INTERROGATING THE GLYCOME USING CLICK CHEMISTRY

by

ERIC NGALLE MBUA

(Under the Direction of Geert-Jan Boons)

ABSTRACT

The past several years has seen a rapid development of the bioorthogonal chemical reporter methodology for the labelling of glycoconjugates of living cells and whole organisms. We have shown that 4-dibenzocyclooctynol (DIBO), which can easily be synthesized, reacts exceptionally fast in the absence of a Cu (I) catalyst with azido-containing compounds to give stable triazoles. The use of several cell lines with known defects in glycoconjugate glycosylation validated DIBO as a reagent for determining relative quantities of cell surface glycoconjugate sialylation.

Using a chemical reporter strategy in combination with pharmacological treatments, we demonstrated a disease-specific and previously unrecognized accumulation of a diverse set of glycoconjugates in NPC1 and NPC2 fibroblasts within endocytic compartments. The labeled vesicles did not co-localize with the cholesterol-laden compartments of NPC cells, and treatment of either NPC1 or NPC2 cells with cyclodextrin was effective in reducing cholesterol storage and also the endocytic accumulation of sialoglycoproteins.

Alterations in protein glycosylation occur during development and progression of many diseases, hence glycomics and glycoproteomics have emerged as important tools in glycobiomarker discovery. An enrichment method is described to covalently capture azide-tagged *O*-GlcNAc proteins, aimed at facilitating mass spectrometric analysis. Furthermore, the modified DIBO-resin is found to be very specific and with efficient enrichment of over 96% of modified *O*-GlcNAc proteins.

A novel phototriggered click strategy is described for activation of cyclopropenones to produce reactive dibenzocyclooctynes upon irradiation for metal-free ligation for labeling of living cells modified with azidocontaining cell surface saccharides. The cyclopropenone-based phototriggered click chemistry offers exciting opportunities to label living organisms in a temporally and spatially controlled manner.

It was found, for the first time, that the substitution pattern of the dibenzylcyclooctynes influences subcellular location. A highly polar sulfated dibenzocyclooctynylamides (S-DIBO) was developed, and we showed that DIBO can enter cells, thereby labeling intra- and extracellular azido-modified glycoconjugates, whereas S-DIBO cannot pass the cell membrane and therefore is ideally suited for selective labeling of cell surface molecules. The ability to selectively label cell surface molecules will yield unique opportunities for glycomic analysis and the study of glycoprotein trafficking.

INDEX WORDS: azide, bioorthogonal chemistry, carbohydrates, click chemistry, glycoconjugates, metabolic labeling, lectin, cycloaddition, O-sulfation, extracellular, cyclooctyne, dibenzocyclooctyne, cyclopropenone, sialylation, cholesterol, trafficking, lysosomes, endosomes, cyclodextrin, glycosylation, O-GlcNAc, enrichment, glycoproteomics, mass spectrometry.

INTERROGATING THE GLYCOME USING CLICK CHEMISTRY

by

ERIC NGALLE MBUA

B.S., University of Buea, Cameroon, 1998

M.S., University of Buea, Cameroon, 2005

A Dissertation Submitted to the Graduate Faculty of The University of Georgia in Partial Fulfillment of the Requirements for the Degree

DOCTOR OF PHILOSOPHY

ATHENS, GEORGIA

2012

INTERROGATING THE GLYCOME USING CLICK CHEMISTRY

by

ERIC NGALLE MBUA

Major Professor: Geert-Jan Boons
Committee: Richard Steet
Lance Wells

Electronic Version Approved:

Maureen Grasso
Dean of the Graduate School
The University of Georgia
December 2012

DEDICATION

To my fiancee Vera Nyonglemuga and son Hansel Lesiga Mbua.

ACKNOWLEDGEMENTS

I sincerely thank my major advisor, Professor Geert-Jan Boons, for his time and efforts supervising and guiding my research and enabling me to become a better scientist. I also wish to thank Professor Richard Steet and Professor Lance Wells. As my committee members, you have offered me invaluable guidance and encouragement when I needed it despite your busy schedules.

Many thanks go to Dr. Margreet Wolfert for giving me the training necessary during the course of my research and Dr. Hearther Flanagan-Steet for her expertise in confocal microscopy.

My gratitude also goes to the past and present members of the Boons Lab for their moral support and encouragement. You all made this laboratory such a pleasant place to work. Special thank you to the following: Drs. Xinghai Ning, Jun Guo, Frederick Friscourt and Mr. Petr Ledin, who supplied the synthetic compounds that were used for my Ph.D. research.

I sincerely thank Mr Richard Yembe Nfor and his family for making it possible for me to be what I am today.

I would like to thank to my fiancée Vera Nyonglemuga for her love and support; aunt, Fanny Joso Mbua, who has been there for me since my early childhood till now; aunt Mary Menyoli for her support and encouragement, my sister Odilia Nanyongo Litumbe and other family members for their moral support.

TABLE OF CONTENTS

Page

LIST OF FIGURES

Page

LIST OF SCHEMES

Page

CHAPTER 1

INTRODUCTION

1.1. PROTEIN GLYCOSYLATION AND IMPORTANT FUNCTIONS OF CARBOHYDRATES

Glycosylation is the most prevalent and important posttranslational modification affecting >50% of eukaryotic proteins.[1] Glycosylated proteins are ubiquitous components of both extracellular matrices and cellular surfaces. Carbohydrates can have a great influence on the physicochemical properties of glycoproteins, affecting their folding, solubility, aggregation and propensity to degrade, and intracellular trafficking. [2-5]

Carbohydrates are implicated in a number of important biological processes involving highly specific events in cell-cell recognition, cell-protein interactions, and targeting of hormones, antibodies and toxins.[6-10] Furthermore, the glycan chains in glycoproteins can serve as specific ligands for lectins and receptors on cell surfaces, thus participating in many important cellular communication processes, such as cell adhesion, cell differentiation, pathogen-host interaction, development, immune response, neural plasticity, inflammation, and disease progression.[3, 6, 11-14]

Cell surface glycoconjugates mediate essential intra and inter-cellular interactions. Some specific sugar residues present on the glycoconjugates regulate many of these recognition events. Sialic acids located at the terminal positions of oligosaccharides to form sialylated molecules serve important regulatory roles for mammalian cells, as well as they are also exploited by many pathogens.[15, 16] For example, influenza viruses utilize hemagglutinin to bind sialylated cell surface receptors and infect

mammalian host, while *Trypanosoma cruzi*'s trans-sialidase transfers sialic acid from host glycoconjugates to the parasite which confers protection against lysis by host serum factors.[17-20] Sialylated glycosphingolipids, known as gangliosides, are of particular interest because they often serve as the principal recognition element for the invasion of host cells by viruses, bacteria, and their secreted toxins.[21, 22]

L-fucose is often a terminal sugar in glycans that participate in important cell-cell interactions and cell migration processes in connection with physiological and pathological processes such as fertilization, embryogenesis, lymphocyte trafficking, immune responses and cancer metastasis.[12, 23-24] The investigation of fucosylated glycans in healthy and disease processes is therefore of great interest.

Consequently, aberrant glycosylation has now been implicated in many diseases, including hereditary disorders, immune deficiencies, neurodegenerative diseases, cardiovascular diseases and cancer.[25] Therefore, detecting such defects in glycosylation, which serve as hallmarks of many human diseases, and cancer, might help diagnose cancer at an early stage.[26, 27] Many clinical biomarkers and therapeutic targets are glycoproteins, including Her2/neu (breast cancer), prostate-specific antigen (PSA, prostate cancer) and CA 125 (ovarian cancer).[28, 29] In order to examine, and understand the disease-related glycosylation alterations in dsease, sensitive, fast and robust analytical methods are required.

1.2. TYPES OF PROTEIN GLYCOSYLATIONS: N- AND O-LINKED

The most common forms of glycosylation of proteins in the secretory pathway found in mammalian cells are *N*-linked attached to asparagine (Asn, N) residues[3, 30] and O-linked attached to serine (Ser, S) or threonine (Thr, T) residues[31] (Figure 1.1). Protein glycosylation takes place inside the lumen of the endoplasmic reticulum (ER) and the Golgi complex, organelles that play central roles in protein trafficking. The addition of glycans to asparagine residues in a consensus sequence Asn-X-Ser/Thr (N-X-S/T; where X can be any amino acid except proline) within a polypeptide chain is known as N-linked glycosylation and occurs widely in eukaryotes and archaebacteria, but only rarely in bacteria.

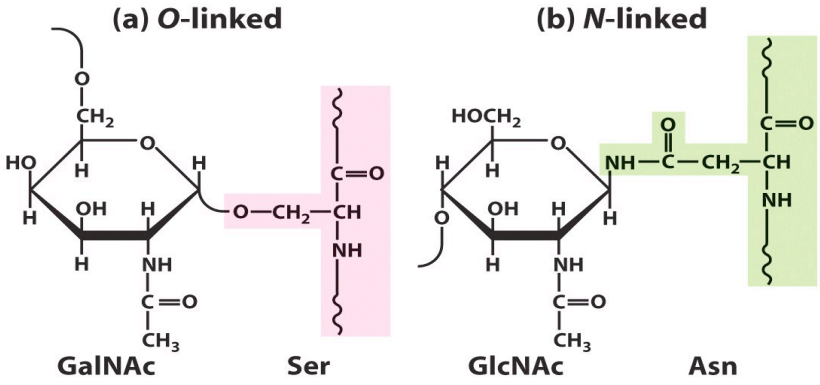

Figure 1.1 Oligosaccharide linkages in glycoproteins.

The *N*-glycosylation occurs on secreted or membrane bound proteins. The diverse assortments of *N*-linked glycans are based on the common core pentasaccharide, Man3GlcNAc2. Further processing in the Golgi results in three main classes of *N*-linked glycan sub-types; high mannose, hybrid and complex type *N*-glycans (Figure 1.2). High mannose type N-linked glycoproteins (Figure 1.2) may contain a variety of oligomannose N-linked oligosaccharides containing between five and nine mannose residues (those that have escaped terminal glycosylation). Further removal of mannose residues leads to a 'core' structure containing three mannose, and two *N*-acetylglucosamine residues, which may then be elongated with a variety of different monosaccharides including *N*-acetylglucosamine, galactose, *N*-acetylgalactosamine, fucose and sialic acid. The addition of an N-acetyllactosamine unit (Galβ1–4GlcNAc; where Gal is Galactose; GlcNAc is *N*-acetylglucosamine), to one arm of the core pentasaccharide in a high mannose type forms the hybrid type *N*-glycans (Figure 1.2).

Complex glycans contain the common trimannosyl core. The addition of an *N*-acetyllactosamine unit to the trimannosy core may be branched by a GlcNAcβ1–6 residue or form repeating *N*-acetyllactosamine units, called poly N-acetyllactosamine extensions. Complex *N*-glycans exist in bi-, tri- and tetraantennary forms (Figure 1.2). Additional modifications may include a bisecting GlcNAc at the mannosyl core and/or a fucosyl residue on the innermost GlcNAc residue. Most often hybrid and complex type *N*-glycans terminate with a sialic acid residue.

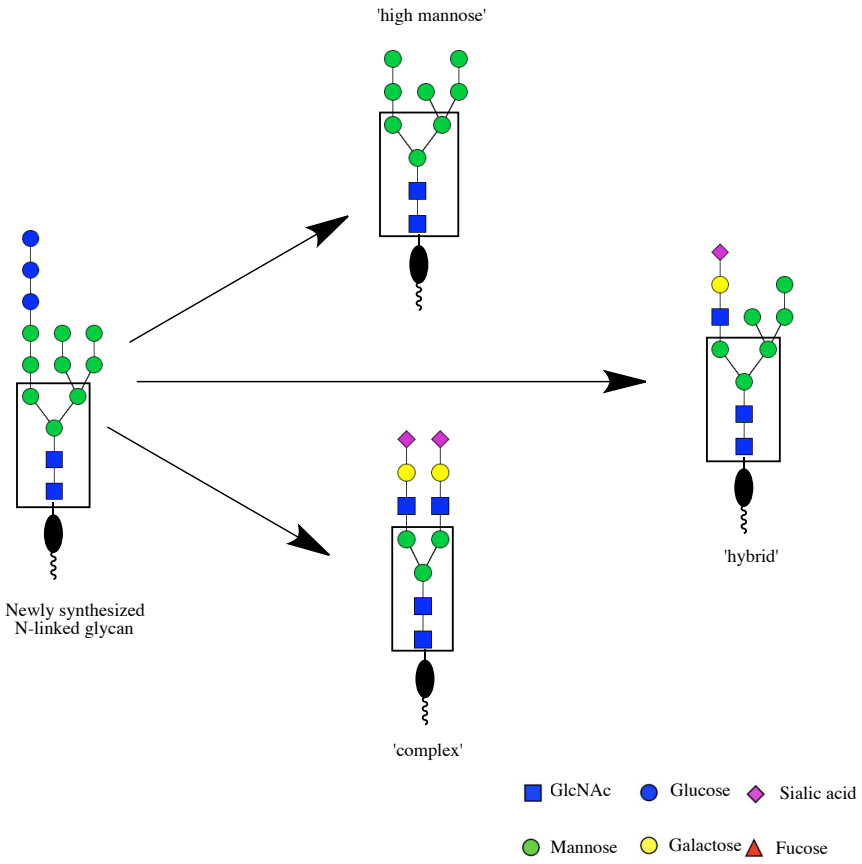

Figure 1.2 Major types of vertebrate N-glycans.

The *O*-glycosylation process produces an immense multiplicity of chemical structures. *O*-linked glycans found in humans are classified on the basis of the first sugar attached to a hydroxyl group of Ser, Thr, or hydroxyl-lysine (hLys) residue of a protein. For most *O*-glycosylation types, a recognition consensus sequence for the attachment of the first sugar residue remains unknown. The most common *O*-linked glycoprotein in humans, the mucin type, has N-acetylgalactosamine (GalNAc) moiety at the reducing end attached to serine or threonine (Figure 1.3).

In total, 8 mucin-type core structures can be distinguished, depending on the second sugar and its sugar linkage, of which cores 1–6 and core 8 have been described in humans.[32] The mucin-type *O*-glycan structures are possible, of which core 1 and 2 are most abundant. The core structures can be further modified; for example, by the addition of *N*-acetylneuraminic acid (NeuAc; sialic acid) to the Tn (GalNAcα1-Ser/Thr) epitope will form sialyl Tn (NeuAcα2–6GalNAcα1-Ser/Thr) epitope; by the addition of an *N*-acetyllactosamine unit (Galβ1–4GlcNAc) which may be branched by a GlcNAcβ1–6 residue or form repeating N-acetyllactosamine units, called poly N-acetyllactosamine extensions. The poly N-acetyllactosamine extensions can also attach to the blood group determinants (A, B, and H) and the type 2 Lewis determinants [LeX, sialyl LewisX (sLeX), and LeY]. The *N*-acetyllactosamine elongations are seen mainly on core 2 O-glycans. Sugars occurring at the nonreducing termini include NeuAc, Fuc, GlcNAc, and GalNAc. GlcNAc and Gal residues can be modified at position 6 or at positions 3 and/or 6, respectively, by sulfation and NeuAc residues can be further modified at positions 4, 7, 8, and 9 with *O*-acetyl ester groups. This gives rise to several hundreds of different mucin-type O-glycan structures.[32] The structures of the other *O*-glycan types seem to show less variability, and they occur mostly in one conformation.

A frequently occurring *O*-linked glycan is the single GlcNAc linked to nuclear and cytosolic proteins (Figure 1.3). This posttranslational modification is more analogous to phosphorylation than to classical complex *O*-glycosylation because it is a reversible process catalyzed by the enzymes O-GlcNAc transferase (OGT) and *O*-GlcNAcase (OGA), respectively[33], and the "normal glycosylation machinery" is not implicated[33, 34]

O-Galactosyl glycans have been found only on collagen domains. Gal or Glcα1–2Gal residues are covalently linked to hydroxyl-lysine (hLys) residues found in collagens, but not all hLys residues become glycosylated. The collagen three-dimensional structure depends on the extent of this posttranslational modification. The quantities and types of *O*-galactosyl glycans vary considerably not only among the different types of collagen, but also among the same collagen type from different tissues and even the same collagen type from different areas of the same type of tissue.[35]

O-Mannosyl glycans are a less common type of protein modification (Figure 1.3), present on a limited number of glycoproteins in the brain, nerves, and skeletal muscle. α-dystroglycan, a skeletal muscle extracellular matrix protein is the best-known *O*-mannosylglycosylated protein.[36]. Only the NeuAcα2–3Galβ1–4GlcNAcβ1–2Man structure has been found in humans, while α-dystroglycan containing Galβ1–4(Fucα1–3)GlcNAcβ1–2Man has been found in sheep brain,[37, 38] and the *O*-mannosyl glycan HSO_3-3GlcAβ1–3Galβ1–4GlcNAcβ1–2Man has been detected in rat brain.[38,39]

Studies have also shown that mammalian N-acetylglucosaminyltransferase IX acts on the GlcNAcβ1,2-Manα1-Ser/Thr moiety, suggesting that 2,6-branched *O*-mannosyl glycan structures are formed in the brain.[40] It is therefore likely that structural diversity of O-mannosyl glycans will also be present in humans.

O-Glucosyl and *O*-fucosyl glycans (Figure 1.3) are also rare types of protein glycosylations that have been found in the epidermal growth factor homology regions (EGF modules) of some human proteins. An EGF module is a common structural motif found in several secreted and cell-surface proteins that is often involved in mediating protein–protein interactions. The EGF repeat is typically 30–40 amino acids long and is

characterized by 6 conserved Cys residues participating in 3 disulfide bridges. Glc is linked to the Ser residue in proteins in the putative consensus sequence C1XSXPC2 (where C1 and C2 are the first and second conserved cysteines of the EGF module, S is the modified Ser residue, and X can be any amino acid).[41] *O*-Linked Glc can be further elongated with 1 or 2 α1–3 linked xyloses and is found on proteins such as human factor VII, factor IX, and protein Z.[42, 43] All *O*-fucosylated glycoproteins are modified with a single *O*-linked Fuc residue (e.g., urinary-type plasminogen activator, tissue-type plasminogen activator, and coagulation factors VII and XII) except for coagulation factor IX, which contains O-linked Fuc that is elongated to the tetrasaccharide NeuAcα2–6Galβ1–4GlcNAcβ1–3Fucα1-Ser/Thr. Most O-Fuc modifications on EGF repeats are found on the consensus site C2X3–5S/TC3 (where C2 and C3 are the second and third conserved cysteines of the EGF repeat, S/T is the modified Ser/Thr residue, and X can be any residue).[43] In a second type of *O*-fucosylation, a disaccharide form of *O*-fucosyl glycans (Glcβ1–3Fucα1-Ser/Thr) is found on the human extracellular matrix protein "thrombospondin-1" in thrombospondin type 1 repeats (TSRs).[44]

TSRs are found in many extracellular proteins and a single TSR is ~60 amino acids long and is characterized by conserved Cys, Trp, Ser, and Arg residues. The putative consensus sequence site for this modification is WX5CX2/3S/TCX2G.[43]

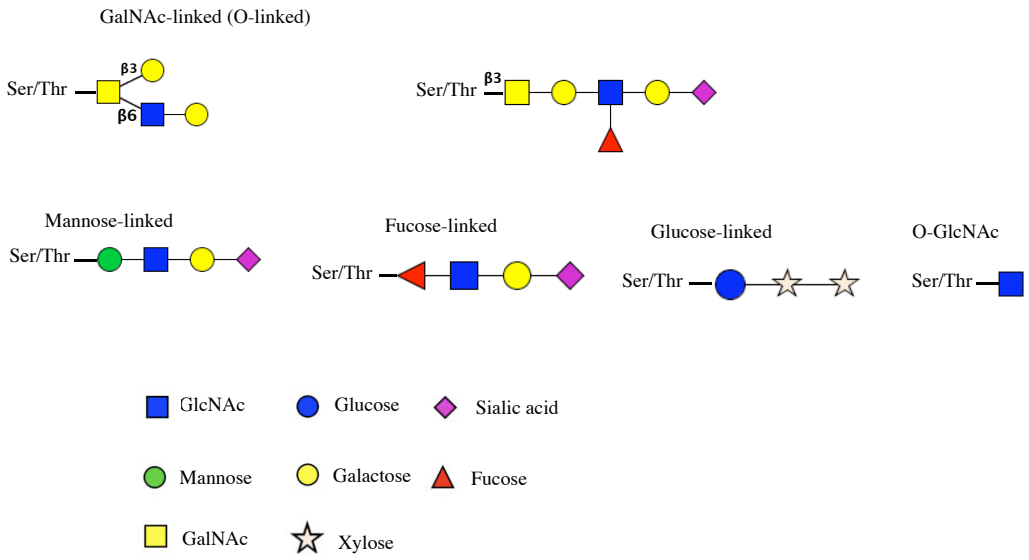

Figure 1.3 Serine/threonine O-linked glycans.

1.3. GLYCOPROTEIN BIOSYNTHESIS AND TRANSPORT

In eukaryotes, *N*-glycosylation begins as a co-translational event in the endoplasmic reticulum (ER) and continues in the Golgi complex, whereas the *O*-linked glycosylation takes place exclusively in the Golgi complex. Glycosylation is a non-templated posttranslational process. It is well known that biosynthesis of glycans takes place in organ- and tissue-specific manners and glycan expression is controlled by various factors including glycosyltransferases. Glycan is synthesized in a stepwise manner by ER- or Golgi-resident glycosyltransferases,[45] and organ- and tissue-specific glycan biosynthesis is achieved by glycosyltransferases, which are also themselves expressed in a tissue-specific manner.[46, 47] The main pathway for the biosynthesis of

complex *N*- and *O*-linked glycans is located in the endoplasmic reticulum (ER) and Golgi compartments, called the secretory pathway. Glycosylation is restricted mainly to proteins that are synthesized and sorted in this secretory pathway, which includes ER, Golgi, lysosomal, plasma membrane, and secretory proteins. There is one exception; nuclear and cytosolic proteins can be modified with a single O-linked GlcNAc.[33] Proteins synthesized by ribosomes and sorted in the secretory pathway are directed to the rough ER by an ER signal sequence in the NH_2 terminus.[48] After protein folding is completed in the ER, these proteins move via transport vesicles to the Golgi complex. The biosynthesis of glycans can be divided into three stages. In the first stage, nucleotide sugars are synthesized in the cytoplasm, except for CMP-NeuAc, which is synthesized in the nucleus.[49] In the second stage, these nucleotide sugars are transported into the ER or the Golgi. In the third stage, specific glycosyltransferases attach the sugars to a protein or to a glycan in the ER or Golgi.

1.3.1. N-LINKED GLYCOPROTEIN BIOSYNTHESIS

The process of N-linked glycosylation is well characterized relative to our understanding of the synthesis of the glycosyl carrier lipid. Fourteen distinct lipid-linked oligosaccharide (LLO) intermediates are synthesized during the assembly of the final *N*-glycan donor molecule in the ER[50]. These steps in LLO biosynthesis take place on both sides of the ER bilayer, with the GlcNAc-1-phosphotransferase catalysing the first step on the cytosolic face of the ER by addition of a GlcNAc-1-P residue from a UDP-GlcNAc donor to dolichol monophosphate (Dol-P). The GlcNAc-P-P-Dol undergoes a series of further reactions at the cytoplasmic leaflet utilizing UDP-GlcNAc and GDP-

Man until it is elongated to Man5GlcNAc2-P-P-Dol (M5-LLO). The LLO intermediates mannose-P-dolichol (Man-P-Dol) and glucose-P-dolichol (Glc-P-Dol) are also synthesized on the cytosolic leaflet of the ER, with GDP-Man and UDP-Glc serving as the respective glycosyl donors. Once synthesized, the M5-LLO, Man-P-Dol, and Glc-P-Dol intermediates are flipped in a protein-dependent manner to the luminal side of the ER, where the M5-LLO is elongated further through addition of four additional mannose units and three glucose residues until it reaches the mature state of Glc3Man9GlcNAc2-P-P-Dol (G3M9-LLO). These sugars are then transferred from Dol-P through the action of oligosaccharyltransferase within the ER lumen to the appropriate Asn acceptor site on the nascent glycoprotein. *N*-linked glycans are installed on target proteins by a single enzyme, oligosaccharyltransferase, which recognizes the consensus sequence Asn-X-Ser/Thr (X is any amino acid apart from proline).[51]

Proteins in the lumen of the ER and in the ER membrane are transported to the Golgi complex, which is a stack of flattened membranous sacs. The Golgi complex has two principal roles. First, carbohydrate units of glycoproteins are altered and elaborated in the Golgi complex. The *O*-linked sugar units are processed here, and the N-linked sugars, arriving from the ER as a component of a glycoprotein, are modified in many different ways. Second, the Golgi complex is the major sorting center of the cell. Proteins proceed from the Golgi complex to lysosomes, secretory granules or the plasma membrane, according to signals encoded within their amino acid sequences and three-dimensional structures.

The Golgi complex of a typical mammalian cell has three or four membranous sacs (cisternae), and those of many plant cells have about twenty. The Golgi complex is differentiated into (1) a cis compartment, the receiving end, which is closest to the ER; (2) medial compartments; and (3) a trans compartment, which exports proteins to a variety of destinations. These compartments contain different enzymes and mediate distinctive functions. The *N*-linked carbohydrate units of glycoproteins are further modified in each of the compartments of the Golgi complex.

In the cis Golgi compartment, three mannose residues are removed from the oligosaccharide chains of proteins destined for secretion or for insertion in the plasma membrane. The carbohydrate units of glycoproteins targeted to the lumen of lysosomes are further modified. In the medial Golgi compartments of some cells, two more mannose residues are removed, and two *N*-acetylglucosamine residues and a fucose residue are added. Finally, in the trans Golgi, another N-acetylglucosamine residue can be added, followed by galactose and sialic acid, to form a complex oligosaccharide unit. The sequence of *N*-linked oligosaccharide units of a glycoprotein is determined both by (1) the sequence and conformation of the protein undergoing glycosylation and by (2) the glycosyltransferases present in the Golgi compartment in which they are processed. Despite all of this processing, *N*-glycosylated proteins have in common a pentasaccharide core (Figure 1.2). Carbohydrate processing in the Golgi complex is called terminal glycosylation to distinguish it from core glycosylation, which takes place in the ER. Tremendous structural diversification can occur as a result of the terminal glycosylation process.

1.3.2. O-LINKED GLYCOPROTEIN BIOSYNTHESIS

The predominant form of *O*-linked glycosylation is the mucin-type characterized by an initial N-acetylgalactosamine (GalNAc) residue α-linked to the hydroxyl groups of Thr or Ser side chains.[52] Mucin-type *O*-linked glycosylation is initiated in the Golgi compartment by a family of polypeptide N-acetyl-α-galactosaminyltransferases (ppGalNAcTs).[53] Multiple isoforms exist in eukaryotes (~ 24 in humans, ~23 in mouse, 15 in Drosophilia and 9 in *C. elegans*), and many of the family members have overlapping tissue distribution and substrate specificity. There is no defined consensus sequence for the ppGalNAcTs, rendering predictions of *O*-linked glycosylation difficult because every pp-GalNAc-T has its own specific attachment site. The biosynthesis of *O*-glycans is initiated after the folding and oligomerization of proteins in the ER and transported to the Golgi compartments[54, 55] O-Glycans are assembled by the sequential action of several specific, membrane-bound glycosyltransferases in a highly controlled fashion.[31] The pathways of *O*-glycosylation are determined by the distinct substrate specificities of glycosyltransferases. Transferases involved in O-glycan biosynthesis are localized mainly in the Golgi. Although many of these enzymes catalyze similar reactions, there is a surprisingly limited sequence homology among different classes. The Golgi glycosyltransferases described to date are all type II transmembrane proteins, with a short N-terminal cytoplasmic domain, a single hydrophobic membrane-spanning domain, and a large C-terminal catalytic domain localized in the lumen of the Golgi.

Only Ser and Thr residues that are exposed on the protein surface will be glycosylated, as *O*-glycosylation is a postfolding event. Therefore, *O*-glycosylation takes place mainly in coil, turn, and linker regions. Furthermore, all attachment sites have high Ser, Thr, and Pro content.[56]

The α-GalNAc residue on mucin-type *O*-linked glycoproteins is elaborated to generate a diversity of structures,[52] for which there is not a single specific lectin.[57] Furthermore, it was recently discovered that human core 1 β3-galactosyltransferase (core 1 β3-Gal-T), which is involved in the formation of core 1 (and core 2) mucin-type *O*-glycans, requires a molecular chaperone for its functioning. This molecular chaperone is called core 1 β3-Gal-T-specific molecular chaperone (Cosmc) and is an ER-localized type II transmembrane protein that appears to be required for the proper folding of the core 1 β3-Gal-T enzyme. In the absence of functional Cosmc, core 1 β3-Gal-T is degraded in the proteosome.[58]

Golgi transferases can recognize a single sugar residue, a sugar sequence, or a peptide moiety, leading to variable specificity. With very few exceptions, each type of transferase is regio- and stereospecific. Glycosyltransferases involved in the linkage of monosaccharides to the protein backbone and those involved in the core processing of mucin-type *O*-glycans are specific and not involved in other classes of glycoconjugates, whereas most glycosyltransferases involved in the elongation, branching, and termination of glycans are not specific for one glycoconjugate class.

For example, the ubiquitous α2,6-sialyltransferase ST6Gal I recognizes the N-acetyllactosamine unit and catalyzes the formation of an α2,6 linkage to terminal N-acetyllactosamine structures found on N-glycans, *O*-glycans, and glycosphingolipids, whereas the β1,4-galactosyltransferase (Gal-T1) galactosylates any terminal GlcNAc residue. An additional prerequisite for proper glycosylation is Golgi trafficking.

1.3.3. GOLGI TRAFFICKING

The Golgi apparatus is a hub of vesicular protein trafficking and is a major site for the glycosylation of proteins and lipids.[59] The Golgi apparatus consists of several cisternae, starting from the nucleus with the cis-Golgi network, through the cis-, medial-, and trans-Golgi compartments, and ending with the trans-Golgi network, which is organized in the form of a stack. The Golgi position and organization within a cell are sustained largely through the combined efforts of a complex cytoskeletal matrix composed of microtubules, an actin–spectrin network, and intermediate filaments. The interaction between these filament systems and Golgi membranes is mediated by mechanochemical enzymes such as dyneins, kinesins, myosins, and dynamin and different structural proteins.[60] The journey of proteins between these compartments starts with the exit from export sites on the ER in coat protein complex II (COPII)-coated vesicles (Figure 1.4). Coatamer proteins (COPs) recognize transport signals present in the cytoplasmic tail of cargo membrane proteins for their incorporation in COPII vesicles.

Most type I membrane proteins have a diacidic or dihydrophobic motif, and the type II glycosyltransferases have a [RK(X)RK] motif proximal to the transmembrane domain.[61] Signals that direct soluble cargo into ER-derived vesicles are less well defined. It is thought that soluble proteins are exported from the ER in 2 ways: (a) through a passive bulk flow process; and (b) through an active receptor-mediated process relying on receptor-like proteins that attach proteins to the inner membrane of the coated vesicle.[62] Different COPII-coated vesicles fuse to form the ER-Golgi intermediate compartment (ERGIC). From here, escaped ER proteins or misfolded proteins are transported back to the ER via COPI-coated vesicles. The ERGIC elements are transported to and fused with the cis-Golgi network. From this point, both anterograde and retrograde transport is mediated via COPI-coated vesicles. Three major protein families regulate vesicle transport. The ARF and Sar1 family GTPases are involved in COPI and COPII vesicle formation, which starts with the activation of ARF and Sar1 by a nucleotide exchange factor into ARF-GTP and Sar1-GTP. ARF-GTP and Sar1-GTP recruit many additional components for the synthesis of the vesicle coat. Subsequently, the Rab family GTPases mediate vesicle targeting. The mammalian Rab protein family includes at least 63 isoforms. All cytosolic Rab proteins form a complex with the Rab guanine nucleotide dissociation inhibitor chaperone, which transports the Rab proteins to the membrane of specific Golgi compartments, where they become activated to the GTP state. Activated Rabs mediate vesicle motility and the tethering of transport intermediates to their target membranes. The third family consists of SNARE proteins, which direct vesicle fusion.

Each type of transport vesicle carries a specific vesicle-SNARE (v-SNARE), which binds to a tethering-SNARE (t-SNARE) on the target membrane, producing the trans-SNARE complex. After fusion, the cargo is transferred to that specific compartment.[63, 64]

Until recently, the Golgi was seen as a static organelle. In this model, Golgi enzymes are retained within one Golgi cisterna, and cargo (the proteins that are transported to and processed in the Golgi) are transported through the different Golgi compartments in the anterograde direction via COPI vesicles. However, at present, the cisternal maturation model is favored. It is now believed that cargo remains in one cisterna and that this Golgi compartment traffics in the anterograde direction, whereas the Golgi enzymes traffic backward by COPI vesicles. This model is based on the experimental observations that cargo indeed remains in a specific cisterna and that COPI vesicles are enriched with Golgi enzymes.[65, 66]

Given the sequential and competing nature of glycosyltransferases, the precise localization of these enzymes within the Golgi is of great importance. It is thought that glycosyltransferases are arranged in an assembly line in the Golgi, whereas early-acting transferases are localized in the cis-Golgi, intermediate-acting transferases in the medial-Golgi, and terminating transferases in the trans-Golgi. A signal targeting glycosyltransferases to a specific Golgi localization has not yet been described. Studies have indicated that glycosyltransferases from a certain Golgi compartment form high–molecular-mass complexes.[67]

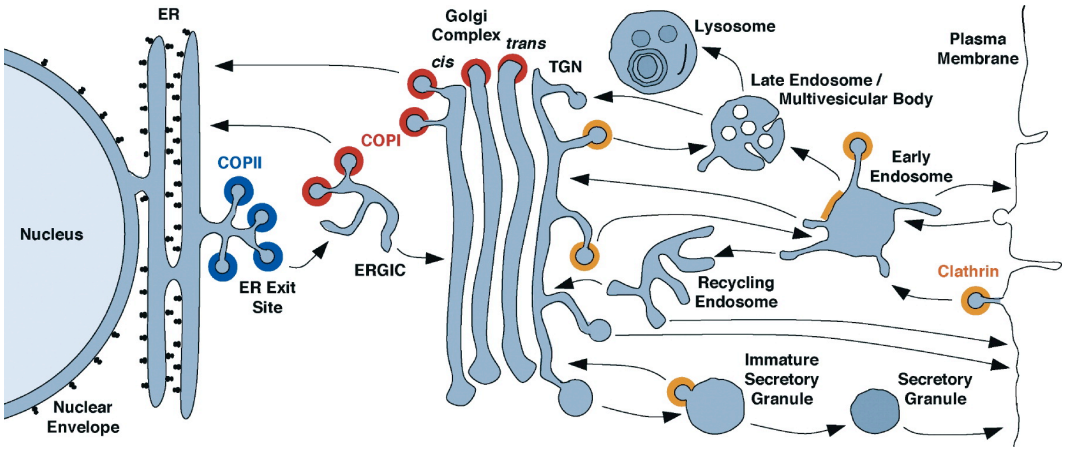

Figure 1.4. Intracellular Transport Pathways. The scheme depicts the compartments of the secretory, lysosomal/vacuolar, and endocytic pathways. Transport steps are indicated by arrows. Colors indicate the known or presumed locations of COPII (blue), COPI (red), and clathrin (orange). Clathrin coats are heterogeneous and contain different adaptor and accessory proteins at different membranes. Only the function of COPII in ER export and of plasma membrane-associated clathrin in endocytosis are known with certainty. Less well understood are the exact functions of COPI at the ERGIC and Golgi complex and of clathrin at the TGN, early endosomes, and immature secretory granules. The pathway of transport through the Golgi stack is still being investigated but is generally believed to involve a combination of COPI-mediated vesicular transport and cisternal maturation. Additional coats or coat-like complexes exist but are not represented in this figure. (Opat AS, *et al., Biochimie* 2001).

The presence of multienzyme complexes is likely to be functionally relevant in the regulation of glycosylation and contribute to the maintenance of the steady-state localization of the Golgi glycosyltransferases.[67] Not all glycosyltransferases form complexes; in particular, those found in the trans-Golgi network seem to be unbound. Another factor that is likely to play a role in the targeting of glycosyltransferases is the thickness of the lipid bilayer, which increases en route to the plasma membrane. The fact that Golgi proteins have shorter transmembrane domains than do plasma membrane proteins suggests that cisternae of a specific compartment can accommodate glycosyltransferases with a transmembrane domain of matching length.

However, it has been shown that some soluble forms of glycosyltransferases, which have lost their transmembrane domain, are retained in the Golgi probably as a result of being associated in complexes.[65, 66] It is likely that more independent signals act together to mediate efficient Golgi localization. The conserved oligomeric Golgi complex (COG) is a hetero-octomeric peripheral membrane protein required for retrograde vesicular transport and glycoconjugate biosynthesis within the Golgi. The mammalian COG complex contains 8 subunits, of which COG1 through -4 form lobe A and COG5 through -8 form lobe B with COG4 as the core component linking the 2 lobes.[68] Mutations in COG subunits (COG1 through -8) of Chinese hamster ovary (CHO), yeast, and *Drosophila melanogaster* sperm cells have been shown to affect the structure and function of the Golgi, producing defects in glycoconjugate biosynthesis, intracellular protein sorting, protein secretion, and in some cases, cell growth.

In the recessive COG1 (ldlB) and COG2 (ldlC)-null CHO mutants, for example, the Golgi showed an abnormal morphology with dilated cisternae[69] and pleiotropic defects in several medial- and trans-Golgi–associated reactions affecting *N*-linked, *O*-linked, and lipid-linked glycoconjugates.[70]

Furthermore, COG works in concert with COPI. Their function is to retrograde transport several Golgi resident proteins to the appropriate Golgi compartment where they reside. COPI coats are found on trafficking vesicles originating within the Golgi, and have an established role in retrograde trafficking.[71] COG complex has a critical role in Golgi structure and function, which, in turn, is involved in protein sorting and glycosylation. Evidence came from the work of Oka et al.[72] who investigated the consequences of the loss and overexpression of COG on a set of Golgi resident type II transmembrane proteins, including members of the SNARE, Rab, and golgin protein families.

The expression and localization of some proteins were COG-dependent, whereas for others this was not the case. The COG-sensitive, integral membrane Golgi proteins called GEARs (Golgi resident integral membrane proteins: mannosidase II, GOS-28, GS15, GPP130, CASP, giantin, and golgin-84) whose abundances were reduced in the mutant cells and, in some cases, increased in COG-overexpressing cells. Dysfunction of COG complex in humans has been associated with new forms of Congenital Disorders of Glycosylation (CDG), therefore highlighting its essential role.[73-75]

1.4. NIEMANN-PICK DISEASE

1.4.1. TYPES OF NIEMANN-PICK DISEASE

Niemann-Pick disease is a group of rare inherited lipid diseases in which harmful quantities of fatty substances (lipids) accumulate in the spleen, liver, lungs, lungs, bone marrow, and the brain. Albert Niemann first described the disease in 1914[76] with its pathology characterized by Ludwig Pick in 1933[77]. The disease usually appears in early childhood, but juvenile and adult forms of the disease are also known and they are currently some approved drugs for treatment still under clinical trials. In 1961, Niemann-Pick (NP) disease was classified into four types based on clinical and biochemical feautures[78, 79]. Type A - acute infantile form presents with severe hepatosplenomegaly and neurological abnormalities. Type B – a juvenile/adult form, is similar to type A, and presents only visceral involvement. NP disease type A and B result from mutations in the gene encoding for the lysosomal enzyme acid sphingomyelinase, that results in the progressive accumulation of sphingomyelin and other lipids in the lysosomes of various tissues. The reticulo-endothelial system is the prominent site of pathology. Characteristic foamy macrophages are observed in the bone marrow, liver, spleen, lung, and other tissues[80, 81]. Type C and D have sub-acute neurological involvement and less hepatoslenomegaly. Type C and D are clinically indistinguishable and so type D is no longer justified as distinct[81].

Niemann-Pick type C (NPC) disease is a fatal neurodegenerative lysosomal storage disorder resulting in abnormal accumulation of unesterified cholesterol, glycosphingolipids, and other lipids in late endosomes/lysosomes (LE/LY) of many cells[81]. NPC disease is predominantly caused by mutations in the NPC1 protein (95% of

all cases)[82, 83]. The second (but much rare; 5%) causative locus for this disease, NPC2, was later identified through a proteomic survey of the lysosome[84]. Both affect intracellular cholesterol trafficking and cause accumulation of unesterified cholesterol and other lipids in lysosomal storage organelles[85]. The incidence of NPC disease is estimated between 1:120,000 and 1:50,000 live births[86]. This NPC1 gene includes sterol-sensing domain, which may relate to cholesterol homeostasis[82]. The most common NPC1 mutation described is I106T, which accounts for 20% of the alleles in the United Kingdom and France and about 15% in the United States of America[83, 87], and leads to severe disruption of cholesterol processing.

The discovery that the hallmark of NPC disease is lysosomal accumulation of LDL-derived unesterified cholesterol, and consequently misregulated sterol biosynthesis, uptake and esterification was made by Peter Pentchev and co-workers in 1984[88, 89]. Patients carrying mutations in either NPC1 or NPC2 display phenotypes that are clinically and biochemically indistinguishable[90-93]. These genes do not encode lysosomal enzymes, thus it is likely that the proteins encoded by these two genes act in a common cellular pathway or act upon downstream target. This result provides genetic evidence for a cellular pathway for the transport of lysosomal lipids in which both proteins participate and in which neither can compensate for loss of the other[90]. Lysosomes play a critical role in protein, lipid, and carbohydrate catabolism, plasma membrane recycling, lipid and sterol trafficking, antigen presenting and autophagy. These processes are mediated by a variety of organelle-contained hydrolytic activities. On the cellular level the most pronounced observation is an abnormal accumulation of lipids such as cholesterol, sphingomyelin, glycosphingolipids, sphingosine, some phospholipids in late endosome/

lysosome (LE/LY)-like storage organelles (LSOs) [90, 94-96]. Proteins involved in both early and late endocytic transport has been shown to be mislocalized because of lipid accumulation in late endosomes in NPC disease[97]. The mechanisms leading to this complex pattern of storage remains unknown and how lipid storage causes neurodegeneration is also not understood. Another defining feature is a profound block in the endocytic pathway at the level of the late endosome (LE) [98].

1.4.2. NIEMANN-PICK C PROTEINS AND THEIR FUNCTION IN THE MOBILIZATION OF CHOLESTEROL

Two genes NPC1 and NPC2 have been linked to the NPC defect and the precise mechanism of action of these proteins are still under investigation. NPC1 is a 1,278 amino acid multi-spanning protein with 13 trans-membrane helices, three large luminal domains and a cytoplasmic tail that is localized in the limiting membrane of the LE/LY[82], [99-102]. NPC1 contains three lumenally oriented domains including an N-terminal domain (NTD), a sequence of 240 amino acids that is postulated to project into the lumen of the lysosome[102, 103] and was shown to be a major oxysterol binding protein found in the liver[101, 103]. Oxysterols are analogs of cholesterol that are modified with 24-, 25- or 27-hydroxyl groups and regulate cholesterol pathways[104]. It was shown that the NTD of NPC1 contained all of the sterol binding capacity and binds oxysterol stronger than cholesterol[103]. Kwon et al.[102] showed that substitution mutations in the adjacent amino acids of the N-terminal domain of NPC1, abolishes its cholesterol binding activity and impairs its ability to export cholesterol from lysosomes of cultured cells lacking NPC1.

Thus, the cholesterol-binding domain in the NTD of NPC1 is essential for cholesterol export from lysosomes in living animals as it is in cultured cells.

NPC2 is a soluble, glycosylated protein of 132 amino acids that is localized in the lumen of the LE/LY and is able to bind cholesterol[105-107]. NPC2 was shown to bind strongly to cholesterol and did not bind oxysterols[101, 103, 108]. It was showed that the NTD of NPC1 binds cholesterol slowly[101, 103], and had slow dissociation rate, while NPC2 binds and release cholesterol rapidly[102]. Thus, NPC1 and NPC2 function as a cellular 'tag team duo' to catalyze mobilization of cholesterol within the multi-vesicular environment of the LE to effect egress through the limiting bilayer of the LE[109].

NPC2 has been shown to shuttle free cholesterol to and from membranes in vitro and the N-terminal cholesterol-binding domain of NPC1[103, 108, 110]. Wang et al.[111] identified NPC1 residues L175/L176 and E191/Y192 being critical for receipt of cholesterol from NPC2. Mutations of these NPC1 residues L175Q/L176Q to form the NPC1 mutant protein, showed a defective egress of cholesterol from the lysosome. Deffieu and Pfeffer[112] showed that NPC1's second luminal domain binds NPC2 in a cholesterol-dependent manner, a process that may facilitate directional transfer of cholesterol from NPC2 onto NPC1's N-terminal domain. The binding of NPC2 to NTD of NPC1, allow cholesterol to slide from NPC2 to NPC1 without having to enter the water phase. This sliding model is supported by crystallography showing the opposite orientation of cholesterol in the two binding site[102, 111]. Furthermore the cholesterol handoff model is supported by alanine-scanning mutagenesis of NPC2 and NPC1 (NTD)[102, 111].

The cholesterol transferred to NPC1 in the limiting membrane of the LE is channelled to a cytosolic sink. Here vesicle trafficking pathways and members of the oxysterol-binding protein-related proteins (ORPs) family are thought to be cyctosolic cholesterol transfer proteins[106].

1.4.3. NPC1 AND NPC2 CHOLESTEROL INDEPENDENT ROLES

The function of NPC1 remains enigmatic but NPC2 function as a cholesterol transporter within the lysosome[110]. Other functions of NPC1 protein have been reported. Carette et al[113] showed that the membrane fusion mediated by filovirus glycoproteins and viral escape from the vesicular compartment require the NPC1 protein. Fibroblasts derived from human Niemann-Pick type C1 disease patients were shown to be resistant to infection by Ebola virus and Marburg virus (filoviruses), but remain fully susceptible to a suite of unrelated viruses. But, NPC2-mutant fibroblasts derived from patients were susceptible to filovirus glycoprotein dependent infection. Thus resistance of NPC1-deficient cells to Ebola virus is not caused by defects in cholesterol transport per se since both NPC1 and NPC2-mutants have accumulation of cholesterol. Thus, NPC1 has a critical role in infection mediated by filovirus glycoproteins that is conserved in mammals and probably independent of NPC1's role in cholesterol transport.

Studies have shown that defects in NPC1/NPC2 pathway of cholesterol efflux from late endosomes/lysosomes can profoundly affect HIV-1 infectivity, highlighting the contribution of intracellular cholesterol transport and localization to virus infectivity and release[114, 115]. Ulatowski et al.[116] showed that the reduction or lack of NPC1 or NPC2 function in cultured cells resulted in a marked accumulation of alpha-tocopherol (vitamin

E). Thus, NPC1/2 proteins may function in the proper bioavailability of vitamin E and that the NPC pathology might involve tissue-specific perturbations of vitamin E status. It has been shown that the expression of the ATP-binding cassette transporter A1 (ABCA1) is impaired in human NPC1-/- fibroblast[117] and NPC2-/- fibroblast[118] cells from patients with NPC disease. This is consistent with the finding that there is impaired oxysterol generation, the key regulator of liver X receptor (LXR)-dependent activation of ABCA1 expression, in both NPC1-/- and NPC2-/- cells[119]. NPC1 protein has also been implicated in endosomal/lysosomal fusion and fission[120], calcium homeostasis[96]; facilitate endocytic transport[98] and fatty acid efflux[121].

1.4.4. CHOLESTEROL METABOLISM AND HOMEOSTASIS

Cholesterol plays an important role in determining the physical properties of biological membranes into discrete microdomains essential for their normal functions[122]. Cholesterol is distributed throughout the cell, including cell membranes, lipid rafts, myelin and synaptic structures. Cholesterol is highly enriched in the central nervous system (CNS) with up to 70% of brain cholesterol present in myelin and required for a variety of membrane structures and functions, including intracellular signal transduction. Cholesterol is also important for synaptic vesicle transport; receptor-mediated endocytosis and receptor mediated post-receptor cell signaling in neurons.

The main sorting station for cholesterol within the cell is the late endosome, an intermediate stage in the endosomal-lysosomal trafficking pathway. Within the lumen of the LE, cholesterol esters are hydrolyzed to free cholesterol by lysosomal acid lipase. Released cholesterol joins the endogenous cholesterol pool for recycling to the cell

surface or transferred to the endoplasmic reticulum (ER) where they are re-esterified and as necessary, placed in storage particles for later use[91]. Evidence suggests that sorting of cholesterol utilizes both vesicular and non-vesicular pathways. Two LE/LY proteins, Niemann-Pick C1 (NPC1) and NPC2 appear to be key players that initiate the sorting process[91, 93, 106, 123].

In normal cells, cholesterol levels are tightly regulated by a number of mechanisms that includes cholesterol uptake, storage and efflux[122]. In cells with normal sterol trafficking, low-density lipoprotein (LDL)-associated cholesteryl esters (CE) are internalized into cells via receptor-mediated endocytosis[124] and delivered to LE/LY, where the hydrolysis of chloesteryl esters by lysosomal acid lipase (LAL) takes place to free cholesterol and fatty acids[125, 126]. Free cholesterol is then exported from the LE/LY and delivered to the plasma membrane and extracellular acceptors, as well as the endoplasmic reticulum (ER), where cholesterol is esterified by acyl-coenzymeA: cholesterol acyltransferase (ACAT) and deposited as lipid droplets[127, 128].

The low-density lipoprotein (LDL) uptake and its delivery to LE/LY, and cholesteryl ester hydrolysis by LAL are all normal in NPC-deficient cells, but the rate of free cholesterol efflux from the LE/LY is severely reduced[129]. As a consequence, there is an obstruction in cholesterol trafficking and hence a significant decrease in the homeostatic responses in NPC-deficient cells. As a result cholesterol cannot reach the ER and regulate the rate of sterol biosynthesis or act as substrate for the esterifying enzyme, ACAT. At the transcriptional level, sterol regulatory element-binding proteins regulate the expression of a large number of genes involved in the synthesis and uptake of cholesterol, fatty acids, triglycerides and phospholipids, as well as NADPH that is needed

for lipid and cholesterol synthesis[130]. In the presence of adequate cholesterol in the ER, these transcription factors fail to translocate to the nucleus, and genes involved in cholesterol synthesis and uptake are no longer activated. The ER cholesterol concentration dictates the processing of sterol response-element-binding protein-2 (SREBP2), which transcriptionally regulates, the expression of many genes involved in cellular cholesterol homeostasis[130, 131]. When ER cholesterol content exceeds ~5% total lipids, the expression of genes in cholesterol biosynthesis is reduced whereas cholesterol storage as cholesterol esters (CE) and expression of genes involved in cholesterol efflux, are increased[132]. Consequently, a low cholesterol level sensed by the ER results in expression of genes involved in cholesterol biosynthesis. Re-esterification by ACAT is reduced and the accumulation of cholesterol and other lipids in the lysosomal storage organells (LSOs) contributes to the pathology of NPC disease.

NPC cells are unable to respond to the accumulation of unesterified cholesterol within late endocytic/lysosomal compartments. In these cells, LDL-receptor expression is not down regulated and consequently LDL uptake continues to occur despite the increased cellular content of free cholesterol[124]. As a result, elevated cholesterol levels are not counterbalanced by sterol homeostatic mechanisms in the ER, and cholesterol and other lipids continue to accumulate, causing the formation of abnormal storage organelles[133]. Xie et al.[134] showed that in NPC disease, it is the cholesterol carried in LDL and chylomicrons that is sequestered in the tissues and not sterol that is newly synthesized and carried in high density lipoproteins (HDL).

Cellular cholesterol is also regulated by liver X Receptors (LXRs) transcription factors, which are activated by cholesterol-derived oxysterols[135]. In increased cellular cholesterol, LXRs activate target genes that participate in the efflux of cellular cholesterol, including the transporters, ATP-binding cassette transporters (ABCA1, ABCG1, ABCG4, ABCG5 and ABCG8). NPC cells are defective in oxysterol generation and subsequent LXR inactivation[119]. Reddy et al.[136] showed that many genes involved in the trafficking and the cellular regulation of calcium, metals and other ions were upregulated in NPC fibroblasts. The NPC cells exhibited a gene expression profile indicative of oxidative stress, which are likely contributors to the pathophysiology of NPC disease.

1.4.5. EFFECTS OF DRUGS ON CHOLESTEROL METABOLISM

Certain small molecules such as 3-ß-[2-(diethylamino)ethoxy]androst-5-ene-17-one (U1866A)[137, 138] and the antidepressant imipramine[139] cause a cellular phenotype similar to NPC deficiency possibly by targeting NPC1[137]. The inhibitory action of imipramine and other hydrophobic amines in cholesterol transport is not well known, but it is suggested that the hydrophobic amines may act by forming a complex with an acidic component that is essential for cholesterol transport[140]. Imipramine has been described to alter the (Na+/K+)- and Mg2+-dependent ATPases and could alter membrane recycling and or properties of the lysosomal membrane[141, 142]. The result is impaired cholesterol transport across the lysosomal membrane and cholesterol will stay within lysosomes. Another potential mechanism might be a raise in the pH of intracellular compartments[141].

1.4.6. TREATMENT OPTIONS

Treatment options for NPC disease are limited. One possible therapeutic option for NPC patients is the reduction of cholesterol within the LSOs. Substrate reduction therapy utilizes imino sugars to inhibit glucosylceramide synthase, a key component in the glycosphingolipid biosynthetic pathway[143] and potentially abrogate the effects of storage. The encouraging but relatively limited success of studies using one such inhibitor N-butyldeoxynojirimycin (Misglustat: NB-DNJ) to treat animal models of NPC disease[144] suggests that additional strategies should be considered. This treatment was shown to slow the disease progression, but it did not reverse the damaged neurons or promote recovery of lost neurons. Misglustat treatment in both feline and murine NPC models responded positively to treatment, resulting in reduced ganglioside accumulation, and a significant increase in lifespan, highlighting the importance of glycosphingolipids in neuropathogenesis[145]. These findings suggest that the mechanism of pathogenesis are complicated and cannot be attributed to cholesterol or GSL storage alone. Later, another imino sugar N-butyldeoxygalactonojirimycin (NB-DGJ) was reported to be a potentially more selective glycosphingolipids biosynthesis inhibitor, in vitro and in vivo[146].

Correction of mutations in NPC2 will focus on approaches that improve 'donor' function i.e. improve cholesterol mobilization within the LE. An example of a class of drugs is the cyclodextrin chemical scaffold. Cyclodextrins (CDs) are composed of cyclical oligosaccharide with a hydrophilic exterior and hydrophobic interior, and are ideal chelators of sterols[147]. Cyclodextrins are nontoxic and are used in humans for drug delivery[148]. Small molecules such as 2-hydroxylpropyl–ß-cyclodextrin or methyl-ß-cyclodextrin are commonly used to modify the cholesterol content of cellular membranes.

Mammalian cells lack the enzymes for degradation of CDs[149], so CDs delivered to LE/LY remain intact. The cyclodextrins provide a sustained shuffling mechanism within the endosomal-lysosomal system to achieve unidirectional flow via the linked activities of NPC1 and ORP or vesicle traffic. The internalized cyclodextrin binds to cholesterol and supplements the shuttle activity of endogenous NPC2 to transfer cholesterol from internal membranes to favor efflux via ABCA1 or the presence of an extracellular sink for cholesterol via vesicular recycling pathways. In vivo studies with NPC1-deficient mice[150, 151] and NPC2-deficient mice[151] treatment with 2-hydroxylpropyl-ß-cyclodextrin (HPCD) prolonged lifespan, corrected cholesterol regulation[150] and reduced intraneuronal cholesterol content[151] in these animals. Cell culture studies also showed reduced lysosomal cholesterol in both NPC1- and NPC2-deficient fibroblasts or neurons and glial cells from NPC1-/- mice treated with HPCD[152-154] or methyl-ß-cyclodextrin[153], as well as correction of cholesterol esterification by ACAT in both cell types[152]. Cycodextrins are thought to act by either direct mobilization of cholesterol within endocytic organelles[153] or by inducing calcium-independent exocytosis from lysosomes[155], by bypassing both NPC1 and NPC2 defects. A limited human trial of cyclodextrin is currently in progress, but there is currently no cure for NPC disease.

Pipalia et al.[156] showed that treatment of NPC human fibroblasts in tissues culture with small molecule histone deacetylase (HDAC) inhibitors corrected the NPC phenotype in cells with either one or more copies of the NPC1 mutation. The correction was associated with increased expression of NPC1 protein. But, the HDAC inhibitor treatment was ineffective in an NPC2 mutant human fibroblast line. HDAC play a regulatory role in chromatin remodelling and gene transcription[157] by mediating

posttranslational deacetylation of many types of proteins including histones transcription factors, and chaperones, such as Hsp90[158] An inbalance in histone acetylation has been hypothesized in NPC disease.

Munkacsi et al.[159] showed that the majority of the 11 histone deactylase (HDAC) genes are transcriptionally up-regulated in fibroblast cell lines from patients with NPC disease, and an approved HDAC inhibitor, suberoylanilide hydroxamic acid (SAHA) reversed the dysregulation of the majority of the HDAC genes.

1.5. THE ENDOCYTIC PATHWAY

Endocytosis is the process by which cells internalise molecules from the outside, plasma membrane lipids, and plasma membrane proteins. Material taken up by endocytosis passes from the early endosomes[160] to the late endosomes and from there may intersect with trafficking pathways from the Golgi apparatus, or may be directed to lysosomes or to the Golgi. The exact pathway depends on the cell and the material that has been internalised. There are several endocytic pathways that utilize different mechanisms to internalize portions of the plasma membrane. This removal of membrane from the cell surface is balanced by endosomal recycling pathways that return much of the endocytosed proteins and lipids back to the plasma membrane[161-164] and contributes to diverse cellular processes, including nutrient uptake, cell adhesion and migration, cytokinesis, cell polarity and signal transduction. Thus, endocytic pathways must be robust and coordinately regulated[165].

Different types of endocytic processes can be distinguished by the size of the vesicle formed, their cargo and the machineries involved and it includes pinocytosis, the uptake of small soluble molecules in vesicles, and phagocytosis, the internalisation of large insoluble particles. Endocytic uptake from the cell surface may occur through clathrin-mediated or clathrin-independent routes[166, 167]. Endocytosis that is mediated by vesicles coated with clathrin is the best-characterized pathway, yet the selection of cargo by adaptor proteins is considerably more complex than initially anticipated[168-170]. Further down the endocytic pathway, lysosomes are the primary catabolic compartments of eukaryotic cells that degrade extracellular material internalized via endocytosis and intracellular components sequestered by autophagy. The importance of lysosomal trafficking pathways is emphasized by recent findings describing new roles of lysosomal membrane proteins in cellular physiology and an increasing number of diseases that is recognized as a defect in lysosome biogenesis[171].

1.5.1. THE CLATHRIN-MEDIATED ENDOCYTOSIS

The major endocytosis pathway in mammalian cells is the clathrin-coated pit pathway[172]. This is the uptake of material into the cell from the surface using clathrin-coated pits. This pathway is versatile as many different cargoes can be packaged using a range of accessory adaptor proteins. In some cases of receptor-mediated endocytosis, covalent attachment of ubiquitin can act as a signal for endocytosis and several proteins appear to control this complex process and some of them are distinguished by the fact that they become tagged with a single copy of the molecule ubiquitin. Monoubiquitination is well established as a signal for endocytosis in yeast, and is

implicated in the regulated removal of cell surface receptors in animal cells[173]. This tagging requires sequentially acting enzymes, the last one being a ubiquitin ligase that attaches ubiquitin to a lysine residue of the target protein.

Clathrin-coated vesicle formation proceeds through five stages that involve initiation, cargo selection, coat assembly, scission and uncoating. Clathrin consists of a heavy chain of molecular weight 180,000 together with a light chain of molecular weight 35,000[174]. Clathrin molecules successively assemble into a polyhedral, cage-like coat on the surface of the coated pit. The clathrin coat is made of sub-assemblies, each consisting of a three-pronged protein complex, a triskelion, each leg of which is made of one heavy and one light chain. The triskelion forms a lattice-like network of hexagons and pentagons, which attaches to the membrane via an adaptor protein (AP) complex[170].

In clathrin-mediated endocytosis, the cytoplasmic domains of many receptors such as the receptors for iron-bound transferrin and low-density lipoproteins (LDLRs) and their associated ligands[166, 175] cluster into clathrin-coated pits by association with clathrin adaptor proteins such as the four-subunit complex AP-2[176]. The most abundant phosphoinositide at the plasma membrane is Phosphatidylinositol 4,5-bisphosphate (PtdIns(4,5)P2), and generation of PtdIns(4,5)P2 by phosphatidylinositol phosphate 5-kinase Iβ recruits AP-2 to the plasma membrane, increases the number of clathrin coated pits at the membrane and permits transferrin receptor internalisation[177]. PtdIns(4,5)P2 binds directly to the epsin N-terminal homology (ENTH) domain of epsin[178] and can hence indirectly recruit epsin binding components of the endocytic machinery, such as AP-2, Eps15 and Intersectin. PtdIns (4,5)P2 was reported to bind directly to AP-2 at two basic sites on the α and μ2 sub-units[179, 180]. Binding of AP-2 to the Yxxϕ sorting motif is

contingent upon coincident PtdIns(4,5)P2 binding thus ensuring that engagement of AP-2 is exclusive to the plasma membrane and not at other sites of the cell where the cytoplasmic tail of receptors may be exposed[181].

Accessory proteins and the GTPase dynamin work together with forces provided by actin polymerization to deform the membrane into a curved bud. The deformation and scission of the vesicle is energy-dependent, and a family of proteins called epsins appears to be involved in this process[182]. Epsin-1 induces membrane curvature and promotes the polymerisation of clathrin. Another protein, AP180, appears to limit the vesicle size, and vesicle scission is mediated by another protein, dynamin, a GTPase that collaborates with the coat proteins to induce budding of clathrin-coated vesicles[183, 184]. Dynamin self-assembles into rings and forms collars at the neck of invaginated coated pits. These collars constrict the neck of the coated pits, which are then severed by hydrolysis of GTP[166, 167]. The ATPase chaperone Hsc70 and the protein auxilin promote clathrin-coated vesicle uncoating, a necessary step for the vesicle to fuse with endosomes[184]. Membrane proteins are sorted throughout the secretory and endocytic pathway by cis-acting sorting motifs that are recognized in trans by a host of protein machinery. While sorting information for some proteins can be an intrinsic nonregulated property embedded within their primary sequence, sorting information for other proteins can be revealed, concealed or appended by post-translational modification. This sorting may involve specific retention signals or phosphorylation-induced changes in the oligomeric structure of the proteins[168, 169].

Clathrin-mediated endocytosis has a range of different functions. These include; regulating the surface expression of proteins; sampling the cell's environment for growth and guidance cues; bringing nutrients into cells; controlling the activation of signaling pathways; retrieving proteins deposited after vesicle fusion; and turning over membrane components by sending these components for degradation in lysosomes. Signaling receptors are thought to be mediated in part through regulated endocytosis. In some cases endocytosis is thought to down-regulate signaling, while in others endocytosis may be required for signaling receptors to contact their downstream effectors located on endosomal membranes[185].

1.5.2. CLATHRIN-INDEPENDENT ENDOCYTOSIS

Many cell surface transmembrane proteins lack cytoplasmic sequences for the recruitment and internalization into clathrin-coated vesicles. The different mechanisms of clathrin-independent endocytosis depend on cell types and cargo molecules being endocytosed[186]. In recent years, non-clathrin-mediated pathways, including macropinocytosis, phagocytosis and caveolin-dependent pathways, have gained considerable interest, which in turn has led to the discovery of new endocytic recycling systems[187]. In many cell types, stimulation by growth factors often induces membrane disturbance, which ultimately leads to macropinocytosis. Macropinocytosis is a non-specific mechanism for internalisation; in which lamellipodia extend at a site of membrane ruffling to form irregular vesicles, containing large volumes of extracellular fluid[188]. The extension of lamellipodia is driven by the extension of actin filaments, in a process controlled by small GTPases belonging to the Rho family[189].

Caveolin-mediated endocytosis proceeds by involution of selective plasma-membrane domains that give rise to smaller pinocytic vesicles. Caveolar endocytosis involves caveolin, is dynamin dependent and is the mechanism that glycosphingolipids and some viruses use for cell internalization[186, 190]. Assembly of endosomal vesicles is often preceded by the formation of domains within the membrane, consisting of specific lipids and proteins. For example, caveolae form from lipid rafts (cholesterol-rich domains within the membrane), which can selectively incorporate or exclude particular proteins. The cytoskeletal protein actin is thought to constrain the lateral mobility of rafts, increasing their stability in the membrane. Moreover, actin is involved in the initial intracellular movement of the caveolae[191].

The endocytosis of fluid-phase markers, glycosylphosphatidylinositol (GPI)-anchored proteins and bacterial toxins have been reported to dependent on CDC42, ADP-ribosylation facotor 1 (ARF1)[192] and actin and is dynamin independent. Another dynamin independent mechaism of clathrin-independent endocytosis, first described in HeLa cells, is associated with the ARF6 GTPase and is responsible for the endocytosis of many cell surface integral membrane proteins that lack the adaptor protein recognition sequences[193]. The ARF6-associated pathway has been shown to be the mechanism through which endogenous proteins enter cells such as the major histocompatibility complex (MHC) class I proteins[193], ß-integrins[194, 195], GPI-anchored protein CD59[196], the ubiquitous glucose transporter GLuT1 and other proteins that are involved in amino acid uptake and cell–extracellular matrix interactions[197], the interleukin 2 receptor α-subunit[193], the β2 adrenergic and M3 muscarinic receptors in the absence of ligand[198].

1.5.3. THE ENDOSOMAL-LYSOSOMAL PATHWAY

In most cases, following internalization into distinct vesicles, the endocytosed cargo is then delivered to the early endosome, where sorting occurs. Cargo-specific sorting leads to distinct subsequent cargo itineraries. Cargo can be routed from the early endosome to the late endosomes and lysosomes for degradation, to the trans-Golgi network (TGN) or to recycling endosomal carriers that bring the cargo back to the plasma membrane[199]. Uncoated endocytic vesicles fuse with early endosomes, a network of tubules and vesicles distributed around the cytoplasm. The fusion is regulated by rab5 GTPase[200, 201]. The ability of early endosomes to host multiple sorting events is crucial for cells. The majority (>95%) of internalized lipid is recycled from early (sorting) endosomes back to the plasma membrane[202]. Some endocytosed receptors, such as low-density lipoprotein (LDL) and transferrin receptors, are efficiently recycled from the sorting endosomes along with the bulk membrane lipids[203, 204]. The slightly acidic pH of the sorting endosomes allows dissociation of ligands destined to lysosomes, e.g. LDL, from their recycling receptors[169]. Apparently, recycling receptors are segregated from the soluble contents into the narrow tubular extensions of sorting endosomes[204-206]. These tubular extensions will then give rise to tubular/vesicular carriers mediating recycling to the plasma membrane. Some recycling cargo also accumulates in a pericentriolar cluster of tubules and vesicles (recycling endosomes)[207-209]. The role of this distinct pool of early endosomes is currently unclear. The recycling through sorting and recycling endosomes appears to be regulated by the resident GTPases, rab4[210, 211] and rab11[212], respectively.

Endosomal sorting complexes required for transport (ESCRTs) dictate cargo selection for the lysosomal pathway and the production of vesicles that bud inwards from the limiting membrane of the sorting endosome[213, 214]. Sorting endosomes can also generate a variety of cell type-specific recycling vesicles, for example, synaptic vesicles in neurons and neuroendocrine cells, insulin-responsive glucose transporter (Glut-4)-containing vesicles in adipocytes and major histocompatibility (MHC) class II-containing vesicles in antigen-presenting cells[168, 169]. Furthermore, these endosomes are capable of sorting certain components for transport to the opposite plasma membrane domain (transcytosis), in which the cargo transport occurs via common apically located recycling endosomes[215, 216] and appears to be regulated by rab17 GTPase[217, 218].

Many ligands do not recycle but instead are transported from early to late endosomes and eventually to lysosomes for degradation. For example, the epidermal growth factor receptor (EGFR), together with its ligand moves from an early endosomal compartment to a late endosome and from there to lysosomes for degradation. This is a mechanism for reducing the number of receptors on the cell surface, a process that is controlled, in many cases, by the phosphorylation of the receptors[219]. Also, a pool of newly synthesized lysosomal proteins and mannose-6-phosphate receptor (MPR)-ligand complexes, harvested to clathrin-coated vesicles in the TGN, reaches the endocytic pathway in sorting endosomes to be further transported to late endosomes and lysosomes[220, 221].

The formation of late endosomes from early endosomes requires the conversion from a Rab5-positive organelle into a Rab7-positive organelle, a process regulated by the homotypic fusion and vacuole protein sorting (HOPS) complex[222]. Two models for the

transport from early to late endosomes have been proposed. One model assumes that early endosomes gradually mature to give rise to late endosomes[223, 224]. According to the other model, transport requires specific carrier vesicles pinching off from early endosomes and fusing to late endosomes[225-227]. Transport to late endosomes is dependent on intact microtubules[225] and dynein[226] and appears to be controlled by rab7, a small GTPase localized to late endosomes[228]. The transport to lysosomes is thought to occur by fusion of late endosomes with preexisting lysosomes[229, 230], while the transport between late endosomes and the TGN is controlled by rab9 GTPase[231].

Lysosomes are membrane-bound organelles responsible for intracellular digestion of substances derived from both inside and outside the cell. Within their membrane an acidic interior (pH ~ 5)[232] is maintained by the action of proton pumps in the membrane. The lysosomes contain a class of enzymes, hydrolases that catalyse hydrolysis of covalent bonds in proteins, lipids, carbohydrates and nucleic acids into simpler, low molecular mass compounds that can be reused. The enzyme content of lysosomes varies in different tissues according to the needs of the tissue. Lysosomes are not just involved in breaking down material arriving via endocytosis, but also degrade intracellular debris, such as defective organelles and macromolecules. Molecules destined to be degraded are tagged (most frequently by ubiquitination) and then taken up by lysosomes, or are first encapsulated within endosomes that fuse with lysosomes[233].

Sorting of ubiquitylated cargo proteins, such as transmembrane receptors into multivesicular bodies (MVBs) is catalysed by the ESCRT machinery[234]. ESCRT-0, ESCRT-I and ESCRT-II bind cargo proteins, ESCRT-III remodels the membrane, and the Vps4–Vta1 complex recycles ESCRTIII following vesicle scission. The physical and

functional link between ESCRT-II and ESCRT-III is pivotal but poorly understood[235]. The method of delivery of endocytosed macromolecules from late endosomes to lysosomes was for long a matter of dispute with vesicular transport, kissing and direct fusion hypotheses all being suggested[236, 237]. The first assumes vesicular transport between the two organelles –largely by analogy with the many membrane traffic steps of both the secretory and endocytic pathways in which such a mechanism operates. The second hypothesis is termed 'kiss and run' and proposes that late endosomes and lysosomes undergo continuous repeated transient fusion and fission[238]. Storrie and Desjardins proposed this hypothesis to explain data from experiments in which small soluble markers appeared to move more readily between lysosomes and endosomes/phagosomes than did larger soluble markers and from experiments in which soluble cargo was delivered to lysosomes faster than membrane proteins. The third hypothesis involves direct and complete fusion between late endosomes and lysosomes with subsequent recovery of lysosomes for re-use. Direct fusion of late endosomes with lysosomes produces a hybrid organelle, from which the lysosome has to be re-formed via a maturation process. The first evidence for the formation of a hybrid organelle came from cell-free studies of endosome–lysosome fusion in which an organelle with a density intermediate between that of endosomes and lysosomes was formed[239]. Vesicle-associated membrane protein 7 (VAMP7) is a key soluble N-ethylmaleimide-sensitive factor-attachment protein receptor (SNARE) for lysosome fusion with late endosomes and with the plasma membrane and its presence on the lysosome membrane may help to define the lysosome[240].

Products of lysosomal degradation are released from lysosomes into the cytosol and are re-used by the cell. Material that cannot be digested accumulates in vesicles called residual bodies, whose contents are removed from the cell by exocytosis[241].

Some residual bodies contain high concentrations of heterogenous pigmented substances, including polyunsaturated fatty acids and proteins, called lipofucsin (or 'age pigment')[242, 243]. Under particular conditions some lysosomal enzymes are secreted from the cell for the digestion of extracellular material in connective tissue[244].

The deficiencies in lysosomal degradation result in so-called 'lysosomal storage diseases'. What accumulates depends on which type of enzyme is deficient[245]. For example, the lack of some endoglycosidases leads to the accumulation of heparan sulfate-containing glycoproteins. As a consequence the undegraded molecules accumulate in tissues and cause damage, particularly in the brain where they produce loss of neurons and progressive dementia[246]. Most of these conditions are rare but extremely serious, and affected individuals often die in childhood.

1.6 O-GlcNAc MODIFICATION OF PROTEINS

Protein glycosylation is one of the most abundant posttranslational modifications (PTM) and plays a fundamental role in the control of biological systems[247]. *O*-GlcNAc glycosylation is a covalent modification of serine (Ser) and threonine (Thr) residues on intracellular proteins by ß-*N*-acetylglucosamine[248] that is found in all metazoans studied[249]. Unlike glycans added on the secretory pathway, O-GlcNAc modification (Figure 1.5) is not further elaborated into larger, more complex oligosaccharide structures. The vast majority of O-GlcNAc-modified proteins are nuclear, cytoplasmic or

mitochondrial proteins that are modified in response to cellular or environmental cues, such as growth factors, signalling molecules, glucose and other nutrient fluxes, and stress[249, 250]. This modification is ubiquitous, inducible, highly dynamic, and almost all O-GlcNAc modified proteins are also phosphorylated, suggesting interplay between the two modifications[249, 251, 252]. The cycling of O-GlcNAc on serine or threonine residues of target proteins is controlled by two highly conserved enzymes, O-GlcNAc transferase (OGT) and β-N-acetylglucosaminidase (OGA or O-GlcNAcase) (Figure 1.5). Whereas OGT catalyses the addition of O-GlcNAc to the hydroxyl group of serine or threonine residues of a target protein[253]; OGA catalyses the hydrolytic cleavage of O-GlcNAc from posttranslationally modified proteins[254]. The OGT enzyme is a soluble protein that is found in the cytosol, nucleus, and mitochondria rather than in the endoplasmic reticulum or Golgi[249].

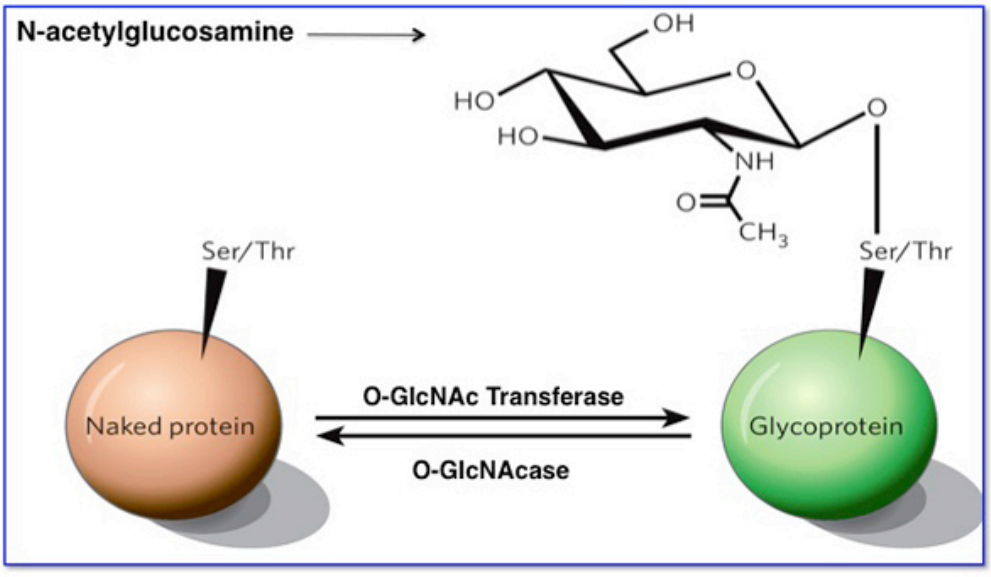

Figure 1.5. O-GlcNAc (ß-N-acetylglucosamine) protein modification.

(Ser = serine Thr= threonine).

OGT contains a C-terminal catalytic domain, and a long stretch of tetratricopeptide repeats that varies in number amongst species within its N-terminal domain. The tetratricopeptide (TPR) repeats serve as protein-protein interaction modules that appear to target OGT to accessory proteins and potential substrates[255, 256], such as OGT interacting protein (OIP106) and protein phosphatase-1[257]. The association between OGT and protein phosphatase-1 is particularly intriguing because it may provide a direct mechanism to couple O-GlcNAc to dephosphorylation of specific substrates. The catalytic activity of OGT is controlled by the concentration of its donor substrate, uridine-diphosphate-*N*-acetylglucosamine (UDP-GlcNAc). UDP-GlcNAc level is highly sensitive to flux in nutrients and energy, mainly through the hexosamine biosynthetic pathway (HBP)[258]. Increased flux through the HBP, either through increased glucose uptake or glucosamine treatment, increases the production of UDP-GlcNAc and stimulates O-GlcNAc modification of proteins[259]. Unlike acidic hexosaminidase in lysosomes, OGA or O-GlcNAcase has a neutral pH optimum and a nucleocytoplasmic distribution[254]. The catalytic domain of O-GlcNAcase is in the N-terminus[260], while the C-terminus has been reported *in vitro* to have a histone acetyl-transferase activity[261].

There exists evidence for the association of O-GlcNAc and neurodegenerative diseases, cancer and diabetes[249]. Thus, it has been proven to be essential for neuronal function and survival in mice[262] and a correlation between the variations of O-GlcNAc levels and Alzheimer's disease has been suggested[262, 263]. There is also considerable evidence linking increased levels of O-GlcNAc to the development of insulin resistance and diabetic complications, such as hyperleptinemia, cardiomyocyte apoptosis, hypertrophy and arteriosclerosis[249].

1.7. METABOLIC CELL LABELING: SIALIC ACID ENGINEERING

Strategies to introduce reactive functional groups into biomolecules include the metabolic incorporation of synthetic labels and chemical modification of native biomolecules.[264, 265] Metabolic oligosaccharide engineering (MOE) provides a method to install novel chemical functional groups into the glycocalyx of living cells. Metabolic oligosaccharide engineering was originally established for sialic acids, which represent another class of terminal components in large glycan structures that play important roles in cell-cell interactions.[266]

Sialic acids (neuraminic acid) refer to a family of over 50 naturally occurring nine carbon α-keto acid sugars attached to glycoproteins and glycosphingolipids. In humans the predominant sialic acid is *N*-acetylneuraminic acid (Figure 1.6(A)).[9] Sialic acid has the potential for additional substitutions with acetyl, methyl, sulphate, and phosphate groups at the hydroxyl groups on the 4-, 7-, 8-, and 9-carbons that gives it additional properties. The negative charge of sialic acid at physiological pH and its terminal position in glycans have given it a predominant role in determining the nature of glycan interactions involved in many essential functions of human physiology.

The biosynthesis of sialic acid (Figure 1.6(B)) begins in the cytosol with the formation of *N*-acetylmannosamine (ManNAc) from a relatively minor proportion of UDP-N-acetylglucosamine (UDP-GlcNAc), obtained form the extracellular environment[268] or derived from GlcNAc via the action of GlcNAc 2-epimerase.[269] In mammals, the ManNAc is then phosphorylated to give ManNAc-6- phosphate (ManNAc-6-P). The second step involves the condensation of either ManNAc or MacNAc-6-P with phosphoenolpyruvate (PEP) to give neuraminic acid or neuraminic acid-9-P, respectively.

A

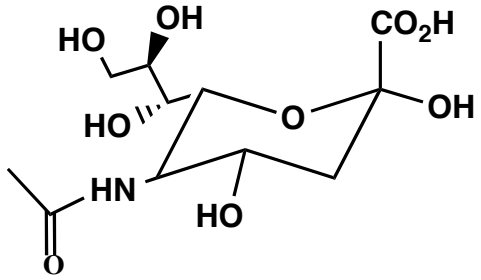

N-acetylneuraminic acid (Neu5Ac; sialic acid)

B

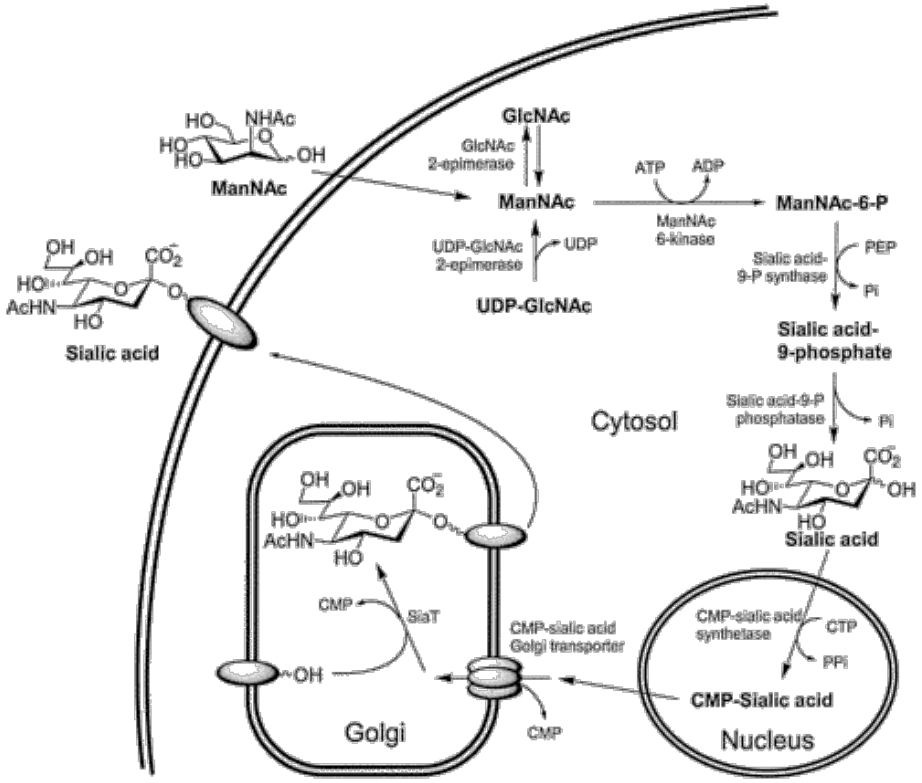

Figure 1.6 (A) Sialic acid structure. (B) Sialic acid biosynthetic pathway. (Jacobs CL *et al., Biochemistry* **2001**).

Scheme 1.1 Natural monosaccharidess and their non-natural analogs used in glycan biosynthetic pathways.

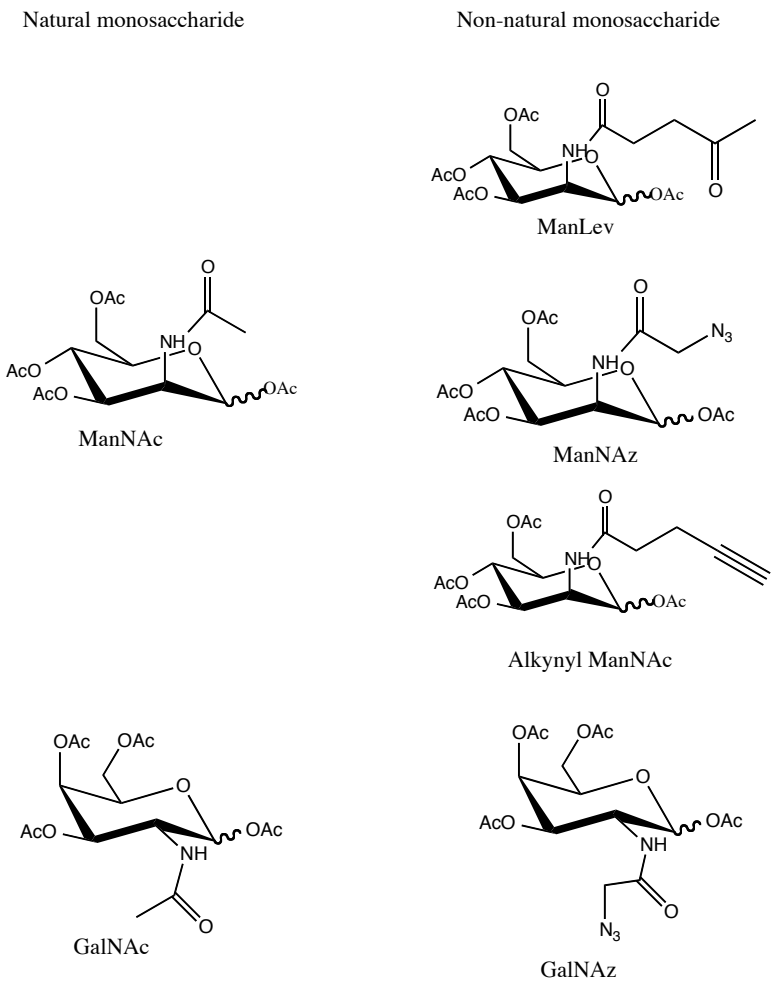

In mammals, neuraminic acid-9-P is then dephosphorylated to generate neuraminic acid. Finally, in the nucleus the activation of sialic acid with cytidine monophosphate (CMP-Sia) is generated with the use of cytosine triphosphate (CTP).[270] Once in the cytosol CMP-Sia is then transported to the Golgi lumen by a specific transporter (CMP-SiaTr) where it is used as donor substrate by more than twenty human sialyltransferases (STs) that incorporate it into the nonreducing end of glycans.[271-273]

The method to remodel the glycocalyx of living cells with nonnatural functional groups expressed in cell surface sialic acids was pioneered by the Reutter group, where analogs of N-acetyl-D-mannosamine (ManNAc, Scheme 1.1) intercept the sialic acid biosynthetic pathway (Figure 1.6) and are presented on the cells surface as the corresponding nonnatural forms of *N*-acetylneuraminic acid (sialic acid: Neu5Ac).[274] Of the different analogue precursors of sialic acid biosynthesis, ManNAc analogues (Scheme 1.1) are ideal candidates for metabolic labeling because ManNAc is the first pathway intermediate to be committed to sialic acid biosynthesis, assuring that imaging of the labeled ManNAc analog reflects glycan sialic acid expression. This method utilizes an easily accessible chemically modified *N*-acetylmannosamine (ManNAc) as demonstrated by Reutter and co-workers.[274, 275] Reutter and co-workers demonstrated that unnatural analogs of N-acetyl-D-mannosamine (ManNAc) that are modified at the N-acyl position can be used to probe terminal sialic acid residues within rodents.[274] This takes advantage of the permissivity of the sialic acid biosynthetic pathway for nonnatural metabolic intermediates.[274, 275]

The Bertozzi group extended this technique by including functional groups not normally found in the glycocalyx such as the ketone[276] and azide[277] into analog design. By hijacking a cell's biosynthetic machinery, a metabolic precursor functionalized with a bioorthogonal functional group termed a 'chemical reporter' is incorporated into target biomolecules including glycans.[276-279] The analogs bearing bioorthogonal functional groups termed a 'chemical reporter' then serve as chemical handles that reacts selectively with a complementary second group installed on a probe reagent.[276-278]

Modified *N*-acetylmannosamine (ManNAc) analogs that contain a functional group of interest such as alkyl, hydroxyl, thiols, and nonnatural functional groups such as ketones, and azides have been carried by the substrate through the biosynthesis of sialic acids, thus ultimately leading to the introduction of chemical modifications into complex biomolecules.

Metabolic labeling requires the uptake of nonnatural monosaccharide analogues into biosynthetic pathways, which allows for their incorporation into numerous glycans. Acetylation of the nonnatural monosaccharide analogues was necessary to increase uptake of the sugar by cells.[277, 280] Upon entering the cell's interior endogenous esterases hydrolyse the acetyl groups and release the intact modified mannose sugar. The synthetic analogs are processed by a series of enzymes to generate activated nucleotide-sugar analogs. The sugar analogs, bearing unique chemical functionality, are subsequently utilized in the biosynthesis of various cellular glycoconjugates. The non-natural sugars must compete with natural sugars and thus often incorporated substoichiometrically into glycoconjugates.

Because enzymes involved in the sialic acid biosynthetic pathway process nonnatural substrates that are similar in structure to the natural substrates, it is easier to encode small groups such as the azide, ketone, and alkyne groups, into biomolecules than it is to incorporate bulky groups. Aldehydes or ketones are a convenient functional group choice since there are few native aldehydes or ketones found at the cell surface. Metabolic labeling using *N*-levulinylmannosamine, ManLev (Scheme 1.1) can selectively introduce ketones into sialic acid containing glycoproteins.[276] The aldehyde or ketone is then selectively ligated using hydrazine or aminooxy compounds with aniline catalysis as a way to accelerate the labeling reaction in aqueous solution.[281-283]

Azides and alkynes are remarkably stable within biological systems, enabling facile introduction of these reactive groups into a wide range of biomolecules. The use of azides and alkynes as reporting moieties is exceptionally appealing, due to their accessibility, small size, inertness, high chemical stability, high selectivity, and absence in biological media.[277, 284] Multiple startegies have been reported for incorporation of azides into biomolecules, providing potential targets for azide-specific, bioorthogonal labeling. For example, azides have beeen incorporated into glycans, lipids, proteins, and nucleic acids by using metabolic machineries of cells. For incorporation into carbohydrates of glycoconjugates, cells are supplied with azide-functionalized carbohydrates precursors.[277] The azide component is introduced through the metabolic incorporation of azide-containing biosynthetic precursor, peracetylated *N*-azidoacetylmannosamine, Ac_4ManNAz (Scheme 1.1).

In the cytosol, Ac_4ManNAz is enzymatically deacetylated by nonspecific esterases and then metabolically converted to the corresponding *N*-azidoacetyl sialic acid (SiaNAz), which is subsequently incorporated into sialoglycoconjugates.[277, 285]

The aldehyde or ketone is then selectively ligated using hydrazine or aminooxy compounds with aniline catalysis as a way to accelerate the labeling reaction in aqueous solution.[281-283] Azides and alkynes are remarkably stable within biological systems, enabling facile introduction of these reactive groups into a wide range of biomolecules. The use of azides and alkynes as reporting moieties is exceptionally appealing, due to their accessibility, small size, inertness, high chemical stability, high selectivity, and absence in biological media.[277, 284]

Multiple startegies have been reported for incorporation of azides into biomolecules, providing potential targets for azide-specific, bioorthogonal labeling. For example, azides have beeen incorporated into glycans, lipids, proteins, and nucleic acids by using metabolic machineries of cells. For incorporation into carbohydrates of glycoconjugates, cells are supplied with azide-functionalized carbohydrates precursors.[277] The azide component is introduced through the metabolic incorporation of azide-containing biosynthetic precursor, peracetylated *N*-azidoacetylmannosamine, Ac_4ManNAz (Scheme 1.1). In the cytosol, Ac_4ManNAz is enzymatically deacetylated by nonspecific esterases and then metabolically converted to the corresponding *N*-azidoacetyl sialic acid (SiaNAz), which is subsequently incorporated into sialoglycoconjugates.[277, 285]

Wong and co-workers used alkynyl ManNAc derivative, peracetylated *N*-(4-pentynoyl)-mannosamine (Ac_4ManNAl) (Scheme 1.1) for metabolic labeling of cultured cells and CuAAC-mediated reaction with an azide-functionalized probe for capture of sialylated glycoproteins.[286, 287] Chang PV et al.[288] metabolically labeled sialic acids in cultured cells and mice with peracetylated *N*-(4-pentynoyl)-mannosamine (Ac_4ManNAl) with greater efficiency than with Ac_4ManNAz. MOE was expanded to GalNAc analogs, GalNAz (Scheme 1.1) which were incorporated into the *O*-glycan chains of extracellular glycoproteins, and GlcNAc analogs, GlcNAz to modifying *O*-linked *N*-acetylglucosamine on intracellular proteins.[289] An azide analog of GalNAc, *N*-azidoacetylgalactosamine (GalNAz), is incorporated into O-linked glycoproteins using the GalNAc salvage pathway (Figure 1.7). The GalNAz-containing molecules are then covalently tagged with imaging probes or epitope tags, either *ex vivo* or *in vivo*, using an azide-specific reaction.[290] Unfortunately, site-specific metabolic labeling of glycans is hindered by multiple factors.

First, nucleotide-sugar analogs are necessarily in direct competition with the cell's endogenous pool of donor sugar, often leading to poor levels of metabolic incorporation of the synthetic analog.[291] The efficiency of sialic acid biosynthesis is very sensitive to the N-acyl structure of the nonnatural ManNAc analogs.[292, 293]

Analogs with long or branched *N*-acyl chains are poor substrates for the biosynthetic enzymes, while those containing short linear chains are better tolerated.[293] Many eukaryotes possess epimerase activity that can interconvert nucleotide-sugar stereochemistries and thereby alter the final metabolic destination of a given monosaccharide.[270, 294]

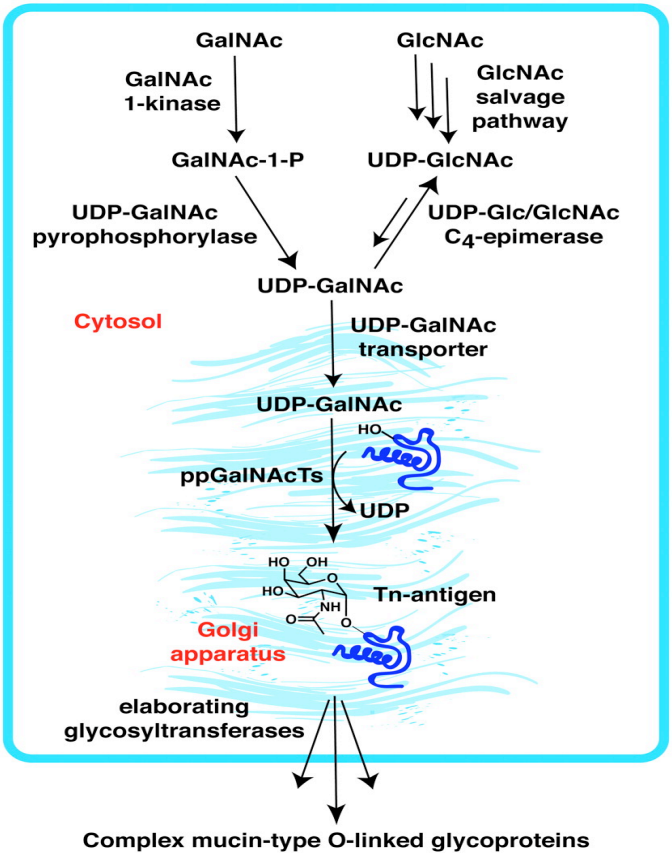

Figure 1.7 Biosynthesis of mucin-type O-linked glycoproteins. UDP-GalNAc is produced endogenously from UDP-GlcNAc, which can be generated from GlcNAc via a salvage pathway. Alternatively, UDP-GalNAc can be generated from GalNAc by the action of GalNAc 1-kinase and UDP-GalNAc pyrophosphorylase enzymes of the salvage pathway. Transport of UDP-GalNAc into the Golgi lumen provides the nucleotide sugar donor for the ppGalNAcTs, which modify Ser or Thr residues with α-GalNAc. Further elaboration of this "Tn-antigen" (α-GalNAc-Thr/Ser) by downstream glycosyltransferases generates more complex mucin-type O-linked glycans. (Hang H C et al. *PNAS* **2003**).

Finally, glycan assembly is not genetically encoded and is therefore inherently prone to michroheterogeneity, targeting analogs to specific positions within a defined class of glycoconjugate is unattenable.

Ketones and azides presented completely new functionalities on cell surfaces, which allowed subsequent chemoselective conjugation reactions. Ketones and aldehydes could be selectively reacted using the hydrazone or oxime ligation with hydrazine or aminooxy compounds, respectively. Several chemical reactions that utilize azides included the Staudinger ligation, CuAAC and strain-promoted [3+2] cycloaddition for the attachment of various biochemical probes into living organisms. A well-known chemical method for introducing the aldehyde functional group in sialic acids is by chemical modification. This strategy for labeling of glycoproteins makes use of sodium periodate to oxidize the glycerol side chain of sialic acid to an aldehyde.[107] This method, periodate oxidation and aniline-catalyzed ligation (PAL) of the aldehyde group on sialic acid on glycoconjugates on cell surfaces using aminooxy-biotin conjugates, and detection by fluorescently labeled streptavidin[283] presents an attractive alternative for the metabolic labeling of sialic acids.

1.8. BIOORTHOGONAL CHEMICAL REACTIONS

Bioorthogonal chemistry relies on coupling exogenous moieties of non-biological origin under mild physiological conditions. To perform a specific chemical reaction in living cells, both reactants need to be bioorthogonal, meaning that neither reacts with endogenous components of the cell to an appreciable degree.[296] The development of bioorthogonal ligation reactions has made it possible to chemoselectively label

biomolecules in living systems, including proteins, nucleic acids, carbohydrates, and lipids.[278, 297] Chemoselective ligation chemistries are important tools for the detection, analysis, and perturbation of proteins, glycoconjugates in order to elucidate structure and function. The main challenge is in the development of a chemoselective ligation reaction that can selectively address a 'bioorthogonal' functional group that is present in the biomolecule of interest while leaving other functional groups of the biomolecule unchanged. The crucial requirement is for ligation reactions that can be conducted in a biological environment (water, high salt concentrations, reducing conditions) to form a stable covalent linkage between the two functional groups with fast kinetics, so that product is formed at a reasonable rate with reactant concentration as required in many biological labeling experiments. In practice, reactions with a second-order rate constants smaller than 10^{-4} $M^{-1}s^{-1}$ will be too slow for practical use when reagents are held at the low concentrations necessary to label biomolecules with minimal background.[298] Because of these unique features, bioorthogonal chemistry has been successfully employed to label chemically modified sugars in glycoproteins, in protein functional studies to visualize protein expression, track protein localization, measure protein activity, identify protein interaction partners, and study protein turnover in living systems. Two sequential steps are typically involved during the implementation of bioorthogonal chemistry: (1) incorporation of a bioorthogonal reporter into the biomolecule of interest by either metabolic labeling or engineered biosynthetic pathway; (2) bioorthogonal reaction between the bioorthogonal reporter and the complementary external chemical probe. A number of bioorthogonal reactions have been developed to show excellent biocompatibility and selectivity in living systems.

1.8.1. CONDENSATION REACTION OF KETONES AND ALDEHYDES

Oxime- and hydrazone-based reactions have found wide application in the conjugation of biomolecules on account of the absence of aldehydes or ketone groups in proteins and their orthogonal reactivity with aminooxy or hydrazide derivatives to give stable oximes or hydrazones. Aldehydes and ketones have a small size and are particularly useful electrophiles, as they have a unique reactivity among the exclusively nucleophilic native amino acid side-chains at neutral pH. Aldehydes and ketones react selectively with aminooxy groups to form oximes (Scheme 1.2(A)) and with hydrazides to form *N*-acyl hydrazones (Scheme 1.2(B)). It should be noted that, although water is produced in these condensation reactions, the products are of sufficient thermodynamic stability under typical reaction conditions (slightly acidic pH) that the reactions are favorable even in aqueous solvents.[299, 300] Under the acidic conditions (pH 5 – 6), the carbonyl group reacts with a primary amine to form a reversible Schiff base where equilibrium typically favors the free carbonyl form. In the presence of hydroxyamines and hydrazines (or hydrazides), the equilibrium favors the imine forms, giving rise to the stable oxime and hydrazone adducts, respectively (Scheme1.2).

Chemoselective ligation reaction between a ketone and an aminooxy or hydrazide group was used to label cell surface glycoconjugates.[276] Ketones were introduced on Jurkat cells through sialic acid biosynthesis pathway using *N*-levulinylmannosamine (ManLev), a ketone-bearing analog of the native sugar *N*-acetylmannosamine (ManNAc), which was converted to the corresponding keto-sialic acid residues on cell surface glycoconjugates.

Scheme 1.2 Imine-based conjugation reactions. (A) Oxime ligation between an aminooxy group and aldehyde/ketone to generate a stable oxime linkage. (B). Hydrazone ligation between a hydrazide and an aldehyde/ketone to generate a reversible hydrazone linkage.

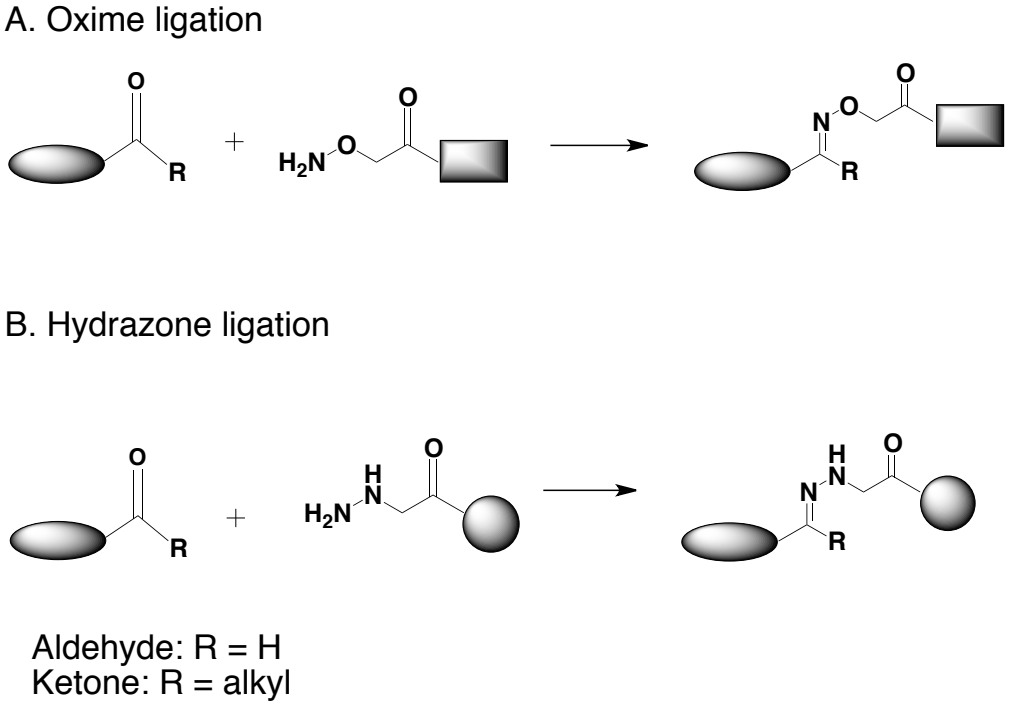

The ketone on cell surface was then selectively ligated with a biotin-aminooxy or hydrazide reagents (probes) to form the stable covalent adducts. Oxime or hydrazone ligations of aminooxy or hydrazide reagents to aldehydes or ketones are convenient but require acidic conditions (pH 5 - 6) and high reagent concentrations (2 - 5 mM) to compensate for the slow reaction rates.[301] While reactions between aldehydes and ketones with aminooxy or hydrazides are generally slow, they can be significantly accelerated by addition of the nucleophilic catalyst aniline.[281, 302] This has resulted in a number of applications ranging from the site-specific labeling of sialylated proteins on cell

surfaces[283] to the fluorescent labeling of bacteria cells.[303] The oxime ligation product is more stable than the hydrazone ligation product.[304] Ketone ligation reactions have limited intracellular use owing to competition with endogenous keto-metabolites.

1.8.2. REACTIONS OF AZIDES

The azide has a major advantage over the aldehyde or ketone in that its reactivity is unique in a cellular context owing to its abiotic nature. Ketones abound inside cells in the form of metabolites such as pyruvate and oxaloacetate, and will interfere with the ketone-based condensation reaction. Azide moieties have excellent properties, such as stability against hydrolysis or dimerization. In addition, the azide group is small in size, and easy to introduce into biomolecules or probe molecules without dramatically changing their functional properties. The azide has been used as a chemical reporter of protein biosynthesis, protein and lipid posttranslational modifications, nucleic acid biosynthesis, and enzyme activity.[264] Azides undergo a number of chemical reactions that involve the loss of nitrogen, a good driving force for a reaction proceeding without catalysis. The first investigated reaction type in this respect is the Staudinger ligation (Scheme 1.3), which was successfully applied to covalently label carbohydrates on cell surfaces.[277]

The azide can also participate in cycloaddition reactions through the Huisgen 1,3-dipolar cycloaddition.[305] Cycloaddition reactions are attractive in this context, since they usually involve weakly polarized reactants, minimizing undesired side reactions with biomolecules. The biocompatibility of these reactions provides efficient tools for the metabolic labeling of cell-surface glycans, lipids, DNA and RNA within their native

environment and would allow the study of the biological processes in which these biomolecules are involved.[264] Three bioorthogonal reactions have been reported for labeling azide-tagged biomolecules viz Staudinger ligation, copper (I)-catalyzed and, strain-promoted azide-alkyne cycloaddition reactions. Azides are incorporated into carbohydrates of glycoconjugates by supplying cells with azide-functionalized carbohydrate precursors[277] incorporated into proteins by supplying cells or organisms with azide-functionalized methionine[306-309] and incorporated into lipids.[310-312]

Scheme 1.3 (A) Classical Staudinger reaction between a phosphine and an azide. (B) Staudinger ligation between an activated phosphine and an azide, yielding a native amide bond.

A. Staudinger reaction

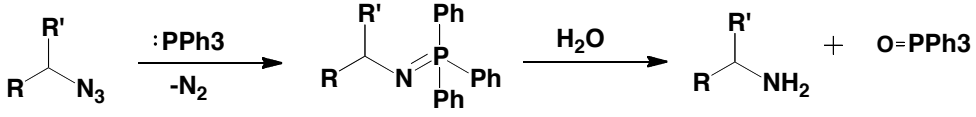

B. Staudinger ligation

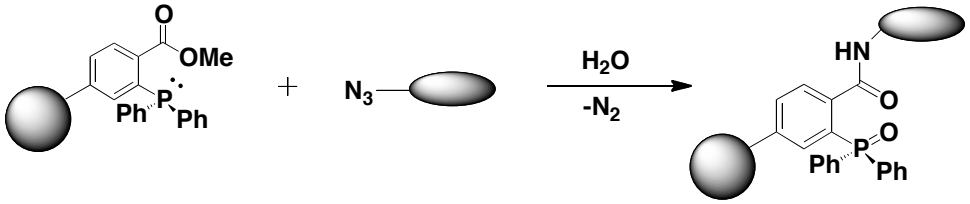

1.8.2.1. STAUDINGER LIGATION

Staudinger reaction, the reduction of azides with phosphines and water to primary amines was reported by Herman Staudinger in 1919.[313] Both phosphines and azides are abiotic and essentially unreactive towards biomolecules inside or on the surfaces of cells, which meets many of the criteria required of a chemoselective ligation in a cellular environment. The Staudinger reduction mechanism proceeds through nucleophilic attack of the phosphine on the azide, followed by loss of nitrogen to yield a reactive aza-ylide species. In aqueous environments, the aza-ylide is rapidly hydrolyzed to produce a phosphine oxide and a primary amine. (Sheme 1.3(A)). The phosphine and azide react with each other rapidly in water at room temperature in high yields. The limitation of the Staudinger reaction is that the intermediate aza-ylide is not stable in water.

Bertozzi and co-workers transformed the Staudinger reaction by redesigning a triphenylphosphine with an intracellular electrophilic trap, such as a methyl ester, within the phosphine structure that could capture the nucleophilic aza-ylide by intramolecular cyclization to form an intermediate, which upon hydrolysis yielded a stable amide-linked product (Scheme 1.3(B)).[277] This led to the reaction known as the Staudinger ligation because of its exquisite ability in covalently linking two molecules together.[314] Though highly specific for the azide group, this reaction suffers from slow kinetics (typical second order rate constants of 2.0×10^{-3} $M^{-1}s^{-1}$),[315, 316] which required the use of high concentration of the phosphine reagent. This resulted in high background signals due to difficulty to wash away excess probe reagent.[317] The phosphine reagents are susceptible to oxidation by molecular oxygen or by metabolic enzymes, which limits their shelf life, and they cannot be used to monitor rapid biological processes *in vivo* because of their

slow reaction kinetics.[318, 319] Staudinger ligation has been widely utilized in various biological systems, for example it has been used in the fluorescent staining of cell-surface azido sugar-labeled glycoconjugates on cultured cells,[277, 317, 320, 321] and in live mice.[290] Other applications include the enrichment of glycoprotein subtypes in the cell lysates,[289, 322] the site-specific fluorescent labeling of proteins,[323] the addition of new functionality to recombinant proteins,[324] the live-cell imaging using a FRET-based fluorogenic phosphine,[316] the tagging of azide-labeled proteins in bacteria,[306, 325] and used for glycoproteomics studies.[326] The Staudinger ligation is chemically orthogonal to ketone ligations.

1.8.2.2. COPPER (I)-CATALYZED AZIDE-ALKYNE CYCLOADDITION REACTION (CLICK CHEMISTRY)

Alkyne and azide groups are very small in size, highly energetic, have a particularly narrow distribution of reactivity and are not normally expressed in biological systems. The 1,2,3-triazole ring system was first formed by the reaction of azides with terminal alkynes in a 1,3-dipolar cycloaddition first described by Huisgen.[305] The classic Huisgen cycloaddition required high temperatures and pressures that are far beyond the limits of biological systems. Another drawback of this approach is the parallel formation of the 1,4- and 1,5-regioisomers. The azide-alkyne cycloaddition using unactivated alkynes had very sluggish kinetics with high activation energy for the cycloaddition reaction.[327] Though the starting materials are easily prepared, the 1,2,3-triazole products are exceptionally stable, and the reaction occurs readily in both organic and aqueous solvents, there is still the need to lower the activation barrier for the reaction.

In 2002, the Meldal group[328] and the Sharpless group[329] reported the Copper (I)-catalyzed azide-alkyne cycloaddition (CuAAC) reaction which takes place with high regioselectivity giving the 1,4-disubstituted 1,2,3-triazole exclusively (Scheme 1.4(A)). They demonstrated that with the addition of Cu (I) catalyst the reaction could proceed at low temperature with high rates, efficiency, and regiospecificity. In 2001, Sharpless and co-workers introduced the term 'click chemistry' to define a set of nearly perfect reactions that resemble natural biochemical ligations.[330] The azide-alkyne cycloaddition is selective, efficient and broad in scope, a paradigmatic example of a 'click reaction.'[330] The copper (I) catalyst used in 'click reactions' is known to lower the activation barrier by 11 kcal/mol, which is sufficient to rapidly drive the reaction forward with high selectivity.[331, 332]

'Click chemistry' reactions are orthogonal, regioselective, and highly efficient and the reactions can be performed in aqueous solutions at room temperature or physiological temperature, and display outstanding functional group tolerance, making them compelling reactions for bioconjugation. However the need for copper catalyst makes the CuAAC ideal for many applications in inorganic and nanomaterial science but nonideal for biological applications because of the toxic effect of Cu (I) to both bacteria cells[307] and mammalian cells at low concentrations.[333] Because of its fast reaction kinetics, the CuAAC has been validated by numerous applications in almost all areas of chemistry, such as drug delivery, bioconjugation, polymer and material science, and supramolecular chemistry.

Scheme 1.4 Variations on 1,3-dipolar cycloaddition reactions. (A) Un-catalyzed azide-alkyne cycloaddition reaction. (B) Cu (I) catalyzed azide-alkyne cycloaddition reaction. (C) Strain-promoted azide-alkyne cycloaddition reaction

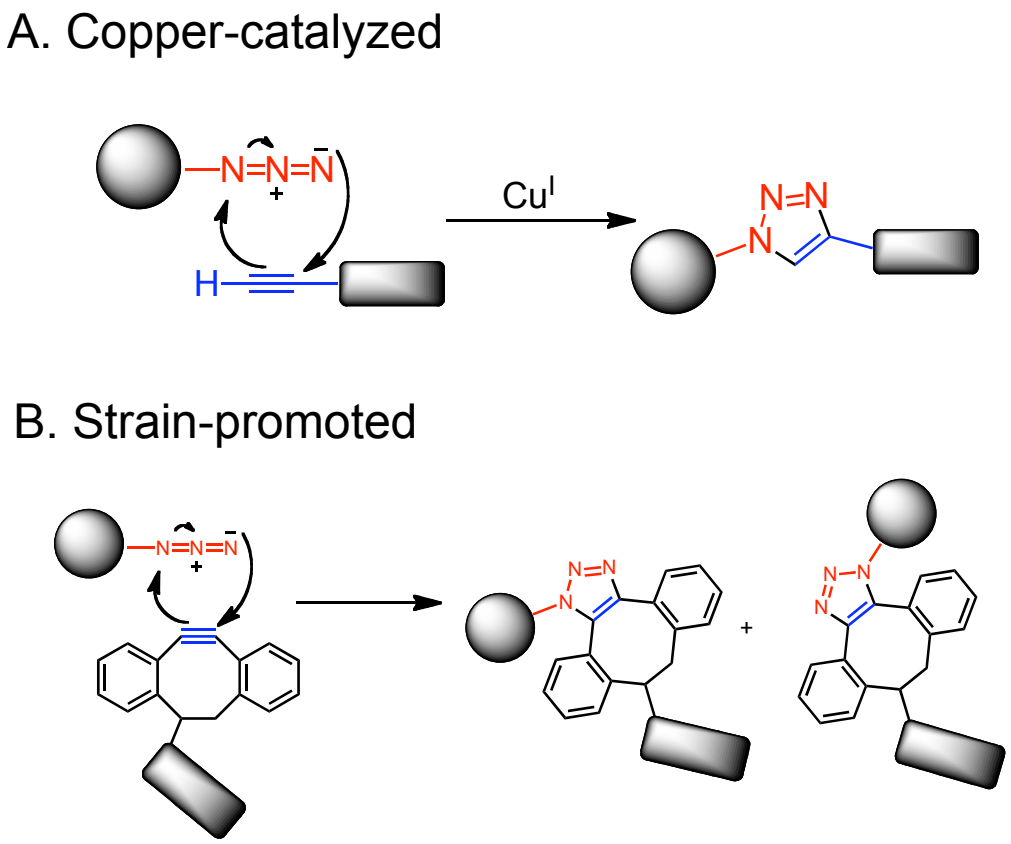

The CuAAC reaction has been applied for special purposes, such as in the preparation of peptide nanotubes,[334] dendrimers,[335, 336] polymers,[49] di, tri-and polyvalent neoglycoconjugates,[338] water soluble calixaranes,[339] fluorescent dyes,[340] labeling of proteins,[308] glycans,[341, 342] lipids,[311-312, 343] RNA,[344] labeling of azido-modified bacterial surface proteins[345] and the activity-based proteome profiling.[283, 346]

With ligands, the CuAAC has been used for live cell imaging of azide and terminal alkyne chemical reporter group.[347-351] The water soluble ligands tris-(hydroxypropyltriazolylmethyl)amine (THPTA),[352] bis[(tertbutyltriazoyl)methyl]-[(2-carboxymethyltriazoyl)methyl]-amine (BTTAA)[349, 351] or bis(l-histidine)[350] for Cu (I) accelerate the cycloaddition reaction and act as sacrificial reductants, helping to protect cells and biomolecules from reactive oxygen species (ROS).[352] Sawa M et al.[342] developed a click-activated fluorogenic labeling technique for imaging of fucosylated glycoconjugates at the cell surface and inside the cell.

1.8.2.3. STRAIN-PROMOTED AZIDE-ALKYNE CYCLOADDITION REACTION (SPAAC)

Different approaches have been developed to circumvent the issue of copper toxicity, and at the same time increase the reactivity of the alkyne group to allow metal-free azide-alkyne cycloadditions under mild conditions.[353] Bertozzi and co-workers[315, 354-355] developed cyclooctyne derivatives to react with azides in a strain-promoted azide-alkyne [3+2] cycloaddition (SPAAC) reaction (Scheme 1.4(B)), from initial work by Blomquist and Liu[356] and later supported by Wittig and Krebs.[357] Wittig and Krebs noted that the strained cyclic alkyne cyclooctyne (OCT), the smallest stable cyclootyne reacts violently when combined neat with phenylazide, forming a triazole product by 1,3-dipolar cycloaddition.[357] The high strain (≈18 kcal/mol) of the ring, primarily as a result of the distorted bond angles surrounding their sp-hybridized carbon atoms,[358, 359] is released in the transition state of the cycloaddition reaction. As a result cyclooctyne reacts selectively with azides to form regioisomeric mixtures of 1,2,3-triazoles at ambient

temperatures and pressures without the need for metal catalysis and with no apparent cytotoxicity.[354] The 1,2,3-triazole product is chemically stable under hydrolytic as well as reductive and oxidative conditions. Because structurally modified cyclooctynes react with azides at rates approaching that of the metal-catalyzed reaction, these cycloaddition reactions were referred to as 'Cu-free click chemistry.'

Thus, for bioorthogonal chemistry application in live cells or living systems, the strain-promoted azide-alkyne cycloaddition (SPAAC) referred to as 'Cu-free click reaction' was introduced. This was based on the design of strain cyclooctyne reagents that react rapidly and selectively with azides on biomolecules. The strain-promoted azide-alkyne cycloaddition takes advantage of ground-state destabilization (strain) to accelerate triazole formation under ambient or physiological conditions.[360] Bioorthogonal reactions have enabled the high precision chemical modification of biomolecules *in vitro*, as well as real-time visualization of molecules and processes in cells and live organisms.[264]

1.9. DEVELOPMENT OF STRAINED CYCLOALKYNES FOR COPPER-FREE CLICK REACTIONS

The metal-free SPAAC process is rapidly evolving in myriad directions, increasing demand for cycloalkyne tools. The stabilities of the clycoalkynes are strongly influenced by ring size, with cycloheptynes being unisolable at room temperature because of rapid oligomerization, and cyclononynes being several orders of magnitude less reactive with azides than cyclooctynes.[361] Cyclooctyne offers 'explosive' reactivity towards azides.[356, 357]

Thus, design synthesis of clycoalkynes that are stable to diverse chemical environments and yet spontaneously reactive towards azides was an important challenge. The high reactivity of clycoalkyne is attributed to ~ 18 kcal mol^{-1} of ring strain resulting from deformation of the bond angles of alkyne from 180^{o} to 158^{o} .[362]

The first generation of cyclooctyne was based on the smallest stable cyclooctyne (OCT, Scheme 1.5) platform. OCT had second order rate constant of 2.4 x 10^{-3} $M^{-1}s^{-1}$ for benzyl azide, which was not faster than the Staudinger ligation and had limited solubility.[354] Despite its slower kinetics, OCT-biotin was used to label azide labeled-biomolecules both *in vitro*, within cell lysates and on live cell surfaces without observable cytotoxicity.[354] OCT derivatives have also been used to selectively label lipids in living cells,[363] site-specific labeling of cell surface proteins.[364]

Further optimization of this reaction led to the development of numerous cyclooctyne analogs based on the OCT platform with accelerated reaction rates with azides because of two major rate-enhancing modifications. The cyclooctyne compounds have been designed bearing fluorine substituents, fused rings and insertion of heteroatoms in the cyclooctyne ring with the goal of increasing the cycloaddition kinetics as well as optimizing solubility, and stability properties. The rationale is to develop reagents with faster reaction kinetics, which is accelerating SPAAC to rate levels that are comparable to its copper-mediated version. Fast-reacting cyclooctyne reagents would allow labeling of biological processes in real-time monitoring experiments. The reactivity of cyclooctynes towards azides was enhanced by two major structural modifications.

The first approach exploited the addition of fluorine atoms known as the fluorine effect. The second generation monofluorinated cyclooctyne, MOFO (Scheme 1.5), with an electron-withdrawing fluorine atom at the propargylic position showed some rate enhancement with a second-order rate constant of 4.3 x 10^{-3} $M^{-1}s^{-1}$ and was used to label azides in cell lysates and on cell surfaces.[365] To accelerate the cycloaddition reactions further a third generation difluorinated cyclooctyne, DIFO (Scheme 1.5) derivative of cyclooctyne was generated. By introducing electron withdrawing fluorine atoms adjacent to the triple bond (propargylic position) in DIFO resulted in increased second order rate constant of 7.6 x 10^{-2} $M^{-1}s^{-1}$.[366] The electron activation was shown to decrease the lowest unoccupied molecular orbital level (LUMO) energy of the alkyne thereby increasing its interaction energy with the highest occupied molecular orbital (HOMO) of the azide.[367] Because of this improved kinetics, the DIFO reagent was used in the dynamic *in vivo* imaging of cells[315] and the developing zebrafish.[355] The poor-yielding synthetic accessibility of DIFO has limited its wide applicability despite its good reaction kinetics. The first generation DIFO was synthesiszed in 12 steps with an overall yield of ~ 1%.[315] The final step of the squence, elimination of a vinyl triflate to form the cyclooctyne, suffered from significant decomposition and low yield. An improvement in the synthesis was carried out for a second generation DIFO that was synthesized in a total of 8 steps with an overall yield of 28 %.[366]

Boons and co-workers exploited the strain effect and prepared an active cyclooctyne, dibenzocyclooctynol (DIBO) (Scheme 1.5) with excellent reaction rates with azides.[368-370] Introducing two benzene rings fused to the cyclooctyne increased the ring strain that resulted in the efficiency of these strained cyclooctynes in click reactions.

Scheme 1.5. Ring-strained cyclooctynes for bioorthogonal cycloaddition reactions with azides.

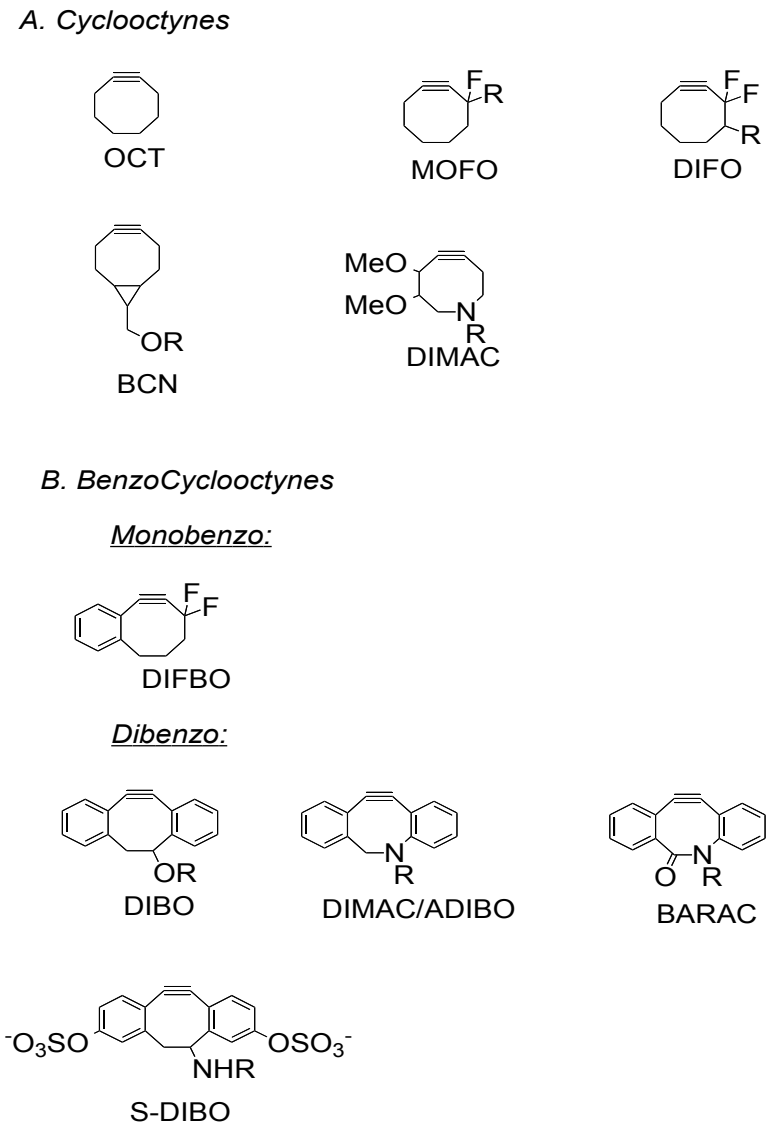

DIBO had an increased second-order rate constant of 5.7 x 10^{-2} $M^{-1}s^{-1}$ with benzyl azide. Goddard and co-workers proposed that the fused aryl rings of DIBO promoted the cycloaddition reaction by augmenting the ring strain in the cyclooctyne.[371] These alkyne-based reagents have been used to visualize the metabolically labelled azide-containing glycoconjugates on the surfaces of living cells.[368-370, 372] Compared to the DIFO reagents, the major advantage of the DIBO-based reagents is their synthetic accessibility and the possibility of further rate enhancement through substituent effect. In addition DIBO had an excellent shelf life and was stable against nucleophiles.

The addition of sp^2-like centers within the cycooctyne ring was sought as another means to increase strain and hence increase the reaction kinetics. The resulting analogs dibenzoazacyclooctyne (DIBAC) / azadibenzocyclooctyne (ADIBO) (Scheme 1.5) with an exocyclic amide had a rate constant of 3.1 x 10^{-1} $M^{-1}s^{-1}$ with benzyl azide.[373, 374] The synthesis of DIBAC was accomplished in 9 steps with > 40% overall yield. Further enhancement was achieved through the addition of an amide bond to the DIBO scaffold to form biarylazacyclooctynone (BARAC) (Scheme 1.5) with second order rate constant of 9.6 x 10^{-1} $M^{-1}s^{-1}$.[375] BARAC reacts rapidly with azides, and is quite stable. Van Delft and co-workers demonstrated that bicyclononyne (BCN) (Scheme 1.5) has second rate constant of $0.1M^{-1}s^{-1}$ which is similar to the reactivity of DIBAC/ADIBO due to the combination of strain effects from the fused cyclopropyl group and reduced steric hindrance surrounding the alkyne.[376] BCN was shown to be the most synthetically accessible cyclooctyne derivative, synthesized in 4 steps with an over all yield of ~ 50% combined yield of *endo* and *exo* diastereomers.[376]

The synthesis of highly reactive cyclooctynes such as difluorobenzocyclooctyne (DIFBO) (Scheme 1.5) unfortunately resulted in unwanted side reactions from the modifications.[361] DIFBO combines features of fused aryl and gem-difluoro modifications. DIFBO has fast reaction rates and the electronic effects of fluorination was reported to augment the ring strain created by the fused aryl ring leading to enhanced reactivity, but also makes DIFBO unstable and prone to decomposition via trimerization.[361] The very reactive DIFBO could be stabilized in an inclusion complex with ß-cyclodextrin and used as a reagent for rapid cycloaddition with azides. The combination of fluorination and a fused ring in DIFBO enhances its reactivity with second-order rate constant of 2.2×10^{-1} $M^{-1}s^{-1}$.[361]

Most of the cyclooctynes employed for Cu-free click chemistry comprise hydrocarbon scaffolds that limit their solubility in aqueous solutions and compromise bioavailability. As a result they are involve in hydrophobic interaction with proteins. Thus, there is the need to design cyclooctynes derivatives with enhanced water solubility. The compound 6,7-dimethoxyazacyclooct-4-yne (DIMAC) (Scheme 1.5) was synthesized with a nitrogen atom within the strained ring system that would interrupt the hydrophobic surface area.[377] The presence of two methoxy groups on the molecule was shown to enhance its water solubility and still had good reaction kinetics with azide-labed proteins and cells. DIMAC is not widely used due to its lengthy synthesis (11 steps, 5% overall yield)[377]. Recently, a highly polar sulfated dibenzocyclooctynylamide (S-DIBO) was synthesized (Scheme 1.5).[370] The molecule had superior polarity and water solubility and had reduced nonspecific binding in azide-labeled cell surface glycoconjugates. Accurate rate measurements of the reaction of benzyl azide with various

dibenzocyclooctyne and SDIBO demonstrated that the aromatic substitution and the presence of the amide function had only a marginal impact on the rate constants. SDIBO was found to be stable against nucleophiles and showed excellent reactivity towards azides with similar reactivity to DIBO.[370] Fluorescence-labeled or biotinylated derivatives of these cyclooctynes have enabled the visualization, distribution of azido-glycoconjugates in cultured cells[315, 354; 361, 365-366; 368-370, 372, 375, 377-378] and in living animals[278-279, 379] live zebrafish,[355] labeling and detection of azido-containing *Candida antartica* lipase B (CAL-B)[373]; to label various biomolecules in cells[364, 380-382]; monitor phospholipid dynamics in live cells,[363] fluorescent staining of the capsid protein of cowpea chlorotic mottle virus and the ligation of azido-containing cell surface glycans on MV3-melanoma cells,[376] labeling of BSA,[383] synthesis of RNA conjugates through solid phase synthesis[384]. Cyclooctynes have been applied in material sciences, for example in microarrays,[374] hydrogels,[385] quantum dots,[386] polymers,[387] and dendrimers.[388] In combination with genetic encoding, bioorthogonal chemistry provides a powerful covalent strategy to probe biomolecular dynamics and function in living systems.

1.10 REFERENCES

(1) Apweiler R, Hermjakob H, Sharon, N. *Biochim. Biophys. Acta*, **1999**, 1473: 4–8.

(2) Imperiali, B. and O'Connor, S. E. *Curr. Opin. Chem. Biol.* **1999**, 3, 643–649.

(3) Helenius A, and Aebi, M. *Science* **2001,** 291, 2364–2369.

(4) Petrescu, A. J, Wormald, M. R, Dwek, R. A. *Curr. Opin. Struct. Biol.* **2006**, 16, 600–607.

(5) Sola R. J, Rodriguez-Martinez, J. A, and Griebenow K. *Cell. Mol. Life Sci.* **2007**, 64: 2133 – 2152

(6) Dwek, R. A. *Chem. Rev.* **1996**, 96, 683–720.

(7) Dove A. *Nat. Biotechnol.* **2001**,19, 913 - 917

(8) Fazio F, Bryan M. C, Blixt O, Paulson J. C, Wong C. H. *J. Am. Chem. Soc.* **2002**, 124:14397-14402

(9) Kiessling, L. L. and Cairo, C. W. *Nature Biotech.* **2002**, 20, 234-235.

(10) Tirrell D. A. *Nature* **2004**; 430 (7002):837.

(11) Varki, A. *Glycobiology* **1993**, 3, 97–130.

(12) Haltiwanger, R. S, Lowe, J. B. *Annu. Rev. Biochem.* **2004**, 73, 491– 537.

(13) Ohtsubo K. and Marth J. D. *Cell* **2006**, 126: 855-867.

(14) Taniguchi N, Miyoshi E, Jianguo G, Honke K, Matsumoto A. *Curr Opin Struct Biol.* **2006**, 16:561–566.

(15) Varki A. *Nature* **2007**, 446: 1023-1029.

(16) Schauer R. *Curr. Opin. Struct. Biol.* **2009**, 19(5):507-14.

(17) Ferrero-Garcia M. A, Trombetta S. E, Sanchez D. O, Reglero A, Frasch A. C, Parodi A. J. *Eur. J Biochem.* 1993, 213:765–771.

(18) Tomlinson S, Pontes de Carvalho L. C, Vandekerckhove F, Nussenzweig V. *J Immunol.* **1994**, 153:3141–3147.

(19) Pereira-Chioccola, V.L., Acosta-Serrano, A., Correia De Almeida, I., Ferguson, M.A., Souto-Padron, T., Rodrigues, M.M., Travassos, L.R., and Schenkman, S. *J. Cell Sci.* **2000**, 113, 1299–1307.

(20) von Itzstein M. *Curr. Opin. Struct. Biol.,* **2008**, 18: 558–566.

(21) Schengrund C. L. *Biochem Pharmacol.* **2003**, 65(5):699-707.

(22) van der Meer-Janssen Y.P.M, van Galen J, Batenburg J. J, Helms J. B. *Prog. Lipid Res.,* **2010**, 49:1–26.

(23) Becker, D. J., and Lowe, J. B. *Glycobiology* **2003**, 13, 41R–53R.

(24) Dube D. H. and Bertozzi C.R. *Nat. Rev. Drug Discovery* **2005**, 4, 477-488.

(25) Lowe J. B, Marth J. D. *Annu Rev. Biochem.* **2003**;72:643–91.

(26) Kim Y. J, Varki A. *Glycoconj J.* **1997**, 14(5):569-76.

(27) Rexach J. E, Clark P. M, Hsieh-Wilson L. C. *Nat Chem Biol.* **2008**, 4:97–106.

(28) Diamandis E P. *Mol Cell Proteomics.* **2004**, 3(4):367-78.

(29) Pan S, Wang Y, Quinn J. F, Peskind E. R, Waichunas D, Wimberger J. T, Jin J, Li J. G, Zhu D, Pan C, Zhang J. *J Proteome Res.* **2006**, 5(10):2769-79.

(30) Kornfeld R, Kornfeld S. *Annu Rev. Biochem.* **1985**;54:631-64.

(31) van den Steen, P., Rudd, P. M., Dwek, R. A., and Opdenakker, G. *Crit. Rev. Biochem. Mol. Biol.* **1998,** 33 151-208.

(32) Brockhausen I. *Biochim. Biophys. Acta.* **1999**: 67-95.

(33) Wells L, Hart GW. *FEBS Lett* **2003**;546:154–8.

(34) Love D. C, Kochan J, Cathey R. L, Shin S. H, Hanover J. A. *J Cell Sci* **2003**;116:647–54.

(35) Pinnell S. R, Fox R, Krane S. M. *Biochim Biophys Acta* **1971**;229:119–22.

(36) Endo T. *Biochim Biophys Acta* **1999**;1473:237–46.

(37) Smalheiser N. R, Haslam S. M, Sutton Smith M, Morris H. R, Dell A. *J. Biol. Chem.* **1998**;273:23698–703.

(38) Endo T. *Glycoconj J* **2004**;21:3–7.

(39) Yuen C. T, Chai W, Loveless R. W, Lawson A. M, Margolis R. U, Feizi T. *J. Biol. Chem.* **1997**;272:8924–31.

(40) Inamori K, Endo T, Gu J, Matsuo I, Ito Y, Fujii S, Iwasaki H, Narimatsu H, Miyoshi E, Honke K, and Taniguchi N. *J. Biol. Chem.* **2004**;279:2337–40.

(41) Shao L, Luo Y, Moloney D. J, Haltiwanger R. *Glycobiology* **2002**;12: 763–70.

(42) Nishimura H, Kawabata S, Kisiel W, Hase S, Ikenaka T, Takao T, Shimonishi Y, and Iwanaga S. *J. Biol. Chem.* **1989**;264: 20320–5.

(43) Shao L, Haltiwanger R. S. *Cell Mol Life Sci* **2003**;60:241–50.

(44) Hofsteenge J, Huwiler K. G, Macek B, Hess D, Lawler J, Mosher D. F, Peter-Katalinic J. *J. Biol. Chem.* **2001**;276:6485–98.

(45) Tu, L., and Banfield, D. K. *Cell Mol. Life Sci.* **2010**, 67, 29–41.

(46) Eckhardt M, Bukalo O, Chazal G, Wang L., Goridis C, Schachner M, Gerardy-Schahn R, Cremer H, and Dityatev A. *J. Neurosci.* **2000**, 20, 5234–5244.

(47) Ohtsubo K, Takamatsu S, Minowa M. T, Yoshida A, Takeuchi M, and Marth J. D. *Cell* **2005**,123;1307–1321

(48) Matlack, K. E., Mothes, W. and Rapoport, T. A. *Cell* **1998**, 92, 381-390.

(49) Kean E. L. *J. Biol. Chem.* **1970**, 245:2301–2308

(50) Burda P, Aebi M. *Biochim Biophys Acta.* **1999**, 1426(2):239-57.

(51) Dempski R.E Jr, Imperiali B. *Curr Opin Chem Biol.* **2002**, 6(6):844-50.

(52) Hanisch F. G. *Biol Chem.* **2001**, 382(2):143-9.

(53) Ten Hagen K. G, Fritz T. A, Tabak L. A. *Glycobiology* **2003**;13:1R–16R.

(54) Rottger S, White J, Wandall H. H, Olivo J. C, Stark A, Bennett E. P, Whitehouse C, Berger E. G, Clausen H, and Nilsson T. *J Cell Sci* **1998**;111:45–60.

(55) Spiro R. G. *Glycobiology* **2002**;12:43R–56R.

(56) Julenius K, Molgaard A, Gupta R, Brunak S. *Glycobiology* **2005**;15:153–64.

(57) Lis H and Sharon N. *Chem. Rev.* **1998**, 98, 637-674.

(58) Ju T, Cummings R. D. *Proc Natl Acad Sci U S A* **2002**;99:16613–8.

(59) Warren G, and Malhotra V. *Curr. Opin. Cell Biol.***1998**, 10:493-498.

(60) Allan V.J, Thompson H. M, and McNiven M.A. *Nat. Cell Biol.* **2002**, 4:E236–E242.

(61) Giraudo C. G, and Hugo J. F. Maccioni. *Mol Biol Cell* **2003**, 14(9): 3753-3766.

(62) Barlowe C. *Trends Cell Biol.* **2003**, 13(6):295-300.

(63) Béraud-Dufour S, Balch W. *J Cell Sci.* **2002**, 115(9):1779-1780.

(64) Bonifacino J. S, Glick B. S. *Cell* **2004,** 116(2):153-66.

(65) de Graffenried C. L, Bertozzi C. R. *Curr Opin Cell Biol.* **2004,** 16(4):356-63.

(66) Young W. W. Jr. *J Membr Biol.* **2004**;198:1–13

(67) Opat A. S, van Vliet C, Gleeson P. A. *Biochimie* **2001**, 83:763-773.

(68) Loh E, Hong W. *J Biol Chem* **2004**, 279:24640-24648.

(69) Ungar D, Oka T, Brittle E. E, Vasile E, Lupashin V. V, Chatterton J. E, Heuser J. E, Krieger M, Waters M. G. *J Cell Biol* **2002**, 157:405-415.

(70) Kingsley D. M, Kozarsky K. F, Segal M, Krieger M. *J Cell Biol* **1986**, 102:1576-1585.

(71) Letourneur F, Gaynor E. C, Hennecke S, Demolliere C, Duden R, Emr S. D, Riezman H, Cosson P. *Cell* **1994**, 79: 1199–1207.

(72) Oka T, Ungar D, Hughson F. M, Krieger M. *Mol Biol Cell* **2004**, 15:2423-2435.

(73) Steet R, and Kornfeld S. *Mol. Biol. Cell* **2006**, 17: 2312–2321.

(74) Zeevaert R, Foulquier F, Jaeken J, Matthijs G. *Mol. Genet. Metab.* **2008**, 93: 261–278.

(75) Foulquier F. *Biochim Biophys Acta.* **2009**, 1792(9):896-902.

(76) Niemann A. *Jahr Kinderh* **1914**; 79:1–10.

(77) Pick L. *Am J Med Sci* **1933**; 185:601–616.

(78) Crocker A.C. J Neurochem 1961, 7: 68–80.

(79) Crocker A. C, Mays, V. B. Am. J. Clin. Nutr. 1961, 9, 63-67.

(80) Vanier M. T, Pentchev P, Rodriguez-Lafrasse C, Rousson R. *J. Inherit Metab Dis.* 1991, 14(4): 580–595.

(81) Vanier M. T, Millat G. Clin Genet. 2003, 64(4):269-81.

(82) Carstea E. D, Morris J. A, Coleman K. G et al. Science 1997, 277 (5323): 228–231.

(83) Park W. D, O'Brien J. F, Lundquist P. A, Kraft D. L, Vockley C. W, Karnes P. S, Patterson M. C, Snow K. *Hum Mutat.* **2003**, 22(4):313-25.

(84) Naureckiene S, Sleat D. E, Lackland H, Fensom A, Vanier M. T, Wattiaux R, Jadot M, Lobel P. Science 2000, 22;290(5500):2298-301.

(85) Walkley S. U, Suzuki K. *Biochim Biophys Acta.* **2004**, 1685:48–62.

(86) Vanier M.T. Orphanet *J. Rare Dis.* **2010**, 5:16.

(87) Millat G, Marçais C, Rafi M. A, Yamamoto T, Morris J. A, Pentchev P. G, Ohno K, Wenger D. A, Vanier, M. T. Am J Hum Genet 1999, 65: 1321–1329.

(88) Pentchev, P. G, Boothe, A. D, Kruth, H. S, Weintroub, H, Stivers, J. and Brady, R. O. J. Biol. Chem. 1984, 259, 5784-5791.

(89) Pentchev P. G, Comly M. E, Kruth H. S, Vanier M. T, Wenger D. A, Patel S, and Brady, R. O. Proc Natl Acad Sci USA 1985, 82: 8247–8251.

(90) Sleat D. E, Wiseman J. A, El-Banna M, Price S. M, Verot L, Shen M. M, Tint G. S, Vanier M. T, Walkley S. U, and Lobel P. Proc Natl Acad Sci USA 2004, 101:5886–5891.

(91) Maxfield, F. R, and Menon, A. K. Curr. Opin. Cell Biol. 2006, 18, 379-385.

(92) Cheruku S. R, Xu Z, Dutia R, Lobel P. and Storch J. J. Biol. Chem. 2006, 281, 31594-31604

(93) Vance J. E. *FEBS Lett.* **2006**, 580(23): 5518-24.

(94) Liscum L, Ruggiero R. M, Faust J. R. *J. Cell Biol*. **1989**, 1085: 1625–1636.

(95) te Vruchte D, Lloyd-Evans E, Veldman R. J, Neville D. C, Dwek R. A, Platt F. M, Van Blitterswijk W. J, and Sillence D. J. *J. Biol. Chem.* **2004**, 279 26167-26175.

(96) Lloyd-Evans E, Morgan A. J, He X, Smith D. A, Elliot-Smith E, Sillence D. J, Churchill G. C, Schuchman E. H, Galione A, and Platt F. M. Nat Med 2008;14: 1247–55.

(97) Mayran N, Parton R. G, and Gruenberg J. EMBO J 2003, 22, 3242-53.

(98) Ko D. C, Gordon M. D, Jin J. Y, Scott M. P. Mol Biol Cell 2001: 12: 601–614.

(99) Davies J. P, Ioannou Y. A. J Biol Chem. 2000, 275:24367–24374.

(100) Liscum L, Sturley S. L. *Biochim. Biophys. Acta* **2004**, 1685(1–3): 22–27.

(101) Infante R. E, Abi-Mosleh L, Radhakrishnan A, Dale J. D, Brown M. S, Goldstein J. L. J. Biol. Chem. 2008, 283:1052–1063.

(102) Kwon H. J, Abi-Mosleh L, Wang M. L, Deisenhofer J, Goldstein J. L, Brown M. S, Infante R. E. Cell 2009, 137: 1213–1224.

(103) Infante R. E, Radhakrishnan A, Abi-Mosleh L, Kinch L. N, Wang M. L, Grishin N. V, Goldstein J. L, Brown M. S. Proc Natl Acad Sci USA 2008, 283:1064-1075.

(104) Vaya J, Schipper H. M. *J. Neurochem.* **2007**, 102:1727–1737.

(105) Friedland N, Liou H. L, Lobel P, Stock A. M. Proc Natl Acad Sci USA 2003, 100: 2512–2517.

(106) Chang T. Y, Chang C. C, Ohgami N, Yamauchi Y. Annu Rev Cell Dev Biol 2006, 22:129–157.

(107) Xu S, Benoff B, Liou H. L, Lobel P, Stock A. M. J Biol Chem 2007, 282:23525–23531.

(108) Xu Z, Farver W, Kodukula S, Storch J. *Biochemistry* **2008**, 47:11134–11143.

(109) Infante R. E, Wang M. L, Radhakrishnan A, Kwon H. J, Brown M. S, Goldstein J. L. Proc. Natl. Acad. Sci. USA. 2008, 105:15287–15292.

(110) Babalola, J. O, Wendeler M, Breiden B, Arenz C, Schwarzmann G, Locatelli-Hoops S, Sandhoff K. J. Biol. Chem. 2007, 388, 617–626.

(111) Wang M. L, Motamed M, Infante R. E, Abi-Mosleh L, Kwon H. J, Brown M. S, Goldstein J. L. Cell Metab 2010, 12:166–173.

(112) Deffieu M. S, Pfeffer S. R. Proc Natl Acad Sci U S A. 2011, 108(47):18932-6.

(113) Carette J. E, Raaben M, Wong A. C, Herbert A. S, Obernostere G, Mulherkar N, Kuehne A. I, Kranzusch P. J, Griffin A. M, Ruthe G, Cin P. D, Dye J. M, Whelan S. P, Chandran K, and Brummelkamp T. R. Nature 2011: 340

(114) Tang Y. Y, Leao I. C, Coleman E. M, Broughton R. S, and Hildreth J. E. K. J. Virol. 2009, 83, 7982–7995.

(115) Coleman E. M, Walker T. N, and Hildreth J. E. K. Virology Journal 2012, 9:31.

(116) Ulatowski L, Parker R, Davidson C, Yanjanin N, Kelley T. J, Corey D, Atkinson J, Porter F, Arai H, Walkley S. U, and Manor D. J. Lipid Res. 2011, 52: 1400-1410.

(117) Choi H. Y, Karten B, Chan T, Vance J. E, Greer W. L, Heidenreich R. A, Garver W. S, Francis G. A. J. Biol. Chem. 2003, 278, 32569–32577.

(118) Boadu E, Nelson R. C, Francis G. A. Biochimica et Biophysica Acta 2011, 1821(3):396–404.

(119) Frolov A, Zielinski S. E, Crowley J. R, Dudley-Rucker N, Schaffer J. E, and Ory D. S. J. Biol. Chem. 2003, 278:25517–25525.

(120) Goldman S. D, and Krise J. P. J. Biol. Chem. 2010, 285, 4983–4994.

(121) Davies J. P, Chen F.W, and Ioannou Y. A. Science 2000, 290, 2295–2298.

(122) Maxfield F. R, and Tabas I. Nature 2005, 438, 612–621.

(123) Yu L. Curr Opin Lipidol 2008, 19: 263–269.

(124) Liscum L, Faust J. R. J. Biol. Chem. 1987, 262: 17002–17008.

(125) Goldstein J. L, Dana S. E, Faust J. R, Beaudet A. L, Brown M. S. J. Biol. Chem. 1975, 250, 8487–8495.

(126) Goldstein J. L, Basu S. K, Brown M. S. Methods Enzymol. 1983, 98, 241–260.

(127) Chang C. C, Huh H. Y, Cadigan K. M, and Chang T. Y. J. Biol. Chem. 1993, 268, 20747–20755.

(128) Chang T. Y, Chang C. C. Y, Cheng D. Annu. Rev. Biochem. 1997, 66, 613–638.

(129) Sokol J, Blanchette-Mackie J, Kruth H. S, Dwyer N. K, Amende L. M, Butler J. D, Robinson E, Patel S, Brady R. O, Comly M. E, Vanier M. T, Pentchev P. G. J. Biol. Chem. 1988, 263, 3411–3417.

(130) Horton J. D, Goldstein J. L, Brown M. S. J Clin Invest 2002, 109:1125–1130.

(131) Brown M. S, and Goldstein J. L. Cell 1997, 89, 331–340.

(132) Radhakrishnan A, Goldstein J. L, McDonald J. G, Brown M. S. Cell Metab. 2008, 8, 512–521.

(133) Goldstein J. L, DeBose-Boyd R. A, and Brown M. S. Cell 2006, 124:35–46.

(134) Xie C, Turley S. D, and Dietschy J. M. Proc Natl Acad Sci U S A. 1999, 96 (21):11992-11997.

(135) Chawla A, Repa J. J, Evans R. M, Mangelsdorf D. J. Science 2001, 294:1866–1870.

(136) Reddy J. V, Ganley I. G, Pfeffer S. R. PLoS ONE 2006, 1(1): e19.

(137) Cenedella R. J. *Lipids* **2009**, 44, 477–487.

(138) Reiners J. J Jr, Kleinman M, Kessel D, Mathieu P. A, Caruso J. A. Free Radic Biol Med. 2011, 50(2):281-94.

(139) Rodriguez-Lafrasse C, Rousson R, Bonnet J, Pentchev P. G, Louisot P, Vanier M. T. Biochim Biophys Acta 1990, 1043, 123–128.

(140) Liscum L, Underwood K. W. J Biol Chem 1995, 270:15443–15446.

(141) Dean R.T, Jessup W, and Roberts C. R. *Biochem. J.* **1984**, 217, 27-40.

(142) Shacoori, V, Leray. G, Gueble-Val F, Le Treut A, and Le Gall J. Y. Res. Commun. Chem. Pathol. Pharmacol. 1988, 59, 11796611806.

(143) Patterson M. C, Vecchio D, Prady H, Abel L, Wraith J. E. Lancet Neurol 2007, 6:765–772.

(144) Zervas M, Dobrenis K, Walkley S. U. J Neuropathol Exp Neurol 2001, 60: 49–64.

(145) Zervas M, Somers K. L, Thrall M. A, Walkley S. U. Curr. Biol 2001, 11(16):1283–1287.

(146) Andersson U, Butters T. D, Dwek R. A, Platt F. M. Biochem Pharmacol. 2000, 59(7):821-9.

(147) Camargo F, Erickson R. P, Garver W. S, Hossain G. S, Carbone P. N, Heidenreich R. A, Blanchard J. Life Sci 2001, 70(2):131–142.

(148) Kiss T, Fenyvesi F, Bácskay I, Váradi J, Fenyvesi E, Iványi R, Szente L, Tósaki A, and Vecsernyés M. Eur. J. Pharm. Sci. 2010, 40, 376–380.

(149) Davis M. E, Brewster M. E. Nat Rev Drug Discov. 2004, 3:1023–1035.

(150) Liu B, Turley S. D, Burns D. K, Miller A. M, Repa J. J, Dietschy J. M. Proc Natl Acad Sci USA 2009, 106:2377–2382.

(151) Davidson C. D, Ali N. F, Micsenyi M. C, Stephney G, Renault S, Dobrenis K, Ory D. S, Vanier M. T, Walkley S. U. PLoS One 2009, 4: e6951.

(152) Abi-Mosleh L, Infante R. E, Radhakrishnan A, Goldstein J. L, Brown M. S. Proc Natl Acad Sci USA 2009, 106:19316–19321.

(153) Rosenbaum A. I, Zhang G, Warren J. D, Maxfield F. R. Proc Natl Acad Sci USA 2010, 107:5477–5482.

(154) Peake K. B and Vance J. E. *J. Biol. Chem*. **2012**, 287, 9290–9298.

(155) Chen F. W, Li C, Ioannou Y. A. PLoS One 2010, 5: e15054.

(156) Pipalia N. H, Cosner C. C, Huang A, Chatterjee A, Bourbon P, Farley N, Helquist P, Wiest O, Maxfield F. R. Proc Natl Acad Sci U S A. 2011, 108(14):5620-5.

(157) Shahbazian M. D, Grunstein M. Annu Rev Biochem 2007, 76:75–100.

(158) Budillon A, Bruzzese F, Di Gennaro E, Caraglia M. Curr Drug Targets 2005, 6: 337–351.

(159) Munkacsi A. B, Chen F. W, Brinkman M. A, Higaki K, Gutierrez G. D, Chaudhari J, Layer J. V, Tong A, Bard M, Boone C, Ioannou Y. A, and Sturley S. L. J. Biol. Chem. 1988, 286, 23842–23851.

(160) Luzio, J.P, Pryor P.R. and Bright N.A. Nat. Rev. Mol. Cell Biol. 2007, 8, 622–632

(161) Goldstein J. L, Brown M. S, Anderson R. G, Russell D. W, and Schneider W. J. Annu. Rev. Cell Biol. 1985, 1, 1–39.

(162) Fuller S. D and Simons K. J. Cell Biol. 1986, 103:1767-1779.

(163) Bomsel M, Prydz K, Parton R. G, Gruenberg J and Simons K. J. Cell Biol. 1989, 109:3243-3258.

(164) Matter K, and Mellman I. *Curr. Opin. Cell Biol.* **1994**, 6:545-554.

(165) Steinman R. M, Mellman I. S, Muller W. A. and Cohn Z. A. J. Cell Biol. 1983, 96, 1–27.

(166) Conner S. D. and Schmid S. L. Nature 2003, 422, 37–44.

(167) Doherty G. J. and McMahon, H. T. Annu. Rev. Biochem. 2009, 78, 857–902.

(168) Mellman I. Annu. Rev. Cell Dev. Biol. 1996, 12:575-625.

(169) Mukherjee S, Ghosh R. N. and Maxfield F. R. Physiol Rev 1997, 77:759-803.

(170) Traub L. M, Downs M. A, Westrich J. L, Fremont D. H. Proc Natl Acad Sci U S A 1999, 96(16):8907-12.

(171) Saftig P, and Klumperman J. Nat Rev Mol Cell Biol. 2009, 10(9):623-35.

(172) Brodsky F. M, Chen C. Y, Knuehl C, Towler M. C, and Wakeham D. E. Annu. Rev. Cell Dev. Biol. 2001, 17, 517–568.

(173) Mukhopadhyay D. and Riezman H. Science 2007, 315(5809): 201-205.

(174) Pearse B. M. Proc Natl Acad Sci U S A. 1976, 73(4): 1255–1259.

(175) Benmerah A. and Lamaze C. Traffic 2007, 8: 970–982.

(176) Motley A, Bright N. A, Seaman M. N. J. and Robinson M. S. J. Cell Biol. 2003, 162:909-918.

(177) Padron D, Wang Y. J, Yamamoto M, Yin H, Roth M. G. J. Cell Biol. 2003, 162; 693–701.

(178) Itoh T, Koshiba S, Kigawa T, Kikuchi A, Yokoyama S, Takenawa T. Science 2001, 291:1047–1051.

(179) Gaidarov I, Keen J. H. J. Cell Biol. 1999, 146:755–764.

(180) Rohde G, Wenzel D, Haucke V. J. Cell Biol. 2002, 158: 209–214.

(181) Honing S, Ricotta D, Krauss M, Spate K, Spolaore B, Motley A, Robinson M, Robinson C, Haucke V, Owen D. J. *Mol. Cell* **2005**, 18: 519–531.

(182) Drake M. T, Downs M. A, Traub L. M. J Biol Chem 2000, 275(9):6479-89.

(183) Urrutia R, Henley J. R.Cook T, McNiven M. A. Proc. Natl Acad. Sci. USA 1997, 94 (2): 377–384.

(184) Henley J. R, Cao H, McNicven M. A. The FASEB Journal 1999, 13, S243-S247; Lemmon S. K. Curr Biol. 2001, 11(2):R49-52.

(185) Sorkin A. and von Zastrow M. Nat Rev Mol Cell Biol. 2009, 10: 609-622.

(186) Mayor S. and Pagano R. E. Nature Rev. Mol. Cell Biol. 2007, 8, 603–612.

(187) Grant B. D. and Donaldson J. G. Nat Rev Mol Cell Biol 2009, 10 (9): 597–608.

(188) Swanson J. A. and Watts C. Trends Cell Biol. 1995, 5:424–428.

(189) Nobes C. D, and Hall A. Cell 1995, 81(1):53-62.

(190) Sandvig K, Torgersen M. L, Raa H. A. and van Deurs B. Histochem. Cell Biol. 2008, 129, 267–276.

(191) Parton R. G. and Richards A. A. Traffic 2003, 4, 724-738.

(192) Kumari S. and Mayor S. Nature Cell Biol. 2008, 10, 30–41.

(193) Radhakrishna H. and Donaldson J. G. J. Cell Biol. 1997, 139, 49–61.

(194) Brown F. D, Rozelle A. L, Yin H. L, Balla T. and Donaldson J. G. J. Cell Biol. 2001, 154, 1007–1017.

(195) Powelka A. M, Sun J, Li J, Gao M, Shaw L. M, Sonnenberg A, Hsu V. W. Traffic 2004, 5, 20–36.

(196) Naslavsky N, Weigert R. and Donaldson J. G. Mol. Biol. Cell 2004, 15, 3542–3552.

(197) Eyster C. A, Higginson J. D, Huebner R, Porat-Shliom N, Weigert R, Wu W. W, Shen R. F, Donaldson J. G. Traffic 2009, 10, 590–599.

(198) Scarselli M. and Donaldson J. G. J. Biol. Chem. 2009, 284, 3577–3585.

(199) Maxfield F. R. and McGraw T. E. Nature Rev. Mol. Cell Biol. 2004, 5, 121–132.

(200) Gorvel J-P, Chavrier P, Zerial M. and Gruenberg J. Cell 1991, 64:915-925.

(201) Bucci C, Parton R. G,Mather I. H, Stunnenberg H, Simons K, Hoflack B and Zerial M. *Cell* **1992**, 70:715-728.

(202) Koval M. and Pagano R. E. J Cell Biol 1989, 108:2169-2181.

(203) Stoorvogel W, Geuze H. J and Strous G. J. J. Cell Biol. 1987, 104:1261-1268.

(204) Mayor S, Presley J. F and Maxfield F. R. J. Cell Biol. 1993, 121:1257-1269.

(205) Geuze H. J, Slot J. W and Schwartz A. L. J. Cell Biol. 1987, 104:1715-1723.

(206) Dunn K. W, McGraw T. E. and Maxfield F. R. J. Cell Biol. 1989, 109:3303-3314.

(207) Hopkins C. R. Cell 1983, 35:321-330.

(208) Hopkins C. R. and Trowbridge I. S. J. Cell Biol. 1983, 97:508-521.

(209) Yamashiro D, Tycko B, Fluss S. and Maxfield F. R. Cell 1984, 37:789-800.

(210) Van der Sluijs P, Hull M, Zahraoui A, Tavitian A, Goud B. and Mellman I. Proc Natl Acad Sci USA 1991, 88:6313-6317.

(211) Van der Sluijs P, Hull M, Webster P, Male P, Goud B. and Mellman I. Cell 1992, 70:729-740.

(212) Ullrich O, Reinsch S, Urbe S, Zerial M. and Parton R. G. J. Cell Biol. 1996, 135:913-924.

(213) Hurley J. H. and Emr S. D. Annu. Rev. Biophys. Biomol. Struct. 2006, 35: 277–298.

(214) Williams R. L. and Urbe S. Nat. Rev. Mol. Cell Biol. 2007, 8: 355–368.

(215) Apodaca G, Katz L. A and Mostov K. E. J. Cell Biol. 1994, 125:67-86.

(216) Knight A, Hughson E, Hopkins C. R. and Cutler D. F. Mol. Biol. Cell 1995, 6:597-610.

(217) Hunziker W. and Peters P. J. J. Biol. Chem. 1998, 273:15734-15741.

(218) Zacchi P, Stenmark H, Parton R. G, Orioli D, Lim F, Giner A, Mellman I, Zerial M. and Murphy C. J. Cell Biol. 1998, 140:1039-1053.

(219) Kirisits A, Pils D, Krainer M. Int J Biochem Cell Biol. 2007, 39(12):2173-82.

(220) Ludwig T, Griffiths G. and Hoflack B. J. Cell Biol. 1991, 115:1561-1572.

(221) Honing S, Griffith J, Geuze H. J. and Hunziker W. EMBO J 1996, 15:5230-5239.

(222) Rink J, Ghigo E, Kalaidzidis Y. and Zerial M. Cell 2005, 122, 735–749.

(223) Stoorvogel W, Strous G. J, Geuze H. J, Oorschot V. and Schwartz A. L. Cell 1991, 65:417-427.

(224) Dunn K. W. and Maxfield F. R. J. Cell Biol. 1992, 117:301-310.

(225) Gruenberg J, Griffiths G. and Howell K. E. J. Cell Biol. 1989, 108:1301-1316.

(226) Aniento F, Emans N, Griffiths G. and Gruenberg J. J. Cell Biol. 1993, 123:1373-1387.

(227) Clague M. J, Urbe S, Aniento F. and Gruenberg J. J. Biol Chem. 1994, 269:21-24.

(228) Feng Y, Press B. and Wandinger-Ness A. J. Cell Biol. 1995, 131:1435-1452.

(229) Van Deurs B, Holm P. K, Kayser L. and Sandvig K. Eur J Cell Biol. 1995, 66(4):309-23.

(230) Mullock B. M, Bright N. A, Fearon C. W, Gray S. R, Luzio J. P. *J. Cell Biol.* **1998**, 140 (3): 591–601.

(231) Lombardi D, Soldati T, Riederer M. A, Goda Y, Zerial M. and Pfeffer S. R. *EMBO J.* 1**993**, 12:677-682.

(232) de Duve C, De Barsy T, Poole B, Trouet A, Tulkens P. and Van Hoof F. Biochem. Pharmacol. 1974, 23, 2495-2531.

(233) Mukhopadhyay D. and Riezman H. Science 2007, 315, 201-205.

(234) Woodman P. G. and Futter, C. E. Curr. Opin. Cell Biol. 2008, 20, 408–414.

(235) Im Y. J, Wollert T, Boura E, and Hurley J. H. Dev. Cell 2009, 17: 234–243.

(236) Luzio J. P, Rous B. A, Bright N. A, Pryor P. R, Mullock B. M. and Piper R. C. J. Cell Sci. 2000, 113, 1515–1524.

(237) Mullins C. and Bonifacino J. S. BioEssays 2001, 23, 333–343.

(238) Storrie B. and Desjardins M. BioEssays 1996, 18, 895-903.

(239) Mullock B. M, Bright N. A, Fearon C. W, Gray S. R. and Luzio J. P. J. Cell Biol. 1998, 140, 591–601.

(240) Pryor P. R, Jackson L, Gray S. R, Edeling M. A, Thompson A, Sanderson C. M, Evans P. R, Owen D. J. and Luzio J. P. Cell 2008, 134, 817–827.

(241) Munnell J. F. and Cork L. C. Am J Pathol 1980, 98(2): 385–394.

(242) Siakotos A. N, Armstrong D, Koppang N, Connole E. Invest Ophthalmol Vis Sci. 1978, 17:618–633.

(243) Elner V. M. Trans Am Ophthalmol Soc. 2002, 100:301–338.

(244) Werb Z and Reynolds J. J. J Exp Med. 1974, 140(6):1482–1497.

(245) Futerman A. H, and van Meer G. Nat Rev Mol Cell Biol 2004, 5, 554-565.

(246) Neufeld,E.F. and Muenzer,J. (1995) The mucopolysaccharidoses. In Scriver,C.R. Beaudet,A.L., Sly,W.S. and Valle,D. (eds.), The Metabolic and Molecular Bases of Inherited Disease. McGraw-Hill, New York, pp. 2465–2494.

(247) Wells, L.; Vosseller, K.; Hart, G. W. *Science* **2001**, *291*, 2376-2378.

(248) Torres C. R, Hart G. W. *J Biol Chem* **1984**, 259:3308-3317.

(249) Hart G. W, Housley M. P, Slawson C.*Nature* **2007**, 446:1017–1022.

(250) Carrillo L. D, Froemming J. A, Mahal L. K. *J. Biol. Chem.* **2010**, 286:6650–6658.

(251) Zachara N. E, Hart G. W. *Trends Cell Biol* **2004**, *14*:218 –221.

(252) Slawson C, Copeland R. J, Hart G. W. *Trends Biochem. Sci*. **2010**, 35:547–555.

(253) Haltiwanger R. S, Holt G. D, Hart G. W. *J. Biol. Chem.* **1990**, 265:2563–2568.

(254) Dong D. L, Hart G. W. *J. Biol. Chem.* **1994**, 269:19321–19330.

(255) Lubas W. A, Hanover J. A. *J. Biol. Chem.* **2000**, 275:10983-10988.

(256) Iyer S. P, Hart G. W. *J. Biol. Chem.* **2003**, 278:24608-24616.

(257) Iyer S. P., Akimoto Y., and Hart G. W. *J. Biol. Chem.* **2003**, 278, 5399-5409.

(258) Kreppel L. K, Hart G. W. *J Biol Chem.* **1999**, 274:32015–32022.

(259) Fulop N, Zhang Z, Marchase R. B, Chatham J. C. *Am J Physiol Heart Circ Physiol.* **2007**, 292:H2227–36.

(260) Toleman C, Paterson A. J, Kudlow J. E. *Biochim Biophys Acta.* **2006**, 1760:829–39.

(261) Toleman C, Paterson A. J, Whisenhunt T. R, Kudlow J. E. *J. Biol. Chem.* **2004**, 279:53665–73.

(262) O'Donnell N, Zachara N. E, Hart G. W, Marth J. D. *Mol Cell Biol* **2004**, 24:1680-1690.

(263) Liu K, Paterson A. J, Zhang F, McAndrew J, Fukuchi K, Wyss J. M, Peng L, Hu Y, Kudlow J. E. *J Neurochem* **2004**, 89:1044-1055.

(264) Sletten E. M, and Bertozzi C. R. *Angew. Chem., Int. Ed.* **2009**, 48, 6974–6998.

(265) Tiefenbrunn T. K, Dawson P. E. *Biopolymers* **2010**, 94(1):95-106.

(266) Varki, A. *Blood* **2004**, 104:3005.

(267) Varki N.M, Strobert E, Dick Jr, E.J, Benirschke K. and Varki A. *Annu. Rev. Pathol. Mech.* **2011**, 6:365-393.

(268) Varki A. *FASEB J* **1991**, 5(2): 226–235.

(269) Maru I, Ohta Y, Murata K, and Tsukada Y. *J. Biol. Chem.* **1996**, 271(27):16294–16299.

(270) Tanner M. E. *Bioorg. Chem.* **2005**, 33(3): 216–228.

(271) Eckhardt M and Gerardy-Schahn R. *Eur. J Biochem.* 1997, 248(1): 187–192.

(272) Harduin-Lepers A, Mollicone R, Delannoy P, Oriol R. *Glycobiology* **2005**, 15(8): 805–817.

(273) Martinez-Duncker I, Dupré T, Piller V, Piller F, Candelier J. J, Trichet C, Tchernia G, Oriol R, Mollicone R. *Blood* **2005**, (105(7): 2671–2676.

(274) Kayser H, Zeitler R, Kannicht C, Grunow D, Nuck R, Reutter W. *J. Biol. Chem.* **1992**, 267:16934–16938.

(275) Keppler O.T, Stehling P, Herrmann M, Kayser H, Grunow D, Reutter W and Pawlita M. *J. Biol. Chem.* **1995**, 270:1303-1314.

(276) Mahal, L. K., Yarema, K. J., and Bertozzi, C. R. *Science* **1997***,* 276, 1125–1128.

(277) Saxon, E.; Bertozzi, C. R. *Science* **2000**, 287, 2007-2010.

(278) Prescher J. A, and Bertozzi C. R. *Nat. Chem. Biol.* **2005**, 1, 13–21.

(279) Laughlin S. T, and Bertozzi C. R. *Proc. Natl. Acad. Sci. U.S.A.* **2009**, 106, 12-17.

(280) Sarkar A. K, Fritz T. A, Taylor W. H, and Esko J. D. *Proc. Natl. Acad. Sci. USA* **1995**, 92:3323-3327.

(281) Dirksen A, Dirksen S, Hackeng T. M, Dawson P. E. *J. Am. Chem. Soc.* **2006**, 128, 15602–15603.

(282) Dirksen A, Hackeng T. M, Dawson P. E. *Angew. Chem. Int. Ed.* **2006**, 45, 7581–7584.

(283) Zeng Y, Ramya T. N, Dirksen A, Dawson P. E, Paulson J. C. *Nat Methods* **2009**, 6, 207–209.

(284) Debets M. F, van der Doelen C. W. J, Floris P. J. T. Rutjes F. P. J. T, and van Delft F. L. *ChemBioChem* **2010**, 11:1168-1184.

(285) Luchansky S. J, Hang H. C, Saxon E, Grunwell J. R, Yu C, Dube D. H, Bertozzi C. R. *Meth. Enzymol*. **2003**, 362, 249-272.

(286) Hanson S. R, Hsu T. L, Weerapana E, Kishikawa K, Simon G. M, Cravatt B. F, Wong C. H. *J. Am. Chem. Soc*. **2007**;129:7266-7267.

(287) Hsu T. L, Hanson S. R, Kishikawa K, Wang S. K, Sawa M, and Wong C. H. *Proc. Natl. Acad. Sci. U. S. A.* **2007**, 104:2614–2619.

(288) Chang P. V, Chen X, Smyrniotis C, Xenakis A, Hu T, Bertozzi C. R, Wu P. *Angew. Chem., Int. Ed.* **2009**, 48, 4030-4033.

(289) Hang H. C, Yu C, Kato D. L, Bertozzi C. R. A *Proc. Natl. Acad. Sci. U.S.A.* **2003**, 100, 14846-14851.

(290) Laughlin S. T, Bertozzi C. R. *Nat. Protoc.* **2007,** 2, 2930-2944.

(291) Luchansky S. J, Argade S, Hayes B. K, Bertozzi C. R. *Biochemistry* **2004**, 43, 12358-12366.

(292) Jacobs C. L, Goon S, Yarema K. J, Hinderlich S, Hang H. C, Chai D. H, Bertozzi C. R. *Biochemistry* **2001**, 40, 12864-12874.

(293) Keppler O. T, Horstkorte R, Pawlita M, Schmidt C, and Reutter W. *Glycobiology* **2001**, 11(2):11R-18R.

(294) Weerapana E, and Imperiali B. *Glycobiology* **2006**, 16(6): 91R–101R.

(295) Van Lenten L, and Ashwell G. *J. Biol. Chem.* **1971**, 246, 1889-1894.

(296) Chen I, and Ting A. Y. *Curr. Opin. Biotechnol.* **2005**, 16:35-40.

(297) Hang H. C, and Bertozzi C. R. *Accounts Chem. Res.* **2001**, 34, 727-736.

(298) Liu D. S, Tangpeerachaikul A, Selvaraj R, Taylor M.T, Fox J. M, and Ting A. Y. *J. Am. Chem. Soc.* **2012**, 134, 792-795.

(299) Jencks W. P. *J. Am. Chem. Soc.* **1959**, 81 (2): 475–481.

(300) Sayer J. M, Peskin M, Jencks W. P. *J. Am. Chem. Soc*. **1973**, 95 (13):4277–4287.

(301) Nauman D. A, and Bertozzi C. R. *Biochim. Biophys. Acta.* **2001**, 1568, 147-154.

(302) Cordes E. H, Jencks W. P. *J. Am. Chem. Soc.* **1962**, 84 (5): 826–831145.

(303) Rayo J, Amara N, Krief P, and Meijler M. M. *J. Am. Chem. Soc.* **2011**, 133 (19): 7469–7475

(304) Kalia J, Raines R. T. *Angew. Chem. Int. Ed.* **2008**;47:7523–7526.

(305) Huisgen, R. Padwa, A., Ed.; Wiley: New York, 1984; Vol. 1, pp 1– 176.

(306) Kiick K. L, Saxon E, Tirrell D. A, Bertozzi C. R. *Proc. Natl. Acad. Sci. U.S.A.* **2002**, 99, 19-24.

(307) Link A J, and Tirrell D. A. *J. Am. Chem. Soc.* **2003**;125:11164.

(308) Dieterich D. C, Link A. J, Graumann J, Tirrell D. A, and Schuman E. M. *Proc. Natl. Acad. Sci. U. S. A.* **2006**;103(25):9482-9487.

(309) Ngo J. T, Champion J. A, Mahdavi A, Tanrikulu I. C, Beatty K. E, Connor R. E, Yoo T. H, Dieterich D. C, Schuman E. M, Tirrell D. A. *Nature Chem Biol.* **2009**;5:715–717.

(310) Hang H. C, Geutjes E. J, Grotenbreg G, Pollington A. M, Bijlmakers M. J, and Ploeghet H. L. *J. Am. Chem. Soc.* **2007**. 129(10):2744-2755.

(311) Charron G, Zhang M. M, Yount J. S, Wilson J, Raghavan A. S, Shamir E, and Hang H. C. *J. Am. Chem. Soc.* **2009**, 131 (13):4967–4975.

(312) Hannoush R. N, and Arenas-Ramirez N. *ACS Chem. Biol.* **2009**, 4 (7):581–587.

(313) Staudinger, H., and Meyer, J. *Helv. Chim. Acta* **1919**, 2, 635–646.

(314) Kohn M, and Breinbauer R. *Angew. Chem. Int. Ed.* **2004**, 43(24):3106-16.

(315) Baskin J. M, Prescher J. A, Laughlin S. T, Agard N. J, Chang P. V, Miller I. A, Lo A, Codelli J. A, Bertozzi C. R. *Proc. Natl. Acad. Sci. U.S.A.* **2007**, 104, 16793-16797.

(316) Hangauer M. J, and Bertozzi C. R. *Angew. Chem., Int. Ed.* **2008,** 47, 2394-2397.

(317) Chang P. V, Prescher J. A, Hangauer M. J, Bertozzi C. R. *J. Am. Chem. Soc.* **2007**, 129, 8400-8401.

(318) Lin F, Hoyt H. M, van Halbeek H, Bergman R. G, Bertozzi C. R. *J. Am. Chem. Soc*. **2005,** 127, 2686-2695.

(319) Zhang H. L, Ma Y, Sun X. L. *Chem. Commun.* **2009**, 21, 3032– 3034.

(320) Saxon E, Luchansky S. J, Hang H. C, Yu C, Lee S. C, Bertozzi C. R. *J. Am. Chem. Soc.***2002**, 124, 14893-14902.

(321) Prescher J. A, Dube D. H, Bertozzi C. R. *Nature* **2004**, 430, 873-877.

(322) Vocadlo D. J, Hang H. C, Kim E. J, Hanover J. A, Bertozzi C. R. *Proc. Natl. Acad. Sci. U.S.A.* **2003**, 100, 9116-9121.

(323) Lemieux G. A, de Graffenried C. L, Bertozzi C. R. *J. Am. Chem. Soc.* **2003**, 128, 4708- 4709.

(324) Luchansky S. J, Argade S, Hayes B. K, Bertozzi C. R. *Biochemistry* **2004**, 43, 12358-12366.

(325) Tsao M. L, Tian F, Schultz P. G. *ChemBioChem.* **2005**, 6:2147–2149.

(326) Kho Y, Kim S. C, Jiang C, Barma D, Kwon S. W, Cheng J. K, Jaunbergs J, Weinbaum C, Tamanoi F, Falck J, Zhao Y. M. *Proc. Natl. Acad. Sci. U.S.A.* **2004**, 101 (34) 12479–12484.

(327) Himo F, Lovell T, Hilgraf R, Rostovtsev V. V, Noodleman L, Sharpless K. B. and Fokin V. V. *J. Am. Chem. Soc.* **2005**, 127, 210–216.

(328) Tornoe C. W, Christensen C, Meldal M. *J. Org. Chem.* **2002**, 67:3057–3064.

(329) Rostovtsev V. V, Green L. G, Fokin V. V, Sharpless K. B. *Angew. Chem. Int. Ed.* **2002**, 41:2596–2599.

(330) Kolb H. C, Finn M. G, and Sharpless K. B. *Angew. Chem. Int. Ed.* **2001**, 40:2004-2021.

(331) Bock V. B. Hiemstra H, van Maarseveen J. H. *Eur. J Org Chem*. **2006**; 2006:51.

(332) Hein C, Liu X-M, Wang D. *Pharm Res.* **2008**, 25:2216.

(333) Wolbers F, ter Braak P, Le Gac S, Luttge R, Andersson H, Vermes I, van den Berg A. *Electrophoresis* **2006**, 27, 5073–5080.

(334) Horne W. S, Stout C. D, and Ghadiri, M. R. *J. Am. Chem. Soc.* **2003**, 125, 9372-9376.

(335) Wu P, Feldman A. K, Nugent A. K, Hawker C. J, Scheel A, Voit B, Pyun J, Fréchet J. M. J, Sharpless K. B, Fokin V. V. *Angew. Chem. Int. Ed.* **2004**, 43, 3928.

(336) Ornelas C, Ruiz J, Cloutet E, Alves S, Astruc D. *Angew. Chem. Int. Ed.* **2007**, 46, 872.

(337) Meldal M. *Macromol. Rapid Commun.* **2008**, 29, 1016.

(338) Perez-Balderas F, Ortega-Munoz M, Morales-Sanfrutos J, Hernández-Mateo F, Calvo-Flores F. G, Calvo-Asín J. A, Isac-García J, Santoyo-González F. *Org Lett.* **2003**;5:1951.

(339) Ryu E. H, and Zhao Y. *Org. Lett.* **2005**, 7: 1035–1037.

(340) Sivakumar K, Xie F, Cash B. M, Long S, Barnhill H. N, and Wang Q. *Org. Lett.* **2004**, 6 (24):4603–4606.

(341) Rabuka D, Hubbard S. C, Laughlin S. T, Argade S. P, Bertozzi C. R. *J. Am. Chem. Soc.***2006**, 128, 12078-9.

(342) Sawa M, Hsu T. L, Itoh T, Sugiyama M, Hanson S. R, Vogt P. K, Wong C. H. *Proc. Natl. Acad. Sci. U. S. A.* **2006**;103(33):12371-12376.

(343) Yang Y.-Y, Ascano J. M, Hang H. C. *J. Am. Chem. Soc.* **2010**, 132, 3640.

(344) Salic A, Mitchison T. J. *Proc. Natl. Acad. Sci. U. S. A.* **2008**, 105, 2415 – 2420.

(345) Link A. J, Vink M. K, Tirrell D. A. *J. Am. Chem. Soc.* **2004**, 126:10598–10602.

(346) Speers A. E, and Cravatt B. F. *J. Am. Chem. Soc.* **2005**, 127 (28): 10018–10019.

(347) Hong V, Steinmetz N. F, Manchester M, and Finn M. G. *Bioconjugate Chem.* **2010**, 21 (10):1912–1916.

(348) Soriano del Amo D, Wang W, Jiang H, Besanceney C, Yan A. C, Levy M, Liu Y, Marlow F. L, and Wu P. *J. Am. Chem. Soc.* **2010**, 132 (47):16893–16899.

(349) Besanceney-Webler C, Jiang H, Zheng T, Feng L, Soriano del Amo D, Wang W, Klivansky L. M, Marlow F. L, Liu Y, and Wu P. *Angew. Chem. Int. Ed.* **2011**, 50, 8051- 8056.

(350) Kennedy D. C, McKay C. S, Legault M. C. B, Danielson D. C, Jessie A. Blake J. A, Pegoraro A. F, Stolow A, Mester Z, and Pezacki J. P. *J. Am. Chem. Soc.* **2011**, 133 (44):17993–18001.

(351) Uttamapinant C, Tangpeerachaikul A, Grecian S, Clarke S, Singh U, Slade P, Gee K. R, and Ting A. Y. *Angew. Chem. Int. Ed.* **2012**, 51, 1 – 6.

(352) Hong V, Presolski S. I, Ma C, and Finn M. G. *Angew. Chem. Int. Ed.* **2009**, 48, 9879 –9883.

(353) Becer C. R, Hoogenboom R, Schubert U. S. *Angew. Chem. Int. Ed.* **2009**, 48(27):4900-8.

(354) Agard N. J, Prescher J. A, Bertozzi C. R. *J. Am. Chem. Soc.* **2004**, 126, 15046-15047.

(355) Laughlin S. T, Baskin J. M, Amacher S. L, Bertozzi C. R. *Science* **2008**, 320, 664-667.

(356) Blomquist, A. T.; Liu, L. H. *J. Am. Chem. Soc.* **1953**, 75, 2153-2154.

(357) Wittig, G.; Krebs, A. *Chem. Ber.* **1961**,94 3260-3275.

(358) Turner R. B, Jarrett A. D, Goebel P, and Mallon B. J. *J. Am. Chem. Soc.* **1973**, 95 (3):790–792.

(359) Petersen H, Kolshorn H, and Meier H. *Angew. Chem. Int. Ed.* **1978**, 17, 461-462.

(360) Sletten E. M, and Bertozzi C. R. *Acc Chem Res*. **2011**, 44, 666-676.

(361) Sletten E. M, Nakamura H, Jewett J. C, Bertozzi C. R. *J. Am. Chem. Soc.* **2010**, 132, 11799-11805.

(362) Krebs A, and Wilke J. *Top Curr. Chem* **1983**, 109, 189-233.

(363) Neef A. B, and Schultz C. *Angew. Chem. Int. Ed.* **2009**, 48(8):1498-500.

(364) Fernández-Suárez M, Baruah H, Martínez-Hernández L, Xie K. T, Baskin J. M, Bertozzi C. R, and Ting A. Y. *Nat. Biotechnol.* **2007**, 25, 1483-1487.

(365) Agard N. J, Baskin J. M, Prescher J. A, Lo A, Bertozzi C. R. *ACS Chem. Biol.* **2006**, 1, 644-8.

(366) Codelli J. A, Baskin J. M, Agard N. J, Bertozzi C. R. *J. Am. Chem. Soc.* **2008,** 130, 11486-11493.

(367) Ess D. H, Jones G. O, and Houk K. N. *Org. Lett.* **2008**, 10 (8):1633–1636.

(368) Ning X, Guo J, Wolfert, M. A, Boons G.-J. *Angew. Chem., Int. Ed.* **2008**, 47, 2253– 2255.

(369) Mbua N. E, Guo J, Wolfert M. A, Steet R, Boons G.-J. *ChemBioChem* **2011**, 12, 1912–1921.

(370) Friscourt F, Ledin P. A, Mbua N. E, Flanagan-Steet H. R, Wolfert M. A, Steet R, and Boons G. J. *J. Am. Chem. Soc.* **2012**, 134, 5381-5389.

(371) Chenoweth K, Chenoweth D, Goddard W. A. III. *Org. Biomol. Chem.* **2009**, 7, 255–5258.

(372) Poloukhtine A. A, Mbua N. E, Wolfert M. A, Boons G.-J, Popik V. V. *J. Am. Chem. Soc.* **2009**, 131, 15769– 15776.

(373) Debets M. F, van Berkel S. S, Schoffelen S, Rutjes F. P. J. T, van Hest J. C. M, van Delft F. L. *Chem. Commun.* **2010**, 46, 97– 99.

(374) Kuzmin A, Poloukhtine A, Wolfert M. A, Popik V. V. *Bioconjugate Chem.* **2010**, 21, 2076– 2085.

(375) Jewett J. C, Sletten E. M, Bertozzi C. R. *J. Am. Chem. Soc.* **2010**, 132, 3688–3690.

(376) Dommerholt J, Schmidt S, Temming R, Hendriks L. J. A, Rutjes F. P. J. T, van Hest J. C. M, Lefeber D. J, Friedl P, van Delft F. L. *Angew. Chem. Int. Ed.* **2010**, 49, 9422– 9425.

(377) Sletten E. M, and Bertozzi C. R. *Org. Lett.* **2008**, 10, 3097-3099.

(378) Chang P. V, Dube D. H, Sletten E. M, Bertozzi C. R. *J. Am. Chem. Soc.* **2010,** 132, 9516-9518.

(379) Chang P. V, Prescher J. A, Sletten E. M, Baskin J. M, Miller I. A, Agard N. J, Lo A, Bertozzi C. R. *Proc. Natl. Acad. Sci. U.S.A.* **2010**, 107, 1821-1826.

(380) Beatty K. E, Fisk J. D, Smart B. P, Lu Y. Y, Szychowski J, Hangauer M. J, Baskin J. M, Bertozzi C. R, Tirrell D. A. *ChemBioChem* **2010**, 11, 2092– 2095.

(381) Winz M. L, Samanta A, Benzinger D, and Jäschke A. *Nucl. Acids Res.* **2012**, 1-13.

(382) Yao J. Z, Uttamapinant C, Poloukhtine A. A, Baskin J. M, Codelli J. A, Sletten E. M, Bertozzi C. R, Popik V. V, Ting A. Y. *J. Am. Chem. Soc*. **2012**, 134, 3720-3728.

(383) Kele P, Mezo G, Achatz D. and Wolfbeis O. S. *Angew. Chem., Int. Ed.* **2009**, 48, 344–347.

(384) Jayaprakash K. N, Peng C. G, Butler D, Varghese J. P, Maier M. A, Rajeev K. G, Manoharan M. *Org Lett.* **2010**, 3;12(23):5410-3.

(385) DeForest C. A, Polizzotti B. D, Anseth K. S. *Nat. Mater.* **2009**, 8, 659–664.

(386) Bernardin A, Cazet A, Guyon L, Delannoy P, Vinet F, Bonnaffe F, Texier I. *Bioconjugate Chem.* **2010**, 21, 583–588.

(387) Johnson J. A, Baskin J. M, Bertozzi C. R, Koberstein J. T, Turro N. J. *Chem. Commun.* **2008**, 3064–3066.

(388) Ornelas C, Broichhagen J, Weck M. *J. Am. Chem. Soc.* **2010**, 132, 3923–3931.

CHAPTER 2
STRAIN-PROMOTED ALKYNE-AZIDE CYCLOADDITIONS (SPAAC) REVEAL NEW FEATURES OF GLYCOCONJUGATE BIOSYNTHESIS

2.1 INTRODUCTION

Metal-free cycloadditions between cyclooctynes and azides that give stable 1,2,3-triazoles, have found wide utility in labeling glycans in proteins and lipids of living cells, glycoprotein enrichment for proteomics, protein and oligonucleotide modification, and tissue reengineering.[1] These reactions, which have been coined "strain-promoted alkyne–azide cycloadditions" (SPAAC) have also made an entry in material sciences and have, for example, been employed for the assembly, cross-linking and surface modification of dendrimers,[2] derivatization of polymeric nanostructures,[3] and patterning of surfaces.[4] The attraction of SPAAC is that it does not require a toxic metal, is highly efficient even in a very complex milieu and proceeds efficiently at ambient temperature. Density functional theory (B3LYP) calculations of the transition states of cycloadditions of phenyl azide with acetylene and cyclooctyne indicate that the fast rate of the strain promoted cycloaddition is due to a lower energy required for distorting the 1,3-dipole and alkyne into the transition-state geometry.[5]

The first generation of cyclooctynes (**1**) suffered from relatively slow reaction rates and as a consequence the scope of these reagents is rather limited (Scheme 2.1). It has, however, been found that electron-withdrawing fluorine groups at the propargylic position of a cyclooctyne (DIFO, **2**) dramatically increase the rate of strain-promoted cycloaddition with azides.[6]

The attractiveness of this methodology has, for example, been demonstrated by visualization of glycans *in vivo* at subcellular resolution during the development of zebrafish embryos.[7]

Scheme 2.1 Reagents for labeling azido-containing biomolecules.

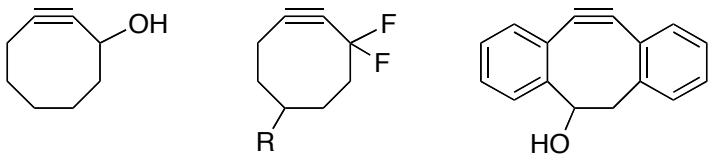

1 **2** **3**

We have found that derivatives of 4-dibenzocyclooctynol (DIBO, **3**) react fast with azido-containing saccharides and amino acids, and can be employed for visualizing metabolically labeled glycans of living cells.[8] While the fluorine atoms of DIFO (**2**) influence rate enhancement by increasing interaction energies, the aromatic rings of **3** accomplish a similar increase in reaction rate through conformational effects that result in decreasing the distortion energy. Attractive features of DIBO (**3**) include easy access to the compounds by a simple synthesis approach, nontoxicity and straightforward attachment of a variety of probes. Furthermore, dibenzocyclooctynes can be generated photochemically by short irradiation by UV light of corresponding cyclopropenones, and thereby provide opportunities for the spatially and temporally controlled labeling of the target substrates.[9] We have also shown that by employing nitrones and nitrile oxides as 1,3-dipoles, the rate of cycloaddition can be further enhanced and this technology has, for

example, made it possible to selectively tag proteins at the N-terminus or perform sequential modifications of complex compounds.[10] Furthermore, several analogues of DIBO have been reported that exhibit even higher rates of cycloaddition with azides.[11]

Scheme 2.2 Biotinylated detection reagents used to probe for the presence of azides.

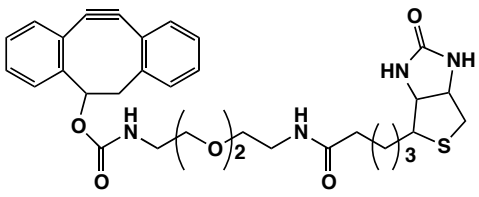

4

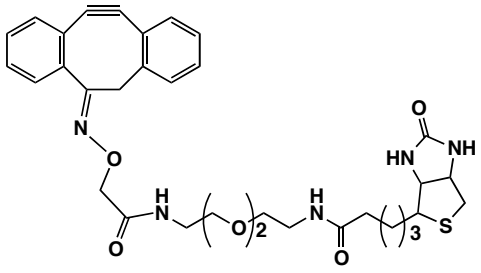

5

We report herein that metabolic labeling combined with SPAAC using compounds **4** and **5** (Scheme 2.2), of wild-type cells and those that have known defects in their glycosylation machinery, showed that relative quantities of sialylation of glycoconjugates can easily and reliably be established. Furthermore, a combined use of metabolic labeling/SPAAC and lectin staining revealed that a defect in the conserved oligomeric Golgi (COG) complex affects terminal processing of *N*-glycans to a greater extent than modification of *O*-glycans.

2.2 RESULTS AND DISCUSSION

The bioorthogonal chemical reporter strategy is emerging as a versatile method for labeling biomolecules, such as nucleic acids, lipids, proteins, and carbohydrates.[1a, c, d] In this approach, an abiotic chemical functionality (reporter) is incorporated into a target

biomolecule, which can then be reacted with a complementary bioorthogonal reagent linked to a probe. Azide is commonly employed as a reporter and can be installed into biomolecules by using azido-containing biosynthetic precursors that can be accepted by the cell's native or engineered biosynthetic machinery. For example, azido-containing glycoconjugates can be biosynthesized by metabolic labeling with peracetylated N-α-azidoacetylmannosamine (Ac_4ManNAz), which is an appropriate substrate for the cell's glycosylation machinery.[12] A subsequently bioorthogonal reaction can then covalently attach a probe to the azido function, which in turn makes it possible to conduct a multitude of functional studies. A number of bioorthogonal reactions have been described for reactions with azides, however, SPAAC is emerging as a particularly attractive approach as it can be performed under physiological conditions and does not require a toxic metal catalyst.

To establish biotin-modified DIBO derivatives **4** and **5** as appropriate bioorthogonal reagents, we employed these compounds to determine relative quantities of cell surface sialylation of wild-type and mutant cells, and compared the results with traditional lectin staining. It is well established that Ac_4ManNAz can be employed by the glycosylation machinery to install azido-containing sialic acid in various glycoconjugates and a subsequent reaction with **4** or **5** was expected to provide quantitative data on cell surface sialylation.[12] Thus, Jurkat cells were cultured in the presence of Ac_4ManNAz (25 μM) for 3 days to metabolically introduce N-azidoacetyl-sialic acid (SiaNAz) moieties into glycoproteins and glycolipids. As a negative control, Jurkat cells were employed that were grown in the presence of peracetylated *N*-acetylmannosamine (Ac_4ManNAc). A time-course experiment was conducted by exposing the cells to 30 μM of **4** and **5** for

different time periods at room temperature, washed and then stained with avidin–FITC for 15 min at 4 °C. The efficiency of the two-step cell surface labeling was determined by measuring the fluorescence intensity of the cell lysates.

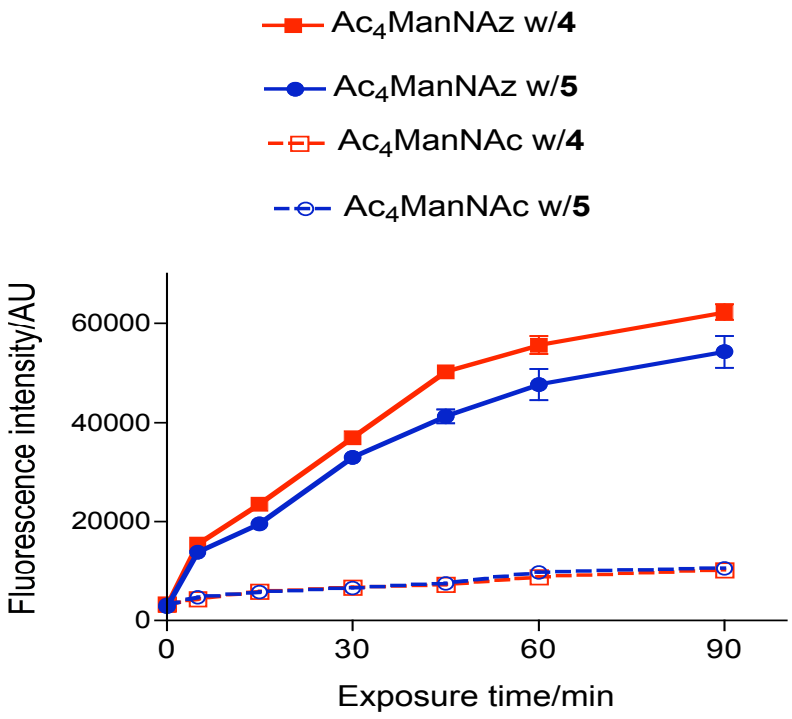

Figure 2.1 Time course of cell surface labeling with compounds **4** and **5**. Jurkat cells grown for 3 days in the presence of Ac_4ManNAc or Ac_4ManNAz (25 μM) and were incubated with compounds **4** or **5** (30 μM) for 0–90 min at room temperature. Next, cells were incubated with avidin–FITC for 15 min at 4 °C, after which cell lysates were assessed for fluorescence intensity. AU indicates arbitrary fluorescence units. Data (n=3) are presented as mean ±SD.

Gratifyingly, the ManNAz-labeled cell exhibited strong fluorescent readings after being stained with the two different DIBO derivatives, and the cell labeling was almost complete after a reaction time of 60 min (Figure 2.1), whereas the control cells gave a very low fluorescence intensity showing that background labeling is negligible. Similar results were obtained when Chinese hamster ovary (CHO)-K1 cells were subjected to the same procedure.

Metabolically labeled cells were also examined by confocal microscopy (Figure 2.2). Thus, adherent Chinese hamster ovary (CHO) cells were cultured in the presence of Ac_4ManNAz (100 μM) for two days.[13] Next, cell surface azido moieties were treated with **4** or **5** (30 μM) for 1 h at ambient temperature, and then visualized with avidin–AlexaFluor488 for 15 min at 4 °C. Staining was mainly observed at the cell surface, and as expected, blank cells exhibited very low fluorescence staining confirming that background labeling is negligible. We also found that the two-step labeling approach with **4** and **5** had no effect on cell viability as determined by morphology and exclusion of trypan blue.

The concentration dependency of the cell surface labeling was studied by incubating Jurkat and CHO-K1 cells with various concentrations of **4** or **5** followed by staining with avidin–FITC (Figure 2.3). As expected, cells displaying azido moieties showed a dose-dependent increase in fluorescence intensity and reliable labeling was achieved at a concentration of 3 μM of **4** or **5**, however, optimal results were obtained at concentrations ranging from 30 to 100 μM. No increase in labeling was observed at concentrations higher than 100 μM due to limited solubility.

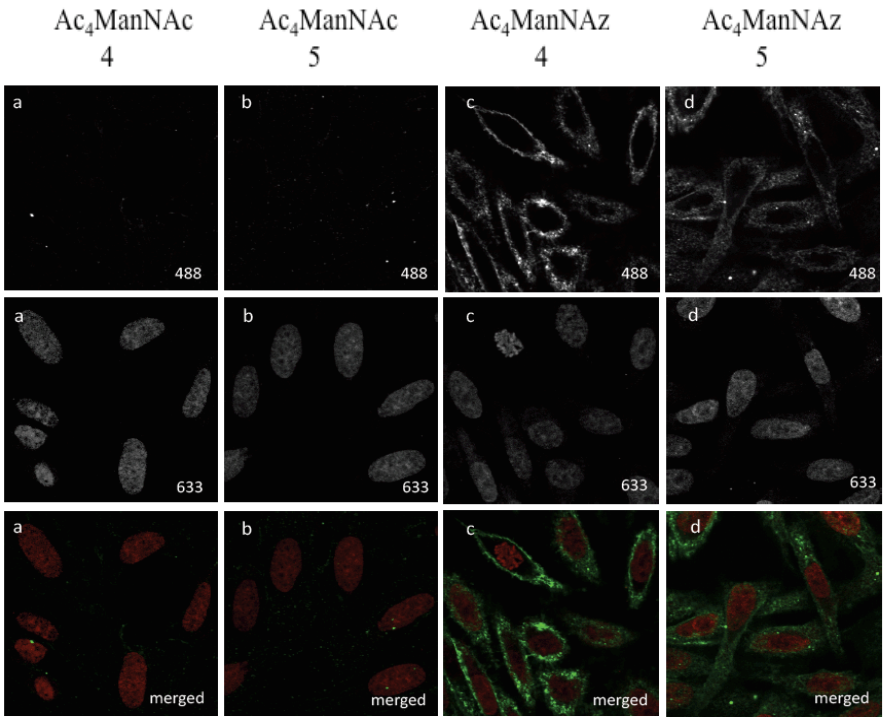

Figure 2.2 Fluorescence images of cells labeled with compounds **4** and **5** and avidin-AlexaFluor 488. CHO cells grown for 2 days in the presence of a, b) Ac_4ManNAc or c, d) Ac_4ManNAz (100 μM) were incubated with compounds a, c) **4** or b, d) **5** (30 μM) for 1 h at room temperature. Next, cells were incubated with avidin-AlexaFluor 488 for 15 min at 4^{o}C and, after washing, fixing, and staining for the nucleus with the far-red-fluorescent dye TOPRO-3 iodide, imaged. Merged indicates that the images of cells labeled with AlexaFluor(488 nm) and TO-PRO (633 nm) are merged and shown in green and red, respectively.

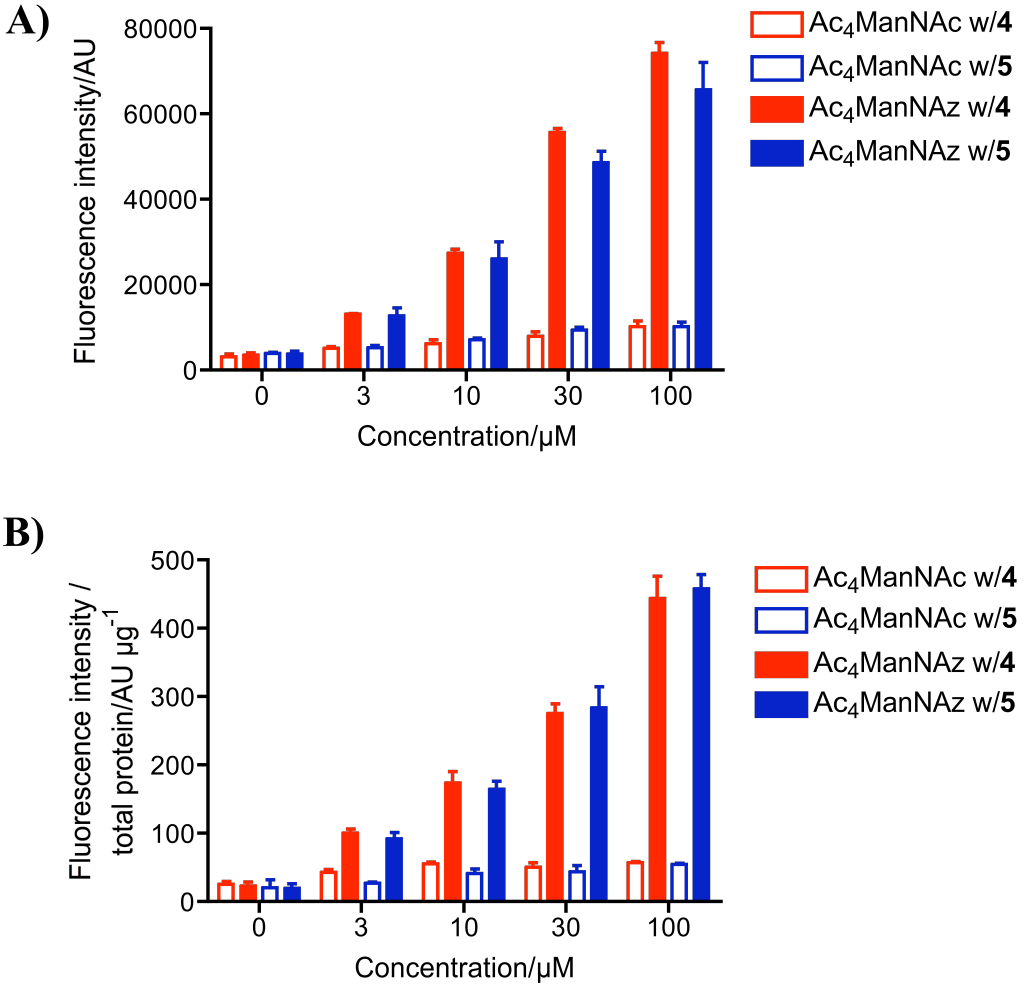

Figure 2.3 Dose-dependency of cell surface labeling with compounds **4** and **5**. A) Jurkat cells grown for 3 days in the presence of Ac_4ManNAc or Ac_4ManNAz (25 μM) and B) CHOK1 cells grown for 2 days in the presence of Ac_4ManNAc or Ac_4ManNAz (100 μM) were incubated with compounds **4** and **5** (0-100 μM) for 1 h at room temperature. Next, cells were incubated with avidin-FITC for 15 min at 4 ^{o}C, after which cell lysates were assessed for fluorescence intensity. AU indicates arbitrary fluorescence units. Data (n=3) are presented as mean ± SD.

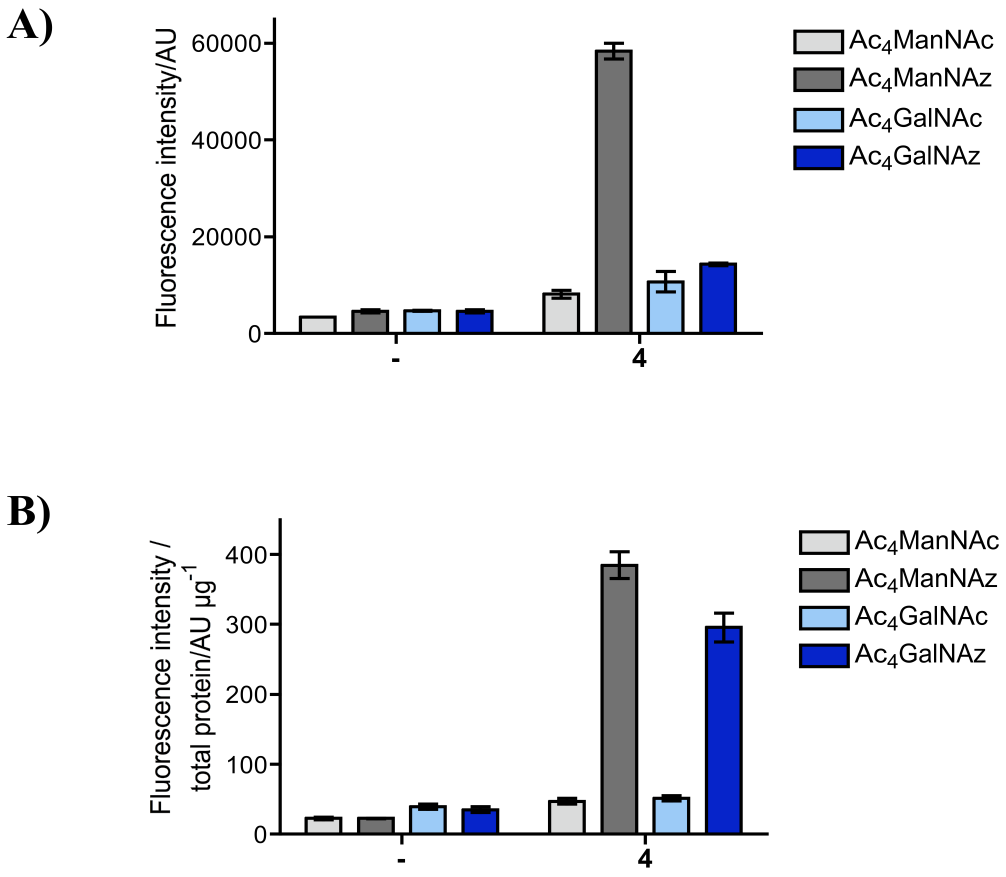

Figure 2.4 Ac_4ManNAz and Ac_4GalNAz labeling of Jurkat and CHO-K1 cells. A) Jurkat cells grown for 3 days in the presence of Ac_4ManNAc, Ac_4ManNAz, Ac_4GalNAc or Ac_4GalNAz (25 µM) and B) CHO-K1 cells grown for 2 days in the presence of Ac_4ManNAc, Ac_4ManNAz, Ac_4GalNAc or Ac_4GalNAz (100 µM) were incubated with compound **4** (30 µM) for 1 h at room temperature. Control cells were incubated in medium only. Next, cells were incubated with avidin-FITC for 15 min at 4°C, after which cell lysates were assessed for fluorescence intensity. AU indicates arbitrary fluorescence units. Data (n=3) are presented as mean ± SD.

Jurkat and CHO-K1 cells were also metabolically labeled with peracetylated *N*-α-azidoacetylgalactosamine (Ac_4GalNAz, 100 μM), which can be metabolized by a number of cells and installed on mucin type glycoproteins.[14] Subsequent treatment of the CHO-K1 cells with **4** followed by avidin–FITC resulted in strong fluorescent labeling whereas weak labeling was observed for Jurkat cells (Figure 2.4). These results are in agreement with the well-known fact that CHO cells produce significant quantities of mucins whereas this is not the case for Jurkat cells.[15]

Having established optimal conditions for SPAAC of azido-modified glycoconjugates of living cells with DIBO reagents, labeling studies were performed with a panel of lectin-resistant (Lec) mutant CHO cells. These cell lines (Lec2, Lec13 and Lec32), which exhibit unique structural changes in surface carbohydrates that reflect specific defects in glycosylation reactions, were expected to be ideally suited for validation of the SPAAC methodology. Lec2 cells have a mutation in the open reading frame of the CMP-sialic acid transporter, and therefore, are unable to translocate CMP-sialic acid into the lumen of the Golgi apparatus, resulting in a marked reduction in glycoprotein and ganglioside sialylation.[16]

Although very small amounts of sialic acid containing glycoconjugates are made by these cells[17] the major class of glycans are asialo, core fucosylated *N*-glycans having LacNAc moieties.[18] Lec32 mutants also exhibit a defect in sialylation due to a reduced expression of CMP-sialic acid synthetase. As a result, these cells have an increase in terminal β-galactoside residues on cell surface glycoproteins.[19] Lec13 mutants exhibit a reduced expression of GDP-Man-4,6-dehydratase activity; this results in a decrease in GDP-fucose biosynthesis and underfucosylation of glycoproteins and glycolipids.[20] The

N-glycan profiles of these cells show increased levels of core nonfucosylated *N*-glycans with the most abundant *N*-glycans being asialo-, mono-, or di-sialylated structures.

Wild-type CHO-K1 and Lec2, Lec13 and Lec32 mutant cells were cultured in the presence of Ac_4ManNAz or Ac_4ManNAz (100 μM) for 2 days and then exposed to biotin-modified DIBO (**4**) for 1 h at room temperature. Next, the cells were washed and labeled with avidin–FITC at 4 °C and the fluorescence intensity measured.

As expected, the wild-type and Lec13 cells gave similar and strong fluorescence intensity readings (Figure 2.5(A)). On the other hand, the Lec2 and Lec32 mutants showed a significant reduction in staining intensity and, in the case of the Lec2 cells; the readings were barely above the control, which indicates that these cells express very low levels of surface sialosides. Thus, the results of these studies are in agreement with the previously described defects in the mutant cell lines and hence support the notion that the chemical reporter strategy can be employed to determine relative quantities of sialylation of glycoconjugates of living cells. Furthermore, treatment of the wild-type cells with *Vibrio cholerae* neuraminidase led to a similar fluorescent reading as control cells, confirming selective azide incorporation into sialic acid (Figure 2.5(A)).

The results of the metabolic labeling studies were compared with traditional lectin staining by using FITC-labeled peanut (*Arachis hypogaea*) agglutinin (PNA) and FITC-labeled *Ricinus communis* (castor bean) agglutinin type 1 (RCA1), which mainly recognize terminal β-Gal-(1-3)-GalNAc residues of *O*-linked structures and β-Gal-(1-4)-GlcNAc (LacNAc) found on *N*-linked glycoproteins, respectively.

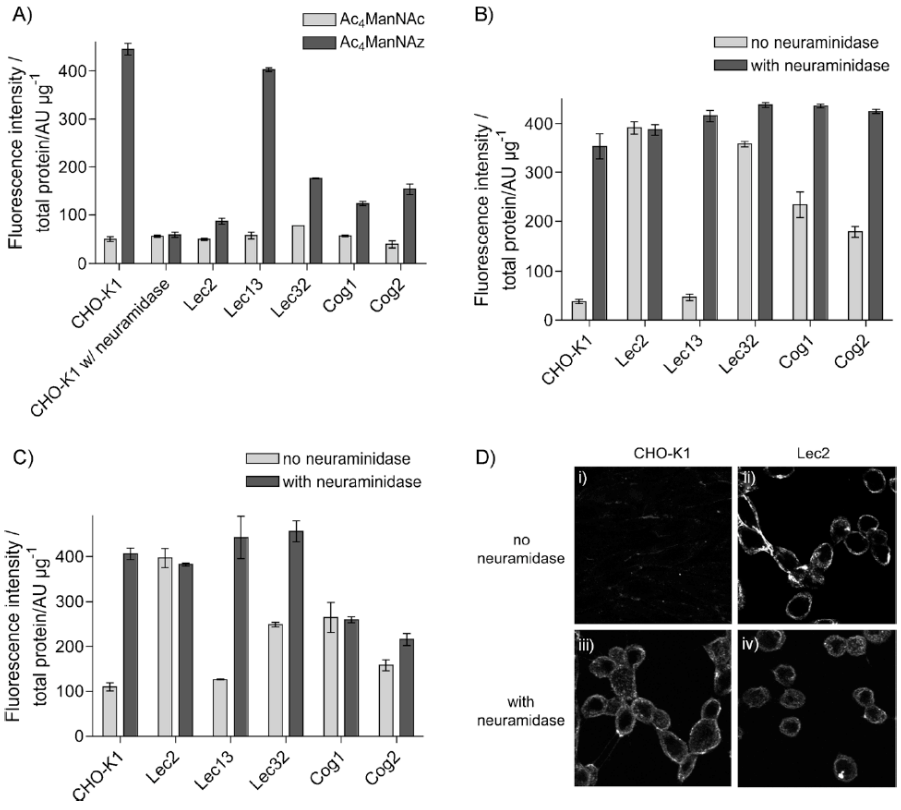

Figure 2.5 SiaNAz expression in CHO-K1 and CHO glycosylation mutant cells and the effect of neuraminidase treatment on cell surface labeling. A) CHO-K1 and CHO mutant cells grown for 2 days in the presence of $Ac_4ManNAc$ or $Ac_4ManNAz$ (100 μM) were incubated, either directly or after treatment with *V. cholerae* neuraminidase (50 mU mL^{-1}) in serum-free culture medium for 2 h at 37 °C, with compound **4** (30 μM) for 1 h at room temperature. Next, cells were incubated with avidin–FITC for 15 min at 4 °C, after which cell lysates were assessed for fluorescence intensity. To assess the effects of desialylation of CHO-K1 and CHO glycosylation mutants on their recognition by PNA and RCA1, cells were incubated, either directly or after treatment with *V. cholerae* neuraminidase (50 mU mL^{-1}), in serum-free culture medium for 2 h at 37 °C with: B) PNA–FITC (50 μg mL^{-1}), or C) RCA1–FITC (50 μg mL^{-1}) for 45 min on ice in the dark. Next cell lysates were assessed for fluorescence intensity. AU indicates arbitrary fluorescence units. Data (n=3) are presented as mean± SD. Similarly, D) CHO-K1 (i, iii) and Lec2 (ii, iv) cells were imaged, either directly (i, ii) or after treatment with *V. cholerae* neuraminidase (iii, iv) with PNA–FITC.

Cells that have intact sialylation machinery modify β-galactosyl residues with sialic acid and hence display low reactivity against PNA and RCA1 lectins. Indeed, the wild-type and Lec13 cells gave fluorescent intensities just above background whereas the Lec2 and Lec32 mutants, which have a defect in sialylation, showed strong staining (Figure 2.5(B–D)). Treatment of the wild-type and Lec13 cells with *V. cholerae* neuramidase resulted in fluorescent intensities similar to that of the Lec2 and Lec32 cells; this indicates that the various cell types express similar quantities of galactosyl-containing glycoproteins.

Furthermore, a similar neuraminidase treatment of Lec2 cells followed by staining with PNA–FITC or RCA1–FITC did not lead to a significant increase in fluorescent intensity; this demonstrates that these cells do not significantly modify their cell surface glycoconjugates with sialic acid. On the other hand, neuraminidase treatment of Lec32 cells resulted in an increase in fluorescence staining with RCA1–FITC, whereas it did not impact the reading of PNA–FITC. These results indicate that the *N*-linked glycans of Lec32 contain some sialosides whereas this modification is absent in *O*-linked residues. The lectin staining (Figure 2.5(B–D)) and metabolic labeling followed by SPAAC (Figure 2.5 (A)) gave similar results and in particular both approaches showed that Lec2 cells express very small quantities of sialosides whereas the Lec32 mutant attach some sialic acid to their glycoconjugates.

Surprisingly, a shortage of CMP-Neu5Ac as in Lec32 cells resulted in differential sialylation of *N*- and *O*-linked glycans and it appears that *N*- but not *O*-linked glycans are modified by some sialic acid. Finally, both approaches showed that a defect in fucosylation does not impact the level of glycoconjugate sialylation. Attempts were made

to directly assess differences in sialylation within the Lec mutants by utilizing lectins that recognize α(2,3)- or α(2,6)-linked terminal sialic acid residues (MAA and LFA). Surprisingly, we found fluorescence intensity for both lectins to be comparable in wild-type and Lec2 mutants; this suggests that these lectins might recognize additional sugar structures other than terminal sialic acid and are not suitable for this study. Thus, we believe that the chemical reporter strategy provides a more reliable approach to determine relative differences in glycoprotein sialylation.

Having established biotin-modified DIBO (**4**) as a reliable reagent for detection of cell surface sialosides, attention was focused on sialylation of the CHO mutants Cog1 (*ldlB*) and Cog2 (*ldlC*). These cell lines were identified in a genetic screen for mutations that block low-density lipoprotein receptor (LDLR) activity.[21] Further examinations have shown that these cell lines have defects in the conserved oligomeric Golgi (COG) complex, which is a protein complex consisting of eight subunits (Cog1–8) that play a critical role in retrograde vesicle transport and intra-Golgi trafficking. Malfunctions in the COG complex impact Golgi integrity and result in defects in protein sorting and glycosylation.[22] Mutations in COG subunits have also been observed in humans and result in severe congenital disorders of glycosylation (CDG).[23]

Metabolic labeling of Cog1 and Cog2 cells with ManNAz followed by SPAAC with **4** and staining with avidin–FITC showed that these cells produce sialylated glycoconjugates, however, at a significantly reduced level compared to wild-type CHO-K1 cells (Figure 2.5(A)). Staining with PNA–FITC demonstrated that that the cells expose terminal galactosyl residues on their *O*-linked glycans (Figure 2.5(B)). Furthermore, treatment of the cells with *V. cholerae* neuraminidase led to a similar

staining intensity as for wild-type cells. This indicates that both cell types express similar quantities of galactosyl moieties, and thus it appears that in Cog1 and -2 cells, glycoprotein sialylation of *O*-glycans is more severely imparted than galactosylation. Interestingly, a different staining profile was obtained when RCA1–FITC was employed (Figure 2.5(C)) and in this case untreated and neuraminidase exposed cells gave similar but reduced fluorescent intensities highlighting that *N*-glycan sialylation and galactosylation are both affected in the Cog1 and Cog2 mutants. These results suggest that loss of COG complex function might affect the localization and/or stability of glycosyltransferases involved in terminal processing of *N*-glycans to a greater extent than those enzymes that modify *O*-glycans.

In support of this hypothesis, recent studies have shown that the stability of β(1,4)-galactosyltransferase is altered in COG-depleted HeLa cells due to altered trafficking and proteasomal degradation.[24] At this point, we can, however, not rule out the possibility that these differences are due to the type and amount of glycoprotein cargo that is modified in the Golgi of these cells.

2.3 CONCLUSIONS

The past several years has seen a rapid development of the bioorthogonal chemical reporter methodology for the labeling of glycoconjugates of living cells and whole organisms. In this chapter, we present DIBO (**4**) and its derivative (**5**), as ideal bioorthogonal reagents for the chemical reporter strategy. Attractive features of DIBO include easy access by a simple and scalable synthesis approach, nontoxicity and straightforward attachment of a variety of probes. The use of several cell lines with

known defects in glycoconjugate glycosylation validated DIBO as a reagent for determining relative quantities of cell surface glycoconjugate sialylation. The chemical reporter strategy in combination with lectin staining revealed that *O*-glycan sialylation of Cog1 and -2 cells is more severely impacted than galactosylation. Surprisingly, sialylation and galactosylation of *N*-glycans were similarly affected in these mutant cell lines. These results suggest that loss of COG complex function might differently affect the localization and/or stability of glycosyltransferases involved in terminal processing of *N*- and *O*-glycans. Differential modulation of *N*- and *O*-linked sialylation was also observed in Lec32 cells, which exhibit a reduced expression of CMP-sialic acid synthetase, and in this case *N*-linked oligosaccharides acquire some sialic acid moieties whereas this is not the case for *O*-linked structures. It is well known that the various cell types express different ensembles of glycans. The results of this study indicate that a limited availability of sugar nucleotides is one way for a cell to selectively modulate the structures of glycoprotein glycans. We anticipate multiple applications of the described chemical reporter methodology in glycobiology and glycomedicine, including the tagging and isolation of glycoproteins from cell and tissue extracts as well as the investigation of trafficking and turnover of glycoconjugates in healthy and diseased cells.

2.4 MATERIALS AND METHODS

2.4.1 REAGENTS

Synthetic compounds **4** and **5** were reconstituted in DMF and stored at −80 °C. Final concentrations of DMF never exceeded 0.56 % to avoid toxic effects. Ac_4ManNAc, Ac_4ManNAz, Ac_4GalNAc and Ac_4GalNAz were synthesized as reported[31] and

reconstituted in ethanol. Avidin–FITC and avidin–AlexaFluor488 were obtained from Molecular Probes, *V. cholerae* neuraminidase was from Sigma–Aldrich, and PNA–FITC and RCA1–FITC were from EY Laboratories.

2.4.2 CELL CULTURE CONDITIONS

Human Jurkat cells (clone E6-1; ATCC) were cultured in RPMI 1640 medium (ATCC) with L-glutamine (2 mM), adjusted to contain sodium bicarbonate (1.5 $g\,L^{-1}$), glucose (4.5 $g\,L^{-1}$), HEPES (10 mM), and sodium pyruvate (1 mM). CHO cells (clone K1; ATCC) were cultured in Kaighn's modification of Ham's F12 medium (ATCC) with L-glutamine (2 mM), adjusted to contain sodium bicarbonate (1.5 $g\,L^{-1}$). Mutant CHO cells (Lec2, Lec13, Lec32 mutants were obtained from Dr. Pamela Stanley and Cog1 and Cog2 mutants (*ldlB* and *ldlC*) obtained from Dr. Monty Kreiger) were cultured in minimum essential medium Alpha 1X (Cellgro) with Earle's salts, ribonucleosides, deoxyribonucleosides and Lglutamine (2 mM). All media were supplemented with penicillin (100 $U\,mL^{-1}$)/streptomycin (100 $\mu g\,mL^{-1}$; Mediatech) and fetal bovine serum (FBS, 10 %; Hyclone). Cells were maintained in a humid 5 % CO_2 atmosphere at 37 °C.

2.4.3 CELL SURFACE AZIDE LABELING

Jurkat cells were seeded at a density of 75 000 cells per mL in a total volume of 40 mL culture medium in the presence of Ac_4ManNAz or Ac_4GalNAz (25 μM final concentration) and grown for 3 days; this led to the metabolic incorporation of the corresponding *N*-azidoacetyl sialic acid (SiaNAz) or azido-GalNAz into their cell surface glycoproteins. Control cells were grown in the presence of Ac_4ManNAc or Ac_4GalNAc

(25 μM final concentration) for 3 days. CHO cells were plated in 12-well plates (250 000 cells per well) and grown in medium that contained Ac_4ManNAz or Ac_4GalNAz (100 μM) and as control cells Ac_4ManNAc or Ac_4GalNAc (100 μM) for 2 days. Expected cell number on day of click chemistry was approximately 1×10^6 per well.

2.4.4 SIALIDASE PRETREATMENT

Cells were washed twice with serum-free culture medium and incubated with *V. cholerae* neuraminidase (50 mU mL^{-1}) in serum-free culture medium for 2 h at 37 °C, washed in PBS and subjected to the respective assay.

2.4.5 CLICK CHEMISTRY AND DETECTION BY FLUORESCENCE INTENSITY

Jurkat cells bearing azides and control cells were washed with labeling buffer (DPBS, pH 7.4 containing 1 % FBS and 1 % BSA) and transferred to round-bottom tubes (1×10^6 cells per sample). CHO cells (untreated or sialidase pretreated) were left in the 12-well plates (~1×10^6 cells per sample) and washed with labeling buffer. Next, cells were incubated with the biotinylated compounds **4** or **5** (0–100 μM) in labeling buffer for 0–90 min at room temperature. The cells were washed three times with cold labeling buffer and then incubated with avidin–FITC (5 μg mL^{-1}) for 15 min at 4 °C in the dark. Following three washes and cell lysis in passive lysis buffer (Promega), lysates were analyzed for fluorescence intensity (λ_{em}=520/λ_{ex}=485) by using a microplate reader (BMG Labtech). Data points were collected in triplicate and are representative of three separate experiments. Fluorescence of Jurkat cell lysates was expressed as fluorescence

(arbitrary units; AU) per 800 000 cells. CHO cell lysates were assayed for total protein by using the bicinchoninic acid assay (BCA; Pierce Biotechnology) and fluorescence intensity was expressed as fluorescence (AU) per μg total protein.

2.4.6 LECTIN BINDING ASSAY

Untreated or sialidase pretreated cells (~1×10^6) were washed twice in cold PBS and subsequently incubated in 300 μL PBS containing PNA–FITC (50 $\mu g\,mL^{-1}$) or RCA1–FITC (50 $\mu g\,mL^{-1}$) for 45 min on ice in the dark. After being washed with cold PBS, the cells were lyzed in passive lysis buffer (Promega) and lysates were analyzed for fluorescence intensity (λ_{em}=520/λ_{ex}=485) by using a microplate reader.

2.4.7 DETECTION OF CELL LABELING AND LECTIN STAINING BY FLUORESCENCE MICROSCOPY

For cell surface labeling, CHO-K1 cells labeled with Ac_4ManNAc or Ac_4ManNAz (100 μM) for 2 days were seeded at a density of 50 000 cells per coverslip (22 mm) and allowed to adhere, overnight, in their original medium. After two washes with wash buffer (DPBS, supplemented with 1 % FBS), live cells were incubated with biotinylated compounds **4** or **5** (30 μM) in wash buffer for 1 h at room temperature, followed by three washes in wash buffer (10 min per wash). Next, the cells were incubated with avidin conjugated with AlexaFluor488 (5 $\mu g\,mL^{-1}$) for 15 min at 4 °C. Cells were washed three times with wash buffer and fixed with formaldehyde (3.7 % in PBS) at room temperature for 15 min.

After the coverslips were washed four times in PBS (5 min per wash), the nucleus was labeled with the far red-fluorescent TO-PRO-3 iodide dye (Molecular Probes). The cells were mounted with PermaFluor (Thermo Electron Corporation) before being imaged.

For lectin staining of cell surface glycans, CHO-K1 and Lec2 cells were seeded at a density of 50 000 cells per coverslip (22 mm) and allowed to adhere, overnight. After two washes with serum-free culture medium, live cells were treated with *V. cholerae* neuraminidase (50 mU mL^{-1}) in serum-free culture medium for 2 h at 37 °C. Coverslips were washed with DPBS and incubated with PNA–FITC (50 μg mL^{-1}) in PBS supplemented with BSA (1 %) for 45 min at 4 °C. Cells were washed with PBS and fixed and mounted as above.

Initial analysis was performed on a Zeiss Axioplan2 fluorescent microscope. Confocal images were acquired by using a 60× (NA1.42) oil objective. Stacks of optical sections were collected in the *z* dimensions. The step size, based on the calculated optimum for each objective, was between 0.25 and 0.5 μm. Subsequently, each stack was collapsed into a single image (*z* projection). Analysis was performed offline by using ImageJ 1.39f software (National Institutes of Health, USA) and Adobe Photoshop CS3 Extended Version 10.0 (Adobe Systems Incorporated), whereby all images were treated equally.

2.4.8 STATISTICAL ANALYSIS

Statistical significance between groups was determined by two-tailed, unpaired Student's *t* test. Differences were considered significant when $P<0.05$.

2.5 REFERENCES

(1) (a) E. M. Sletten, C. R. Bertozzi. *Angew. Chem. Int. Ed.* **2009**, 48, 6974- 6998; (b) G. J. *Boons, in Carbohydrate Chemistry: Chemical and Biological Approaches*, Vol. 36 (Eds.: A. Pilar Rauter, T. K. Lindhorst), RSC Publishing, **2010**, pp. 152-167; (c) M. F. Debets, C. W. J. van der Doelen, F. P. J. T. Rutjes, F. L. van Delft. *ChemBioChem* **2010**, 11, 1168-1184; (d) J. C. Jewett, C. R. Bertozzi. *Chem. Soc. Rev*. **2010**, 39, 1272-1279.

(2) (a) J. A. Johnson, J. M. Baskin, C. R. Bertozzi, J. T. Koberstein, N. J. Turro. *Chem. Commun.* **2008**, 3064-3066; (b) C. Ornelas, J. Broichhagen, M. Weck. *J. Am. Chem. Soc.* **2010**, 132, 3923-3931; (c) P. A. Ledin, F. Friscourt, J. Guo, G. J. Boons. *Chem.-Eur. J.* **2011**, 17, 839-846.

(3) E. Lallana, E. Fernandez-Megia, R. Riguera. *J. Am. Chem. Soc.* **2009**, 131, 5748-5750.

(4) S. V. Orski, A. A. Poloukhtine, S. Arumugam, L. Mao, V. V. Popik, J. Locklin. *J. Am. Chem. Soc.* **2010**, 132, 11024-11026.

(5) (a) D. H. Ess, G. O. Jones, K. N. Houk. *Org. Lett.* **2008**, 10, 1633-1636; (b) R. D. Bach. *J. Am. Chem. Soc.* **2009**, 131, 5233-5243; (c) K. Chenoweth, D. Chenoweth, W. A. Goddard. *Org. Biomol. Chem.* **2009**, 7, 5255-5258; (d) F. Schoenebeck, D. H. Ess, G. O. Jones, K. N. Houk. *J. Am. Chem. Soc.* **2009**, 131, 8121-8133.

(6) (a) J. M. Baskin, J. A. Prescher, S. T. Laughlin, N. J. Agard, P. V. Chang, I. A. Miller, A. Lo, J. A. Codelli, C. R. Bertozzi. *Proc. Natl. Acad. Sci. U. S. A.* **2007**, 104, 16793 16797; (b) J. A. Codelli, J. M. Baskin, N. J. Agard, C. R. Bertozzi. *J. Am. Chem. Soc.* **2008**, 130, 11486-11493.

(7) S. T. Laughlin, J. M. Baskin, S. L. Amacher, C. R. Bertozzi. *Science* **2008**, 320, 664-667.

(8) X. H. Ning, J. Guo, M. A. Wolfert, G. J. Boons. *Angew. Chem. Int. Ed.* **2008**, 47, 2253-2255.

(9) A. A. Poloukhtine, N. E. Mbua, M. A. Wolfert, G. J. Boons, V. V. Popik. *J. Am. Chem. Soc.* **2009**, 131, 15769-15776.

(10) (a) X. Ning, R. P. Temming, J. Dommerholt, J. Guo, D. B. Ania, M. F. Debets, M. A. Wolfert, G. J. Boons, F. L. van Delft. *Angew. Chem. Int. Ed.* **2010**, 49, 3065-3068; (b) B. C. Sanders, F. Friscourt, P. A. Ledin, N. E. Mbua, S. Arumugam, J. Guo, T. J. Boltje, V. V. Popik, G. J. Boons. *J. Am. Chem. Soc.* **2011**, 133, 949-957.

(11) (a) M. F. Debets, S. S. van Berkel, S. Schoffelen, F. P. J. T. Rutjes, J. C. M. van Hest, F. L. van Delft. *Chem. Commun.* **2010**, 46, 97-99; (b) J. C. Jewett, E. M. Sletten, C. R. Bertozzi. *J. Am. Chem. Soc.* **2010**, 132, 3688-3690; (c) E. M. Sletten, H. Nakamura, J. C. Jewett, C. R. Bertozzi. *J. Am. Chem. Soc.* **2010**, 132, 11799-11805.

(12) E. Saxon, C. R. Bertozzi. *Science* **2000**, 287, 2007-2010.

(13) H. C. Hang, C. Yu, D. L. Kato, C. R. Bertozzi. *Proc. Natl. Acad. Sci. U. S. A.* **2003**, 100, 14846-14851.

(14) V. Piller, F. Piller, M. Fukuda. *J. Biol. Chem.* **1990**, 265, 9264-9271.

(15) M. Eckhardt, B. Gotza, R. Gerardy-Schahn. *J. Biol. Chem.* **1998**, 273, 20189-20195.

(16) (a) P. Stanley, T. Sudo, J. P. Carver. *J. Cell Biol.* **1980**, 85, 60-69; (b) S. F. Lim, M. M. Lee, P. Zhang, Z. Song. *Glycobiology* **2008**, 18, 851-860.

(17) S. J. North, H. H. Huang, S. Sundaram, J. Jang-Lee, A. T. Etienne, A. Trollope, S. Chalabi, A. Dell, P. Stanley, S. M. Haslam. *J. Biol. Chem.* **2010**, 285, 5759-5775.

(18) B. Potvin, T. S. Raju, P. Stanley. *J. Biol. Chem.* **1995**, 270, 30415-30421.

(19) (a) J. Ripka, A. Adamany, P. Stanley. *Arch. Biochem. Biophys.* **1986**, 249, 533-545; (b) C. Ohyama, P. L. Smith, K. Angata, M. N. Fukuda, J. B. Lowe, M. Fukuda. *J. Biol. Chem.***1998**, 273, 14582-14587; (c) F. X. Sullivan, R. Kumar, R. Kriz, M. Stahl, G. Y. Xu, J. Rouse, X. J. Chang, A. Boodhoo, B. Potvin, D. A. Cumming. *J. Biol. Chem.* **1998**, 273, 8193- 8202.

(20) M. Krieger, M. S. Brown, J. L. Goldstein. *J. Mol. Biol.* **1981**, 150, 167-184.

(21) (a) T. Oka, D. Ungar, F. M. Hughson, M. Krieger. *Mol. Biol. Cell* **2004**, 15, 2423-2435; (b) S. N. Zolov, V. V. Lupashin. *J. Cell. Biol.* **2005**, 168, 747- 759; (c) A. Shestakova, S. Zolov, V. Lupashin. *Traffic* **2006**, 7, 191-204; (d) R. Steet, S. Kornfeld. *Mol. Biol. Cell* **2006**, 17, 2312-2321.

(22) (a) X. Wu, R. A. Steet, O. Bohorov, J. Bakker, J. Newell, M. Krieger, L. Spaapen, S. Kornfeld, H. H. Freeze. *Nat. Med.* **2004**, 10, 518-523; (b) F. Foulquier, E. Vasile, E. Schollen, N. Callewaert, T. Raemaekers, D. Quelhas, J. Jaeken, P. Mills, B. Winchester, M. Krieger, W. Annaert, G. Matthijs. *Proc. Natl. Acad. Sci. U. S. A.* **2006**, 103, 3764-3769; (c) F. Foulquier, D. Ungar, E. Reynders, R. Zeevaert, P.

Mills, M. T. Garcia- Silva, P. Briones, B. Winchester, W. Morelle, M. Krieger, W. Annaert, G. Matthijs. *Hum. Mol. Genet.* **2007**, 16, 717-730; (d) C. Kranz, B. G. Ng, L. Sun, V. Sharma, E. A. Eklund, Y. Miura, D. Ungar, V. Lupashin, R. D. Winkel, J. F. Cipollo, C. E. Costello, E. Loh, W. Hong, H. H. Freeze. *Hum. Mol. Genet.* **2007**, 16, 731-741; (e) R. Zeevaert, F. Foulquier, J. Jaeken, G. Matthijs. *Mol. Genet. Metab.* **2008**, 93, 15-21; (f) P. Paesold-Burda, C. Maag, H. Troxler, F. Foulquier, P. Kleinert, S. Schnabel, M. Baumgartner, T. Hennet. *Hum. Mol. Genet.* **2009**, 18, 4350-4356; (g) E. Reynders, F. Foulquier, E. Leao Teles, D. Quelhas, W. Morelle, C. Rabouille, W. Annaert, G. Matthijs. *Hum. Mol. Genet.* **2009**, 18, 3244-3256.

(23) R. Peanne, D. Legrand, S. Duvet, A. M. Mir, G. Matthijs, J. Rorher, F. Foulquier. *Glycobiol.* **2010**, Epub ahead of print.

(24) S. T. Laughlin, C. R. Bertozzi. *Nat. Protoc.* **2007**, 2, 2930-2944.

CHAPTER 3

ABNORMAL ACCUMULATION OF SIALYLATED GLYCOPROTEINS VISUALIZED IN NIEMANN-PICK TYPE C CELLS USING THE CHEMICAL REPORTER STRATEGY

3.1 INTRODUCTION

The fatal lysosomal disorder, Niemann-Pick type C (NPC) results from mutations in genes encoding NPC1 or NPC2, proteins that act in coordination to mediate the efflux of unesterified cholesterol from lysosomes.[1, 2] Loss of these proteins causes abnormal accumulation of cholesterol in neurons and other cell types, resulting in neuronal degeneration and hepatosplenomegaly.[3, 4] The pathophysiology of NPC disease is complex and may be related to the primary accumulation of cholesterol and secondary storage of other lipids such as glycosphingolipids and sphingosine.[5, 6] Accompanying lipid storage, NPC cells exhibit defects in endocytic transport such as altered recycling of specific cell surface glycoproteins.[7-9] The molecules and pathways implicated in the latter defects have been difficult to analyze due to a lack of technology that can monitor the localization and accumulation of endogenous glycoproteins and glycolipids *en masse.* Most cellular studies have instead relied on the exogenous addition of tagged glycolipids and non-natural dextrans, which may behave differently than their natural counterparts,[10] or the analysis of single glycoprotein markers that limits the range of itinerant trafficking pathways that can be effectively probed. The chemical reporter strategy is emerging as a versatile approach to visualize and capture glycoconjugates of living systems.[11, 12] In this approach, a unique chemical functionality (reporter) is incorporated into glycoconjugates

by feeding a modified biosynthetic precursor. The latter can then be reacted with a complementary bio-orthogonal functional group, which in turn is linked to a probe. The azide is the most versatile chemical reporter because of its small size, bio-orthogonality and diverse mode of reactivity. It can be tagged by Staudinger ligation using modified phosphines, by a copper (I)-catalyzed cycloaddition with terminal alkynes (CuAAC), or by a strain-promoted alkyne-azide cycloaddition (SPAAC) using cyclooctynes.[13, 14]

Although chemical reporter strategies have been applied to visualize glycans in living cells and model organisms, insights into the functional relevance of glycans in normal and disease biology have yet to emerge from these technologies.[14-17] Here, we demonstrate a previously unrecognized accumulation of glycoproteins in NPC1 and NPC2 fibroblasts using, for the first time, a powerful combination of SPAAC-based chemical reporter strategy and pharmacological treatments. It provides new insights into trafficking defects in NPC cells and highlights the utility of visualizing glycoconjugates *en masse* to uncover novel aspects of human disease.

3.2 RESULTS AND DISCUSSIONS

Control and disease fibroblasts were fed the sialic acid precursor, peracetylated *N*-α-azidoacetylmannosamine (Ac_4ManNAz), which can be incorporated into glycoproteins and gangliosides as *N*-azidoacetyl sialic acid (SiaNAz). The resulting azido-modified glycoconjugates were visualized by confocal microscopy after cycloaddition with biotin-modified dibenzylcyclooctynol (DIBO) followed by treatment with streptavidin-568. The DIBO compound was chosen for this study due to its ability to detect both intracellular and extracellular glycoconjugates.[18] While staining of Golgi, cell surface and

extracellular matrix (ECM) was primarily detected in control fibroblasts, striking additional accumulation of sialylated glycoconjugates was observed within intracellular vesicles in NPC1 (Figure 3.1) and NPC2 cells (Figure 3.2). This phenotype appeared to be specific to NPC cells as no obvious vesicular accumulation was noted in mucolipidosis IV (ML-IV) or mucopolysaccharidosis I (MPS-I) fibroblasts (Figure 3.2), which exhibit different types of storage defects.

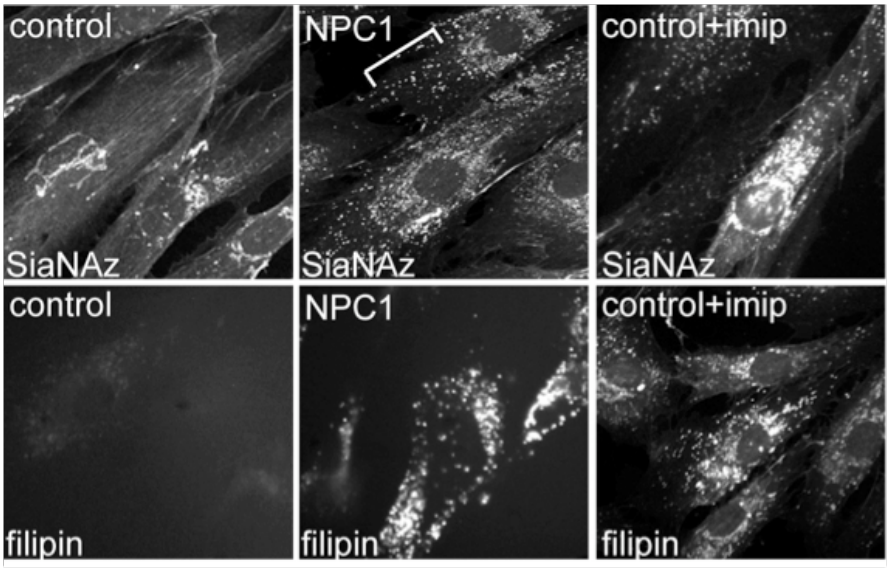

Figure 3.1 Sialylated molecules accumulate within intracellular vesicles in NPC1-null fibroblasts and imipramine-treated control fibroblasts. (top panels) Ac_4ManNAz-labeled control, NPC1 fibroblasts and imipramine (imip)-treated control fibroblasts incubated with DIBO and streptavidin-conjugated fluorophore; (bottom panels), filipin staining of the same cells and conditions. Imipramine treatment of control fibroblasts leads to a similar accumulation of sialylated molecules as noted in NPC fibroblasts.

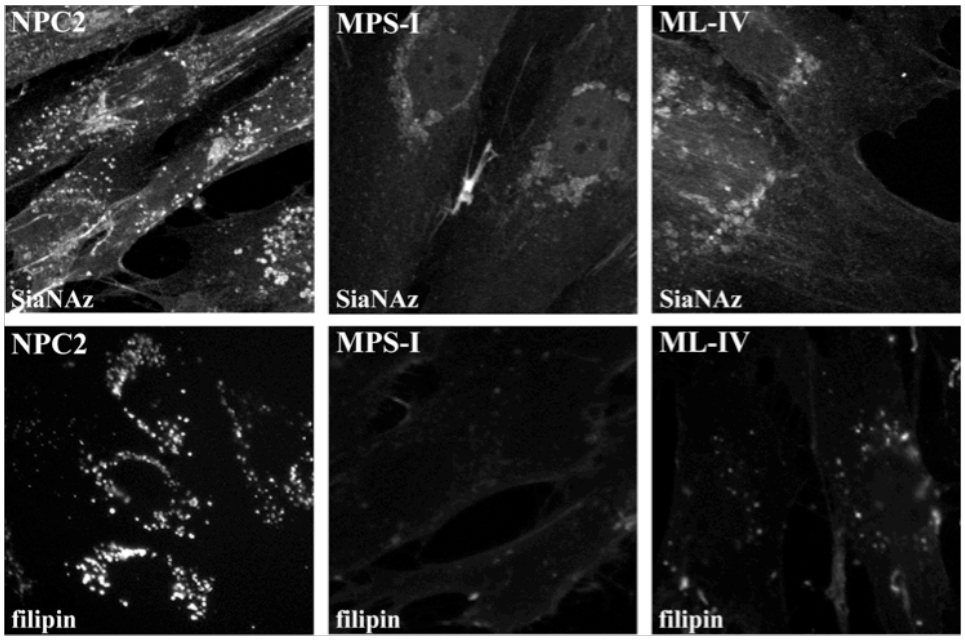

Figure 3.2 Vesicular SiaNAz staining is detected in NPC2 but not MPS-I and ML-IV fibroblasts. NPC2, MPS-I and ML-IV fibroblasts were cultured in the presence of Ac_4ManNAz for 24 h prior to incubation with DIBO and filipin. Filipin-stained cells were imaged by fluorescence microscopy while the SiaNAz-stained cells were analyzed by confocal microscopy. Note the lack of vesicular SiaNAz staining and cholesterol storage in MPS-I and ML-IV cells.

Furthermore, treatment of control fibroblasts with the anti-depressant imipramine, which is a known chemical inducer of intracellular cholesterol storage,[19] also resulted in the accumulation of sialylated glycoconjugates (Figure 3.1), whereas treatment with phenelzine, which is another anti-depressant that does not induce cholesterol storage, did not cause this type of phenotype. These observations suggest a correlation between cholesterol and glycoconjugate storage.

To further probe the specificity of the storage, cells were labeled with peracetylated *N*-α-azidoacetylgalactosamine (Ac_4GalNAz), which can be incorporated into *O*-linked glycans and glycosaminoglycans. In this case, azido-modified glycoconjugates in control cells were primarily detected within the nucleus, ECM and Golgi whereas NPC1-null fibroblasts again exhibited additional vesicular staining (Figure 3.3).

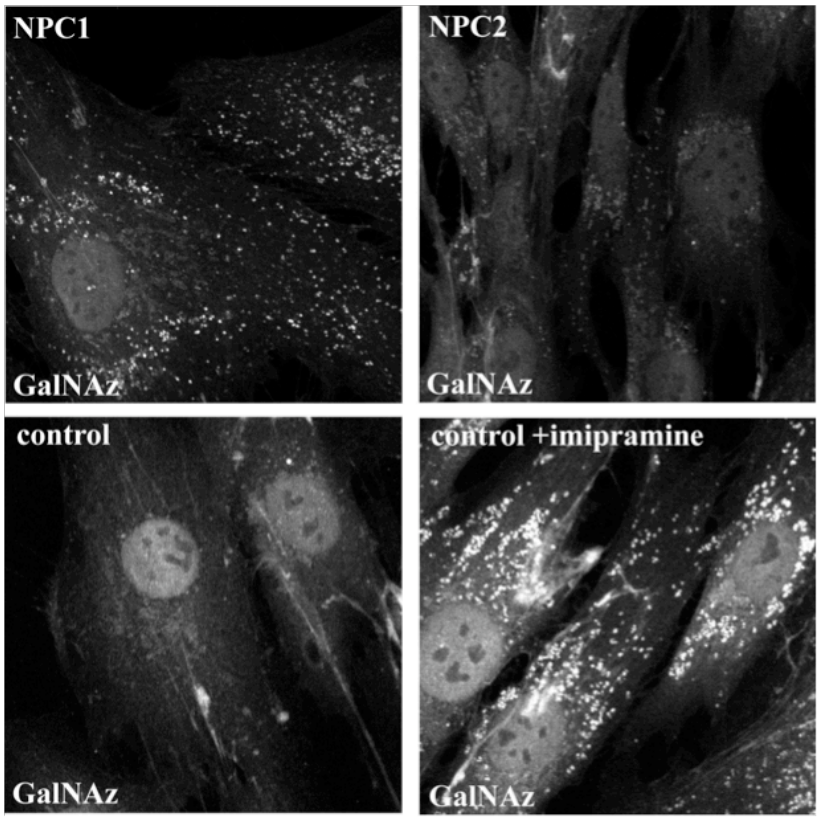

Figure 3.3 Vesicular GalNAz staining is detected in NPC1, NPC2 and imipramine treated control fibroblasts. Fibroblast cultures were labeled in the presence of Ac_4GalNAz for 24 h prior to incubation with DIBO. Stained cells were imaged by confocal microscopy.

This finding indicates that intracellular vesicles of NPC1-null fibroblasts contain glycosaminoglycans and/or O-glycans, in addition to sialoglycoproteins and gangliosides. The GalNAz phenotype was also seen in NPC2 fibroblasts and imipramine-treated control cells, although the intensity of staining was somewhat reduced compared to SiaNAz. Together, these data indicate that storage of cholesterol, induced by genetic or chemical means, is associated with the intracellular accumulation of a wide variety of glycoconjugates.

To examine possible co-localization of the accumulated glycoconjugates with cholesterol-filled lysosomes, NPC1 cells were metabolically labeled with Ac_4ManNAz and the resulting sialylated compounds visualized by successive treatment with DIBO-biotin and streptavidin-568. Co-staining with filipin was performed to detect cholesterol and the resulting fluorescence images clearly demonstrated little or no co-localization of cholesterol- and SiaNAz-positive vesicles (Figure 3.4(A)), indicating that internalized cell surface sialoglycoconjugates are excluded from cholesterol-laden lysosomes of NPC cells. Complete separation of sialylated glycoconjugates and cholesterol was also seen in NPC2 deficient fibroblasts, further demonstrating that cholesterol storage, and not impaired NPC1 function, is the primary mechanism underlying the exclusion of SiaNAz-positive molecules from cholesterol-containing compartments (Figure 3.5).

To better define the localization of the SiaNAz-positive vesicles in NPC1-null fibroblasts, Ac_4ManNAz-labeled control and NPC1 fibroblasts were subjected to DIBO-biotin and incubated with antibodies against early endosome antigen protein 1 (EEA1) for early endosome identification, CD63 for late endosomes and multivesicular bodies and lysosomal associated membrane protein 1 (LAMP1) for lysosomes.

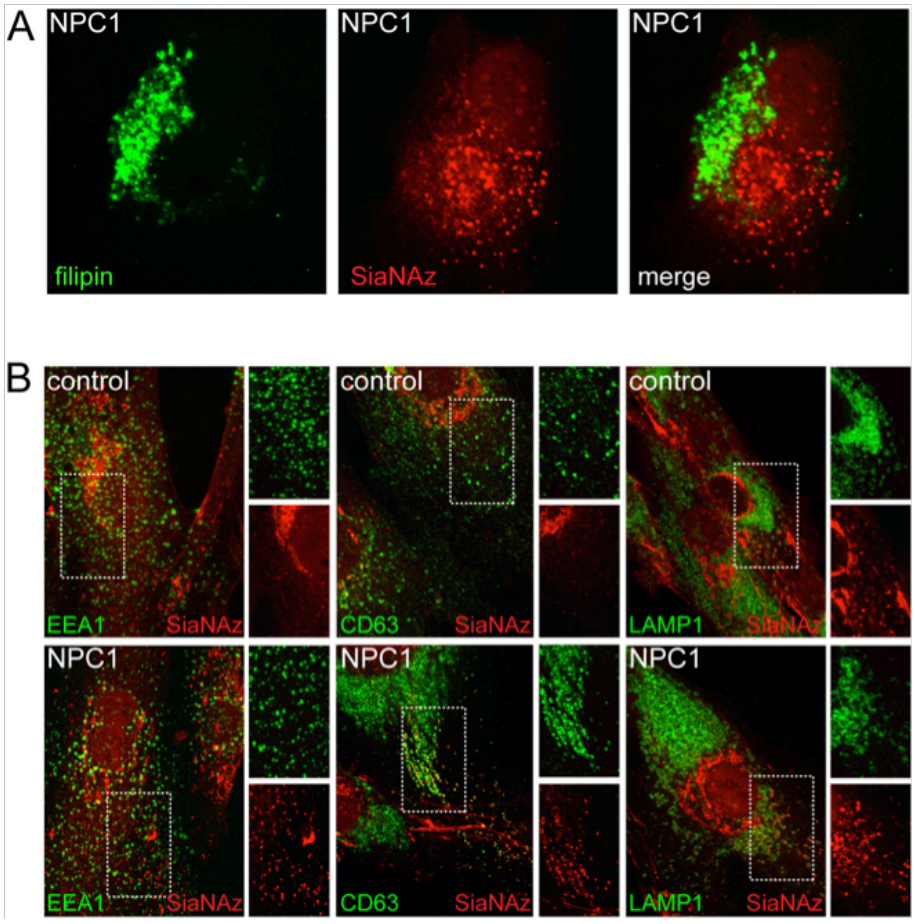

Figure 3.4 SiaNAz-labeled molecules are excluded from cholesterol-laden compartments and exhibit partial co-localization with endosomal markers in NPC1 fibroblasts. (A) NPC1-null fibroblasts were labeled with Ac_4ManNAz and incubated with DIBO and streptavidin-568 followed by filipin staining. A representative image is shown. (B) Ac_4ManNAz-labeled control and NPC1 fibroblasts were incubated with DIBO, co-stained with monoclonal antibodies to EEA1, CD63, and LAMP1 and then incubated with appropriate secondary antibodies and visualized by confocal microscopy.

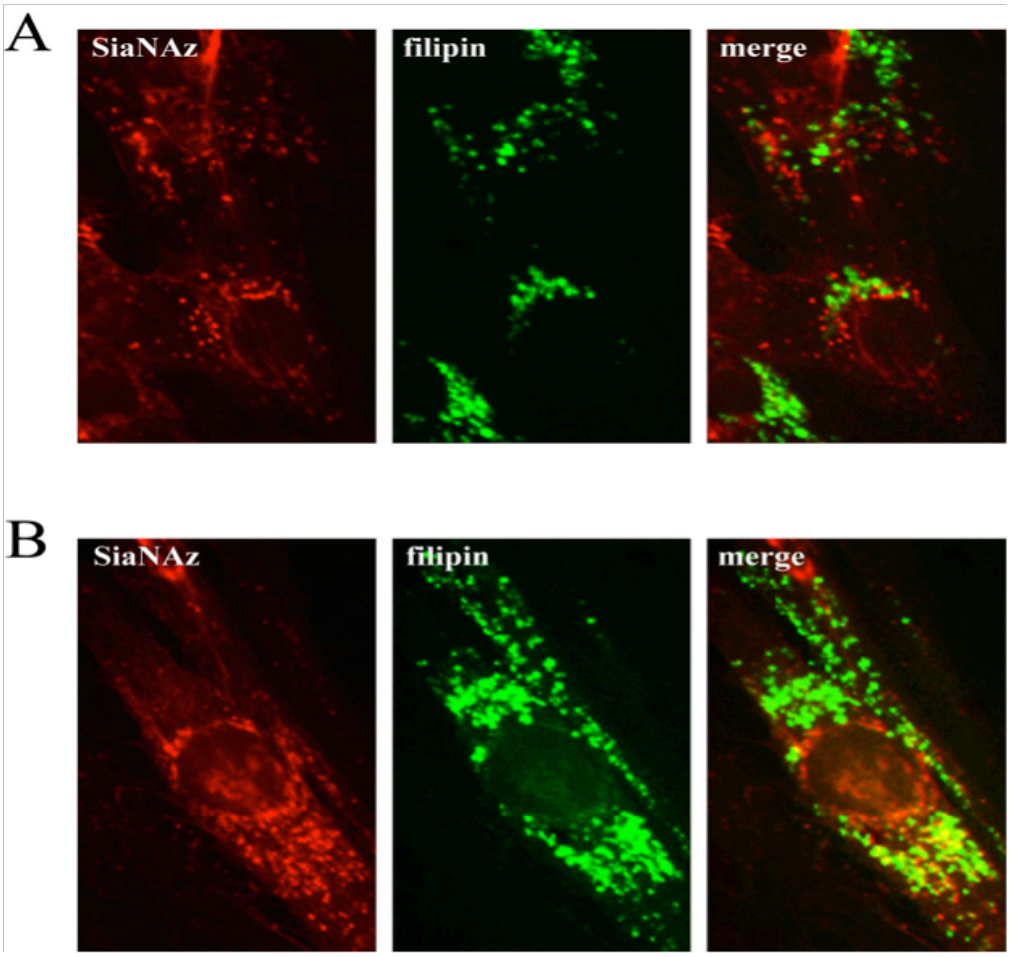

Figure 3.5 Co-localization of cholesterol and SiaNAz in NPC2 and imipramine-treated control fibroblasts. NPC2 fibroblasts (panel A) and imipramine-treated control fibroblasts (panel B) were labeled with Ac_4ManNAz for 48 h, incubated with DIBO and AlexaFluor 568 (to label sialylated molecules) and filipin (to label cholesterol) and prepared for imaging as described in the Materials and Methods. Staining was visualized on an epifluorescence microscope. Note the lack of co-localization in the NPC2 fibroblasts between cholesterol and SiaNAz. In contrast, imipramine treatment of control cells results in cholesterol and SiaNAz accumulation within common compartments.

Partial co-localization of SiaNAz-positive vesicles with CD63, but not EEA1 and LAMP1, was apparent in NPC1 cells, suggesting that much of the NPC-dependent glycoconjugate storage is within late endosomes (Figure 3.4(B)). The lack of co-localization with LAMP1 was expected since this marker exhibited a high degree of overlap with filipin-stained cholesterol in NPC1 cells. In contrast, no significant co-localization with any of the markers was detected in control cells. We cannot rule out the possibility that CD63 is mislocalized in NPC1 cells.

Indeed, there is a marked increase in CD63 staining in NPC1-null cells, likely reflecting a proliferation of late endosomal or lysosomal vesicles. Nonetheless, these results strongly indicate that the accumulation of SiaNAz-containing glycoconjugates is within endosomes and not lysosomes. Since the NPC1 fibroblasts we employed for this study completely lack the NPC1 protein, it is also possible that some co-localization with this lysosomal marker would be observed in cells with partial loss of NPC1 function. Consistent with this notion, we did observe the highest degree of co-localization between SiaNAz and LAMP1 in NPC2 fibroblasts (Figure 3.6), with some additional co-localization found with CD63 but not EEA1.

Treatment strategies approved or proposed for NPC disease include alleviation of cholesterol storage by treatment with cyclodextrin, or inhibition of glycolipid biosynthesis using *N*-butyl-deoxynojirimycin (NB-DNJ).[6] We examined whether these compounds are capable of reversing the accumulation of sialylated glycoconjugates in NPC1-null cells. Ac_4ManNAz-labeled cells were treated with NB-DGJ or cyclodextrin followed by SPAAC with DIBO-biotin, and visualized by confocal microscopy (Figure 3.7 and Figure 3.8).

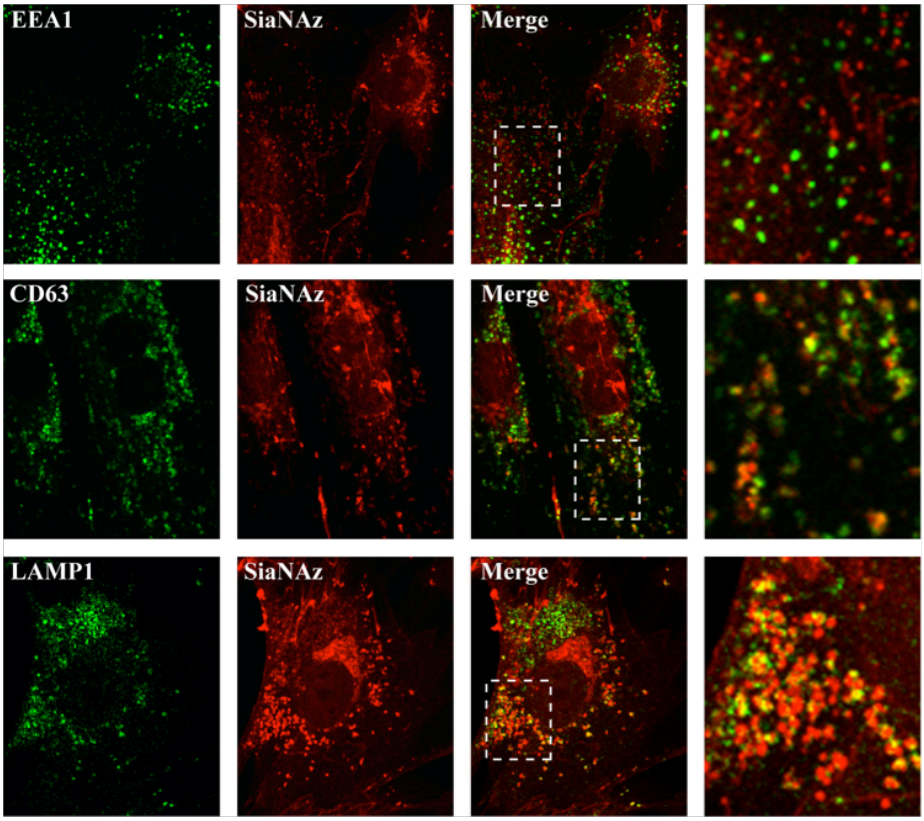

Figure 3.6 Co-localization of SiaNAz with endosomal and lysosomal markers in NPC2 fibroblasts. NPC2 cells were cultured in the presence of Ac_4ManNAz for 24 h prior to incubation with DIBO. After fixation, coverslips were incubated with mouse monoclonal antibodies against EEA1 (to mark early endosomes), CD63 (to mark late endosomes and multivesicular bodies) and LAMP1 (to mark lysosomes). Cells were then incubated with appropriate secondary antibodies and visualized by confocal microscopy. Maximum intensity z-projections are shown. While the vesicular SiaNAz staining in NPC1 fibroblasts exhibited a high degree of co-localization with the late endosomal marker CD63, the SiaNAz staining in NPC2 cells has the most apparent overlap with the lysosomal marker LAMP1.

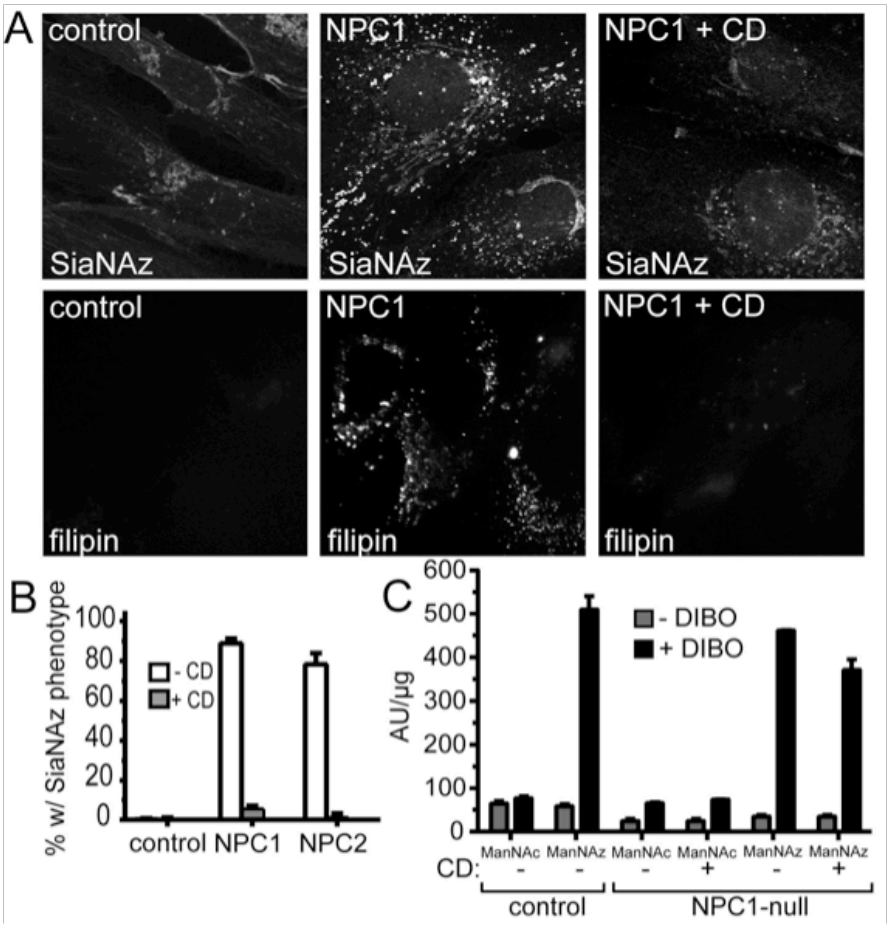

Figure 3.7 Cyclodextrin treatment of NPC1 fibroblasts corrects cholesterol storage and the intracellular accumulation of sialylated molecules. (A) Cells were labeled with peracetylated ManNAz in the presence or absence of 300µM methyl-ß-cyclodextrin (CD) for 48 h followed by reaction with DIBO and filipin staining and visualization by fluorescence microscopy. (B) The percentage of cells that display vesicular SiaNAz staining were quantified in control, NPC1-null and NPC2-deficient fibroblasts. Results represent the average of three independent experiments. Error bars represent standard deviations. (C) Control and NPC1-null fibroblasts were labeled with Ac_4ManNAz, in the presence or absence of CD and cell surface fluorescence intensity measured as described.

NB-DGJ was used instead of NB-DNJ since it has been shown to be a more specific and potent inhibitor of glucosylceramide synthase in cells.[20] Filipin staining was performed in parallel to gauge the effects of these compounds on cholesterol storage. No decrease in filipin staining or the accumulation of SiaNAz-positive vesicles was detected upon treatment of NPC1-null and NPC2-deficient fibroblasts with NB-DGJ (Figure 3.8). These observations indicate that the majority of the labeling is due to the build-up of sialoglycoproteins as opposed to gangliosides. To confirm this notion, Ac_4ManNAz-labeled NPC1 and NPC2 fibroblasts were treated with the *O*-glycan biosynthesis inhibitor, benzyl-α-GalNAc (GB) or the *N*-glycan processing inhibitor kifunensine (Kf) and analyzed by confocal microscopy.

Both compounds were effective at reducing the overall SiaNAz staining as well as the intensity and amount of vesicular staining, confirming that primarily endocytosed glycoproteins were labeled (Figure 3.8). In contrast, treatment of NPC1 cells with methyl ß-cyclodextrin was effective at reducing both cholesterol and sialylated glycoconjugate accumulation (Figure 3.7(A)). Qualitative assessment of the data revealed that filipin and vesicular SiaNAz staining was minimal. Moreover, quantification of three independent experiments showed correction of the SiaNAz phenotype in >90% of cyclodextrin-treated NPC1 and NPC2 cells (Figure 3.7(B)). Cyclodextrin has been shown to inhibit endocytosis by modulating cholesterol levels within lipid rafts. To rule out that decreased endocytosis of sialylated molecules accounts for the loss of intracellular SiaNAz staining, control, NPC1 and NPC2 fibroblasts were labeled with Ac_4ManNAz and Ac_4ManNAc in the presence or absence of cyclodextrin for 24 h and total surface fluorescence intensity measured (Figure 3.7(C) and Figure 3.9).

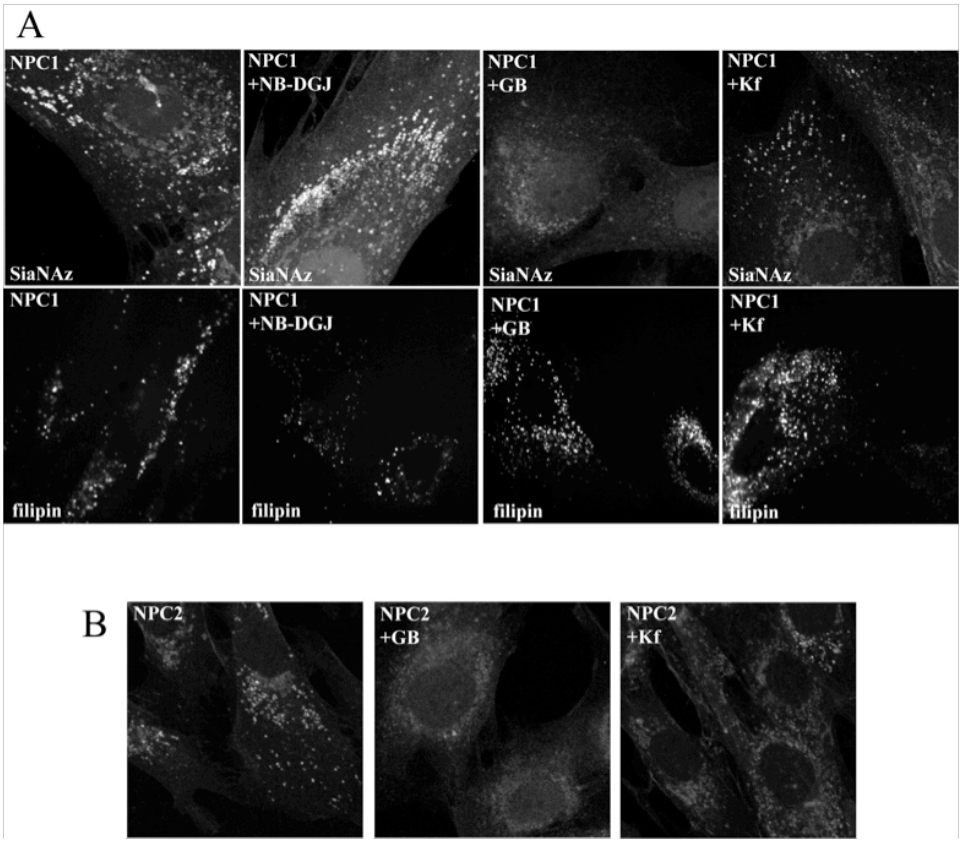

Figure 3.8 Inhibitors of glycoprotein but not glycolipid glycosylation reduce the SiaNAz phenotype in NPC fibroblasts. A) NPC1 and B) NPC2 cells were labeled with Ac_4ManNAz for 2 days in the absence or presence of the following inhibitors: N-butyldeoxygalactonojirimycin (NB-DGJ;100 μM); benzyl-α-GalNAc (GB; 2 mM), and kifunensine (Kf; 10 μM). Treated and non-treated NPC fibroblasts were incubated with DIBO (30 μM); for 1 h at RT, followed by streptavidin-conjugated fluorophore; (SiaNAz: top panels); filipin staining of the same cells and conditions (lower panels). Treatment of NPC fibroblasts with inhibitors of glycoprotein biosynthesis leads to a reduction of accumulated sialylated molecules.

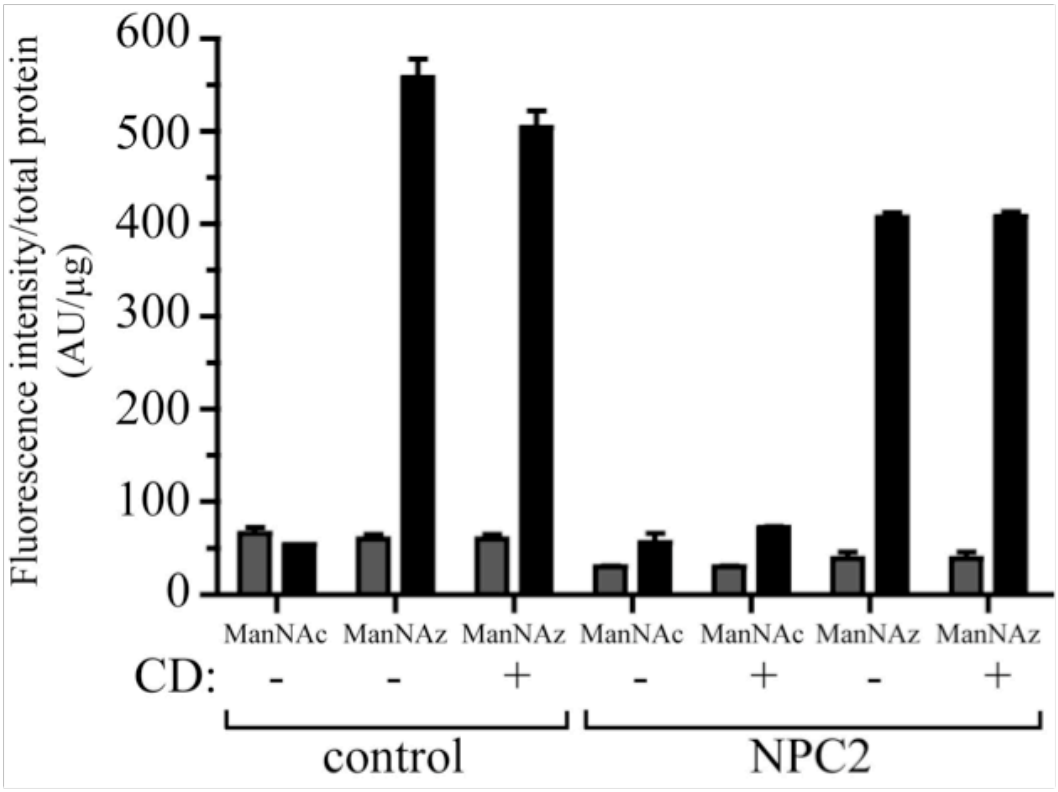

Figure 3.9 Cyclodextrin treatment of control and NPC2 fibroblasts does not significantly alter cell surface sialylation. Control and NPC2 fibroblasts were labeled with Ac_4ManNAz and cell surface fluorescence intensity was measured as described.

Only slight changes in total cell surface fluorescence intensity were detected in all treated cells, indicating that surface sialylation is not overtly altered by the presence of cyclodextrin. Thus, it appears that the loss of intracellular SiaNAz in NPC fibroblasts induced by cyclodextrin treatment is due to alleviation of cholesterol storage and the restoration of normal lysosomal turnover of sialoglycoproteins.

3.3 CONCLUSIONS

The results presented here demonstrate for the first time that the chemical reporter strategy combined with pharmacological treatments can provide unprecedented insight into endocytic trafficking defects associated with this disease. We show that cholesterol storage leads to accumulation of primarily sialoglycoproteins and not gangliosides in the endosomes. Although secondary storage of glycolipids and other lipid molecules is well documented in NPC disease,[8, 21] there are only a few reported examples of endosomal accumulation of specific cell surface glycoproteins. Since many signal transduction events including ligand-receptor binding and coordination of second messengers occur within endosomes, we speculate that some of the phenotypes associated with NPC disease may arise due to impaired trafficking of glycoproteins involved in cell signaling. The decreased residence of these glycoproteins at the cell surface of neurons or other sensitive cell types or their prolonged localization within endosomes may disrupt the balance of key pathways involved in survival and function of affected tissues. In addition, it has been found that cholesterol-filled lysosomes are incapable of receiving endocytosed molecules. In light of the fact that cholesterol-independent functions for NPC1 have been proposed, including a role for this protein in Ebola virus infection,[22, 23] it is possible that aspects of the SiaNAz phenotype are due to altered fusion of endosomal and lysosomal vesicles in the absence of the NPC1 protein.[24, 25] However, the similarity of the phenotypes in NPC1 and NPC2 cells and the cyclodextrin-induced alleviation point instead to cholesterol storage as the underlying mechanism for the accumulation of sialylated glycoproteins within late endosomal network of NPC cells.

These findings pave the way for the use of chemical reporter strategies to study the impact of altered glycosylation on the pathophysiology of human diseases. We believe this approach will find value in the diagnosis of certain disorders and in the identification of other diseases that have alered trafficking of endocytosed glycoconjugates.

3.4 MATERIALS AND METHODS

3.4.1 CHEMICALS AND BIOLOGICAL REAGENTS

Curcumin, imipramine, filipin and methyl-ß-cyclodextrin were obtained from Sigma-Aldrich (St. Louis, MO, USA). Goat anti-rabbit IgG(H+L) Alexa-Fluor488, goat anti-mouse IgG(H+L) Alexa-Fluor488, Strepavidin Alexa-Fluor 568 were obtained from Invitrogen. N-butyldeoxygalactonojirimycin (NB-DGJ) was obtained from Toronto Research Chemicals Inc. The monocolonal mouse antibody anti-CD63 (H5C6) and LAMP-1 antibody (1D4B) were from the Developmental Studies Hybridoma Bank, developed under the auspices of the NICHD and maintained by the University of Iowa, Department of Biology, Iowa City, IA 52242. Mouse monoclonal antibody to EEA1 was obtained from BD Biosciences. Synthetic compound, biotinylated dibenzocyclooctyne (DIBO), was reconstituted in DMF and stored at –80 ^{o}C until required for use. Final concentrations of DMF never exceeded 0.56% to avoid toxic effects.

3.4.2 CELL LINES AND CULTURE

Human skin control fibroblasts (CRL-1509; from ATCC), NPC1-null fibroblasts (gift from Dr. Daniel Ory), NPC2-deficient (GM18455; from NIGMS Human Genetic Cell Repository), ML-IV fibroblasts (GM02048; from NIGMS Human Genetic Cell

Repository) and MPS I fibroblasts (GM00798; from NIGMS Human Genetic Cell Repository) were cultured in Dulbecco's Modified Eagle's Medium (DMEM) (ATCC) with L-glutamine (2 mM), sodium bicarbonate (1.5 g/L), glucose (4.5 g/L), HEPES (10 mM), and sodium pyruvate (1.0 mM). Media was further supplemented with penicillin (100 u/ml) / streptomycin (100 μg/ml; Mediatech) and fetal bovine serum (FBS, 10% or 20%; Hyclone). Cells were maintained in a humid 5% CO_2 atmosphere at 37^{o}C and subcultured every 2-3 days.

3.4.3 METABOLIC LABELING, CYCLOADDITION CHEMISTRY AND CELL STAINING

Fibroblast cultures were seeded at a density of 50000 cells/coverslip (22 mm) and allowed to adhere overnight and then labeled with 25 μM Ac_4ManNAz or Ac_4GalNAz for 2 days. Monolayers were incubated with 30 μM DIBO for 1 h at RT followed by three washes in PBS, fixed with 3.7% formaldehyde for 15 min at RT. The cells were permeabilized for 10 min at RT using 0.2% Triton X-100 in PBS, washed and incubated with strepavidin Alexa-Fluor 568 (1:100) in PBS containing 0.2% Triton X-100 for 30 min at RT. Coverslips were washed 3X in PBS and mounted on to glass slides for imaging by fluorescence or confocal microscopy.

In some experiments, cells were co-stained with filipin prior to imaging. Following streptavidin Alexa-Fluor 568 incubation, cells were incubated with 0.05 mg/ml filipin in PBS containing 10% FBS for 1 h at RT in the dark followed by three washes with PBS. For co-staining of ManNAz-labeled cells with antisera to protein markers, cells were first incubated with DIBO, then permeabilized for 10 min at RT using 0.2%

Triton X-100 in PBS, washed and incubated with the following specific monoclonal antibodies: mouse anti-EEA1 (early endosomes), mouse anti-CD63 (late endosomes/ multivesicular bodies (MVBs)), and mouse anti-LAMP1 (lysosomes) for 1 h. After washing, the slides were incubated with goat anti-mouse Alexa-Fluor 488 (to stain the protein markers) and streptavidin Alexa-Fluor 568 (to stain the SiaNAz-containing molecules) and imaged by confocal microscopy.

3.4.4 DRUG TREATMENTS

NPC1 and NPC2 fibroblasts were treated with 25 μM Ac_4ManNAz in the presence of the drug *N*-butyldeoxygalactonojirimycin (NB-DGJ; a glucosylceramide synthase inhibitor) (100 μM), imipramine (50 μM), phenelzine (50 μM), benzyl-α-GalNAc (GB; 2 mM), and kifunensine (Kf; 10 μM) for 48 h; or methyl-ß-cyclodextrin (MβCD) (300 μM) for 1 day prior to preparation for imaging as described above. Cells were washed 3X and incubated with DIBO (30 μM) for 1 h at RT, fixed, permeabilized and stained with streptavidin–Alexa Fluor568; or cells were washed, fixed and stained with filipin as described previously. Coverslips were washed 3X in PBS (5 min each wash) and mounted on to glass slides. Fluorescent cells were observed using a confocal microscope or fluorescence microscope using a UV filter set. To quantify the extent of correction in drug-treated NPC1 cells, 150-200 cells from three independent experiments were assessed for the presence of peripherally localized vesicular SiaNAz staining. The average percentage of corrected cells (with standard deviations) is presented.

3.4.5 SURFACE AZIDE LABELING AND DETECTION BY FLUORESCENCE INTENSITY

Fibroblast cultures were grown in the presence of peracetylated *N*-azidoacetylmannosamine (Ac_4ManNAz; 100 μM final concentration) for 3 days, as before. The cells were either not treated or treated with 300 μM methyl-ß-cyclodextrin (MβCD) for 1 day. Wild type human skin fibroblast, NPC1 and NPC2-mutant cells bearing azides and control cells grown in the presence of peracetylated *N*-acetylmannosamine (Ac_4ManNAc; 100 μM final concentration) were incubated with the biotinylated compound DIBO (30 μM) in labeling buffer (PBS, pH 7.4 containing 1% FBS) for 1 h at room temperature. The cells were washed three times with labeling buffer and then incubated with avidin conjugated to fluorescein isothiocyanate (FITC; 0.5 μg/mL; Molecular Probes) for 15 min at 4 ^{o}C. Following three washes and cell lysis, cell lysates were analysed for fluorescence intensity (485 ex / 520 em) using a microplate reader (BMG Labtech). Data points were collected in triplicate and are representative of three separate experiments. Cell viability was assessed at different points in the procedure with exclusion of trypan blue.

3.4.6 FLUORESCENCE AND CONFOCAL MICROSCOPY

Initial analysis was performed on a Zeiss Axioplan2 fluorescent microscope. Confocal images were acquired using a 60X (NA1.42) oil objective. Stacks of optical sections were collected in the *z* dimensions. The step size, based on the calculated optimum for each objective, was between 0.25 and 0.5 μm.

Subsequently, each stack was collapsed into a single image (*z*-projection). Analysis was performed offline using ImageJ 1.39f software (National Institutes of Health, USA) and Adobe Photoshop CS3 Extended Version 10.0 (Adobe Systems Incorporated), whereby all images were treated equally.

3.5 REFERENCES

(1) Infante, R.E., *et al. Proc Natl Acad Sci U S A* 105, 15287-15292 (2008).

(2) Wang, M.L., *et al. Cell Metab* 12, 166-173 (2010).

(3) Rosenbaum, A.I. & Maxfield, F.R. *J Neurochem* 116, 789-795 (2011).

(4) Walkley, S.U. & Suzuki, K. *Biochim Biophys Acta* 1685, 48-62 (2004).

(5) Lloyd-Evans, E., *et al. Nat Med* 14, 1247-1255 (2008).

(6) Madra, M. & Sturley, S.L. *Clin Lipidol* 5, 387-395 (2010).

(7) Pipalia, N.H., Hao, M., Mukherjee, S. & Maxfield, F.R. *Traffic* 8, 130-141 (2007).

(8) te Vruchte, D., *et al. J Biol Chem* 279, 26167-26175 (2004).

(9) Devlin, C., *et al. Traffic* 11, 601-615 (2010).

(10) Martin, O.C. & Pagano, R.E. *J Cell Biol* 125, 769-781 (1994).

(11) Ning, X., Guo, J., Wolfert, M.A. & Boons, G.J. *Angew Chem Int Ed Engl* 47, 2253-2255 (2008).

(12) Sletten, E.M. & Bertozzi, C.R. *Angew Chem Int Ed Engl* 48, 6974-6998 (2009).

(13) Laughlin, S.T. & Bertozzi, C.R. *Nat Protoc* 2, 2930-2944 (2007).

(14) Mbua, N.E., Guo, J., Wolfert, M.A., Steet, R. & Boons, G.J. *Chembiochem* 12, 1912-1921 (2011).

(15) Dehnert, K.W., *et al. ACS Chem Biol* 6, 547-552 (2011).

(16) Laughlin, S.T., Baskin, J.M., Amacher, S.L. & Bertozzi, C.R. *Science* 320, 664-667 (2008).

(17) Rabuka, D., Hubbard, S.C., Laughlin, S.T., Argade, S.P. & Bertozzi, C.R. *J Am Chem Soc* 128, 12078-12079 (2006).

(18) Friscourt, F.*, et al. J Am Chem Soc* 134, 5381-5389 (2012).

(19) Rodriguez-Lafrasse, C.*, et al. Biochim Biophys Acta* 1043, 123-128 (1990).

(20) Andersson, U., Butters, T.D., Dwek, R.A. & Platt, F.M. *Biochem Pharmacol* 59, 821-829 (2000).

(21) Zhou, S.*, et al. Am J Pathol* 179, 890-902 (2011).

(22) Miller, E.H.*, et al. EMBO J* 31, 1947-1960 (2012).

(23) Carette, J.E.*, et al. Nature* 477, 340-343 (2011).

(24) Goldman, S.D. & Krise, J.P. *J Biol Chem* 285, 4983-4994 (2010).

(25) Zhang, M.*, et al. Acta Paediatr Suppl* 92, 63-73; discussion 45 (2003).

CHAPTER 4

SELECTIVE ENRICHMENT OF AZIDE-CONTAINING O-GlcNAc MODIFIED PROTEINS FROM THE NUCLEOCYCTOSOLIC FRACTION FOR GLYCOPROTEOMIC ANALYSIS

4.1 INTRODUCTION

While it is increasingly appreciated that O-GlcNAcylation is an abundant PTM, it has been very difficult to detect due to the low stoichiometry of modification with an estimated 5–10% occupancy at a particular site[1]; the fragile nature of the O-linkage during tandem mass spectrometric (MS/MS) sequencing, and the lack of tools available to study this modification. Thus, the challenge still remains, in the availability of more effective tools for the detection and study of *O*-GlcNAc modification of proteins. However, recent breakthroughs in enrichment strategies and mass spectrometric sequencing approaches will greatly facilitate the unambiguous identification of O-GlcNAc modified peptides. These techniques will reveal the ubiquitous and dynamic nature of this posttranslational modification, which has been shown to provide an additional layer of posttranslational regulation of protein function.

Several methods have been reported for the identification of *O*-GlcNAc modifications on proteins. The tritium methodology using the enzymatic transfer of [^{3}H] galactose by β-1,4-galactosyltransferase (GalT), is labor intensive, expensive, lacks sensitivity, and involves handling of radioactive material, and requires exposure times of days to months.[2] Lectins are a class of proteins isolated from plants, fungi, bacteria and animals that have a unique affinity towards carbohydrates. Lectin affinity approaches

have been used for mapping N-glycosylation sites on proteins[3] and for quantitative profiling.[4] Advantages of lectin affinity approaches include simplicity, cost-effectiveness, and flexibility and can be used either in combination or in series. But, lectin chromatography of *O*-GlcNAc proteins suffers from low specificity because lectins may bind strongly to proteins with other forms of glycosylation or non-specific binding to nonglycosylated proteins often occur.[5] Therefore, the use of lectin to enrich O-linked glycoproteins requires extensive prior digestion with glycosidases and is not generally applicable.

The enrichment *O*-GlcNAc proteins using antibody chromatography cannot rule out false-positives.[6] High affinity pan-specific antibodies are expected to offer convenient and robust tools for exploring the *O*-GlcNAc proteome. The pan-specific anti-O-GlcNAc antibodies (CTD110.6, Pierce; RL2 Covance) have proven invaluable for monitoring changes in global protein O-GlcNAc modification by immunoblotting or for probing for the presence of the modification on a specific protein of interest. However, these antibodies vary greatly in their specificity and sensitivity toward different OGT substrates and thus recognize only a subset of O-GlcNAc modified proteins. Although, such antibodies are powerful tools in many contexts, they have limited sensitivity.[2] However, monitoring the dynamics of *O*-GlcNAc glycosylation on specific proteins is challenging because monoclonal *O*-GlcNAc site-specific antibodies are difficult to generate.[7] The generated suite of monoclonal anti-O-GlcNAc antibodies when coupled to MS/MS facilitated the identification of over 200 candidate O-GlcNAc modified proteins.[7]

Recently, Hsieh-Wilson and co-workers developed an improved O-GlcNAc specific labeling strategy which relies on specific modification of proteins containing a

terminal GlcNAc moiety with a ß-1,4-galactosyltransferase that has been engineered, GalT1 (Y289L) to transfer a ketone-containing galactose, from UDP-keto-galactose to the C4 hydroxyl of a GlcNAc.[8] The single mutation of GalT (Y289L) enlarges the binding pocket and enhances the catalytic activity toward UDP-GalNAc substrates with minor substitutions at the C-2 position without compromising specificity.[9] The ketone then becomes the tagging target of an aminooxy biotin derivative for the purpose of detection by Western blot. The chemoenzymatic labeling approach capitalizes on the substrate tolerance of ß-1,4-galactosyltransferase, GalT, which allows for chemoselective installation of an unnatural functionality such as ketone, and azide[10] to *O*-GlcNAc modified proteins. The detection of purified *O*-GlcNAc proteins by this approach is still time-consuming requiring long incubation time for the formation of the oxime linkage for subsequent detection.

Here, we report a practical method using a Cu-free 1,3-dipolar cycloaddition reaction for enrichment of chemoenzymatically labeled *O*-GlcNAc modified proteins and metabolically labeled O-GlcNAz-proteins from the nucleocytosolic fraction. The *O*-GlcNAc proteins were tagged with a C-2 azide galactose using and engineered GalT1, which transfers GalNAz to C4 position of GlcNAc using UDP-N-azido-acetylgalactosamine (UDP-GalNAz) as donor substrate **(2,** Scheme 4.1**)**.

The azide moiety on *O*-GlcNAc glycosylated proteins was then tagged via Cu-free click cycloaddition reaction for detection by western blot or affinity enriched using a covalent reaction with a modified Ultralink Biosupport resin with cyclooctyne **3** (DIBO-resin, Scheme 4.1) for glycoproteomic analysis.

Scheme 4.1 Synthetic organic compounds for chemoenzymatic labeling of O-GlcNAc protiens

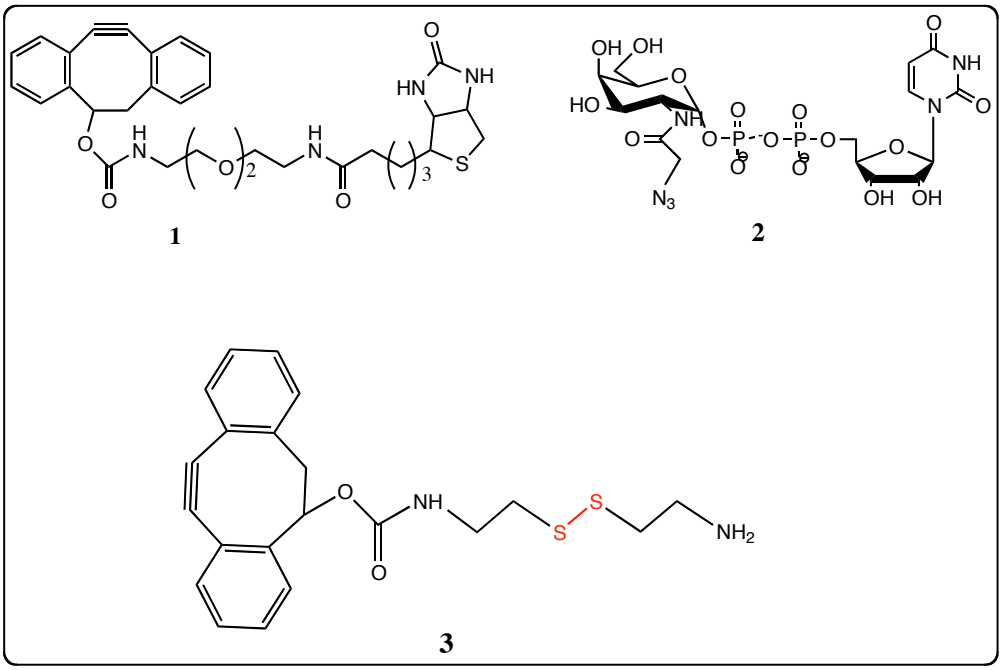

4.2 RESULTS AND DISCUSSIONS

4.2.1 SYNTHESIS OF THE DIBO-RESIN

Among the bioorthogonal reactions reported so far, Cu (I)-catalyzed 1,3-dipolar Huisgen-type cycloaddition ('click reaction') is most frequently employed to immobilize proteins onto solid supports[11] due to its effectiveness and simplicity. However, proteins are often degraded in the presence of the copper ion or may cause Cu (I)-induced oxidation of peptides, which might hamper identification.[12] In contrast, the cyclooctyne

reagents give a clean and selective reaction with azides in proteins and peptides and it was therefore chosen as the reactive group for our purification method. Synthesis of the DIBO-resin started by mixing resin with DIBO **3** with the cleavable S−S bond linker in which the amine group reacts with the azlactone group on the UltraLink Biosupport resin, yielding a stable amide bond with no leaving group or toxic chemical byproduct (Scheme 4.2). The UltraLink Biosupport resin, a hydrophilic resin, swells well in polar solvents and is not affected by organic solvents, and shows very little nonspecific binding and leaching, making it a good choice as a solid support. The coupling of the cyclooctyne **3** to the resin was assessed by examining conjugation to azido-coumarin. The azlactone group was blocked with reaction with ethanolamine and used for negative control experiments. The DIBO-resin reacted with the azide-coumarin, which becomes fluorescent after the cycloaddition reaction when the resins were excited with UV light in the dark (Figure 4.1). Conjugation to and release of the model test protein, BSA-azide, was used to probe the DIBO-resin effectiveness.

The coupling efficiency was determined indirectly by comparing the total amount of protein, using BCA assay in the collected supernantant to the starting BSA-azide protein solution incubated with the DIBO-resin. From this, a coupling efficiency of 66% was determined and the modified resin had a binding capacity of 2.503 mg (20 μmol) BSA-azide/ mL of resin.

Scheme 4.2 Modification of UltraLink Biosupport with DIBO **3.**

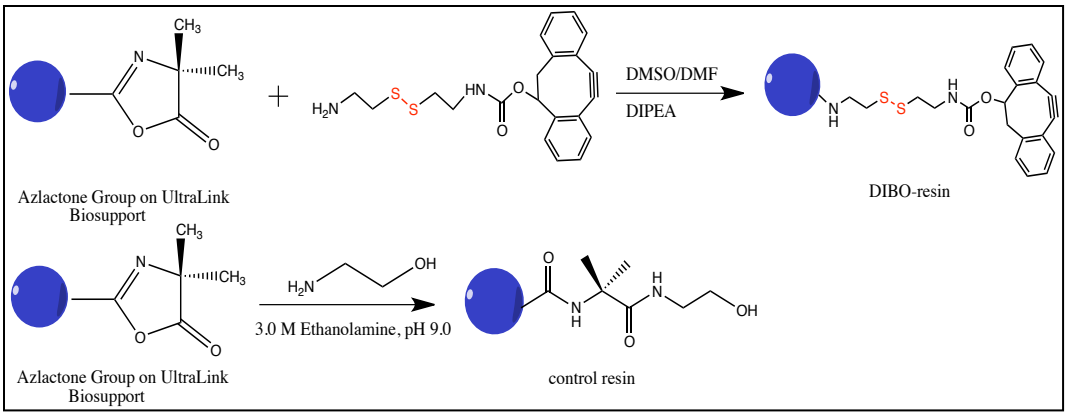

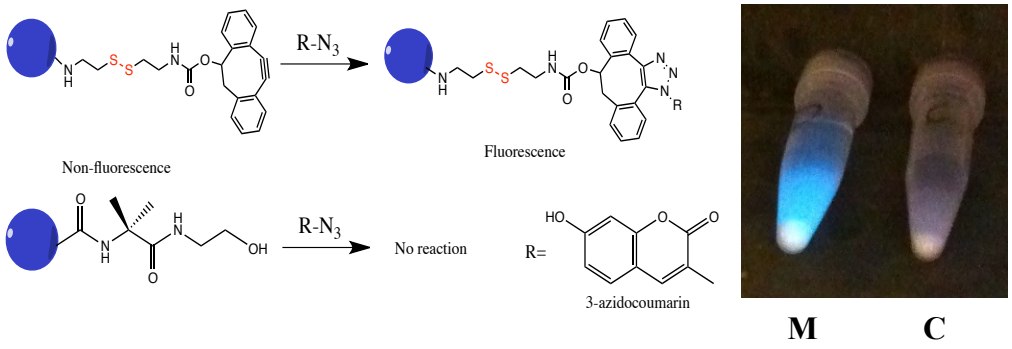

Figure 4.1 Fluorescence image of modified and control UltraLink Biosupport resins after immobilization with the low molecular weight compound N_3-coumarin. The resins were excited with UV light. Both tubes were incubated with N_3-coumarin and were stringently washed to remove unreacted fluorophore. (M =DIBO-resin; C = control resin).

The efficiency of the reductive cleavage of the S−S bond of the linker was determined using DIBO-resin which were reacted with either biotin-azide or azide-modified BSA (BSA-azide) as a model protein. For the biotin-azide reaction, the control

and DIBO-resin were incubated for 1 h on an end-to-end rotator. After the Cu-free click chemistry, the resins were washed, incubated with avidin-FITC for 15 min at 4^{o}C, after which resins were assessed for fluorescence intensity. The resins were next treated with 50 mM dithiothreitol (DTT) and the fluorescence of the supernatant measured. Remarkably, the cleavage of the DIBO-resin was efficient upon treatment with 50 mM DTT at room temperature resulting in > 96% cleavage (Figure 4.2(A)). An azide-modified BSA with a single azide reporter (site) was used to reduce complications that might arise from multiple labeling and cleaving events. BSA-azide was incubated with the control and DIBO-resin for 1 h with end-to-end shaking. After the Cu-free click chemistry, the resin was washed sequentially with 1% NP-40 in PBS, 600 mM NaCl in PBS, and 1 M urea in PBS to remove non-specifically bound protein. The resin was subjected to cleavage conditions by incubation with 50 mM DTT for 1 h to release the bound BSA from the resin. From the protein concentration of BSA-azide before and after cleavage, the cleaving efficiency was > 80% of all BSA-azide cleaved from the resin.

The released BSA was also separated by SDS-PAGE and compared to the amount that was loaded on to the resin. As expected, BSA-azide was bound to the resin through out all the washes, and then efficiently recovered after treatment with DTT to elute the protein, with no elution of protein from the control resin (Figure 4.2(B)).

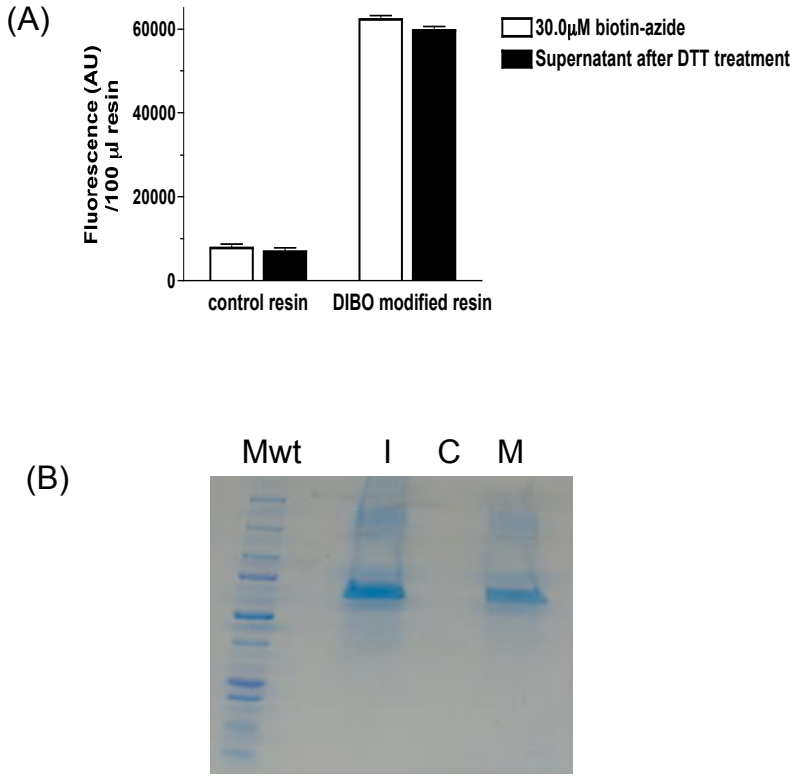

Figure 4.2 Determination of the cleaving efficiency of DIBO-resin. (A) Control and DIBO-modified resins were incubated at room temperature with 30 µM biotin-azide for 1 h. Next, resins were washed, incubated with avidin-FITC for 15 min at 4^{o}C, after which resins were assessed for fluorescence intensity. Resins were next treated with DTT and the fluorescence of the supernatant was measured (485 ex / 520 em). AU indicates arbitrary fluorescence units. (B) SDS-PAGE of released BSA-azide from resins after DTT treatment. Protein stained using Coomassie Brilliant Blue dye (I= input BSA-azide; C = control resin; M= DIBO-resin).

These results show that the azido-tagged protein can be separated cleanly from both non-specifically bound proteins. This feature makes the DIBO-resin especially attractive for use in glycoproteomics studies.

4.2.3 PREPARATION OF NUCLEOCYTOSOLIC FRACTION FROM HEK293T CELLS

As O-GlcNAc is the only known endogenous protein glycoconjugate in mammalian nuclear and cytoplasmic compartments, this fractionation allows for the specific examination of O-GlcNAcylated proteins. A commonly used approach for increasing global *O*-GlcNAc levels is to prevent the removal of *O*-GlcNAc from proteins by pharmacologically inhibiting OGA. PUGNAc [O-(2-acetamido-2-deoxy-d-glucopyranosylidene)amino-N-phenylcarbamate] is an O-GlcNAc analog that is a competitive inhibitor of OGA and has been widely used to increase O-GlcNAc levels.[13] HEK293T cells were cutured for 2 days in the presence of 50 μM PUGNAc. Cell pellet were lysed into 10 volumes of homogenization buffer, and fractionated into nucleocytosolic fraction as described by Teo et al.[7] Briefly, cells were homogenized using a hypotonic buffer (5 mM Tris-HCl pH 7.5 containing protease inhibitor cocktail), followed by a hypertonic buffer (100 mM Tris-HCl, 2M NaCl, 5 mM EDTA, 5 mM DTT and protease inhibitor cocktail) and centrifuged at 14,000 RPM at 4^{o}C for 25 min. The supernatant was collected and labeled as the nucleocytosolic fraction.

The metabolic labeling approach was used to append the azide group to O-GlcNAc proteins as O-GlcNAz. This approach was reported to be much more robust for the metabolic labeling of O-GlcNAc modified proteins using Ac_4GalNAz.[14] To overcome

the low level of incorporation of GlcNAz into proteins by exploiting the GlcNAc salvage pathway using Ac_4GlcNAz for metabolic labeling, HEK293T cells were fed with N-azidoacetylgalactosamine (GalNAz) as a source of GlcNAz for metabolic labeling in the presence of PUGNAc to increase global protein O-GlcNAcylation or Ac_4GalNAc as control. UDP-GalNAz can be converted to UDP-GlcNAz by UDP galactose 4′-epimerase (GALE); following epimerization, UDP-GlcNAz is incorporated into O-GlcNAc modified proteins by OGT. The nucleocytosolic fraction was obtained as described by Teo et al.[7] The protein concentration in the nucleocytosolic fractions was determined by using the bicinchonic acid assay (BCA; Pierce Biotechnology) and samples stored at -80^{o}C until required for use.

4.2.4 CHEMOENZYMATIC LABELING AND DETECTION OF O-GlcNAc MODIFIED PROTEINS DETECTION BY WESTERN BLOT

The model O-GlcNAc modified protein α-crystallin (chain A) contains one major site of glycosylation, and detection of the O-GlcNAc moiety on α-crystallin has been reported to be particularly difficult due to its low stoichiometry of glycosylation (~10%).[15] α-crystallin was enzymatically labeled with the azide functionality (Scheme 4.3) and chemically reacted with DIBO **1** (Scheme 4.1). The mixture was resolved by SDS-PAGE, transferred to a nitrocellulose membrane, and probed with antibiotin-HRP. Strong labeling of α-crystallin was observed by chemiluminescence when exposed to a film (Figure 4.3). In contrast, no signal was observed when reactions were performed in the absence of either **2** or GalT1 (Y289L), demonstrating the selectivity of the reaction.

Scheme 4.3. Strategy for the chemoenzymatic labeling of O-GlcNAc proteins using strain-promoted [3+ 2] azide-alkyne cycloaddition reaction.

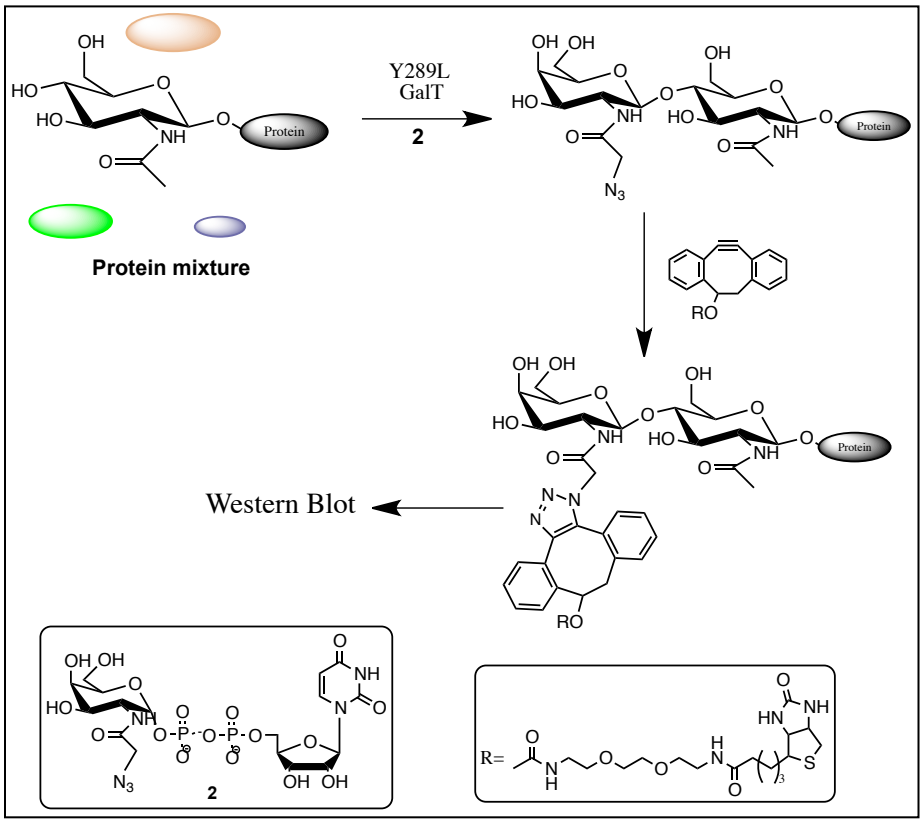

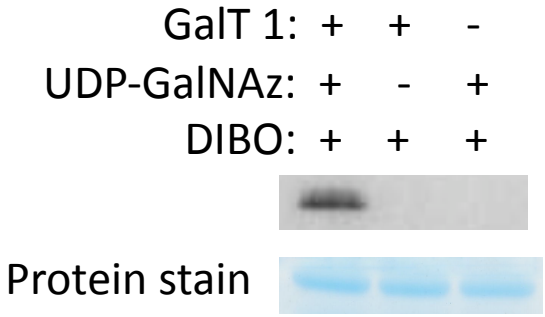

Figure 4.3 Selective labeling of glycosylated αA-crystallin by chemoenzymatic labeling.

4.2.5 IMMUNOBLOT AND CHEMOENZYMATIC LABELING AND DETECTION OF O-GLCNAC MODIFIED PROTEINS DETECTION BY WESTERN BLOT

O-GlcNAc modified proteins in the nucleocytosolic fraction from HEK293T cells were detected using the monoclonal O-GlcNAc mouse IgG_{2a} antibody.[7] Figure 4.4(A) shows Western blot of nucleocytosolic fractions prepared from cells, treated with or without PUGNAc, and developed with an antibody that specifically recognizes O-GlcNAc-modified proteins. Cells that were cultured in the presence of PUGNAc showed clearly increased O-GlcNAc modification of numerous proteins. The azide group on O-GlcNAc modified proteins introduced chemoenzymatically or via metabolic labeling using GalNAz was reacted with DIBO **1** in a strain-promoted [3+2] azide-alkyne cycloaddition (SPAAC) (Scheme 4.3). The mixtures were resolved by SDS-PAGE, transferred to a nitrocellulose membrane, and probed with antibiotin-HRP. By comparing the labeling efficiency of the chemoenzymatic and metabolic approaches, the latter showed a weaker detection in O-GlcNAc-modified proteins (Figure 4.4(B) and 4.4(C)).

Taken together, the data indicate that the chemoenzymatic labeling approach and the metabolic labeling with GalNAz are effective in detecting O-GlcNAc modification on proteins. Thus, Ac_4GalNAz is a useful tool for specifically labeling O-GlcNAcylated proteins in live mammalian cells indicating that the azide modification on these proteins is O-GlcNAz, as predicted. In contrast, no signal was observed when reactions were performed in the absence of UDP-GalNAz **2**, enzyme GalT1, or labeling with GalNAc demonstrating the selectivity of the labeling and detection method.

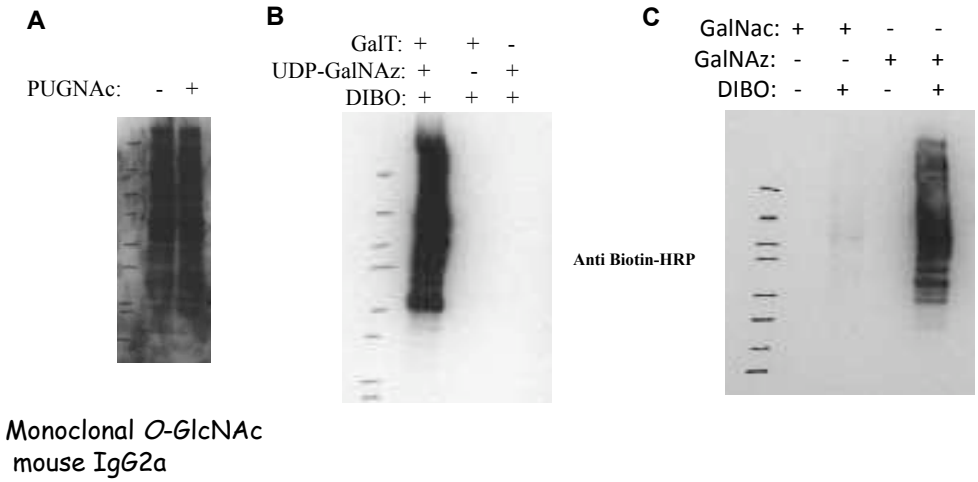

Figure 4.4 (A) Western blot prepared from nucleocytosolic fractions detected with an antibody (monoclonal *O*-GlcNAc mouse IgG_{2a}) that specifically recognizes *O*-GlcNAc-modified proteins. HEK293T cells cultured in the presence of PUGNAc, show clearly increased *O*-GlcNAcylation of several protein bands. (B) Selective chemoenzymatic labeling and detection of *O*-GlcNAc proteins in nucleocytosolic fraction. (C) Detection of metabolically labeled *O*-GlcNAz proteins in nucleocytosolic fractions labeled with GalNAz or GalNAc.

4.2.6 ENRICHMENT OF CHEMOENZYMATICALLY LABELED AND METABOLICALLY LABELED O-GlcNAc PROTEINS

To show the efficiency of the enrichment of azide-containing O-GlcNAc proteins on the DIBO-resin, chemoenzymatically labeled and metabolically labeled O-GlcNAc proteins were incubated with the control or DIBO-resins, captured and released (Figure 4.5).

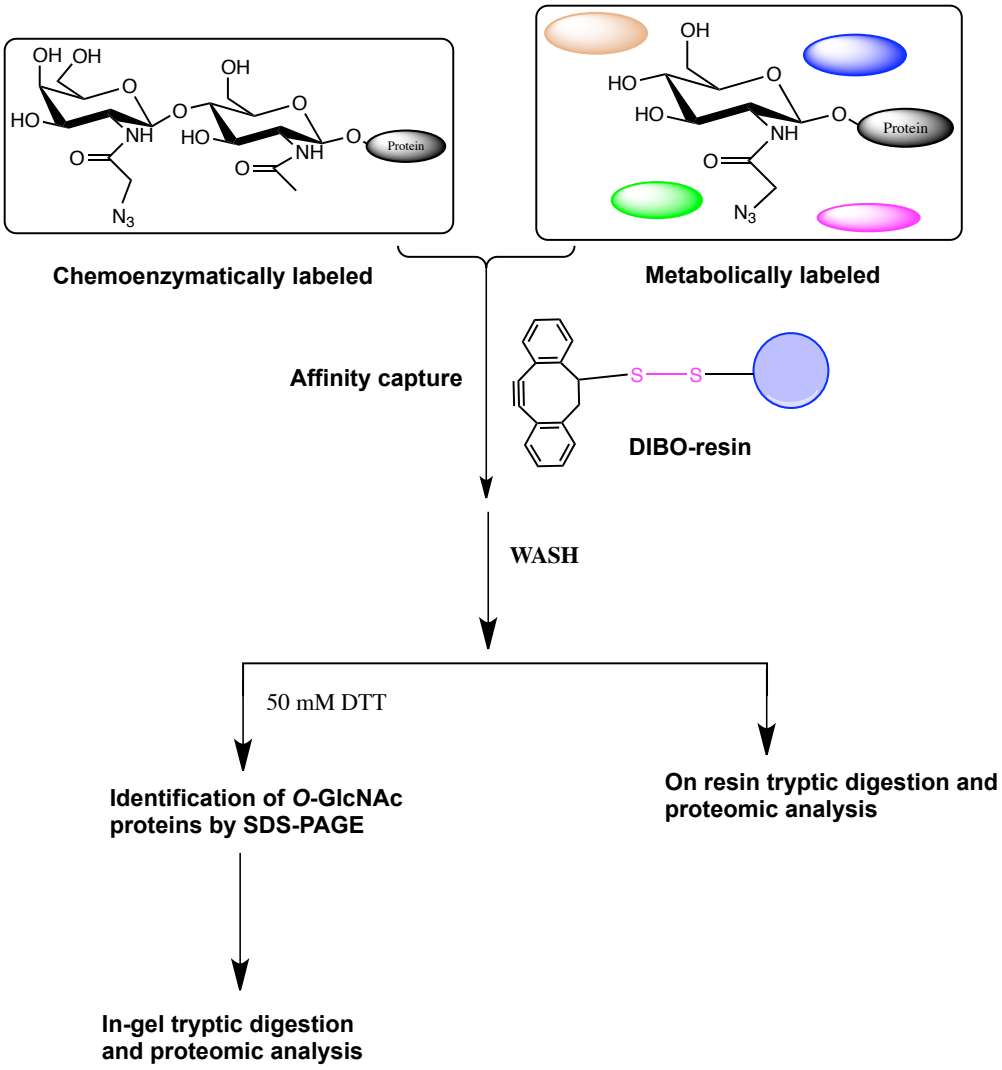

Figure 4.5 Schematic representation of the enrichment of O-GlcNAc proteins. Chemoenzymatically labeled and metabolic incorporated of of azide onto O-GlcNAc proteins were captured with DIBO-resin via SPAAC and subsequently released for SDS-PAGE detection and mass spectrometry analysis.

The DIBO-resin was used to enrich azido-tagged chemoenzymatically labeled O-GlcNAc proteins from the nucleocytosolic fraction of HEK293T cells, and O-GlcNAz proteins from the nucleocytosolic fraction by metabolically labeling HEK293T cells with Ac_4GalNAz. The nucleocytosolic fraction was subjected to chemoenzymatic labeling using the Click-it *O*-GlcNAc enzymatic labeling system (Molecular Probes) according to the manufacturer's instructions. Upon cycloaddition, a triazole is formed and proteins are captured on the resin via their azide moiety. Reductive cleavage of the disulfide bond liberates the thiol bond, which were then resolved on an SDS-PAGE and stained with Coommassie Brilliant blue dye. Figure 4.6(A) shows the results for the capture of labeled proteins by SPAAC and released by DTT treatment of the resin. The elution lane shows clean enrichment of modified proteins from a complex mixture, indicating efficient cleavage of the probe and elution of proteins. The absence of bands (significant) corresponding to proteins in elution fractions of the control resin indicates the specificity of the enrichment strategy.

4.2.7 ENRICHMENT OF O-GlcNAcYLATED PROTEIN FOR MS/MS

O-GlcNAc modification, however, is not stable during conventional MS/MS approaches; upon collision with gas molecules, the GlcNAc moiety is lost from the Ser/Thr side chain prior to fragmentation of the peptide backbone precluding direct detection of the site of modification. Thus, O-GlcNAc as well as other fragile modifications go undetected during routine mass spectrometric analysis.

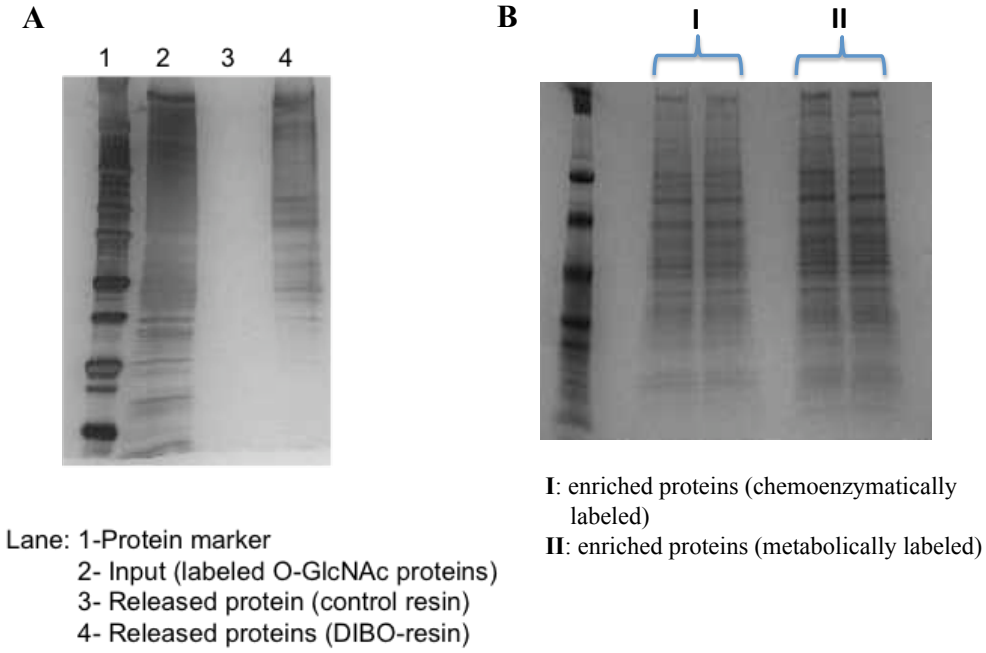

Figure 4.6 SDS-PAGE of released azide-modified O-GlcNAc proteins from DIBO-resin. (A) Azido tagged O-GlcNAc proteins were incubated with DIBO-resin and control resin, and captured proteins released after DTT treatment. Released proteins were resolved by SDS-PAGE and stained with Commassie Brilliant Blue (G250). (B) Chemoenzymatic and metabolically aziide-tagged O-GlcNAc proteins released from DIBO-resin and resolved by SDS-PAGE for subsequent in-gel digestion and mass spectrometry analysis.

We next sought to identify putative azide-labeled O-GlcNAcylated proteins using a mass spectrometry method. We incubated the nucleocytosolic fractions chemoenzymatically labeled and from Ac_4GalNAz treated HEK293T cells with DIBO-resin for 2 h with end-to-end shaking, to capture the azide-modified proteins. After the Cu-free click chemistry, the resin was washed sequentially with 1% NP-40 in PBS, 600

mM NaCl in PBS, and 1 M urea in PBS to remove non-specifically bound protein. To release proteins from the solid support, the disulfide bond, S−S bond was cleaved under mild conditions with 50 mM DTT for 1 h and it was very efficient. The released proteins were separated by SDS-PAGE, stained with Coommassie Brilliant blue (Figure 4.6(B)) and protein bands were excised, digested with trypsin and alkylated (In-gel digestion) before analysis using an LTQ Orbitrap mass spectrometer. Alternatively the captured O-GlcNAc proteins were digested with trypsin on the resin. Released peptides were alkylated and analyzed with an LTQ Orbitrap mass spectrometer. We identified 446 proteins with diverse cellular functions by MS/MS from the in-gel trypsin digestion (Figure 4.7).

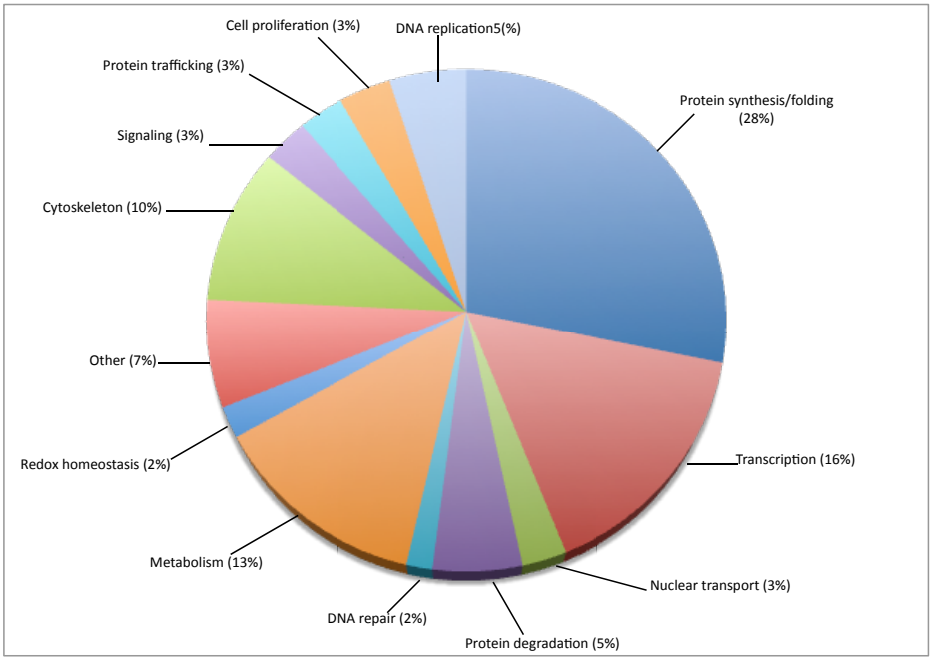

Figure 4.7 Functional classification of O-GlcNAc modified proteins. Pie chart showing the functional categories of the 446 identified O-GlcNAc modified proteins.

To facilitate the identification of the sites of modification, the chemoenzymatically labeled and Ac_4GalNAz-labeled O-GlcNAc proteins were digested with trypsin to produce a mixture of azide-glycopeptides and unmodified peptides. The O-GlcNAcylated peptides were enriched with DIBO-resin through SPAAC reaction (Figure 4.8). The peptides were released from the resin by base catalyzed β-elimination to enable mass spectrometric identification of azide-tagged O-GlcNAc modified peptides. This approach, which relies on β-elimination followed by Michael addition with dithiothreitol (BEMAD), results in replacement of the labile GlcNAc moiety with a more stable sulfide adduct.[16] As this adduct is not cleaved upon collision induced dissociation (CID), sites of glycosylation can be more readily determined. Although the chemoenzymatic tagging approach requires multiple sample preparation steps, advantages of this workflow include the ability to couple this approach to established quantitative proteomic procedures.

4.2.9 DETECTION OF THE SITES OF O-GlcNAc MODIFICATION BY TANDEM MASS SPECTROMETRY (MS/MS)

The development of chemical tools coupled to mass spectrometry has greatly facilitated the localization of O-GlcNAc to short peptide sequences within proteins, and this combination can be used to determine exact glycosylation sites. Recent advances in alternative fragmentation approaches, electron capture dissociation (ECD) and electron transfer dissociation (ETD), permit sequencing of peptides with fragile modifications, such as O-GlcNAc.[17] The chemoenzymatic approach combined with existing ß-elimination strategies, provides a powerful tool to identify precise sites of glycosylation.

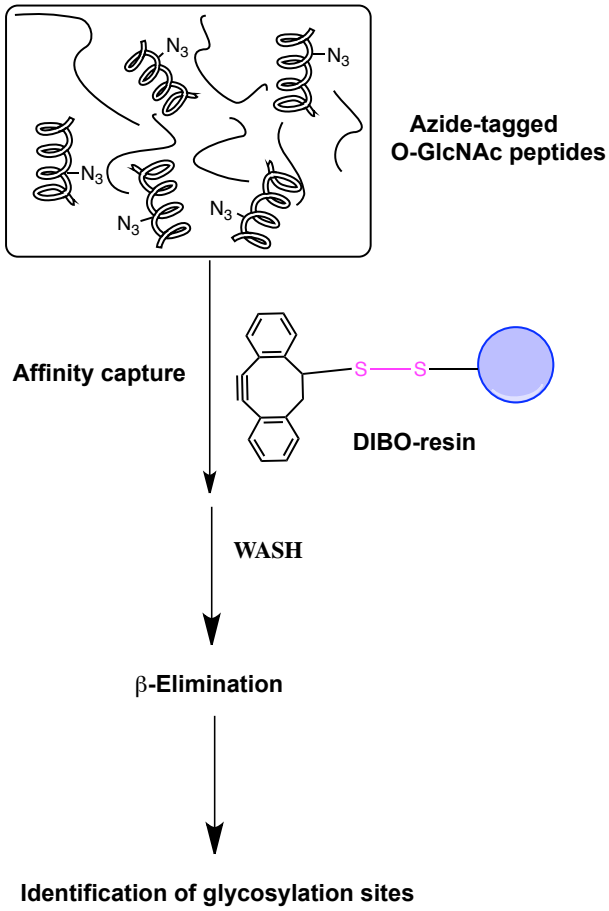

Figure 4.8 Schematic representation of the enrichment of O-GlcNAc peptides. Chemoenzymatically labeled and metabolic incorporation of O-GlcNAz into proteins digested by trypsin to produce azide-tagged peptides. Glycopeptides were captured with DIBO-resin via SPAAC for subsequent ß-elimination on resin to facilitate the identification of O-GlcNAc modification sites by mass spectrometry.

4.3 CONCLUSIONS

Glycoproteomics is currently experiencing a rapid growth both in terms of methodologies and the range of applications facilitated by the novel approaches and advancements in instrumentation. Proteomic studies are designed to elucidate the nature, causes and consequences of spatial and temporal variation in the protein contents of cells. Studying the profiles of glycoproteins is likely to provide critical information regarding the roles they play in a particular biological system and will shed more light to the mechanism and pathogenesis of certain diseases. Additional, the aberrant glycosylation patterns might provide clues to disease-relevant biomarkers in cancer,[18, 19] Alzheimer's disease.[20, 21] *O*-GlcNAc modification allows cells to link nutrient availability and cellular metabolism to the regulation of crucial cellular processes, such as cell cycle regulation, stress response and gene expression. Alteration in O-GlcNAcylation is one mechanism through which cell cycle progression, adaptability to the local environment and changes in gene expression are modulated. Furthermore, changes in O-GlcNAcylation can then disrupt the flow of information from other signalling systems, such as phosphorylation, ubiquitylation and acetylation.

In this study we designed a cyclooctyne (DIBO)-functional probe with a cleavable disulfide bond between the cyclooctyne and resin. By using this DIBO-containing probe, we have shown the enrichment of chemoenzymatically tagged and metabolically Ac_4GalNAz labeled O-GlcNAc proteins. Additionally, the cleavable disulfide linker moiety allowed us to efficiently released enriched proteins under mild conditions at room temperature.[22] Enrichment is the key for mass spectrometric identification of GlcNAcylated proteins because of their low stoichiometry and the issue of ion

suppression contributed by unmodified peptide ions in the mass spectrometer.[5] The Ultralink Biosupport resin was used instead of agarose to avoid the non-specific binding of proteins and the stability of the resin in organic solvents used during the immobilization of small ligands to the resin. In addition, the high affinity streptavidin/biotin binding interaction is also avoided because extremely low pH and high concentrations of chaotropic agents are required to dissociate the complex.[23] This can lead to inactivation of targets such as antibodies, enzymes, bioconjugates, or other labile molecules.

The unique selectivity of the SPAAC reaction would allow loading of the resin with the cyclooctyne (DIBO) without resorting to an extensive protecting group scheme. The azido-GlcNAc-modified proteins thus contain an azide handle for chemoselective conjugation to the DIBO-resin. The azide moiety on *O*-GlcNAc after modification will allow for fast and unambiguous detection of *O*-GlcNAc proteins. The efficiency hereof the DIBO-resin was evaluated showing the wide applicability of the method. Using this strategy, we identified 447 azido-O-GlcNAc-modified proteins in HEK293T cells. This result corroborates the presence of this modification of proteins in the nucleocytosolic fraction identified using a panel of specific monoclonal O-GlcNAc antibodies.[7] Our results reveal that proteins with a wide range of functions are modified by O-GlcNAc, implying its diverse cellular functions.

Importantly, this method can be used for other azide-containing biomolecules; For instance, proteins modified with the azide-functional group for successful capture and release from the DIBO-resin, opening possibilities to map protein−protein interactions in more complex protein systems. The strategy for glycoprotein enrichment and quantitative

MS analysis reported in this study can provide great opportunities for biomarker research. Comparative glycoproteomics have found applications in cancer biomarker research, diagnosis for neurodegenerative diseases and infectious diseases. This method herein will enable the rapid labeling, detection and the affinity purification of *O*-GlcNAc modified proteins from any cell type or tissue for proteomics studies. It will not require the purification of individual proteins and can be extended to the mapping of modification sites. To understand the molecular mechanism of diseases, a higly specific and targeted proteomics approach such as those targeted for glycosylations and phosphorylations will accelerate the pace to uncover the underlying mechanisms of various diseases and offer new insight into development of effective therapeutic strategies for these diseases.

The ability to couple quantitative proteomic approaches to the site-specific identification of O-GlcNAc modification will permit the unbiased discovery of the temporal dynamics and regulation of this modification during signal transduction.

The expected high sensitivity of this method will allow the detection of low abundance regulatory proteins that are *O*-GlcNAcylated and comparing low-abundant glyco-biomolecules at different physiological/pathological stages for identification of glycan-related biomarkers and targets, for example, in cancer cells. In summary, a global enrichment and glycoproteomic analysis method has been developed that allows selective enrichment for azide-containing O-GlcNAc proteins and peptides from complex mixtures in HEK293T cells.

4.4 MATERIALS AND METHODS

4.4.1 REAGENTS

Synthetic compounds **1** and **3** were reconstituted in DMF and stored at −80 °C. Click-iT O-GlcNAc peptide standard and Click-iT O-GlcNAc enzymatic labeling kit were obtained from Invitrogen (Eugene, OR). All other chemicals were obtained from Sigma (St. Louis, MO).

4.4.2 CELL CULTURE CONDITIONS

Human embryonic kidney cell-line 293T (HEK293T) cells were cultured in Dulbecco's modified Eagle's medium (DMEM) with L-glutamine (2 mM), adjusted to contain sodium bicarbonate (1.5 g/L), glucose (4.5 g/L), HEPES (10 mM), and sodium pyruvate (1 mM) and supplemented with penicillin (100 U/ml)/streptomycin (100 μg/mL; Mediatech) and fetal bovine serum (FBS, 10%; Hyclone) at 37 °C under humidified air containing 5% CO_2.

4.4.3 PREPARATION OF NUCLEOCYTOSOLIC FRACTION FROM CELL LYSATE

HEK293T cells were cultured in the presence of *O*-GlcNAse (OGA) inhibitor, PUGNAc [O-(2-acetamido-2-deoxy-D-glucopyranosylidene)amino-*N*-phenylcarbamate) for 2 days at 50 μM final concentration. Cell pellet were resuspended in hypotonic buffer (5 mM Tris-HCl pH 7.5 containing protease inhibitor cocktail) and kept on ice for 10 min and homogenized on ice for 5 mins. Two (2) mL of hypertonic buffer (100 mM Tris-HCl, 2M NaCl, 5 mM EDTA, 5 mM DTT and protease inhibitor cocktail) was added to the

mixture and allowed on ice for 5 min. The mixture was then homogenized and centrifuged at 14,000 RPM at 4^{o}C for 25 min. The supernatant was collected and labeled as the nucleocytosolic fraction.

4.4.4 IMMUNOSTAINING OF *O*-GLCNAC MODIFIED PROTEINS

The protein samples in the nucleocytosolic fraction (25 µg protein) was resolved on a 4−20% SDS-PAGE gel (Bio-Rad) and transferred to a nitrocellulose membrane. Next the membrane was blocked in blocking buffer (nonfat dry milk (5%; Bio-Rad) in PBST (PBS containing 0.1% Tween-20 and 0.1% Triton X-100) for 2 h at RT. The blocked membrane was incubated for 1 h at room temperature with monoclonal O-GlcNAc mouse IgG2a antibody (1:2500) (Teo et al., 2010). Following washing, the membrane was incubated in goat anti-mouse IgG antibody (1:10,000, Jackson Immunoresearch) for 1 h, washed, developed with ECL Plus chemiluminescent substrate (Amersham), exposed to film (Kodak) and development using a digital X-ray imaging machine (Kodak).

4.4.5 CHEMOENZYMATIC LABELING OF *O*-GLCNAC MODIFIED PROTEINS

Labeling of the model *O*-GlcNAc-bearing protein, α-crystallin and *O*-GlcNAc proteins in the nucleocytosolic fraction by GalNAz was done using the Click-it *O*-GlcNAc enzymatic labeling system (Invitrogen) according to the manufacturer's instructions. After labeling, the sample was precipitated using the methanol/chloroform protocol and resuspended in 50 µl of 50 mM Tris/HCl, pH 8.0, containing 1% (w/v) SDS.

The *O*-GlcNAc proteins tagged with the azide group were then detected by western blot or were affinity enriched by a DIBO **3** modified UltraLink Biosupport resin. The tagged O-GlcNAc proteins were resolved on SDS-PAGE and stained with Coomassie Brilliant Blue dye.

4.4.6 WESTERN BLOT ANALYSIS

The samples (25 μg of protein) was resolved on a 4−20% SDS-PAGE gel (Bio-Rad) and transferred to a nitrocellulose membrane. Next, the membrane was blocked in blocking buffer (nonfat dry milk (5%; Bio-Rad) in PBST (PBS containing 0.1% Tween-20 and 0.1% Triton X-100) for 2 h at RT. The blocked membrane was incubated for 1 h at RT with an antibiotin antibody conjugated to horseradish peroxidase (HRP) (1:100000; Jackson ImmunoResearch Lab, Inc.) in blocking buffer and washed with PBST (4 × 10 min). Final detection of HRP activity was performed using ECL Plus chemiluminescent substrate (Amersham), exposure to film (Kodak) and development using a digital X-ray imaging machine (Kodak). Next the blot was stripped and reprobed for loading control (β-actin) using an anti- β-actin antibody (1:100,000) for 1 h at RT. Coomassie staining was also used to confirm total protein loading.

4.4.7 PREPARATION AND CHARACTERIZATION OF DIBO 3 MODIFIED RESIN

250 μL of dibenzocyclooctyne-amine (DIBO **3**) (11.5 mg in DMF) were added directly to dry UltraLink Biosupport resin (80 mg; ~ 30 μmol reactive group, Pierce), DMSO/DMF (0.8 ml/0.8 ml) and 200 μL of *N,N*-diisopropylethylamine added to the

mixture and votexed briefly, and the suspension was gently rocked at 30^{o}C overnight. The suspension was centrifuged at 1,200 x g at RT for 5 min to pellet the resin. The supernatant was discarded, being careful to retain the resin. Non-reacted sites were blocked by incubation with the primary amine buffer 3 M ethanolamine, pH 8.0 at RT for 2.5 hours with gentle shaking. The resin was washed 5 times with PBS pH 7.4 (1mL/wash) over 15 min and resuspended in PBS. The DIBO-modified resin was stored at 4^{o}C until required for use. The control resin was prepared by quenching the azlactone groups on the resin with the primary amine buffer 3 M ethanolamine, pH 8.0 at RT for 2.5 hours with gentle shaking. The control resin was rinsed extensively with PBS and stored at 4^{o}C in PBS until required for use.

4.4.8 DETERMINATION OF COUPLING EFFICIENCY OF THE DIBO-RESIN

100 µl of resin (modified and control) were pre-equilibrated with PBS, pH 7.4 and incubated with BSA-azide, for 2 h at RT with gentle shaking. The suspension was centrifuged at 1,000 x g for 5 min and the supernatant collected. The amount of protein in the supernatant was determined using the bicinchonic acid assay (BCA; Pierce Biotechnology). The amount of BSA-azide 'clicked' to the resins was then calculated by subtracting the amount of protein in the supernatant from the amount of total BSA-azide that was added to the resins, from which the coupling efficiency was determined.

4.4.9 DETERMINATION OF BINDING CAPACITY OF THE DIBO-RESIN

Typically, columns with a bed volume of 1 ml were used. Unless indicated otherwise, experiments were performed in PBS. The binding capacity of modified resin was determined by sequentially loading 100- to 500 µl aliquots of BSA-azide (1mg/ml) on the 1 ml column bed volume. Sample application was continued until absorbance at 280 nm was detected in the outflow. To determine non-specifically bound protein, separate 1 ml column of control resin was treated similarly. After washing until $A_{280} = 0$, retained proteins were released by cleaving the linker with 50 mM DTT for 2 h at RT with gentle shaking. The mixtures were centrifuged at 1,000 x g for 5 mins to collect the supernatants which were concentrated by centrifugation at 10,000 x g for 10 min. The binding capacity was calculated as the total amount of protein loaded on the modified resin prior to the first appearance of A_{280} in the outflow minus the amount of protein eluted from the control resin. The total protein concentration was determined using the bicinchonic acid assay (BCA; Pierce Biotechnology).

4.4.10 DETERMINATION OF RECOVERY OF CAPTURED PROTEINS

The DIBO-modified resin with cleavable linker was used. BSA-azide was incubated with the DIBO-modified resin as described previously. After washing the unbound protein from the resin, the protein was released by cleaving the disulfide linker with 50 mM DTT for 2 h at RT with gentle shaking. A_{280} from the eluted protein was measured and the recovery determined. A protein profile was also produced after separation on an SDS-PAGE followed by Coomassie Blue staining (Thermo Scientific).

4.4.11 AFFINITY CAPTURE OF CHEMOENZYMATICALLY LABELED *O*-GLCNAC MODIFIED PROTEINS

The azide-tagged *O*-GlcNAc modified proteins or metabolically labeled O-GlcNAz-proteins in the nucleocytosolic fraction were incubated with DIBO-modified resin (100 µL) pre-equilibrated with PBS buffer pH 7.4 for 2 h with end-to-end shaking at RT. The suspension was then centrifuged and the supernatant was collected. The resin was washed by centrifugation at 1000 x g, for 5 min per wash with 10 column volumes of buffer as follows: 0.5% NP-40 in PBS (3X); 600 mM NaCl (3X) in PBS; 1 M urea in PBS (3X). The resin was then rinsed finally with PBS and resuspended in 1 column volume of PBS.

4.4.12 IN-GEL DIGESTION TO OBTAIN PEPTIDES FOR MASS SPECTROMETRY (MS) ANALYSIS

To release bound proteins from the column, the resin was incubated with SDS-PAGE sample buffer and boiled for 10 min. The released proteins were resolved on a 4−20% SDS-PAGE gel (Bio-Rad). Separated proteins were stained using Coomassie Brilliant Blue (G-250). G-250-stained bands were excised, and placed in 40 mM ammonium bicarbonate. The supernatant was discarded and gel pieces placed in solution E (Acetonitrile; HPLC grade) for 10 min and rehydrated with 50 µl of a fresh 1:1 mixture of solution A (30 mM potassium ferricyanide in water) and solution B (100 mM sodium thiosulfate in water) for 1-3 min with brief vortexing every 30 seconds. The gel pieces were rinsed 3X with water and incubated for 10 minutes with 200 mM NH_4HCO_3 (50/50 with water from stock of solution C (400 mM ammonium bicarbonate, pH ~8.15). Next,

the gel pieces were swollen with buffer F (10 mM DTT in Buffer D) and reduced for 1 h at 56^{o}C. After 5 min at RT, the supernatant was discarded and replaced with a solution of G (55 mM Iodoacetamide in Buffer D) and alkylated in the dark for 45 min, with brief vortexing every 15 min. The supernatant was discarded and buffer D added and incubated for 10 min, followed by another incubation for 10 min with buffer E and these previous two steps repeated 1X. The samples were dried in Speed Vac and resuspended in ice-cold freshly made 20 ng/µl trypsin in buffer D and stored on ice for 45 min to slowly swell the gel and digestion carried out at 37^{o}C for 6 hrs to overnight. After addition of 25 µl of buffer D, the supernatant was transferred to a cleaned tube and treated for 15 min intervals as follows; 50 µl solution X (5% formic acid/25% acetonitrile/70% water), 50 µl of buffer Y (5% formic acid/50% acetonitrile/45% water) and finally with 50 µl of buffer Z (5% formic acid/75% acetonitrile/20% water). The final supernatant was transferred to a clean peptide tube and dried in a Speed Vac and resuspended as desired for analysis.

4.4.13 TRYPSIN DIGEST ON RESIN TO OBTAIN PEPTIDES FOR MS/MS ANALYSIS

The resin (100 µL) was washed with 500 µL of 1M urea containing 40 mM NH_4HCO_3 followed by a wash with 40 mM NH_4HCO_3. The resin was then incubated with 90 µL of 40 mM NH_4HCO_3 and 10 µL of 1M DTT for 2 h at 37^{o}C. The suspension was allowed to cool to RT and the supernatant removed and replaced with 100 µL of 55 mM iodoacetamide, and the resin incubated in the dark for 1 hr with occasional vortexing every 15 minutes. The resin was washed with 500 µL of 1M urea containing 40 mM NH_4HCO_3 followed by the addition of 80 µL of 1M urea containing 40 mM NH_4HCO_3

and 20 µL of trypsin (20 µg in 200 µl of 40 mM NH_4HCO_3; ~ 0.1µg/µl) and incubated overnight at 37°C. The supernatant was removed and saved while the peptides were extracted 2 times by adding 100 µL of 25% acetonitrile in 1% formic acid and incubating for 20 min at RT. The peptides obtained from the supernatant were dried in a Speed-Vac and resuspended in 100 µL of 0.1% formic acid (buffer A) for clean up using reverse phase C-18 spin column. The spin column was cleaned first with 250 µL of buffer B (0.1% formic acid/80% acetonitrile) and then twice with buffer A. The sample was then applied to the spin column and spun for 4 minutes at 2,000 x g. The flow through was passed through the column once and the column washed 2 times with buffer A. The peptides were eluted with 250 µL of buffer B after spinning for 4 minutes at 2,000 x g and dried using a Speed Vac.

4.4.14 ENRICHMENT AND SITE MAPPING OF GLYCOPEPTIDES

Both the chemoenzymatically labeled and metabolically (GalNAz) labeled O-GlcNAc proteins were precipitated using methanol/chloroform and digested overnight at 37 °C by the addition of 1:10 (w/w) trypsin (Promega). Tryptic peptides mixtures were dried down in a Speed Vac. The azido-glycopeptides and peptides were dried down, resuspended in 200 µL of 25% acetonitrile in PBS, and the azido-glycopeptides and peptides were incubated with DIBO-modified resin (100 µL) pre-equilibrated with PBS buffer pH 7.4 for 3 h with end-to-end shaking at room temperature. The suspension was then centrifuged, supernatant discarded, and the resin washed by centrifugation at 1000 x g, for 5 min per wash with 10 column volumes of buffer as follows: 0.5% NP-40 in PBS (3X); 600 mM NaCl (3X) in PBS; 1 M urea in PBS (3X). The resin was then be rinsed

finally with PBS and resuspended in 1 column volume of PBS. The affinity captured azido-glycopeptides were ß-eliminated and subjected to Michael addition with DTT via resuspension of the resin in 1% triethylamine, 0.1% NaOH, 20% ethanol, and 10 mM DTT. The final pH was adjusted with triethylamine to 12.0–12.5 if necessary. The reaction was incubated at 50 °C for 2.5 h, and the reaction was quenched with trifluoroacetic acid (final concentration, 1%). The peptides were cleaned up via reverse phase C18 spin columns, eluted in 0.1% trifluoroacetic acid, 70% acetonitrile, and dried in a Speed Vac.

DTT-modified peptides were purified over activated thiol-Sepharose (thiol column) from Amersham Biosciences. Resin was swelled in degassed PBS containing 1 mM EDTA (PBS/EDTA), and dried peptides suspended in the same buffer were bound with a 1-h incubation in 200 µl of 50% slurry. The column was washed with 15 ml of PBS/EDTA and eluted three times sequentially with 150 µl of PBS/EDTA containing 20 mM free DTT. Peptides eluted from thiol affinity columns were acidified (brought to 1% trifluoroacetic acid), desalted with reverse-phase C18 spin columns (eluted in 70% acetonitrile, 0.1% trifluoroacetic acid), and dried for subsequent analysis.

4.4.15 MASS SPECTROMETRY (MS) ANALYSIS

Peptides obtained from in-gel, on-resin tryptic digestion and from ß-elimination were resuspended with 19.5 µL of 0.1% formic acid and 0.5 µL of 80% acetonitrile in 0.1% formic acid. The peptides were pressure loaded on a 75 µm x 8.5 cm C18 reverse phase column/emitter (packed in-house, YMC GEL ODS-AQ120ÅS-5) using a nitrogen pressure bomb. Peptides were eluted over a 160-min linear gradient increasing from 5 to

100 % solvent B over 90 min at a flow rate of 250 nl/min. Full scans were collected over 200-2000m/z using the orbitrap which was followed by six MS/MS events based upon intensity in the full scan. A decision tree method was used for the analysis of the collected peptides. By using this method, either CID or ETD was used to generate the resulting MS/MS scans, which was based on charge and m/z and analyzed by TurboSequest with data searched against NCBI non-redundant human database for protein identification.

4.5 REFERENCES

(1) Klein A. L, Berkaw M. N, Buse M. G, Ball L. E. *Mol Cell Proteomics* **2009**, 8:2733–45.

(2) Roquemore E. P, Chou T. Y, Hart G. W. *Methods Enzymol.* **1994**, *230*, 443-460.

(3) Kaji H, Saito H, Yamauchi Y, Shinkawa T, Taoka M, Hirabayashi J, Kasai K, Takahashi N, Isobe T. *Nat. Biotechnol.* **2003**, 21, 667–672.

(4) Han D. K, Eng J, Zhou H. and Aebersold, R. *Nat. Biotechnol.* **2001**, 19, 946–951.

(5) Wang Z, Hart G. W. *Clin Proteomics*. **2008**, *4*:5–13.

(6) Wells L, Vosseller K, Cole R. N, Cronshaw J. M, Matunis M. J. and Hart G. W. *Mol. Cell. Proteomics* **2002**, *1*:791–804.

(7) Teo C. F, Ingale S, Wolfert M. A, Elsayed G. A, Nöt L. G, Chatham J. C, Wells L, and Boons G-J. *Nat. Chem. Biol*., **2010**, *6*: 338-43.

(8) Khidekel N, Arndt S, Lamarre-Vincent N, Lippert A, Poulin-Kerstien K. G, Ramakrishnan B, Qasba P. K. and Hsieh-Wilson L. C. *J. Am. Chem. Soc*. **2003**, 125, 16162–16163.

(9) Ramakrishnan B, and Qasba P. K. *J. Biol. Chem*. **2002**, *277*, 20833-20839.

(10) Clark P. M, Dweck J. F, Mason D. E, Hart C. R, Buck S. B, Peters E. C, Agnew B. J, Hsieh-Wilson L. C. *J. Am. Chem. Soc.* **2008**, 130(35):11576-7.

(11) Camarero J. A. *Biopolymers* **2008**, 90, 450.

(12) Meldal M, and Tornoe C. W. *Chem. Rev.* **2008**, 108, 2952.

(13) Haltiwanger R. S, Grove K, Philipsberg G. A. *J. Biol. Chem.* **1998**, 273:3611–7.

(14) Boyce M, Carrico I. S, Ganguli A. S, Yu S. H, Hangauer M. J, Hubbard S. C, Kohler J. J, and Carolyn R. Bertozzi C. R. *Proc. Natl. Acad. Sci. USA* **2011**, 108:3141–6.

(15) Chalkley R. J, and Burlingame A. L. *J. Am. Soc. Mass Spectrom*. **2001**, 12, 1106–1113.

(16) Wells L, Vosseller K, Cole R. N, Cronshaw J. M, Matunis M. J. and Hart G. W. *Mol. Cell. Proteomics* **2002**, 1:791–804.

(17) Mikesh L. M, Ueberheide B, Chi A, Coon J. J, Syka J. E, Shabanowitz J, Hunt D. F. *Biochim Biophys Acta* **2006**;1764:1811–22.

(18) Kobata A. *Glycoconjugate J* **1998**, 15: 323–31.

(19) Butler M, Quelhas D, Critchley A. J, Carchon H, Hebestreit H. F, Hibbert R. G, Vilarinho L, Teles E, Matthijs G, Schollen E, Argibay P, Harvey D. J, Dwek R. A, Jaeken J, Rudd P. M. *Glycobiology* **2003**, 13, 601–622.

(20) Liu F, Zaidi T, Grundke-Iqbal I, Iqbal K, and Gong C.-X. *Neuroscience* **2002**, 115, 829–837.

(21) Liu F, Iqbal K, Grundke-Iqbal I, Hart G. W, and Gong C.-X. *Proc. Natl. Acad. Sci. USA* **2004**, 101:10804–9.

(22) Shimkus M, Levy J, and Herman T. *Proc. Natl. Acad. Sci. USA* **1985**, 82:2593–7.

(23) Wilchek M, and Bayer E, *Applications of avidin-biotin technology: literature survey,* in: M. Wilchek, E. Bayer (Eds.), *Methods in Enzymology*, vol. 184, Academic Press, New York, 1990, pp. 14–45.

CHAPTER 5

SELECTIVE LABELING OF LIVING CELLS BY A PHOTO-TRIGGERED CLICK REACTION

5.1 INTRODUCTION

The bioorthogonal chemical reporter strategy is emerging as a versatile method for labeling of biomolecules such as nucleic acids, lipids, proteins, and carbohydrates.[1, 2] In this approach, a unique chemical functionality is incorporated into a targeted biomolecule, preferably by the biosynthetic machinery of the cell, followed by a specific chemical reaction of the functional group with an appropriate probe. In particular, the azide is an attractive chemical reporter because of its small size, diverse mode of reactivity, and bio-orthogonality. Azides can be incorporated into biomolecules using a variety of strategies such as post synthetic modification,[3] *in-vitro* enzymatic transfer,[4] the use of covalent inhibitors,[5] and metabolic labeling by feeding cells a biosynthetic precursor modified with an azido function.[1]

The most commonly employed bioorthogonal reactions with azides include the Staudinger ligation with phosphines,[6] copper (I)-catalyzed cycloaddition with terminal alkynes,[7] and strain-promoted cycloaddition with cyclooctynes.[8, 9] The latter type of reaction, which was coined copper-free click chemistry, does not require a cytotoxic metal catalyst thereby offering a unique opportunity for labeling living cells. The attraction of this type of technology was elegantly demonstrated by a study of the Bertozzi laboratory in which glycans of the developing zebrafish were imaged using a difluorinated cyclooctyne derivative.[10]

We have recently demonstrated that derivatives of 4-dibenzocyclooctynol (**1** DIBO, Scheme 5.1) react exceptionally fast in the absence of a Cu (I) catalyst with azido-containing saccharides and amino acids, and can be employed for visualizing glycoconjugates of living cells that are metabolically labeled with azido-containing monosaccharides.[9]

Scheme 5.1. Structures of cyclooctyne compounds for strain-promoted cycloaddition reaction.

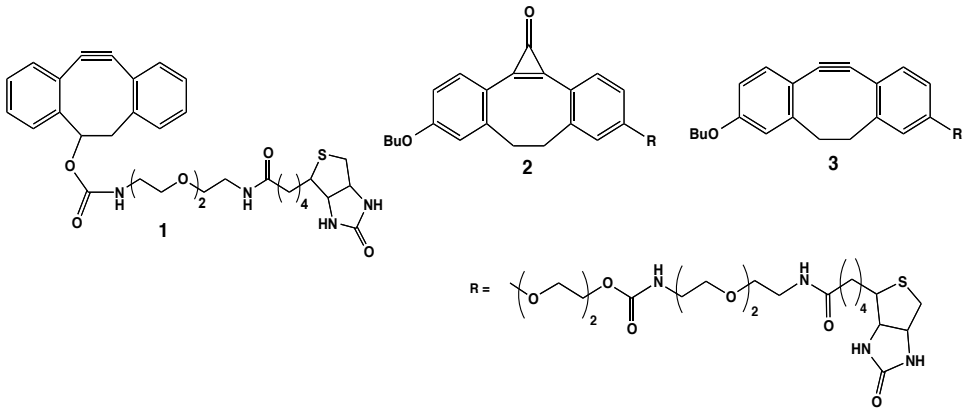

The utility of azide-based bioorthogonal reporter strategy can be further extended by the development of a photochemically-triggered click reaction as this approach provide opportunities for the spatial and temporal control of the labeling of the target substrates. In fact, photochemical release or generation of an active molecule is a widely employed strategy to deliver bioactive compounds to addressable target sites in a time-controlled manner.[11] To achieve this goal; we have explored photochemical generation of

reactive dibenzocyclooctynes. It is known that single[12, 13] or two-photon[14] excitation of cyclopropenones results in the formation of corresponding acetylenes. Photochemical decarbonylation of thermally stable diaryl-substituted cyclopropenones is especially efficient (Φ = 0.2 – 1.0) and produces alkynes in a quantitative yield.[13] This reaction is also extremely fast and is complete within few hundred picoseconds after excitation.[15] We have already employed cyclopropenone moiety in the development of photoswitchable enediynes.[16] Here we report a novel photo-triggered click strategy for metal-free ligation of azides (Scheme 5.2). Cyclopropenones, such as **2** (Scheme 1), do not react with azides under ambient conditions in the dark but efficiently produce reactive dibenzocyclooctynes **3** (Scheme 5.1) upon irradiation. The latter type of compound could be employed for labeling of living cells modified with azido-containing cell surface saccharides.

Scheme 5.2. Photochemical initiation of the copper-free acetylene-azide cycloaddition.

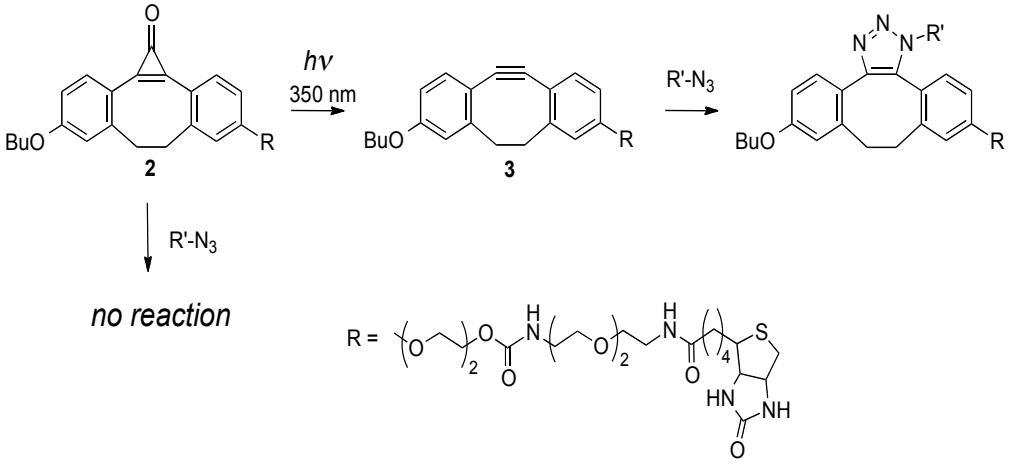

5.2 RESULTS AND DISCUSSION

Having established that light activation of cyclopropenones results in the clean formation of the corresponding dibenzocyclooctynes, which can undergo metal-free cycloadditions with azides to give corresponding triazoles, attention was focused on labeling living cells modified with azido moieties. Thus, Jurkat cells were cultured in the presence of 25 μM of peracetylated *N*-azidoacetylmannosamine (Ac_4ManNAz) for 3 days to metabolically introduce *N*-azidoacetyl-sialic acid (SiaNAz) moieties into glycoproteins and glycolipids.[17] As a negative control, Jurkat cells were employed that were grown in the presence of peracetylated *N*-acetylmannosamine (Ac_4ManNAc). The cells were exposed to 30 μM of compound **1**, **2**, and **3** for 1 h at room temperature. In addition, cells and cyclopropenone **2** were exposed to light (350 nm) for 1 min to form *in-situ* cyclooctyne **3** and then incubated for 1 h at room temperature. Next, the cells were washed and stained with avidin-fluorescein isothiocyanate (FITC) for 15 min at 4°C. The efficiency of the two-step cell surface labeling was determined by measuring the fluorescence intensity of the cell lysates. Cyclooctynes **1** and **3** exhibited strong labeling of the cells (Figure 5.1).

Furthermore*, in-situ* activation of **2** to give **3** resulted in equally efficient cell labeling. As expected, low fluorescence intensities were measured when cells were exposed to cyclopropenone **2** in the dark demonstrating that this compound can be selectively activated by a short irradiation with 350 nm light. Similar staining patterns were obtained when the living cells were analyzed by flow cytometry (Figure 5.2).

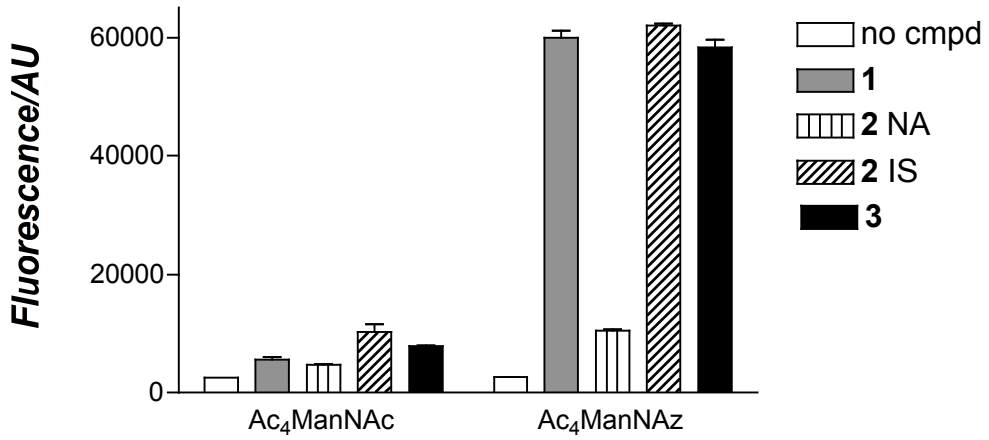

Figure 5.1 Cell surface labeling with compounds **1**, **2**, and **3**. Jurkat cells grown for 3 days in the presence of Ac_4ManNAc (25 μM) or Ac_4ManNAz (25 μM) were incubated at room temperature with compounds **1**, **2**, and **3** at 30 μM for 1 h. Compound **2** was assessed without activation (**2** NA), after immediate light activation *in situ* (1 min at 350 nm; **2** IS). Next, cells were incubated with avidin-FITC for 15 min at 4°C, after which cell lysates were assessed for fluorescence intensity. AU indicates arbitrary fluorescence units.

Some background labeling was observed when the control cells (labeled with Ac_4ManNAc) were exposed to **2** or **3** and then treated with avidin-FITC (Figure 5.1). To exclude the possibility that the background labeling is due to unwanted side reactions of the compounds with protein, the cell lysates were analyzed by Western blotting using an anti-biotin antibody conjugated to HRP (Figure 5.3). Gratifyingly, the control cells gave negligible staining, demonstrating that background staining is not due to chemical reactions of the compounds with protein and probably arises from non-covalent interactions with the cell membrane.

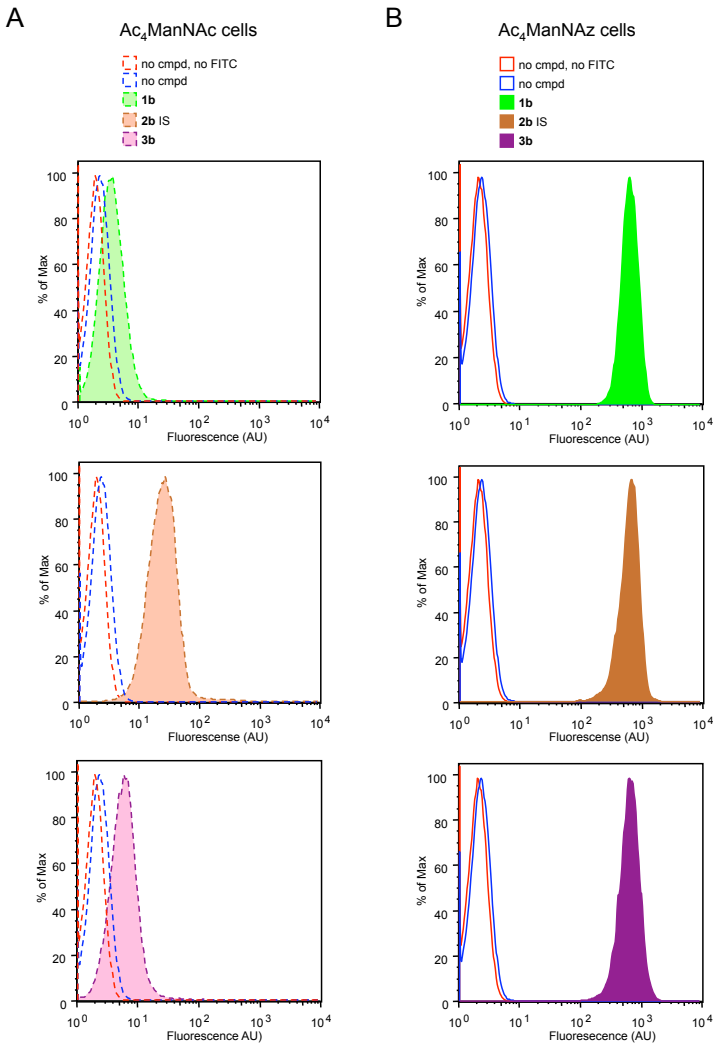

Figure 5.2 Flow cytometry analysis of cell surface labeling with compounds **1**, **2**, and **3**. Jurkat cells grown for 3 days in the presence of $Ac_4ManNAc$ (25 μM; A) or $Ac_4ManNAz$ (25 μM; B) were incubated at room temperature with compounds **1**, **2**, and **3** at 30 μM for 1 h. Compound **2** was assessed after light activation *in situ* (1 min at 350 nm; **2** IS). Next, cells were incubated with avidin-FITC for 15 min at 4°C, after which living cells were analyzed by flow cytometry. AU indicates arbitrary fluorescence units.

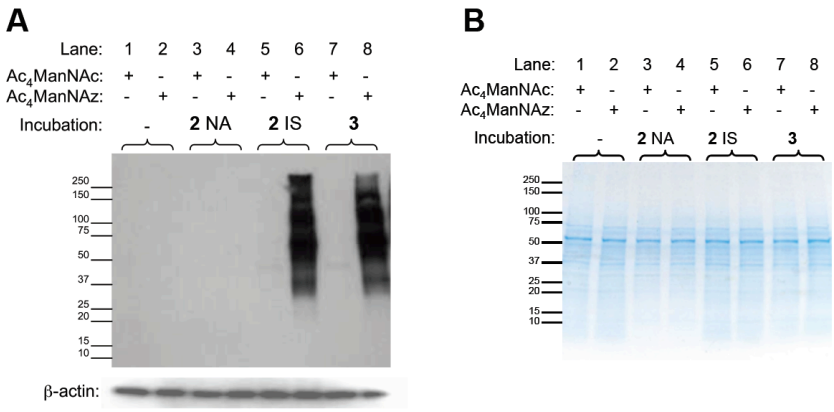

Figure 5.3 Western blot of Jurkat cells after labeling with compounds **2** and **3**. Jurkat cells grown for 3 days in the presence of Ac_4ManNAc (25 μM) or Ac_4ManNAz (25 μM) were incubated at room temperature with compounds **2** and **3** at 30 μM for 1 h. Compound **2** was assessed without activation (**2** NA), after immediate light activation *in situ* (1 min at 350 nm; **2** IS). Next, cells were lysed and cell lysates (15 μg total protein per lane) were resolved by SDS-PAGE and the blot was probed with an anti-biotin antibody conjugated to HRP (A). Total protein loading was confirmed by Coomassie staining (B).

As expected, similar patterns of staining were observed for cells labeled with Ac_4ManNAz and then exposed to **3** or *in-situ* activated **2**. The concentration-dependency of the cell surface labeling was examined by incubating cells with various concentrations of **1**, *in-situ* activated **2**, and **3**, followed by staining with avidin-FTIC (Figure 5.4). The cells displaying azido moieties showed a dose-dependent increase in fluorescence intensity. Reliable fluorescent labeling was achieved at a concentration of 3 μM, however, optimal results were obtained at concentrations ranging from 10 to 100 μM.

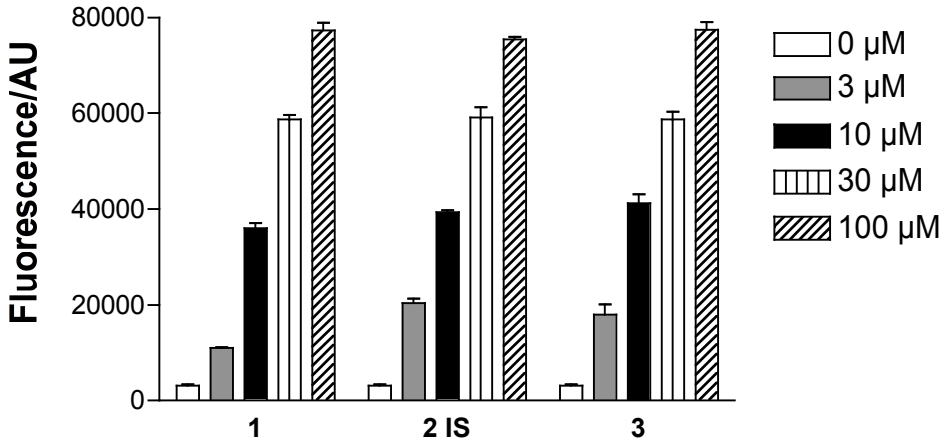

Figure 5.4 Concentration dependence of cell surface labeling with compounds **1**, **2**, and **3**. Jurkat cells grown for 3 days in the presence of $Ac_4ManNAc$ (25 μM) or $Ac_4ManNAz$ (25 μM) were incubated at room temperature with compounds **1**, **2**, and **3,** 0-100 μM for 1 h. Compound **2** was assessed after immediate light activation *in situ* (1 min at 350 nm; **2** IS). Next, cells were incubated with avidin-FITC for 15 min at 4°C, after which cell lysates were assessed for fluorescence intensity. AU indicates arbitrary fluorescence units.

Interestingly, at low concentration, **3** gave a somewhat higher fluorescent reading than **1**. A time course experiment demonstrated that labeling with **1** and **3** (30 mm) at 25°C reaches an apparent plateau after an incubation time of approximately 45 min, which gradually increased after prolonged exposure (Figure 5.5). A similar experiment at a lower temperature (4°C) also showed an initial fast- followed by a slow and gradual increase in fluorescent intensity; however, the responses were somewhat lower compared to the reaction at 25°C (Figure 5.6).

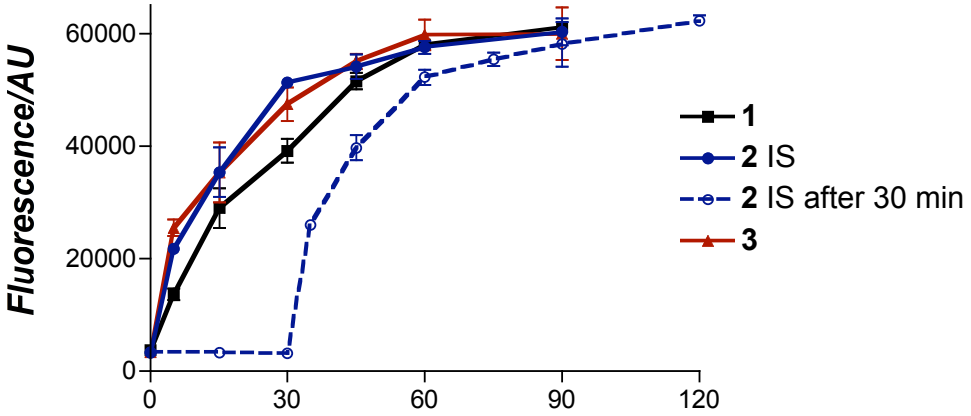

Figure 5.5 Time course for cell surface labeling with compounds **1**, **2**, and **3**. Jurkat cells grown for 3 days in the presence of Ac_4ManNAc (25 μM) or Ac_4ManNAz (25 μM) were incubated at room temperature with compounds **1**, **2**, and **3** at 30 μM for 1 h. Compound **2** was assessed after immediate light activation *in situ* (1 min at 350 nm; **2** IS), and after delayed light activation for 30 min *in situ* (**2** IS after 30 min). Next, cells were incubated with avidin-FITC for 15 min at 4°C, after which cell lysates were assessed for fluorescence intensity. AU indicates arbitrary fluorescence units.

Light activation of cyclopropenone **2** provides and attractive opportunity for labeling cells in a temporal controlled manner. To establish a proof of principle for such labeling, a time course experiment was performed whereby cells were first incubated in the presence of **2** for 30 min in the dark, and then exposed to UV light to form *in-situ* alkyne **3**, which was allowed to react with cell surface azide moieties for different periods of time. Importantly, an identical pattern of labeling was observed compared to cells immediately exposed to UV light, however, with a 30 min delay (Figure 5.5).

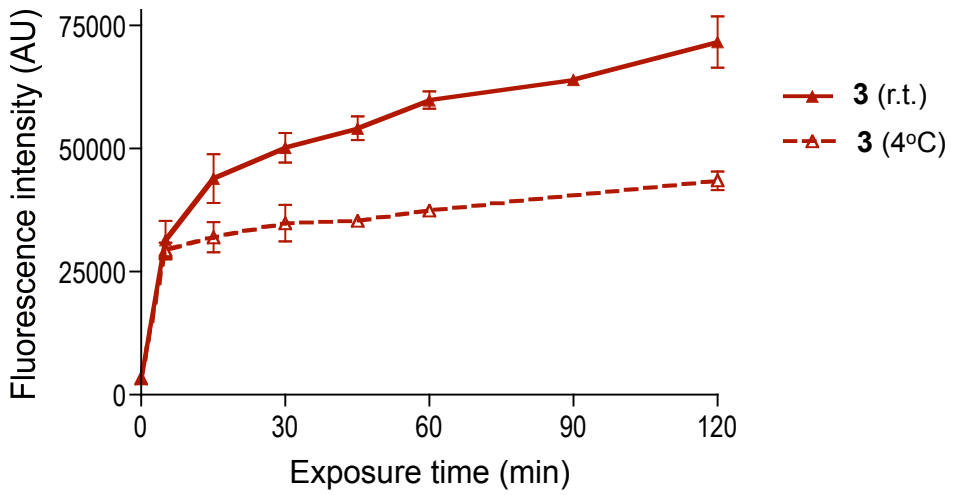

Figure 5.6 Time course of cell surface labeling with **3** at room temperature and 4°C. Jurkat cells grown for 3 days in the presence of Ac_4ManNAz (25 μM) were incubated at room temperature or 4°C with compound **3** at 30 μM for 0-120 min. Next, cells were incubated with avidin-FITC for 15 min at 4°C, after which cell lysates were assessed for fluorescence intensity. AU indicates arbitrary fluorescence units.

The heat-sensitivity of the cyclopropenone extrusion reaction was examined by exposing cells labeled with Ac_4ManNAz to **2** at 37°C in the dark, and no significant increase in fluorescence was observed compared to exposure at room temperature (Figure 5.7). To ensure that *in situ* activation of **2** had no effect on cell viability and morphology, cells were assessed for the ability to exclude trypan blue and fortunately no changes were observed compared to cells that were not exposed to **2** both with and without UV light activation.

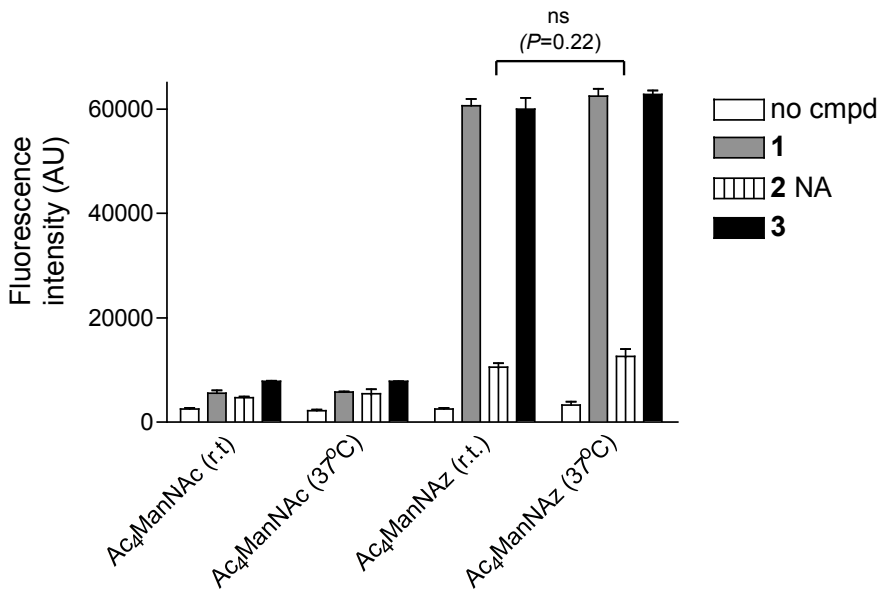

Figure 5.7 Effect of higher temperature on cell surface labeling with compounds **1**, **2**, and **3**. Jurkat cells grown for 3 days in the presence of Ac_4ManNAc (25 μM) or Ac_4ManNAz (25 μM) were incubated in the dark with compounds **1, 2**, and **3** at 30 μM at room temperature or 37°C for 1 h. Compound **2** was assessed without light activation (**2** NA). Next, cells were incubated with avidin-FITC for 15 min at 4°C, after which cell lysates were assessed for fluorescence intensity. AU indicates arbitrary fluorescence units and ns indicates no statistical difference.

Cell viability was also examined after incubation with **2** with and without light activation followed by reincubation for 5 and 24 h (Figure 5.8). In each case, there was no significant difference in the ability of the cells to reduce MTT to its insoluble formazan salt as compared to control cells.

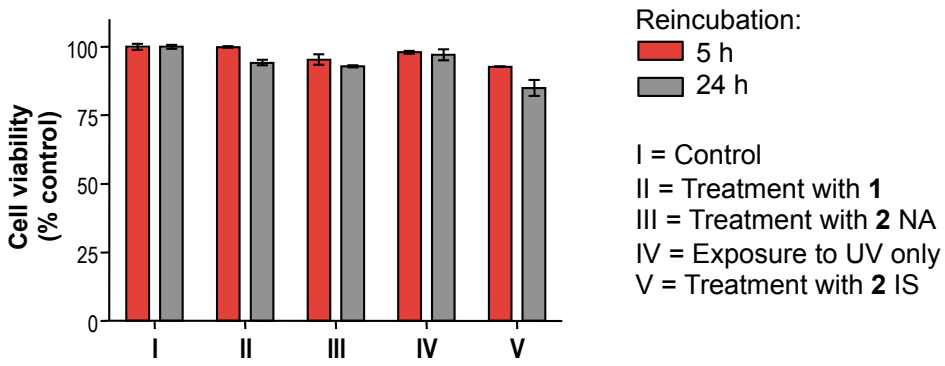

Figure 5.8 Toxicity assessment of cycloaddition reaction with compounds **1** and **2**. Jurkat cells grown for 3 days in the presence of Ac_4ManNAz (25 μM) were incubated with compounds **1** (II) and **2** at 30 μM for 1 h at room temperature. Cell viability after incubation with **2** was assessed with (**2** IS; V) and without (**2** NA; III) light activation *in situ* (1 min at 350 nm). Control cells were treated similarly, but without exposure to compounds and with (IV) and without (I) UV light. After reincubating the cells in cell culture medium for 5 h (red bars) or 24 h (grey bars), the cell viability was assessed by their ability to reduce MTT to its insoluble formazan salt. Cell viability values were normalized for the amount of viable cells of the sample with control cells (100%; I).

Finally, attention was focused on visualizing azido-containing glycoconjugates of cells by confocal microscopy. Thus, adherent Chinese hamster ovary (CHO) cells were cultured in the presence of Ac_4ManNAz (100 μM) for three days. The resulting cell surface azido moieties were reacted with *in situ* generated **3** (30 μM) and then visualized with avidin-Alexa fluor 488. As expected, staining was only observed at the cell surface (Figure 5.9) and showed similar cell surface labeling as obtained by staining with **1.**[9]

Cells cultured in the presence of Ac_4ManNAc (100 μM) exhibited very low fluorescence staining. As expected, cells metabolically labeled with Ac_4ManNAz and exposed to **2** in the dark showed also negligible staining.

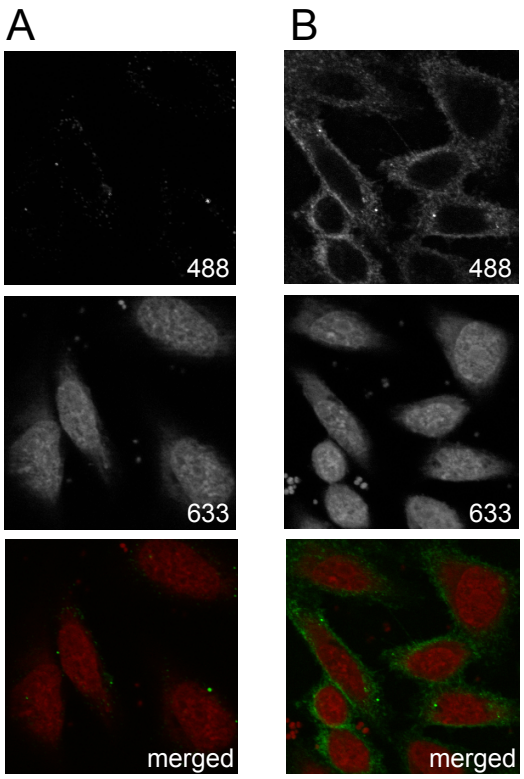

Figure 5.9 Fluorescence images of cells labeled with compound **2** and avidin-Alexa fluor 488. CHO cells grown for 3 days in the presence of Ac_4ManNAc (100 μM; A) or Ac_4ManNAz (100 μM; B) were given compound 2 (30 μM), subjected to 1 min UV light for in situ activation (2 IS), and further incubated for 1 h at room temperature. Next, cells were incubated with avidin-Alexa Fluor 488 for 15 min at 4^{o}C and, after washing, fixing, and staining for the nucleus with the far-red-fluorescent dye TO-PRO-3 iodide, imaged. Merged indicate that the images of cells labeled with Alexa Fluor (488 nm) and TO-PRO iodide (633 nm) are merged and shown in green and red, respectively.

5.3 CONCLUSIONS

It has been shown that light activation of cyclopropenone **2** results in the clean formation of the corresponding dibenzocyclooctyne **3** which can undergo fast and catalyst-free cycloadditions with azides to give corresponding triazoles. *In-situ* light activation of **2** made it possible to efficiently label living cells expressing glycoproteins containing *N*-azidoacetyl-sialic acid. It is to be expected that the properties of compounds such as **2** will make it possible to label living organisms in a temporal and/or spatial controlled manner. It has already been demonstrated that glycoconjugates of model organisms, such as zebrafish, can be metabolically labeled with azido-containing sugars and such an approach has been employed to demonstrate tissue specific expression of glycoconjugates.[10] It is to be expected that the use of compounds such as **2** will make it possible to visualize azido-labeled biomolecules in model organisms or tissues in a more controlled and reliable manner.

In this respect, differences in staining intensities and patterns may arise when classical metal-free click reagents[18] such as **1** are employed due to possible concentration gradients. On the other hand, the use of a photo-triggered click reaction will make it possible to achieve a homogeneous concentration of reagent before initiating the click reaction. The photo-triggered click reagent reported here has a much higher quantum yield than the previously described photo-activated Diels-Alder reaction and hence will exhibit much less light induced toxicity.

It is to be expected that compounds such as **2** can be activated in a spatial controlled manner, however, the resulting alkyne (**3**) is a stable derivative, which may diffuse to surrounding space thereby reducing the resolution of labeling. Although future

studies will need to establish the spatial resolution of the photo-triggered click reaction, it is to be expected that it can selectively label organs or tissues of model organisms. Such an approach provides a unique opportunity for biotinylation of glycoconjugates of specific organs or tissues, which can then be isolated for glycomics or glycoproteomics studies. Wong and coworkers have already reported a combined use of metabolic labeling, Cu-mediated click reactions and glycoconjugate isolation for glycomics.[19] However, such an approach cannot be employed for living organisms.

It is to be expected that other fields of science such as the fabrication of microarrays and the preparation of multifunctional materials, may benefit from photo-triggered click chemistry. In this respect, Cu-mediated click reactions have been used for the fabrication of saccharide microarrays by offering a convening approach to immobilize azide-modified saccharides to an alkyne-modified surface.[20] It is to be expected that surface modification with compounds **2** will offer exciting opportunities for spatially controlled ligand immobilization using light activation followed by copper-free ligation. Furthermore, metal-free click reactions have been applied in material chemistry,[21] and the obvious advantage of such a synthetic approach is that it offers a reliable approach for macromolecule modification without the need of using toxic reagents. Therefore, it is to be expected that the combined use of traditional- and photo-activated metal-free click reactions will offer an attractive approach for multi-functionalization of polymers and macromolecules.[22]

5.4 MATERIALS AND METHODS

5.4.1 REAGENTS AND GENERAL PROCEDURE FOR BIOLOGICAL EXPERIMENTS

Synthetic compounds **1**, **2**, and **3** were reconstituted in DMF and stored at –80^{o}C. Final concentrations of DMF never exceeded 0.56% to avoid toxic effects. The *in situ* photo-activation of biotinylated cyclopropenone **2** was performed using a mini-Rayonet® photoreactor equipped with two 350 nm florescent tubes (4W). The irradiated cell suspensions were kept in plastic vials, which served as an additional short band-path filter. The vial wall absorbs *ca.* 60% of light at 350 nm, 70% at 300 nm, and is virtually not transparent below 275 nm.

5.4.2 CELL CULTURE CONDITIONS

Human Jurkat cells (Clone E6-1; ATCC) were cultured in RPMI 1640 medium (ATCC) with L-glutamine (2 mM), adjusted to contain sodium bicarbonate (1.5 g/L), glucose (4.5 g/L), HEPES (10 mM), and sodium pyruvate (1 mM) and supplemented with penicillin (100 u/ml) / streptomycin (100 μg/mL; Mediatech) and fetal bovine serum (FBS, 10%; Hyclone). Chinese hamster ovary (CHO) cells (Clone K1; ATCC) were cultured in Kaighn's modification of Ham's F-12 medium (F-12K) with L-glutamine (2 mM), adjusted to contain sodium bicarbonate (1.5 g L^{-1}) and supplemented with penicillin (100 U mL^{-1}) / streptomycin (100 μg mL^{-1}) and FBS (10%). Cells were maintained in a humid 5% CO_2 atmosphere at 37^{o}C.

5.4.3 CELL SURFACE AZIDE LABELING

Jurkat cells were seeded at a density of 75,000 cells mL^{-1} in a total volume of 40 mL culture medium in the presence of peracetylated *N*-azidoacetylmannosamine (Ac_4ManNAz; 25 μM final concentration) and grown for 3 days, leading to the metabolic incorporation of the corresponding *N*-azidoacetyl sialic acid (SiaNAz) into their cell surface glycoproteins. Control cells were grown in the presence of peracetylated *N*-acetylmannosamine (Ac_4ManNAc; 25 μM final concentration) for 3 days. Similarly, CHO cells were grown for 3 days in the presence of Ac_4ManNAz (100 μM final concentration) or Ac_4ManNAc (100 μM final concentration).

5.4.4 CLICK CHEMISTRY AND DETECTION BY FLUORESCENCE INTENSITY

Jurkat cells bearing azides and control cells were washed with labeling buffer (DPBS, pH 7.4 containing 1% FBS and 1% BSA), transferred to round bottom tubes (1 $x10^6$ cells/sample) and incubated with the biotinylated compounds **1**, **2**, or **3** (0-100 μM) in labeling buffer for 0-90 min at r.t. To activate **2** *in situ*, the cell suspension was subjected to UV light (350 nm) for 1 min immediately after adding the compound to the cells, unless stated otherwise. The cells were washed three times with cold labeling buffer and then incubated with avidin conjugated with fluorescein (0.5 μg/ml; Molecular Probes) for 15 min at 4^oC. Following three washes, cells were either lysed in passive lysis buffer (Promega) and cell lysates were analysed for fluorescence intensity (485 ex / 520 em) using a microplate reader (BMG Labtech) or live cells were assessed by flow cytometry using the FACSCalibur flow cytometer (Becton Dickinson Immunocytometry

Systems) and data analysis was performed with FlowJo software (Tree Star, Inc.). Data points were collected in triplicate and are representative of three separate experiments. Fluorescence of Jurkat cell lysates was expressed as fluorescence (arbitrary units; AU) per 800,000 cells.

5.4.5 MEASUREMENT OF CYTOTOXICITY

Cell viability and cell morphology were assessed by exclusion of trypan blue and microscopic evaluation immediately after photoactivation or after reincubation of the labeled cells in cell culture medium for 5 or 24 h. After the reincubation, viability was measured by quantifying the cellular ability to reduce the water-soluble tetrazolium dye 3-4,5-dimethylthiazole-2,5-diphenyl tetrazolium bromide (MTT) to its insoluble formazan salt (25). Data points were collected in triplicate and expressed as normalized values for control cells (100%).

5.4.6 WESTERN BLOT ANALYSIS

Jurkat cells were harvested by centrifugation (5 min at 500 x *g*) and resuspended as 5 x10^6 cells/mL. The cell suspensions (200 μL per sample) were incubated with biotin-conjugated alkynes **1**, **2**, and **3** (30 μM) or without compound as control for 1 h. To activate **2** *in situ*, immediately after adding the compound to the cells, the cell suspension was subjected to UV light (350 nm) for 1 min. The cells were washed (4 x 10 min) with cold DPBS, pH 7.4 containing FBS (1%) and lysed in passive lysis buffer. The cell lysates were clarified by centrifugation at 22,000 x *g* for 15 min and the total protein content of the clear supernatants was assessed using the bicinchonic acid assay (BCA;

Pierce Biotechnology). Cell lysate samples (20 μg protein) in SDS-PAGE sample buffer containing 2-mercaptoethanol were boiled for 5 min, resolved on a 4-20% Tris-HCl gel (Bio-Rad) and transferred to nitrocellulose membrane. Next the membrane was blocked in blocking buffer (non-fat dry milk (5%; Bio-Rad) in PBST (PBS containing 0.1% Tween-20 and 0.1% Triton X-100)) for 2 h at r.t. The blocked membrane was incubated for 1 h at r.t. with an anti-biotin antibody conjugated to horseradish peroxidase (HRP) (1:100,000; Jackson ImmunoResearch Lab, Inc.) in blocking buffer and washed with PBST (4 x 10 min). Final detection of HRP activity was performed using ECL Plus chemiluminescent substrate (Amersham^{TM}), exposure to film (Kodak) and development using a digital X-ray imaging machine (Kodak). Next the blot was stripped and reprobed for loading control (β-actin) as described above. Coomassie staining was used to confirm total protein loading.

5.4.7 DETECTION OF CELL LABELING BY FLUORESCENCE MICROSCOPY

CHO cells bearing azides and untreated control cells were transferred to glass coverslips and cultured for 36 h in their original medium. Live CHO cells were treated with the biotinylated compound **2** (30 μM) in labeling buffer (DPBS, supplemented with FBS (1%)) for 1 h at r.t. To activate **2** *in situ*, immediately after adding the compound to the cells, the cells were subjected to UV light (350 nm) for 1 min. Next, the cells were incubated with avidin conjugated with Alexa Fluor 488 (Molecular Probes) for 15 min at 4^{o}C. Cells were washes 3 times with labeling buffer and fixed with formaldehyde (3.7% in PBS). The nucleus was labeled with the far red-fluorescent TO-PRO-3 dye (Molecular Probes). The cells were mounted with PermaFluor (Thermo Electron Corporation) before

imaging. Initial analysis was performed on a Zeiss Axioplan2 fluorescent microscope. Confocal images were acquired using a 60X (NA1.42) oil objective. Stacks of optical sections were collected in the *z* dimensions. The step size, based on the calculated optimum for each objective, was between 0.25 and 0.5 μm. Subsequently, each stack was collapsed into a single image (*z*-projection). Analysis was performed offline using ImageJ 1.39f software (National Institutes of Health, USA) and Adobe Photoshop CS3 Extended Version 10.0 (Adobe Systems Incorporated), whereby all images were treated equally.

5.4.8 STATISTICAL ANALYSIS

Statistical significance between groups was determined by two-tailed, unpaired Student's *t* test. Differences were considered significant when $P<0.05$.

5.5 REFERENCES

(1) Baskin, J. M.; Bertozzi, C. R. *QSAR Comb. Sci.* **2007**, *26*, 1211-1219.

(2) Johnsson, K. *Nat. Chem. Biol.* **2009**, *5*, 63-65; Laughlin, S. T.; Bertozzi, C. R. *Proc. Natl. Acad. Sci. U. S. A.* **2009**, *106*, 12-17.

(3) Gramlich, P. M.; Wirges, C. T.; Manetto, A.; Carell, T. *Angew. Chem. Int. Ed. Engl.* **2008**, *47*, 8350-8358; Weisbrod, S. H.; Marx, A. *Chem. Commun.* **2008**, 5675-5685.

(4) Fernandez-Suarez, M.; Baruah, H.; Martinez-Hernandez, L.; Xie, K. T.; Baskin, J. M.; Bertozzi, C. R.; Ting, A. Y. *Nat. Biotechnol.* **2007**, *25*, 1483-1487; Ochiai, H.; Huang, W.; Wang, L. X. *J. Am. Chem. Soc.* **2008**, *130*, 13790-13803.

(5) Speers, A. E.; Adam, G. C.; Cravatt, B. F. *J. Am. Chem. Soc.* **2003**, *125*, 4686-4687.

(6) Saxon, E.; Bertozzi, C. R. *Science* **2000**, *287*, 2007-2010.

(7) Kolb, H. C.; Finn, M. G.; Sharpless, K. B. *Angew. Chem. Int. Ed.* **2001**, *40*, 2004-2021; Breinbauer, R.; Kohn, M. *Chembiochem* **2003**, *4*, 1147-1149.

(8) Agard, N. J.; Prescher, J. A.; Bertozzi, C. R. *J. Am. Chem. Soc.* **2004**, *126*, 15046-15047; Baskin, J. M.; Prescher, J. A.; Laughlin, S. T.; Agard, N. J.; Chang, P. V.; Miller, I. A.; Lo, A.; Codelli, J. A.; Bertozzi, C. R. *Proc. Natl. Acad. Sci.* **2007**, *104*, 16793-16797.

(9) Ning, X. H.; Guo, J.; Wolfert, M. A.; Boons, G. J. *Angew. Chem. Int. Ed.* **2008**, *47*, 2253-2255.

(10) Laughlin, S. T.; Baskin, J. M.; Amacher, S. L.; Bertozzi, C. R. *Science* **2008**, *320*, 664-667.

(11) Pelliccioli, A. P.; Wirz, J. *Photochem. Photobiol. Sci.* **2002**, *1*, 441-458; Mayer, G.; Heckel, A. *Angew. Chem. Int. Ed.* **2006**, *45*, 4900-4921; Ellis-Davies, G. C. R. *Nat. Methods* **2007**, *4*, 619-628; Song, W.; Wang, Y.; Qu, J.; Lin, Q. *J. Am. Chem. Soc.* **2008**, *130*, 9654-9655.

(12) Chapman, O. L.; Gano, J.; West, P. R.; Regitz, M.; Maas, G. *J. Am. Chem. Soc.* **1981**, *103*, 7033–7036; Dehmlow, E. V.; Neuhaus, R.; Schell, H. G. *Chem. Ber.* **1988**, *121*, 569-571; Murata, S.; Yamamoto, T.; Tomioka, H. **1993**, *115*, 4013–4023; Chiang, Y.; Kresge, A. J.; Paine, S. W.; Popik, V. V. *J. Phys. Org. Chem.* **1996**, *9*, 361-370; Kuzmanich, G.; Natarajan, A.; Chin, K. K.; Veerman, M.; Mortko, C. J.; Garcia-Garibay, M. A. *J. Am. Chem. Soc.* **2008**, *130*, 1140-1141.

(13) Poloukhtine, A.; Popik, V. V. *J. Org. Chem.* **2003**, *68*, 7833-7840.

(14) Urdabayev, N. K.; Poloukhtine, A.; Popik, V. V. *Chem. Commun.* **2006**, 454-456.

(15) Takeuchi, S.; Tahara, T. *J. Chem. Phys.* **2004**, *120*, 4768-4776; Poloukhtine, A.; Popik, V. V. *J. Phys. Chem. A* **2006**, *110*, 1749-1757.

(16) Poloukhtine, A.; Popik, V. V. *Chem. Commun.* **2005**, 617-619; Poloukhtine, A.; Popik, V. V. *J. Org. Chem.* **2005**, *70*, 1297-1305; Poloukhtine, A.; Popik, V. V. *J. Org. Chem.* **2006**, *71*, 7417-7421; Pandithavidana, D. R.; Poloukhtine, A.; Popik, V. V. *J. Am. Chem. Soc.* **2009**, *131*, 351-356.

(17) Luchansky, S. J.; Bertozzi, C. R. *Chembiochem* **2004**, *5*, 1706-1709.

(18) van Berkel, S. S.; Dirks, A. T. J.; Debets, M. F.; van Delft, F. L.; Cornelissen, J. J. L. M.; Nolte, R. J. M.; Rutjes, F. P. J. T. *Chembiochem* **2007**, *8*, 1504-1508; Blackman, M. L.; Royzen, M.; Fox, J. M. *J. Am. Chem. Soc.* **2008**, *130*, 13518-13519; Codelli, J. A.; Baskin, J. M.; Agard, N. J.; Bertozzi, C. R. *J. Am. Chem.*

Soc. **2008**, *130*, 11486-11493; Devaraj, N. K.; Weissleder, R.; Hilderbrand, S. A. *Bioconjug. Chem.* **2008**, *19*, 2297-2299; Becer, C. R.; Hoogenboom, R.; Schubert, U. S. *Angew. Chem. Int. Ed. Engl.* **2009**, *48*, 4900-4908; Gutsmiedl, K.; Wirges, C. T.; Ehmke, V.; Carell, T. *Org. Lett.* **2009**, *11*, 2405-8; Singh, I.; Zarafshani, Z.; Lutz, J. F.; Heaney, F. *Macromolecules* **2009**, *42*, 5411–5413.

(19) Hanson, S. R.; Hsu, T. L.; Weerapana, E.; Kishikawa, K.; Simon, G. M.; Cravatt, B. F.; Wong, C. H. *J. Am. Chem. Soc.* **2007**, *129*, 7266-7267.

(20) Sun, X. L.; Stabler, C. L.; Cazalis, C. S.; Chaikof, E. L. *Bioconjugate Chem.* **2006**, *17*, 52-57.

(21) Johnson, J. A.; Baskin, J. M.; Bertozzi, C. R.; Koberstein, J. T.; Turro, N. J. *Chem. Commun.* **2008**, 3064-3066; Lallana, E.; Fernandez-Megia, E.; Riguera, R. *J. Am. Chem. Soc.* **2009**, *131*, 5748-5750; Inglis, A. J.; Sinnwell, S.; Stenzel, M. H.; Barner-Kowollik, C. *Angew. Chem. Int. Ed. Engl.* **2009**, *48*, 2411-2414.

(22) Fournier, D.; Hoogenboom, R.; Schubert, U. S. *Chem. Soc. Rev.* **2007**, *36*, 1369-1380; Lutz, J. F. *Angew. Chem. Int. Ed. Engl.* **2007**, *46*, 1018-1025; Lundberg, P.; Hawker, C. J.; Hult, A.; Malkoch, M. *Macromol. Rapid Comm.* **2008**, *29*, 998-1015.

CHAPTER 6

SYNTHETIC DIBENZOCYCLOOCTONYL PROBES FOR LIVE CELL LABELING AND VISUALIZATION OF CELL SURFACE AND INTRACELLULAR GLYCOCONJUGATES

6.1 INTRODUCTION

Metal free cycloadditions of cyclooctynes with azides to give stable 1,2,3-triazoles have found wide utility in labeling glycans, proteins, and lipids of living cells, glycoprotein enrichment for proteomics, and tissue reengineering.[1] These reactions, which have been coined "Strain-Promoted Alkyne-Azide Cycloadditions (SPAAC)" have also made entry in material sciences and have for example been employed for the assembly and surface modification of dendrimers,[2] derivatization of polymeric nanostructures,[3] and patterning of surfaces.[4, 5] The first generation of cyclooctynes (compound **1**, Scheme 6.1) exhibited relatively slow rates of reaction,[6] however, it has been found that significant increases in the rate of strain-promoted cycloaddition can be accomplished by appending electron-withdrawing groups to the propargylic position of cyclooctyne. For example, difluorinated cyclooctyne (DIFO, **2**) reacts with azides approximately sixty-times faster than similar cycloadditions with an unsubstituted cyclooctyne.[7] We have found that derivatives of 4-dibenzocyclooctynol (DIBO, **3**, **4**) react fast with azido-containing biomolecules and can be employed for visualizing metabolically labeled glycans of living cells.[8] Attractive features of DIBO include easy access to the compound by a simple synthetic approach, non-toxicity, and the possibility of straightforward attachment of a variety of probes. Furthermore, dibenzocyclooctynes

can be generated photochemically from corresponding cyclopropenones by short irradiation with UV light thereby providing opportunities for the spatial and temporal controlled labeling of the target substrates.[9] It has also been shown that by employing nitrones and nitrile oxides as 1,3-dipoles,[10, 11] the rate of cycloaddition can be further enhanced and this technology has for example made it possible to selectively tag proteins at the *N*-terminus or perform sequential modifications of complex compounds.[11] Several analogs of DIBO have also been reported that exhibit even higher rates of cycloaddition with azides.[5, 12]

Scheme 6.1 Reagents for labeling of azido-containing biomolecules.

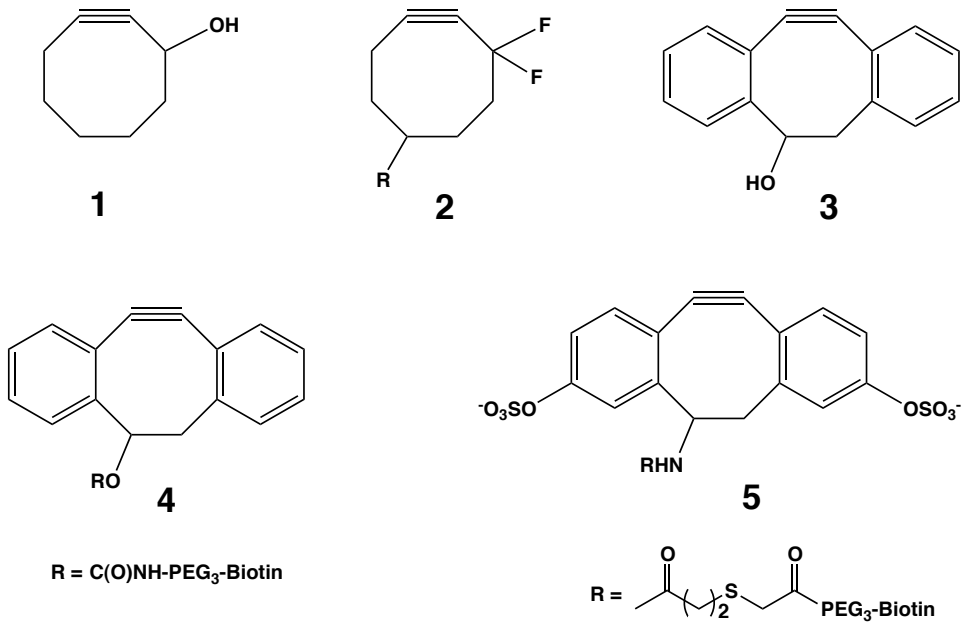

Despite the many attractive features of the second-generation cyclooctynes, their hydrophobicity and resulting limited water solubility represents a serious shortcoming. In particular, it can cause sequestration by membranes or non-specific binding to serum

proteins thereby reducing bio-availability.[13] To address these difficulties, we report here a highly polar sulfated dibenzocyclooctynylamide (S-DIBO) derivative **5**, which was successfully used for labeling azido-containing glycoconjugates of living cells. Sulfate esters of phenols have excellent stabilities under moderately acidic and basic conditions[14] and are found in nature as post-translational modifications of tyrosine.[15] Therefore, it was expected that compounds such as **5** would possess appropriate properties for cell-based studies. The properties of **5** have been compared with those of parent derivative **4** and it was found, for the first time, that their substitution pattern determines membrane permeability and in particular DIBO (**4**) can enter cells thereby labeling intra- and extracellular azido-modified glycoconjugates, whereas S-DIBO (**5**) cannot pass the cell membrane and therefore is ideally suited for selective labeling of cell surface molecules.

6.2 RESULTS AND DISCUSSION

The focus of the study was to use the synthetic sulfated DIBO derivative **5**, in the labeling of living cells modified with azido moieties. Azides can be incorporated into biomolecules using a variety of strategies[21] such as post synthetic modification, *in-vitro* enzymatic transfer, the use of covalent inhibitors, and metabolic labeling by feeding cells a biosynthetic precursor modified with an azido function. We opted for metabolic labeling with peracetylated *N*-α-azidoacetylmannosamine (Ac_4ManNAz), which is an appropriate substrate for the cell's glycosylation machinery, resulting in the incorporation of azido-containing sialic acids in glycoconjugates.[22]

Elegant studies by Bertozzi and coworkers have demonstrated that glycoconjugates of various model organisms can be metabolically labeled with azido-containing sugars and such an approach has been employed to demonstrate tissue specific expression of glycoconjugates.[23]

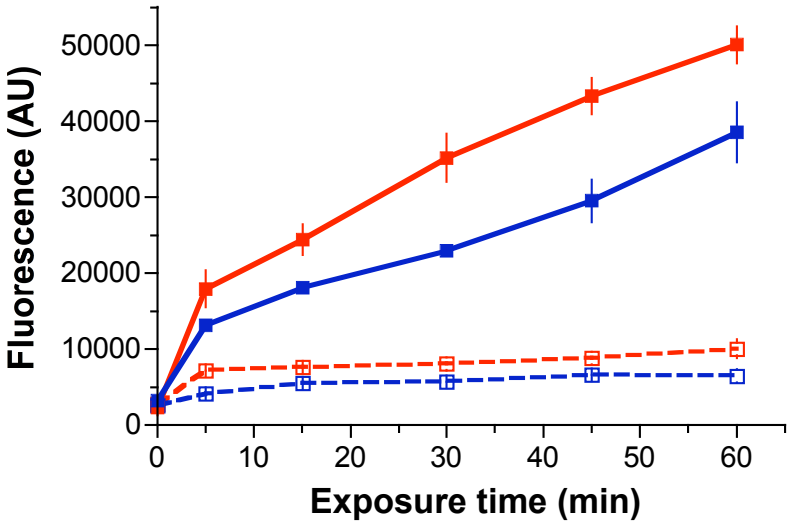

Figure 6.1 Cell surface labeling with compounds DIBO **4** and SDIBO **5**. Jurkat cells grown for 3 days in the presence of Ac_4ManNAc (25 μM; dashed lines) or Ac_4ManNAz (25 μM; solid lines) were incubated at room temperature with compounds **4** (red) and **5** (blue) at 30 μM for 0-60 min. Next, cells were incubated with avidin-FITC for 15 min at 4 ^{o}C, after which cell lysates were assessed for fluorescence intensity. AU indicates arbitrary fluorescence units.

Thus, Jurkat cells were cultured in the presence of Ac_4ManNAz (25 μM) for 3 days to metabolically introduce *N*-azidoacetyl-sialic acid (SiaNAz) moieties into glycoproteins.[22] As a negative control, cells were employed that were grown in the presence of peracetylated *N*-acetylmannosamine (Ac_4ManNAc). The cells were exposed to 30 μM of **4** and **5** for various time periods and after washing, stained with avidin-FITC for 15 min at 4 ^{o}C. The efficiency of the two-step cell surface labeling was determined by measuring the fluorescence intensity of the cell lysates. As can be seen in Figure 6.1, the two compounds gave similar labeling intensities.

The concentration dependency of the cell surface labeling was studied by incubating the cells with various concentrations of **4** and **5** followed by staining with avidin-FITC (Figure 6.2). As expected, cells displaying azido moieties showed a dose-dependent increase in fluorescence intensity. Reliable fluorescent labeling was achieved at a concentration of 3 μM of cyclooctyne, however optimal results were obtained at concentrations ranging from 30 to 100 μM. Importantly, apolar DIBO derivative **4** is not soluble at high concentrations in aqueous solutions and therefore required DMF as a co-solvent (stock solution of 45 mM in DMF). On the other hand, polar S-DIBO **5** is readily soluble in water even at high concentrations (stock solution of 45 mM in water).

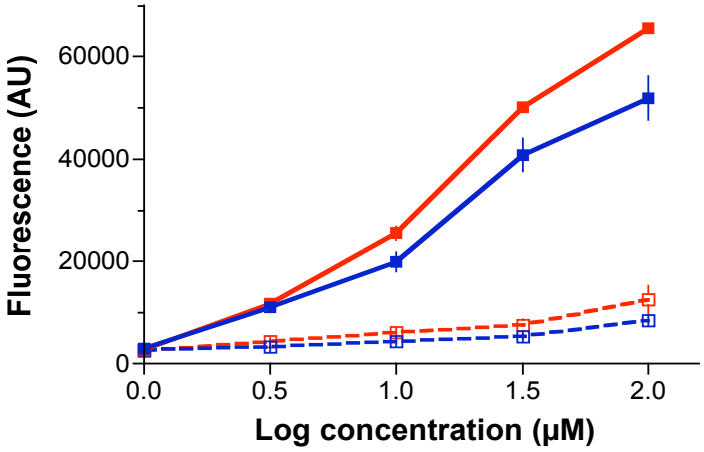

Figure 6.2 Concentration effect for cell surface labeling with compounds DIBO **4** and SDIBO **5**. Jurkat cells grown for 3 days in the presence of Ac_4ManNAc (25 μM; dashed lines) or Ac_4ManNAz (25 μM; solid lines) were incubated at room temperature with compounds **4** (red) and **5** (blue) at 0−100 μM for 1 h. Next, cells were incubated with avidin-FITC for 15 min at 4 °C, after which cell lysates were assessed for fluorescence intensity. AU indicates arbitrary fluorescence units.

To examine whether DIBO (**4**) and S-DIBO (**5**) can cause unwanted side reactions with side chain functional groups of proteins, the cell lysates were analyzed by Western blotting using an anti-biotin antibody conjugated to HRP for detection (Figure 6.3). Gratifyingly, the control cells gave negligible staining demonstrating an absence of unwanted chemical reactions. A surprising observation was, however, that S-DIBO **5** exhibited a less robust and different pattern of staining compared to parent DIBO **4**.

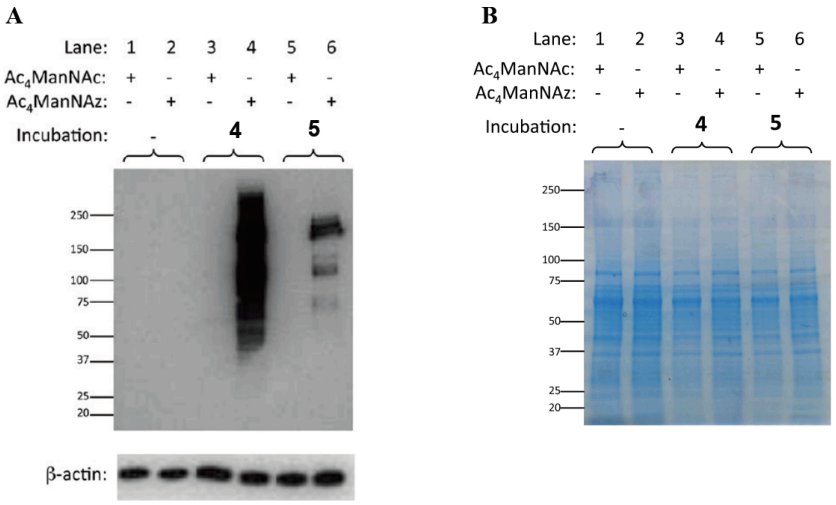

Figure 6.3 Western blot of Jurkat cells after labeling with compounds DIBO **4** and SDIBO **5**. Jurkat cells grown for 3 days in the presence of Ac_4ManNAc (25 μM) or Ac_4ManNAz (25 μM) were incubated at room temperature with compounds **4** and **5** at 30 μM for 1 h. Next, cells were lysed and cell lysates were resolved by SDS-PAGE and the blot was probed with an anti-biotin antibody conjugated to HRP (A). Total protein loading was confirmed by Coomassie staining (B). Coomassie staining of cell lysates indicating comparable levels of protein loading.

Human fibroblasts were chosen since their flat morphology and large size facilitate the visualization of intracellular organelles such as the Golgi apparatus. As shown in Figure 6.4(A), intracellular staining using **4** was readily detected. This staining was primarily due to labeling of Golgi-localized sialoglycoproteins, as determined by the high degree of co-localization with the medial Golgi protein, giantin. Nuclear ManNAz staining was also observed with **4** as judged by the co-localization with the ToPro stain. In contrast, very little or no intracellular staining (nuclear or Golgi) was observed with S-

DIBO **5** demonstrating that this compound is much less cell-permeable compared to the parent compound **4**. The lack of Golgi staining was also confirmed by separating the individual confocal stacks of the maximum intensity projections shown in Figure 6.4(A) (Figure 6.5). Extracellular staining, consistent with the fibrillar network synthesized by fibroblasts, could also be detected in cells incubated with both compounds.

Azido-modified fibroblasts were also stained with Alexa Fluor 568-conjugated streptavidin prior to fixation and permealization to yield only staining of extracellular glycoproteins. As shown in Figure 6.4(B), staining of cell surface glycoproteins, including those located within the fibrillar network, was observed but no intracellular molecules could be seen. Together, these findings demonstrate that DIBO derivatives can exhibit variable cell permeability that is evident under specific staining conditions.

In order to test whether the S-DIBO derivative **5** is capable of crossing the cell membrane following cycloaddition to ManNAz-labeled glycoproteins at the cell surface, labeled fibroblasts were incubated with either **4** or **5** for 4 h at 37 ^{o}C. This extended labeling time was used to allow for a greater fraction of cell surface molecules to be labeled and internalized. As shown in Figure 6.6, staining of Golgi-localized sialoglycoproteins was again observed for **4**, but not for **5**. Since the lack of intracellular staining in the case of **5** may be caused by the rapid degradation of internalized molecules within the lysosome, labeled cells were treated with the compounds in the presence of chloroquine to disrupt lysosomal pH and prevent efficient catabolism within this compartment.[24]

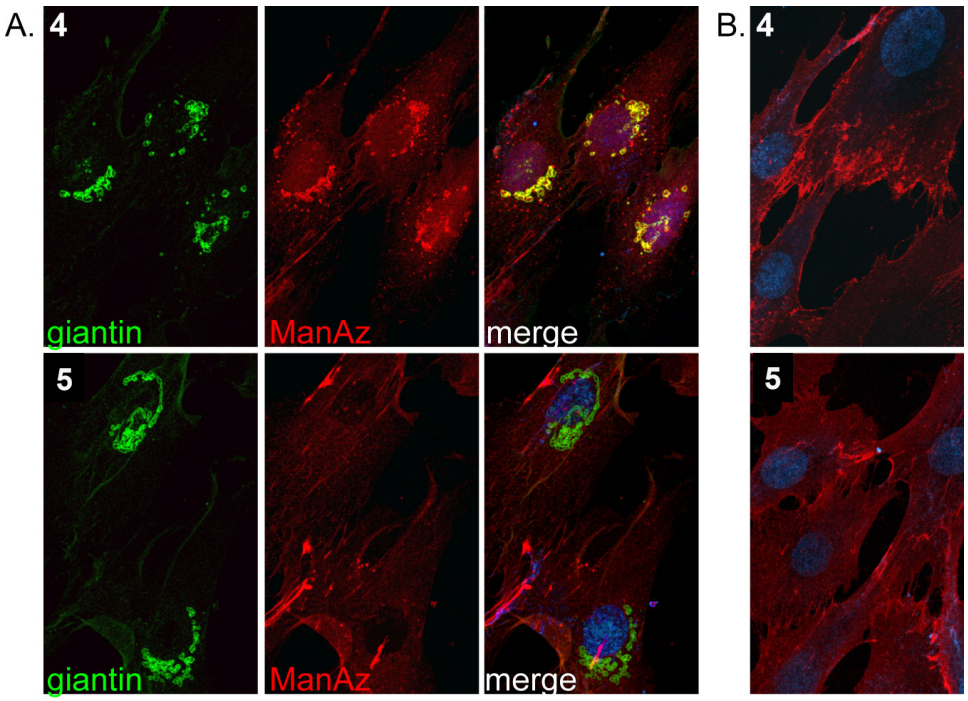

Figure 6.4 DIBO derivatives exhibit selective permeability in cultured human fibroblasts. Human skin fibroblasts grown for 2 days in the presence of Ac_4ManNAz (25 μM) were incubated for 1 h with **4** and **8** (30 μM) at room temperature. Following fixation, cells were permeabilized and incubated with a polyclonal antibody to the Golgi marker giantin. After incubation with appropriate conjugated fluorophores and a ToPro stain (blue) to mark the nucleus, cells were imaged. Only **4** was capable of labeling intracellular Golgi-localized proteins, indicating that this compound is cell permeable (A). Similar to (A), cells were labeled with Ac_4ManNAz and incubated with **4** and **5**, but staining with Alexa Fluor 568-conjugated streptavidin was performed prior to fixation and permeabilization to prevent internalization of labeled molecules. Under these conditions, DIBO **4** and its derivative **5** yield only surface staining of sialylated molecules (B). In both panels, maximum intensity projections of 6−8 individual confocal stacks are shown.

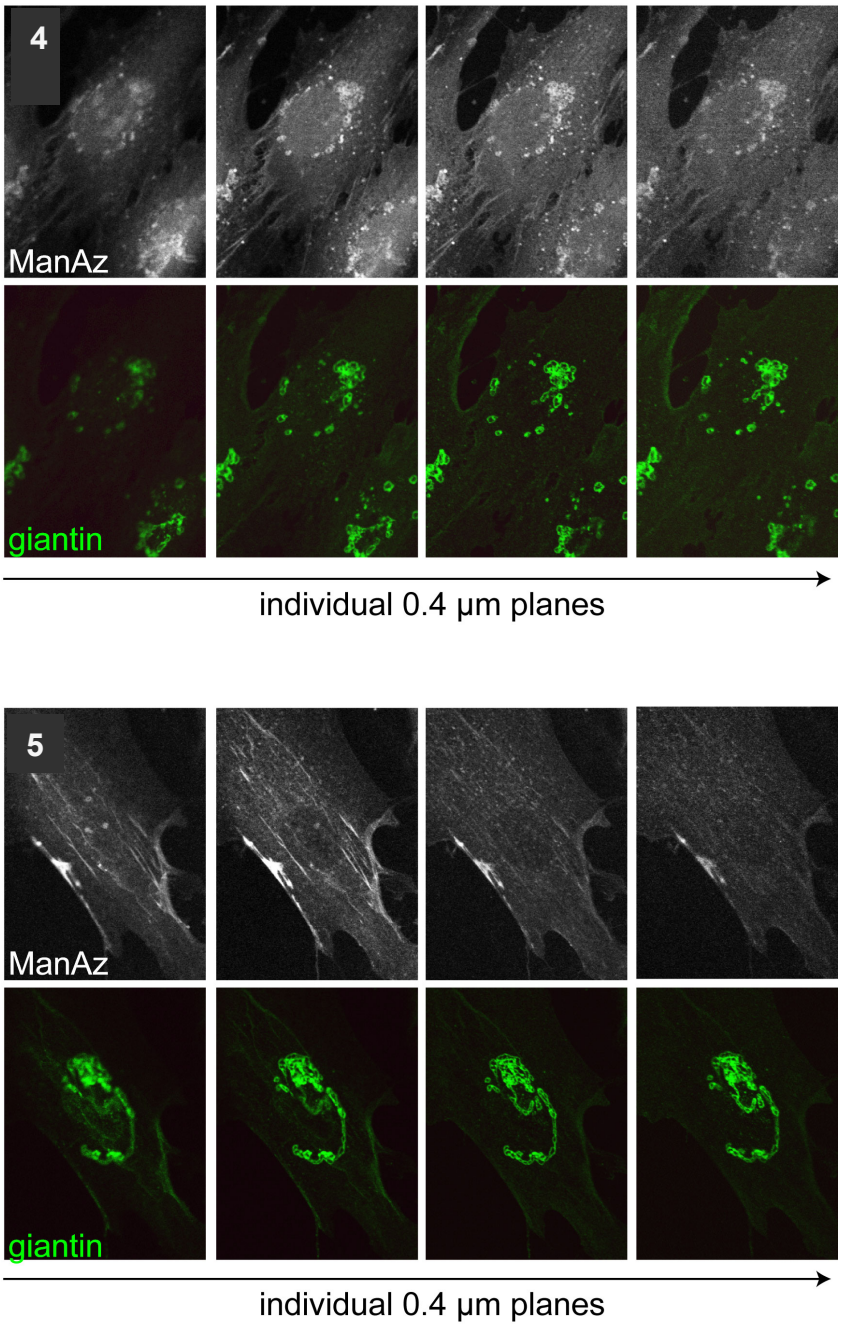

Figure 6.5 A montage of individual 0.4 μm confocal stacks taken from the original images in Figure 6.4(A). Note the complete lack of co-localization between giantin and ManNAz staining in these stacks when compound **5** is used.

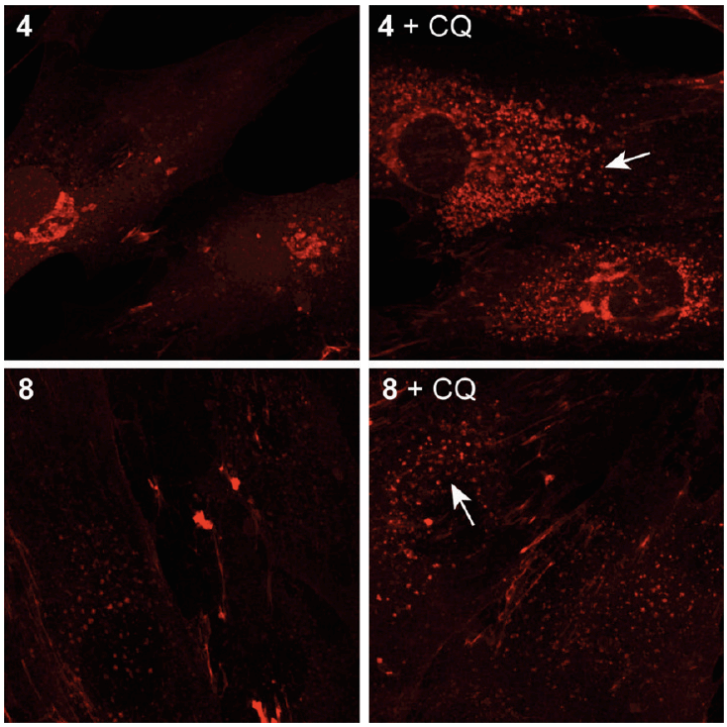

Figure 6.6 Intracellular staining of sialylated molecules can be detected using a non-permeable DIBO derivative following chloroquine (CQ) treatment. Human skin fibroblasts grown for 2 days in the presence of $Ac_4ManNAz$ (25 μM) were incubated for 4 h with **4** and **5** (30 μM) in the absence or presence of chloroquine (50 μM). Following fixation, cells were incubated with Alexa Fluor 568-conjugated streptavidin and imaged by confocal microscopy. Staining of intracellular vesicles can be readily detected using both compounds in the presence of chloroquine.

Under these conditions, labeled molecules, localized within intracellular vesicles resembling late endosomes/lysosomes, are clearly noted for both **4** and **5**. The increased intensity of this intracellular staining when compound **4** is used is likely due to the ability

of this molecule to cross the plasma membrane and react with sialylated molecules already present inside the cell. These results demonstrate that although certain DIBO derivatives have very poor cell permeability, they can be internalized following reaction with cell surface sialylated molecules.

6.3 CONCLUSIONS

Strain promoted cycloadditions of azides with cyclooctyne derivatives provide unique opportunities for labeling biomolecules such as glycoconjugates. The currently employed reagents are, however, apolar resulting in limited bioavailability. In our quest to develop highly polar cyclooctynes, we found that sulfated dibenzylcyclooctynamides can be prepared by an expedient synthetic route, react fast with azides, have excellent stabilities under moderately acidic and basic conditions and can be employed for labeling azido-modified glycoconjugates of living cells. A surprising finding was that biotinylated dibenzylcyclooctynol **4** can enter cells thereby labeling intra- and extracellular azido-modified glycoconjugates, whereas sulfated dibenzylcyclooctynamine **5** cannot pass the cell membrane. Therefore, such sulfated DIBO derivatives are ideally suited for selective labeling of cell surface molecules. The ability to selectively label cell surface glycoconjugates will offer unique opportunities for glycomics and glycoproteomics studies. For example, SPAAC can be employed for the isolation of glycoproteins. However, samples may be contaminated by biosynthetic intermediates complicating the determination of biological relevant cell surface glycoconjugates. Labeling azido-modified glycoconjugates with reagents such as S-DIBO (**5**) that cannot pass the cell membrane will address this problem. Furthermore, selective labeling of cell surface

glycoconjugates will provide new opportunities for monitoring retrograde trafficking. Upon endocytosis from the cell surface, most glycoproteins are either recycled through endosomes or targeted to lysosomes for degradation. Several human diseases are caused by defects in proteins involved in retrograde transport through the endosomal network or in enzymes responsible for the lysosomal catabolism of glycosylated molecules. We expect that selective tagging of cell surface glycoconjugates will make it possible to monitor trafficking and turnover of glycoproteins in healthy and diseased cells. For example, the studies reported here have already shown that accumulation of glycoconjugates in vesicular structures can easily be detected following chloroquine-induced disruption of intracellular transport and normal lysosomal function. Finally, the new polar dibenzylcyclooctynes have the obvious advantage that they are water-soluble and do not need an organic co-solvent for administration. We predict they will also have improved bioavailability and intend to address this in future studies.

6.4 MATERIALS AND METHODS

6.4.1 REAGENTS

Synthetic compound **4** was reconstituted in DMF and **5** was reconstituted in double distilled water. Storage was at –80 ^{o}C. Final concentrations of DMF never exceeded 0.56% to avoid toxic effects.

6.4.2 CELL SURFACE AZIDE LABELING AND DETECTION BY FLUORESCENCE INTENSITY

Human Jurkat cells (Clone E6-1; ATCC) were cultured in RPMI 1640 medium (ATCC) with L-glutamine (2 mM), adjusted to contain sodium bicarbonate (1.5 g/L), glucose (4.5 g/L), HEPES (10 mM), and sodium pyruvate (1.0 mM) and supplemented with penicillin (100 u/ml) / streptomycin (100 μg/ml; Mediatech) and fetal bovine serum (FBS, 10%; Hyclone). Cells were maintained in a humid 5% CO_2 atmosphere at 37 ^oC. Jurkat cells were grown in the presence of peracetylated *N*-azidoacetylmannosamine (Ac_4ManNAz; 25 μM final concentration) for 3 days, leading to the metabolic incorporation of the corresponding *N*-azidoacetyl sialic acid (SiaNAz) into their cell surface glycoproteins. Jurkat cells bearing azides and control cells grown in the presence of peracetylated *N*-acetylmannosamine (Ac_4ManNAc) were incubated with the biotinylated compound **4** and with the hydrophilic analogue **5** (0-100 μM) in labeling buffer (PBS, pH 7.4 containing 1% FBS) for 0-60 min at room temperature. The cells were washed three times with labeling buffer and then incubated with avidin conjugated to fluorescein isothiocyanate (FITC; 0.5 μg/mL; Molecular Probes) for 15 min at 4 ^oC. Following three washes and cell lysis, cell lysates were analyzed for fluorescence intensity (485 ex / 520 em) using a microplate reader (BMG Labtech). Data points were collected in triplicate and are representative of three separate experiments. Cell viability was assessed at different points in the procedure with exclusion of trypan blue.

6.4.3 WESTERN BLOT ANALYSIS

Jurkat cells were harvested by centrifugation (5 min at 500× *g*) and resuspended as 5×10^6 cells/mL. The cell suspensions (200 μL per sample) were incubated with biotin-conjugated compounds **4** and **5** (30 μM) or without compound as control for 1 h. The cells were washed (4 × 10 min) with cold DPBS, pH 7.4 containing FBS (1%) and lysed in passive lysis buffer. The cell lysates were clarified by centrifugation at 22,000 × *g* for 15 min and the total protein content of the clear supernatants was assessed using the bicinchonic acid assay (BCA; Pierce Biotechnology). Cell lysate samples (20 μg protein) in SDS-PAGE sample buffer containing 2-mercaptoethanol were boiled for 5 min, resolved on a 4-20% Tris-HCl gel (Bio-Rad) and transferred to a nitrocellulose membrane. Next the membrane was blocked in blocking buffer (nonfat dry milk (5%; Bio-Rad) in PBST (PBS containing Tween-20 (0.1%) and Triton X-100 (0.1%)) overnight at 4 ^{o}C. The blocked membrane was incubated for 1 h at room temperature with an antibiotin antibody conjugated to horseradish peroxidase (HRP) (1:100 000; Jackson ImmunoResearch Lab, Inc.) in blocking buffer and washed with PBST (4 × 10 min). Final detection of HRP activity was performed using ECL Plus chemiluminescent substrate (Amersham), exposure to film (Kodak) and development using a digital X-ray imaging machine (Kodak). Coomassie staining with GelCode® Blue Stain Reagent (Pierce, USA) was used to confirm total protein loading.

6.4.4 CELL LABELING AND DETECTION BY CONFOCAL MICROSCOPY

Human skin fibroblasts were cultured in Dulbecco's modified Eagle's medium (DMEM) with L-glutamine (2 mM), adjusted to contain sodium bicarbonate (1.5 g/L) and supplemented with penicillin (100 u/mL) / streptomycin (100 μg/mL) and FBS (10%). Cells were maintained in a humid 5% CO_2 atmosphere at 37 ^oC. Cells (50 000 cells) were grown on coverslips in the presence of Ac_4ManNAz (25 μM final concentration) for 2 days to metabolically incorporate SiaNAz into their glycoproteins. Fibroblast cells bearing azides were treated with the biotinylated compounds **4** and **5** (30 μM) in labeling buffer (PBS, pH 7.4 containing 1% FBS) for 1 h at room temperature or 4 h at 37 ^oC in the absence or presence of chloroquine (50 μM; Sigma), followed by fixation with formaldehyde (3.7% in PBS) for 15 min at room temperature. Cells were washed 4 times and permeabilized for 10 min at room temperature with Triton X-100 (0.2%) in PBS. The cells were incubated with rabbit anti-giantin polyclonal antibody (1:2000) in Triton X-100 (0.2%) in PBS for 1 h at room temperature.

Cells were washed 4 times and incubated with goat anti-rabbit antibody conjugated with Alexa Fluor 488 (1:500; Abcam) and Alexa Fluor 568-conjugated streptavidin (10 μg/mL; Molecular Probes) for 1 h at room temperature. Cells were washed 3 times with PBS and mounted with PermaFluor (Thermo Electron Corporation) before imaging. Initial analysis was performed on a Zeiss Axioplan2 fluorescent microscope. Confocal images were acquired on an Olympus FV-1000 laser scanning confocal microscope using a 60X (NA1.42) oil objective. Stacks of optical sections were collected in the *z* dimensions. The step size, based on the calculated optimum for each objective, was between 0.25 and 0.5 μm. Subsequently, each stack was collapsed into a

single image (*z*-projection). Analysis was performed offline using ImageJ 1.39f software (National Institutes of Health, USA) and Adobe Photoshop CS3 Extended Version 10.0 (Adobe Systems Incorporated), whereby all images were treated equally.

6.5 REFERENCES

(1) (a) Sletten, E. M.; Bertozzi, C. R. *Angew. Chem. Int. Ed.* **2009**, *48*, 6974-6998. (b) Jewett, J. C.; Bertozzi, C. R. *Chem. Soc. Rev.* **2010**, *39*, 1272-1279. (c) Debets, M. F.; van Berkel, S. S.; Dommerholt, J.; Dirks, A. T.; Rutjes, F. P.; van Delft, F. L. *Acc. Chem. Res.* **2011**, *44*, 805-815.

(2) (a) Ornelas, C.; Broichhagen, J.; Weck, M. *J. Am. Chem. Soc.* **2010**, *132*, 3923-3931. (b) Ledin, P. A.; Friscourt, F.; Guo, J.; Boons, G. J. *Chem.-Eur. J.* **2011**, *17*, 839-846.

(3) (a) Kele, P.; Mezö, G.; Achatz, D.; Wolfbeis, O. S. *Angew. Chem. Int. Ed.* **2009**, *48*, 344-347. (b) Lallana, E.; Fernandez-Megia, E.; Riguera, R. *J. Am. Chem. Soc* . **2009**, *131*, 5748-5750. (c) Canalle, L. A.; van der Knaap, M.; Overhand, M.; van Hest, J. C. *Macromol. Rapid Commun.* **2011**, *32*, 203-208. (d) DeForest, C. A.; Anseth, K. S. *Angew. Chem. Int. Ed.* **2011**, In press (DOI: 10.1002/anie.201106463). (e) Xu, J.; Prifti, F.; Song, J. *Macromolecules* **2011**, *44*, 2660-2667.

(4) (a) Canalle, L. A.; van Berkel, S. S.; de Haan, L. T.; van Hest, J. C. M. *Adv. Funct. Mater.* **2009**, *19*, 3464-3470. (b) Orski, S. V.; Poloukhtine, A. A.; Arumugam, S.; Mao, L.; Popik, V. V.; Locklin, J. *J. Am. Chem. Soc.* **2010**, *132*, 11024-11026. (c) Canalle, L. A.; Vong, T.; Adams, P. H.; van Delft, F. L.; Raats, J. M.; Chirivi, R. G.; van Hest, J. C. *Biomacromolecules* **2011**, *12*, 3692-3697.

(5) Kuzmin, A.; Poloukhtine, A.; Wolfert, M. A.; Popik, V. V. *Bioconjug. Chem* . **2010**, *21*, 2076-2085.

(6) Agard, N. J.; Prescher, J. A.; Bertozzi, C. R. *J. Am. Chem. Soc.* **2004**, *126*, 15046-15047.

(7) (a) Baskin, J. M.; Prescher, J. A.; Laughlin, S. T.; Agard, N. J.; Chang, P. V.; Miller, I. A.; Lo, A.; Codelli, J. A.; Bertozzi, C. R. *Proc. Natl. Acad. Sci. U. S. A* . **2007**, *104*, 16793-16797. (b) Codelli, J. A.; Baskin, J. M.; Agard, N. J.; Bertozzi, C. R. *J. Am. Chem. Soc.* **2008**, *130*, 11486-11493.

(8) (a) Ning, X. H.; Guo, J.; Wolfert, M. A.; Boons, G. J. *Angew. Chem. Int. Ed.* **2008**, *47*, 2253-2255. (b) Mbua, N. E.; Guo, J.; Wolfert, M. A.; Steet, R.; Boons, G. J. *ChemBioChem* **2011**, *12*, 1912-1921.

(9) Poloukhtine, A. A.; Mbua, N. E.; Wolfert, M. A.; Boons, G. J.; Popik, V. V. *J. Am. Chem. Soc.* **2009**, *131*, 15769-15776.

(10) (a) McKay, C. S.; Moran, J.; Pezacki, J. P. *Chem. Commun.* **2010**, *46*, 931-933. (b) Ning, X.; Temming, R. P.; Dommerholt, J.; Guo, J.; Ania, D. B.; Debets, M. F.; Wolfert, M. A.; Boons, G. J.; van Delft, F. L. *Angew. Chem. Int. Ed.* **2010**, *49*, 3065-3068. (c) McKay, C. S.; Blake, J. A.; Cheng, J.; Danielson, D. C.; Pezacki, J. P. *Chem. Commun.* **2011**, *47*, 10040-10042.

(11) Sanders, B. C.; Friscourt, F.; Ledin, P. A.; Mbua, N. E.; Arumugam, S.; Guo, J.; Boltje, T. J.; Popik, V. V.; Boons, G. J. *J. Am. Chem. Soc.* **2011**, *133*, 949-957.

(12) (a) Debets, M. F.; van Berkel, S. S.; Schoffelen, S.; Rutjes, F. P. J. T.; van Hest, J. C. M.; van Delft, F. L. *Chem. Commun.* **2010**, *46*, 97-99. (b) Dommerholt, J.; Schmidt, S.; Temming, R.; Hendriks, L. J.; Rutjes, F. P.; van Hest, J. C.; Lefeber, D. J.; Friedl, P.; van Delft, F. L. *Angew. Chem. Int. Ed.* **2010**, *49*, 9422-9425. (c) Jewett, J. C.; Sletten, E. M.; Bertozzi, C. R. *J. Am. Chem. Soc.* **2010**, *132*, 3688-

3690. (d) Sletten, E. M.; Nakamura, H.; Jewett, J. C.; Bertozzi, C. R. *J. Am. Chem. Soc.* **2010**, *132*, 11799-11805. (e) Stockmann, H.; Neves, A. A.; Stairs, S.; Ireland-Zecchini, H.; Brindle, K. M.; Leeper, F. J. *Chem. Sci.* **2011**, *2*, 932-936.

(13) (a) Sletten, E. M.; Bertozzi, C. R. *Org. Lett.* **2008**, *10*, 3097-3099. (b) Chang, P. V.; Prescher, J. A.; Sletten, E. M.; Baskin, J. M.; Miller, I. A.; Agard, N. J.; Lo, A.; Bertozzi, C. R. *Proc. Natl. Acad. Sci. U. S. A.* **2010**, *107*, 1821-1826.

(14) Balsved, D.; Bundgaard, J. R.; Sen, J. W. *Anal. Biochem.* **2007**, *363*, 70-76.

(15) Stone, M. J.; Chuang, S.; Hou, X.; Shoham, M.; Zhu, J. Z. *New Biotechnol.* **2009**, *25*, 299-317.

(16) Perlmutter, P. *Conjugate Addition Reactions in Organic Synthesis*; Pergamon Press Ltd.: Oxford, 1992.

(17) Hoyle, C. E.; Bowman, C. N. *Angew. Chem. Int. Ed.* **2010**, *49*, 1540-1573.

(18) Gregg, B. T.; Golden, K. C.; Quinn, J. F.; Wang, H.-J.; Zhang, W.; Wang, R.; Wekesa, F.; Tymoshenko, D. O. *Tetrahedron Lett.* **2009**, *50*, 3978–3981.

(19) Tobey, S. W.; West, R. *J. Am. Chem. Soc.* **1964**, *86*, 1459.

(20) Weissman, S. A.; Zewge, D. *Tetrahedron* **2005**, *61*, 7833-7863.

(21) Hao, Z.; Hong, S.; Chen, X.; Chen, P. R. *Acc. Chem. Res.* **2011**, *44*, 742-751.

(22) Saxon, E.; Bertozzi, C. R. *Science* **2000**, *287*, 2007-2010.

(23) (a) Laughlin, S. T.; Baskin, J. M.; Amacher, S. L.; Bertozzi, C. R. *Science* **2008**, *320*, 664-667. (b) Laughlin, S. T.; Bertozzi, C. R. *ACS Chem. Biol.* **2009**, *4*, 1068-1072.

(24) Lie, S. O.; Schofield, B. *Biochem. Pharmacol.* **1973**, *22*, 3109-3114.